



**TÉCNICO**  
LISBOA

**UNIVERSIDADE DE LISBOA**  
**INSTITUTO SUPERIOR TÉCNICO**

**Energy extraction from black holes**

**Filip Hejda**

**Supervisor:** Doctor José Pizarro de Sande e Lemos

**Co-supervisor:** Doctor Vítor Manuel dos Santos Cardoso

**Thesis approved in public session to obtain the PhD Degree in Physics**

**Jury final classification: Pass with Distinction**

**2019**



**UNIVERSIDADE DE LISBOA**  
**INSTITUTO SUPERIOR TÉCNICO**

**Energy extraction from black holes**

**Filip Hejda**

**Supervisor:** Doctor José Pizarro de Sande e Lemos

**Co-supervisor:** Doctor Vítor Manuel dos Santos Cardoso

**Thesis approved in public session to obtain the PhD Degree in Physics**

**Jury final classification: Pass with Distinction**

**Jury**

**Chairperson:**

Doctor Jorge Manuel Rodrigues Crispim Romão, Instituto Superior Técnico, Universidade de Lisboa

**Members of the Committee:**

Doctor Jiří Bičák, Institute of Theoretical Physics, Faculty of Mathematics and Physics, Charles University, Czech Republic

Doctor Jorge Manuel Rodrigues Crispim Romão, Instituto Superior Técnico, Universidade de Lisboa

Doctor José Pizarro de Sande e Lemos, Instituto Superior Técnico, Universidade de Lisboa

Doctor Filipe Artur Pacheco Neves Carteador Mena, Instituto Superior Técnico, Universidade de Lisboa

Doctor Oleg Borisovich Zaslavskii, V. N. Karazin Kharkiv National University, Ukraine

Doctor João Lopes Costa, Escola de Tecnologias e Arquitetura do ISCTE – Instituto Universitário de Lisboa

**Funding institution:** Fundação para a Ciência e a Tecnologia

**2019**



# Resumo

Os buracos negros são responsáveis por alimentar alguns dos processos mais energéticos no nosso Universo. Como tal, é importante estudar os diversos métodos que podem ser usados para extrair energia de buracos negros. O processo de Penrose é um exemplo típico destes métodos; se uma partícula se desintegra em dois fragmentos perto de um buraco negro, um dos fragmentos pode adquirir energia adicional a troco de o outro fragmento cair no buraco negro, reduzindo o momento angular do buraco negro. No entanto, a viabilidade do processo de Penrose para efeitos práticos é limitada, uma vez que os dois fragmentos precisam de ter uma velocidade relativa muito elevada.

Ainda assim, se considerarmos difusão de partículas em vez de decaimento de partículas, esta velocidade relativa elevada pode surgir naturalmente em colisões de altas energias. O processo de Penrose colisional recebeu então grande atenção após Bañados, Silk e West (BSW) discutirem a possibilidade de ocorrência de colisões de partículas de teste com energias do centro-de-massa arbitrariamente elevadas perto do horizonte de buracos negros de Kerr em rotação máxima. Curiosamente, este efeito BSW está na verdade presente em todos os buracos negros extremos; o efeito é causado pela existência de um tipo distinto de movimento de partículas perto dos horizontes de buracos negros extremos. Estas chamadas partículas críticas apenas se aproximam assintoticamente do horizonte, e isso permite-lhes que a energia de colisão do centro-de-massa com outras partículas genéricas cresça sem limite.

Apesar da variante original do efeito BSW requerer partículas com um ajuste fino do momento angular que orbitem buracos negros rotacionais extremos, Zaslavskii encontrou um efeito análogo para partículas carregadas com ajuste fino da carga em movimento radial em torno de um buraco negro estático, um buraco negro carregado extremo. Apesar de terem a mesma natureza cinemática, as duas variantes diferem significativamente em termos de energias extraídas. Enquanto a energia e massa das partículas de escape pro-

duzidas no efeito original estão sujeitas a limites superiores incondicionais, tais restrições não são encontradas na versão carregada do efeito. Como tal, estas duas variantes do efeito BSW representam um dilema impossível; o caso mais próximo de ser astrofisicamente relevante é limitado no que toca a extração de energia, enquanto que o caso que permite uma extração de energia relevante requer um cenário menos realista.

Como demonstrado por Wald, buracos negros astrofísicos podem conter uma carga diferente de zero graças à acreção de carga causada pela interação com campos magnéticos externos. No entanto, esta carga tenderá a ser extremamente pequena. Logo, surge a questão da possibilidade de generalizar a versão carregada do efeito BSW a buracos negros de carga arbitrariamente pequena e combiná-la com a versão original, e que consequências terá isso na viabilidade da energia extraída. Nesta tese, pretendemos responder a estas questões.

Primeiro consideramos soluções magnetizadas de Kerr-Newman (MKN), que descrevem interações de buracos negros carregados em rotação com um campo magnético externo num regime de campo forte. Estudamos as geometrias perto de horizontes dos casos extremos de MKN e descobrimos que existe um mapa de correspondência entre estes e as geometrias perto de horizontes de buracos negros extremos de Kerr-Newmann sem um campo externo. Isto pode também estar ligado a outros tópicos, como a elevada simetria de horizontes extremos ou o efeito de Meissner de expulsão de campos externos de buracos negros extremos. Além disso, se considerarmos buracos negros extremos como uma aproximação de buracos negros astrofísicos em rotação rápida, a correspondência fornece uma justificação para usar buracos negros de Kerr-Newman como substitutos de buracos negros magnetizados em processos que ocorram perto do horizonte.

No restante da tese, examinamos generalizações do efeito BSW. Descobrimos que a versão carregada do efeito é possível também para partículas em movimento ao longo do eixo de simetria de buracos negros de electrovácuo em rotação extremos com carga arbitrariamente pequena. Apesar de não surgirem limitações na energia extraída, encontramos algumas ressalvas que podem tornar a extração de energia inexequível.

Estudamos também a unificação das duas versões do efeito BSW, que previamente apenas foram estudadas isoladamente, para partículas carregadas em movimento no plano equatorial de buracos negros de electrovácuo em rotação extremos. Neste caso, também, constatamos que não existem limites na energia extraída quando tanto o buraco negro

como as partículas em escape são carregados, independentemente da magnitude da carga do buraco negro. Adicionalmente, demonstramos que as limitações de aplicabilidade encontradas nas colisões de partículas ao longo do eixo, podem ser contornadas através das colisões no plano equatorial num processo adequado.

**Palavras-chave:** buracos negros, campos electromagnéticos, horizonte, colisões de partículas, extração de energia



# Abstract

Black holes are understood as the engines powering some of the most energetic and most violent processes in our Universe. Therefore, it is important to study various ways in which energy can be extracted from black holes. Penrose process remains a textbook example of such a possibility; if a particle disintegrates into two fragments near a black hole, one of the fragments might gain energy at the expense of the other fragment falling inside and reducing slightly the angular momentum of the black hole. However, practical viability of the original Penrose process is limited, as the two fragments must have a very high relative velocity.

Nevertheless, if one considers particle scattering instead of particle decays, the high relative velocity might naturally arise in high-energy collisions. Collisional Penrose process thus received a lot of attention after Bañados, Silk and West (BSW) pointed out the possibility of test particle collisions with arbitrarily high centre-of-mass energy near the horizon of maximally rotating Kerr black holes. Curiously enough, this BSW effect turned out to be ubiquitous among extremal black holes; it is caused by the existence of a distinct type of particle motion near their horizons. These fine-tuned, so-called critical particles can only asymptotically approach the horizon radius, and this allows the centre-of-mass collision energy in their collisions with generic particles to grow without bound.

Although the original variant of the BSW effect requires particles with fine-tuned angular momentum orbiting around rotating extremal black holes, Zaslavskii found an analogous effect with fine-tuned charged particles moving radially in a static, maximally charged black-hole spacetime. Despite having the same kinematic nature, the two variants differ significantly in terms of energy extraction. Whereas the energy and mass of escaping particles produced in the original version is subject to unconditional upper bounds, no such restrictions were found for the charged version. Thus, the two variants of the BSW effect represent an impossible dilemma; the one which is closer to astrophysically relevant

situations fares badly on energy extraction, and the one which permits significant energy extraction requires settings that are not realistic.

As famously shown by Wald, astrophysical black holes can maintain a non-zero charge thanks to charge accretion caused by interaction with external magnetic fields. This charge will be extremely small, however. Therefore, questions naturally arise, whether it is possible to generalise the charged version of the BSW effect to black holes with arbitrarily small charges and combine it with the other variant, and what will be the resulting prospects for energy extraction. In the present thesis, we would like to give answers to such questions.

We first consider magnetised Kerr-Newman (MKN) solutions, which describe interaction of charged, rotating black holes with external magnetic field in the strong-field regime. We study the near-horizon geometries of the extremal cases of MKN spacetimes and we find that there exists a correspondence map between them and the near-horizon geometries of extremal Kerr-Newman black holes without the external field. This can be linked to other interesting issues like the high symmetry of extremal horizons or the Meissner effect of expulsion of external fields from extremal black holes. Moreover, if we consider extremal black holes as an approximation for fast-spinning astrophysical black holes, the correspondence also gives us justification to use Kerr-Newman black holes as surrogates for magnetised black holes for processes happening near the horizon.

In the rest of the thesis, we examine generalisations of the BSW effect. We find that the charged version is possible also for particles moving along the axis of symmetry of extremal rotating electrovacuum black holes with arbitrarily small value of charge. Although no restrictions on the extracted energy appear for this generalisation, we find numerous caveats that can make the energy extraction unfeasible despite the lack of unconditional kinematic bounds.

We also study the unification of the two versions of BSW effect, which were previously studied only separately, for charged particles moving in the equatorial plane of extremal rotating electrovacuum black holes. In this case, too, it turns out that there are no bounds on the extracted energy whenever both the black hole and the escaping particles are charged, regardless of the magnitude of the black-hole charge. Furthermore, we show that the practical limitations found for particle collisions along the axis can be circumvented for collisions in the equatorial plane in suitable processes.

**Keywords:** black holes, electromagnetic fields, horizon, particle collisions, energy extraction



# Acknowledgements

First and foremost, I would like to thank my supervisor, José Lemos, for his endless support, and for giving me the opportunity to study in Portugal, which is a great place to be, and to do gravitational physics especially. José Lemos and my co-supervisor, Vítor Cardoso, gave me a bright example of leadership in international science and enabled me to foster collaborations and embark on scientific visits that would not be possible otherwise.

Among all the people I met during my PhD, the versatile personality of Masashi Kimura stands out. Big thanks belong to him for making our lives better in all regards by his presence.

I am also grateful to Jiří Bičák, Oleg Zaslavskii, Tomohiro Harada and Roberto Oliveri, my collaborators on completed, ongoing and prospective projects for the inspiration and for helping me develop my scientific skills.

I would like to thank my colleagues and friends from CENTRA, IDPASC, and from γαμιάδες office, who kept me company and gave me advice on my scientific journey, in particular Miguel Ferreira, Pedro Cunha, Kyriakos Destounis, Lorenzo Annuli and João Luís.

I am very indebted to my teachers, among others Oldřich Semerák, Jiří Hořejší, Pavel Kratochvíl, Dalibor Pražák and Miroslav Zelený, for giving me the solid foundations of knowledge and skills in various areas of theoretical physics and pure mathematics.

I am grateful to Natália Antunes, Dulce Conceição and Rita Sousa for support in bureaucratic issues, which helped me to get the most of my life in Portugal. I would also like to thank Sérgio Almeida and João Vasconcelos for repairing my computer and to Tomáš Benedikt and Rui André for ready assistance at key moments.

I gladly pay my respect to people of HuBB, especially to the hero of our times, Miguel Duarte. This group reminded me that scientific deadlines are not the worst thing on

Earth and kept me engaged with socio-political issues.

Many thanks belong to my friends from the Czech republic, among others Jan Fabián, Alžběta Kadlecová, Jiří Jiruš, Josefina Wichsová, Adam Stíbal and Lenka Velcová, who warmly received me during my visits to Central Europe. I am also grateful to my grandmother for hosting me at her place.

Last, but not least, I would like to express my gratitude to some special people that I met in Portugal outside the realms of physics, in particular Maria Leonardo, Mexitli Sandoval, Pedro Durão, Marija Čosović and Carmine Piparo.

# Contents

<b>1</b>	<b>Introduction</b>	<b>1</b>
1.1	Frame dragging – a hallmark of relativistic gravitation . . . . .	1
1.2	Charged black holes and external magnetic fields . . . . .	3
1.3	Penrose process and its generalisations . . . . .	8
1.4	BSW effect and related phenomena . . . . .	9
<b>2</b>	<b>Near-horizon description of extremal magnetised stationary black holes and Meissner effect</b>	<b>13</b>
2.1	Outline and summary . . . . .	13
2.2	Charged, rotating black holes in magnetic fields . . . . .	17
2.2.1	Stationary Ernst solution . . . . .	17
2.2.2	Ernst-Wild solution and a general MKN black hole . . . . .	18
2.2.3	Global properties of magnetised black holes . . . . .	20
2.3	The near-horizon description of extremal configurations . . . . .	21
2.3.1	General prescription . . . . .	21
2.3.2	Near-horizon description of extremal black holes in strong magnetic fields . . . . .	25
2.4	Near-horizon degeneracy of extremal cases of MKN solutions . . . . .	27
2.4.1	Special cases . . . . .	27
2.4.2	Effective parameters . . . . .	29
2.4.3	Dimensionless parameters . . . . .	33
2.4.4	Remark on invariants and uniqueness theorems . . . . .	36
<b>3</b>	<b>Particle collisions in the equatorial plane: kinematic restrictions</b>	<b>39</b>
3.1	Outline . . . . .	39

3.2	Electrogeodesic motion in black-hole spacetimes . . . . .	40
3.3	Collision energy and critical particles . . . . .	44
3.4	Kinematics of critical particles . . . . .	46
3.4.1	Derivative of the effective potential . . . . .	47
3.4.2	Remarks on motion towards $r_0$ . . . . .	48
3.4.3	The hyperbola . . . . .	49
3.4.4	Parametric solution . . . . .	54
3.4.5	Remarks on class II critical particles . . . . .	55
3.4.6	The second derivative . . . . .	56
3.5	Results for the Kerr-Newman solution . . . . .	59
3.5.1	The hyperbola . . . . .	60
3.5.2	The second derivative . . . . .	61
3.5.3	Important special cases . . . . .	63
3.5.4	Energy considerations . . . . .	70
3.5.5	The mega-BSW phenomena . . . . .	73
3.6	Summary . . . . .	74
<b>4</b>	<b>Particle collisions along the axis of symmetry: kinematic restrictions and energy extraction</b>	<b>79</b>
4.1	Outline and summary . . . . .	79
4.2	Motion and collisions of test particles along the axis . . . . .	81
4.2.1	Equations of motion and effective potential . . . . .	82
4.2.2	Critical particles and collision energy . . . . .	83
4.2.3	Motion towards $r_0$ , nearly critical particles and class II critical particles . . . . .	85
4.3	Kinematic restrictions . . . . .	86
4.3.1	General formulae for critical particles . . . . .	86
4.3.2	Results for the Kerr-Newman solution . . . . .	88
4.4	Energy extraction . . . . .	90
4.4.1	Application of conservation laws . . . . .	90
4.4.2	Kinematic regimes . . . . .	92
4.4.3	Discussion of caveats . . . . .	96

<b>5</b>	<b>Particle collisions in the equatorial plane: energy extraction</b>	<b>101</b>
5.1	Outline and summary . . . . .	101
5.2	Motion and collisions of charged test particles . . . . .	102
5.2.1	General equations of equatorial motion . . . . .	102
5.2.2	Near-horizon expansions and (nearly) critical particles . . . . .	104
5.2.3	BSW effect and its Schnittman variant . . . . .	108
5.3	Approach phase . . . . .	108
5.3.1	Admissible region in the parameter space . . . . .	109
5.3.2	Degenerate case . . . . .	115
5.4	Energy extraction . . . . .	116
5.4.1	Conservation laws and kinematic regimes . . . . .	116
5.4.2	Structure of the parameter space . . . . .	120
5.4.3	Special cases and the degenerate case . . . . .	127
5.5	Results for Kerr-Newman solution . . . . .	129
5.5.1	Admissible region in the parameter space . . . . .	130
5.5.2	Structure of the parameter space with regard to energy extraction .	131
5.6	Discussion of caveats . . . . .	136
5.6.1	Restrictions on processes with (marginally) bound microscopic particles . . . . .	137
<b>6</b>	<b>Conclusions</b>	<b>141</b>
<b>A</b>	<b>Killing vectors and tensors in the near-horizon spacetimes</b>	<b>145</b>
<b>B</b>	<b>Harrison transformation</b>	<b>149</b>
B.1	Ernst formalism . . . . .	149
B.2	Generating “magnetised” solutions . . . . .	151
B.3	Remark on rigidity theorems . . . . .	153
<b>C</b>	<b>Auxiliary calculations</b>	<b>157</b>
C.1	Derivatives of effective potentials . . . . .	157
C.1.1	Conditions for circular orbits . . . . .	157
C.1.2	Relations for critical particles . . . . .	158
C.2	The decomposition (3.71) . . . . .	160



# Preface

Official research presented in this thesis has been carried out at Centro de Astrofísica e Gravitação (CENTRA) in the Physics Department of Instituto Superior Técnico, and was supported by Fundação para a Ciência e a Tecnologia (FCT) through Grant No. PD/BD/113477/2015 awarded in the framework of the Doctoral Programme IDPASC-Portugal.

I declare that this thesis is not substantially the same as any that I have submitted for a degree, diploma or other qualification at any other university and that no part of it has already been or is concurrently submitted for any such degree, diploma or other qualification.

The work was done in collaboration with my supervisor Professor José Pizarro de Sande e Lemos (Chapter 5), with Professor Oleg Borisovich Zaslavskii (Chapters 4 and 5), and with Professor Jiří Bičák (Chapters 2, 3 and 4). Chapters 2, 3 and 4 were published in international peer-reviewed journal, whereas Chapter 5 is being prepared for publication.

The works published or to be published presented in this thesis are listed below:

- J. Bičák, F. Hejda: Near-horizon description of extremal magnetized stationary black holes and Meissner effect, *Phys. Rev. D* **92**, 104006 (2015), arXiv:1510.01911 [gr-qc] (Chapter 2).
- F. Hejda, J. Bičák: Kinematic restrictions on particle collisions near extremal black holes: A unified picture, *Phys. Rev. D* **95**, 084055 (2017), arXiv:1612.04959 [gr-qc] (Chapter 3).
- F. Hejda, J. Bičák, O. B. Zaslavskii: Extraction of energy from an extremal rotating electrovacuum black hole: Particle collisions along the axis of symmetry, *Phys. Rev. D* **100**, 064041 (2019), arXiv:1904.02035 [gr-qc] (Chapter 4).

- F. Hejda, J. P. S. Lemos, O. B. Zaslavskii: Extraction of energy from an extremal rotating electrovacuum black hole: Particle collisions in the equatorial plane, *in final stages of preparation* (Chapter 5).

# Chapter 1

## Introduction

### 1.1 Frame dragging – a hallmark of relativistic gravitation

In the Newtonian theory of gravity, the gravitational field can be described by a single scalar function, which is sourced by the matter density distribution. Therefore, if we consider two axially symmetric objects, one at rest and the other spinning around its axis, their Newtonian gravitational field will be precisely the same as long as their matter distribution is the same.

On the other hand, in metric theories of gravity, in particular in Einstein’s General relativity, the gravitational field, encoded in the metric, is sourced by the energy-momentum tensor. Because of that, the metric is sensitive both to the direction and to the rate of spin of a source object. Consequently, test bodies, which follow geodesics of the metric, will also be influenced by the spin of the source object. This type of effects in relativistic gravity is commonly called “frame dragging”, or just “dragging” for short.

As early as 1918, the potentially observable consequences of dragging were calculated by Lense and Thirring using the weak-field approximation. In particular, they studied the way in which a gyroscope precesses due to frame dragging by a nearby massive spinning object. (A modern rederivation of the Lense-Thirring effect is given in §40.7 in [1].)

Regarding the study of dragging in the *strong-field regime*, a breakthrough came with the discovery of an exact solution of Einstein’s equations describing a rotating black hole by Kerr [2]. (This was in 1963, more than 47 years after the solution for a static black hole

was found by Schwarzschild.) The Kerr solution turned out to be even more remarkable thanks to several results by Carter. He has first shown that the geodesic equations for the Kerr metric are fully integrable [3]. Moreover, Carter realised that the requirements for integrability of equations of motion for test particles and fields actually provide restrictions on the metric form that can be used to *derive* the Kerr solution from scratch. This new formulation allowed Carter to find a whole generalised class of solutions [4] with several additional parameters, which include the cosmological constant and also pathological curiosities like NUT (Newman-Unti-Tamburino) charge and a magnetic monopole charge.

In the present thesis, we shall mostly work with the electrically charged version, i.e. Kerr-Newman solution [5]. In Carter-like form its metric reads

$$\mathbf{g} = \frac{[a \mathbf{d}t - (r^2 + a^2) \mathbf{d}\varphi]^2 \sin^2 \vartheta - \Delta (\mathbf{d}t - a \sin^2 \vartheta \mathbf{d}\varphi)^2}{\Sigma} + \Sigma \left( \frac{\mathbf{d}r^2}{\Delta} + \mathbf{d}\vartheta^2 \right), \quad (1.1)$$

where

$$\Delta = r^2 - 2Mr + a^2 + Q^2 \qquad \Sigma = r^2 + a^2 \cos^2 \vartheta. \quad (1.2)$$

The corresponding electromagnetic potential reads

$$\mathbf{A} = -\frac{Qr}{\Sigma} (\mathbf{d}t - a \sin^2 \vartheta \mathbf{d}\varphi). \quad (1.3)$$

The original Kerr black-hole solution with mass  $M$  and an angular momentum  $J = aM$  is recovered simply by putting  $Q = 0$  in (1.2).

A very detailed, thorough, and long-running research into orbits of test particles influenced by strong frame dragging was enabled by the full integrability of their equations of motion in the Kerr family of spacetimes (see e.g. [6, 7] and references therein). An elementary, yet very important result is that the static limit, under which no particles can remain at rest with respect to a distant observer, and the event horizon, from which particles cannot return, do not need to coincide. Indeed, for Kerr black hole the static limit is located at

$$r_S = M + \sqrt{M^2 - a^2 \cos^2 \vartheta}, \quad (1.4)$$

whereas the black hole horizon at

$$r_+ = M + \sqrt{M^2 - a^2} , \quad (1.5)$$

and thus they differ for any  $a \neq 0$ . Moreover, it turns out that the dragging causes objects crossing the horizon to rotate precisely with the angular velocity of the black hole. As shown by Anderson and Lemos [8], this can have surprising consequences; when a slowly-rotating black hole is surrounded by a fast-rotating fluid, the fluid will be forced by the frame dragging to slow down its rotation close to the horizon, and this can lead to reversal of the viscous torque.

## 1.2 Charged black holes and external magnetic fields

The first exact solution of the Einstein-Maxwell system of equations, later understood to describe a static charged black hole, was derived independently by Reissner and Nordström. (Reissner made the discovery particularly fast, less than three months after Schwarzschild found the uncharged version.) The Reissner-Nordström solution also forms a subcase  $a = 0$  of the Kerr-Newman solution (1.1), (1.3). Its metric reads

$$\mathbf{g} = - \left( 1 - \frac{2M}{r} + \frac{Q^2}{r^2} \right) \mathbf{d}t^2 + \frac{\mathbf{d}r^2}{1 - \frac{2M}{r} + \frac{Q^2}{r^2}} + r^2 (\mathbf{d}\vartheta^2 + \sin^2 \vartheta \mathbf{d}\varphi^2) , \quad (1.6)$$

and it is accompanied by electrostatic field with potential

$$\mathbf{A} = -\frac{Q}{r} \mathbf{d}t . \quad (1.7)$$

Here  $Q$  is the black-hole charge.

For rotating black holes, the charged generalisation by Newman *et al.* [5] mentioned above was also found quite fast, within two years of Kerr's result. In the metric form (1.1), the influence of the charge  $Q$  on the geometry of the Kerr-Newman solution is carried solely by function  $\Delta$  (1.2). Let us emphasise that in an analogy with a charged rotating sphere, the electromagnetic field (1.3) of the charged rotating black hole acquires a magnetic part.

Besides not representing as major conceptual shift as the rotation, the black-hole

charge has also been questionable with regard to its astrophysical relevance. Indeed, several mechanisms are known that can rapidly discharge a black hole (see [9] for a short review and references). What is then the motivation to study charged black holes?

First part of the answer stems from the fact that astrophysical black holes can be surrounded by external magnetic fields and interact with them. An important analysis of this phenomenon was carried out by Wald [10] in the test-field approximation. He noted that close to an arbitrary rotating black hole, all observers will experience an electric component of the external field even when it is required to asymptotically approach a homogeneous, purely magnetic field at the spatial infinity. Because of this electric component, a “magnetised” rotating black hole will selectively accrete particles with one sign of charge, until it acquires a charge with value  $Q = 2BJ$  (where parameter  $B$  characterises the strength of the external magnetic field and  $J$  is the angular momentum of the black hole). Therefore, the black-hole charge can be non-negligible for fast-spinning black holes interacting with very strong external magnetic fields.

It is natural to ask what happens to this Wald’s result in the strong-field regime, when back-reaction of the electromagnetic field on the metric is taken into account. Difficulties arise from the fact that asymptotically homogeneous field is incompatible with an asymptotically flat universe, as it would carry an infinite amount of energy. Consequences of this problem can be seen on the example of a simple solution of the Einstein-Maxwell system, which was first discovered by Bonnor [11] and later studied by Melvin [12]. Written in cylindrical coordinates ( $R = r \sin \vartheta$ ,  $z = r \cos \vartheta$ ), metric of this “magnetic universe” reads

$$\mathbf{g} = \left(1 + \frac{1}{4}B^2R^2\right)^2 (-\mathbf{d}t^2 + \mathbf{d}R^2 + \mathbf{d}z^2) + \frac{R^2}{\left(1 + \frac{1}{4}B^2R^2\right)^2} \mathbf{d}\varphi^2, \quad (1.8)$$

whereas the potential takes the form

$$\mathbf{A} = \frac{\frac{1}{2}BR^2}{1 + \frac{1}{4}B^2R^2} \mathbf{d}\varphi. \quad (1.9)$$

Observing that  $g_{\varphi\varphi} \rightarrow 0$  for  $R \rightarrow \infty$ , whereas  $g_{zz} \sim R^4$ , we can see that Bonnor-Melvin magnetic universe has indeed a non-flat, pathological asymptotic behaviour.

In a key step, Ernst reformulated the axially symmetric stationary problem, for both the vacuum Einstein equations [13] and the Einstein-Maxwell system [14], using complex-valued potentials (see also chapter 18 in [15] for broader discussion). In this framework,

it was possible to associate symmetries of the field equations in the new formulation with solution generating techniques, as explained by Kinnersley [16] (cf. also chapter 34 in [15]). The generation technique previously described by Harrison [17] is a particularly important example. It turned out that when applied on a “seed” Minkowski solution, the Harrison transformation produces the Bonnor-Melvin magnetic universe (1.8), provided that the Ernst potentials employed are based on the axial Killing vector  $\partial/\partial\varphi$  and a real continuous parameter is used. By analogy, applying the same type of Harrison transformation on asymptotically flat black-hole spacetimes is thus a way to derive new solutions describing interaction of black holes with strong external magnetic fields.

This possibility was first explored by Ernst [18] for Schwarzschild and Reissner-Nordström (1.6) black holes. Subsequently, Ernst and Wild [19] outlined the application of the magnetising Harrison transformation on the whole Kerr-Newman (1.1) family of solutions. They performed the full integration of the resulting solution in the Kerr case, and found that in the weak-field approximation it corresponds to the Wald solution with  $Q = 2BJ$ . However, it should be noted that in the strong-field case,  $J$  is the angular momentum of the *seed* solution, not of the final one.

A lot more research was devoted to finding new solutions via the Harrison transformation. García Díaz [20] integrated the magnetised Kerr-Newman case. It was also discussed that the Harrison transformation with imaginary continuous parameter can be used to generate solutions describing accelerated black holes in an external electric field [21, 22]. The most general “magnetised” solutions that were published involve many additional parameters including electric and magnetic monopole charges, external magnetic and electric fields, and also coefficients of a linear combination of Killing vectors ( $\partial/\partial t$  and  $\partial/\partial\varphi$ ) on which the Harrison transformation is based [23], or acceleration of the black holes and NUT charge [24]. Such solutions however comprise extremely lengthy mathematical expressions, which restricts the possibilities of deeper analysis of their meaning. We will thus limit ourselves to the magnetised Kerr-Newman black holes (MKN) as outlined in [19] (i.e. generated by the Harrison transformation based on  $\partial/\partial\varphi$  and using real continuous parameter).

Various properties of the MKN class of solutions were studied in detail in the literature. Hiscock [25] prove that Schwarzschild-Melvin solution is the only static case among magnetised black holes. Although the asymptotic behaviour of the solutions produced by

the magnetising Harrison transformation generally resembles the Bonnor-Melvin magnetic universe, Hiscock also found that only Schwarzschild-Melvin solution really approaches it. Indeed, he has shown that for other magnetised black holes the electric field on the axis does not vanish when we go to the spatial infinity. This differs from the behaviour of the magnetic universe, which contains no electric field.

More recently, a complementary issue was described by Gibbons, Mujtaba and Pope [26]. They studied ergoregions in the MKN spacetime and found them to extend to the spatial infinity, except for the case when the parameters of the seed solution and the strength of the external magnetic field are related by  $Q = -BMa$ .

A very challenging issue is how to define global quantities like mass and angular momentum for MKN black holes, and how to formulate the first law of black-hole thermodynamics employing those quantities. Karas and Vokrouhlický [27] made an early attempt in this direction using Komar formulae. However, despite a number of interesting results, their study was only partially successful. Much more complete analysis of the thermodynamics of MKN black holes was delivered by Gibbons, Pang and Pope [28]. A different suggestion was presented in a preprint by Booth *et al.* [29]. They calculated the global quantities for MKN using two methods, the isolated horizon formalism and a modification of Komar formulae that the authors proposed. The two approaches were found to completely agree with each other, but not with the results of [28]. In particular, whereas the expression for the angular momentum in [29] turned out to be the same as the one of [28], the expression for the mass did not. This issue became somewhat controversial, since the results of Booth *et al.* regarding the mass of the MKN black hole had to be excluded from the journal version [30]. However, Astorino *et al.* [31] recently confirmed the disputed results of [29] using yet another method of determining the mass of the MKN black hole. To explain the source of this tension remains an open issue.

A further frequently studied aspect of the interaction of black holes with external magnetic fields is the expulsion of the external field by extremal black holes, the so-called black-hole Meissner effect. The name refers to an analogy with Meissner effect for superconductors, which expel magnetic field when they reach the superconducting state. Let us note that black-hole Meissner effect also manifests itself by vanishing of the magnetic flux across a hemisphere of the horizon. It was first noticed in the test-field

regime with the Kerr black hole [32, 33], where the flux is given by

$$\mathcal{F}_H = B\pi r_+^2 \left( 1 - \frac{a^4}{r_+^4} \right). \quad (1.10)$$

This expression indeed vanishes in the extremal case, in which  $r_+ = M = |a|$ .

The black hole Meissner effect is actually quite general; it takes place for *all* axially symmetric stationary test fields around a rotating black hole [33] and it also arises for extremal charged (non-rotating) black holes even for test (electromagnetic) fields that are in general coupled to gravitational perturbations [34]. There are, however, field configurations which penetrate even the horizons of extremal black holes (see e.g. [33, 35]).

Regarding the strong field regime, Karas and Vokrouhlický [27] correctly identified the uncharged and non-rotating cases of extremal MKN black holes and found out that the Meissner effect does occur in these cases. In the uncharged case, this was also noted in [28]. The black-hole Meissner effect has also recently been studied from very general perspectives, including its relation to mode entanglement [36] and its analysis in the framework of weakly isolated horizons [37] and almost isolated horizons [38].

In recent years, yet another astrophysical motivation to study black-hole charge appeared, when multiple authors realised that charged black holes might be needed to explain the mechanism behind fast radio bursts. For example, Zhang [39] suggested that the burst can be produced due to the rapidly changing magnetic dipole moment during a black-hole merger, in which at least one of the black holes is sufficiently charged. Punsly and Bini [40] proposed another model, in which the burst results from a prompt discharge of a metastable Kerr-Newman black hole formed by gravitational collapse of a suitable neutron star. A numerical study of such a collapse was performed by Nathanail *et al.* [41].

Anyway, regardless of all the intricacies, there always remains the simple fact that elementary particles have incredibly large charge-to-mass ratios. Therefore, even if the charge-to-mass ratio of the black hole in the centre of our Galaxy has been constrained to be smaller than about  $10^{-19}$  [42], this is still non-negligible with respect to electrons, which have charge-to-mass ratio of order  $10^{21}$ .

### 1.3 Penrose process and its generalisations

In the zone between the static limit (1.4) and the event horizon (1.5) of the Kerr black hole, later named ergoregion, all particles are forced to corotate with the black hole. Furthermore, inside the ergoregion, particles can have negative energies with respect to the reference system of a distant observer. Penrose [43] realised that the properties of the ergoregion make it possible to extract rotational energy from the black hole, and proposed mechanisms to do so. In the most interesting one, the so-called Penrose process, a particle coming from far away enters the ergoregion and then disintegrates into two fragments. If one of the fragments has negative energy, the other will have more energy than the original particle. The black hole will thus lose energy, if the boosted fragment escapes.

This was further elucidated by Christodoulou [44], who introduced the framework of reversible and irreversible transformations into black-hole physics. In particular, he has shown that although the mass and angular momentum of the black hole can be reduced through the Penrose process, there also exists an irreducible mass of the black hole which can never decrease. Only the rotational mass-energy can be extracted from vacuum black holes.

Bardeen, Press and Teukolsky looked into Penrose process, among other things, in their seminal paper [45]. They noted that putting one of the fragments into the negative energy state would require a boost of about half the velocity of light during the disintegration of the initial particle. This was corroborated by a more detailed calculation by Wald [46], who derived an inequality constraining the relative velocity of the fragments.

Christodoulou and Ruffini [47] soon extended the framework of reversible and irreversible transformations [44] to the case of charged, rotating black holes. This enabled the Penrose process to be generalised likewise, as demonstrated on the example of Reissner-Nordström black holes (1.6) by Denardo and Ruffini [48]. A more significant step in the electromagnetic generalisation of the Penrose process was taken more than a decade later by Wagh, Dhurandhar and Dadhich [49]. They used the astrophysically motivated setup of a black hole interacting with an external magnetic field (in the test-field regime [10]), and realised that the relative velocity restrictions can be circumvented for charged particles in this setting. (For a detailed review, see [50].)

Another way to tackle the Wald inequality is to consider particle collisions instead of decays [51, 52]. In such a case, the required high relative velocity of the particles after

the interaction can result naturally from high relative velocity of the colliding particles. Therefore, it makes sense to search for possibilities of high-energy collisions. Both of the early studies identified limiting cases, in which the relative Lorentz factor between the colliding particles actually diverges. Piran, Shaham and Katz (PSK) [51] found that this is the case for a collision of an (azimuthally) orbiting particle with an infalling particle, if the point of collision approaches the horizon and the black hole approaches extremality. (Note that for the extremal Kerr black hole, various circular orbits exist all the way down to the horizon radius [45].) Piran and Shaham (PS) [52] further noted that the relative Lorentz factor also diverges for a collision between a radially outgoing and a radially incoming particle, if the collision point is taken to the horizon.

## 1.4 BSW effect and related phenomena

Both the PSK and PS effects mentioned above are not very realistic *per se*, as it is not clear, where an orbiting or an outgoing particle near the horizon could possibly originate from. However, for the PSK effect, this deficiency was later remedied by Bañados, Silk and West (BSW) [53], who discovered a variant of the effect with particles coming from rest at infinity. The key observation is that in the extremal Kerr spacetime, there exist fine-tuned, so-called critical particles, which do not fall into the black hole, yet only asymptotically approach the horizon radius. This type of motion resembles a situation when a particle asymptotically approaches a circular orbit; hence the correspondence between the BSW and PSK near-horizon collisions.

Upon its discovery, the BSW effect was connected to an idea of a black hole acting as a Planck-scale “particle accelerator”, and in this way becoming a probe for certain types of dark matter. However, such a possibility turned out to be unfeasible. First, astrophysical black holes cannot get arbitrarily close to extremality through spin-up [54], and this limits the achievable centre-of-mass energy in particle collisions [55, 56]. Second, even in the case of an extremal black hole, achieving arbitrarily high centre-of-mass collision energy would require arbitrarily long time [56, 57]. (See also Section 3.1 of [58] for further discussion.)

Despite all the practical limitations, the BSW effect (and its generalisations) continued to attract attention, representing both an interesting theoretical issue on its own and a “best-case scenario” of a collisional Penrose process. (The idea of BSW-type processes

serving as a dark matter probe also continued to be updated and observable signatures or lack thereof were estimated, cf. for example [59–61].)

Several authors studied in detail alternatives of the BSW effect for subextremal black holes. For example, Grib and Pavlov [57, 62] considered processes with multiple subsequent collisions. They realised that arbitrarily high centre-of-mass energies are possible even for subextremal black holes, if one considers collisions involving particles confined by the effective potential to an arbitrarily small range of radii close to the horizon. Such particles could be produced by a previous collision of particles coming from rest at infinity. In this way, a multiple-scattering process can overcome the limitations mentioned above.

Various generalisations of the original BSW effect for extremal Kerr black holes were also discussed in the literature. First, Zaslavskii [63] showed that BSW effect is in principle possible for arbitrary rotating black holes, yet in some cases the critical particles might not be able to approach the horizon radius. This was confirmed on the example of extremal black Kerr-Newman black holes [64, 65], for which the BSW effect (with uncharged particles) is possible only when the spin parameter is above a certain threshold value.

Similarly to the Penrose process, an analogy of the BSW effect was found for charged particles in the extremal Reissner-Nordström spacetime [66]. In this version of the effect, critical particles need to have a fine-tuned value of charge instead of angular momentum, and thus they can also move purely radially. Regardless of the differences, Zaslavskii demonstrated that the ubiquity of the BSW effect stems from its kinematic nature related to properties of the spacetime in the vicinity of a horizon [67, 68].

Most of the research of the BSW effect and its generalisations concerns particles moving in the equatorial plane. Nevertheless, Harada and Kimura [69] considered the BSW effect with non-equatorial particles in the extremal Kerr spacetime and they found out that it does not work around poles. These results were further generalised in [65, 70].

As mentioned above, high-energy collisions seem to be a natural workaround of the limitations related to the Wald inequality. However, can they really lead to significant extraction of energy from a black hole via the collisional Penrose process? The stringent early assessment of bounds on energy extracted through BSW collisions, presented in [56], was later identified as too crude in [62]. More detailed analyses were performed using both numerical simulation [71] and analytical calculations [72, 73]. It turned out that energy

extraction through BSW effect in rotating black-hole spacetimes is possible, but limited by unconditional bounds on the energy and mass of the escaping particles. In particular, Harada, Nemoto and Miyamoto [72] claimed the maximum efficiency of the collisional Penrose process in the Kerr spacetime to be 146.6%.

However, these bounds had to be revised, when it turned out that BSW effect is not the actual best-case scenario. As revealed by a numerical study conducted by Schnittman [74], particles that are not precisely critical can get reflected by the effective potential very close to the horizon, and then, while still moving in the vicinity of the horizon, be involved in collisions with other particles. The reversed sign of the radial velocity of the colliding nearly critical particle is advantageous for the energy extraction. Including this Schnittman effect, the maximum efficiency of the collisional Penrose process in the Kerr spacetime is 1392%. Analytical studies of the Schnittman effect [75, 76] however revealed that this value can be reached only when the particle absorbed by the black hole in the process is very massive. It was further demonstrated that even the efficiency bound established by Schnittman can be lifted in principle [77]. However, the process studied in [77] is in fact a more sophisticated version of the PS effect, and thus it is not as relevant for practical purposes [78, 79]. Thus, the efficiency bound of 1392% was confirmed for realistic initial conditions in the Kerr spacetime [78].

Curiously enough, for the charged version of the BSW effect in the extremal Reissner-Nordström spacetime, analytical studies [80, 81] found no unconditional bounds on the energy or mass of the escaping particles at all.

Studies of the Penrose process, together with various effects of high-energy collisions, mostly stay within the test particle approximation, neglecting all influence of backreaction. Due to the considerable difficulty of taking the backreaction into account for point particles, some authors turned to thin gravitating shells, which are easier to describe consistently. In the case of the Reissner-Nordström spacetime, it turned out that a BSW-like collision of charged spherical shells can happen only under a horizon, and thus it does not lead to extraction of energy [82]. Nevertheless, a follow-up work found that a single charged-shell collision in the Reissner-Nordström case can actually extract nearly all the energy permitted by the area law, but in a setting which is not related to the BSW-type effect [83]. Furthermore, results of [82] were extended to rotating three-dimensional (Bañados-Teitelboim-Zanelli) case [84].

However, in contrast with the results for gravitating shells, analyses that either considered particle trajectories with inclusion of some self-force contributions [85], or used model-independent estimates for non-geodesic effects [86], indicate that BSW effect can be possible even when backreaction is taken into account.

# Chapter 2

## Near-horizon description of extremal magnetised stationary black holes and Meissner effect

### 2.1 Outline and summary

As we discussed in the Introduction, inclusion of the black-hole charge is chiefly motivated by the fact that it arises from interaction of black holes with external magnetic fields. In the present chapter (accompanied by Appendices A and B), we would like to underpin this motivation using the concrete example of magnetised Kerr-Newman (MKN) black holes. As mentioned above, we use the designation “MKN” for solutions obtained from Kerr-Newman spacetime through application of the Harrison transformation employing Ernst potentials based on the axial Killing vector and utilising a real continuous parameter (cf. Appendix B).

Our MKN solutions thus form a subclass in the branch  $\text{MKN}(\alpha = 0, \beta = 1)$  of general solutions  $\text{MKN}(\alpha, \beta)$  of [23]; here  $\alpha$  and  $\beta$  are coefficients in the linear combination of the Killing vectors  $\partial/\partial t$  and  $\partial/\partial \varphi$ . They also coincide with the solutions rederived recently by Gibbons, Mujtaba and Pope [26] by the use of the  $\text{SU}(2, 1)$  global symmetry which arises after a Kaluza-Klein reduction of the four-dimensional Einstein-Maxwell theory.

By putting the magnetic charge  $g = 0$  in the branch  $\text{MKN}(\alpha = 0, \beta = 1)$ , one obtains solutions described by García Díaz in [20], which include the “addition” of both electric and magnetic fields. Here we restrict ourselves to pure magnetisation. In this way we

guarantee that the new solutions preserve the “mirror symmetry”, i.e. are invariant under reflections  $\vartheta \rightarrow \pi - \vartheta$ . For the same reason it is necessary to put the magnetic charge  $p = 0$  in the solutions of [26].

The way to generate a MKN solution by the Harrison transformation of the Kerr-Newman metric is summarised in Appendix B. Here it is also demonstrated that the rigidity theorems for dragging and electromagnetic potentials (and some related properties) are preserved by the transformation.

The specific aim of this chapter is to analyse some aspects of interaction of black holes with the external field in the strong-field regime, especially the Meissner effect, by applying the near-horizon limit to extremal cases of the MKN metric and its accompanying electromagnetic field. We use the term near-horizon (limiting) “description” in our work.

The issue of describing the near-horizon geometry of extremal black holes has a long history. Indeed, some indications can already be found in the well-known work by Carter [4], in which metrics enabling a separable wave equation are derived. The Kerr metric (1.1) is the best known example, as we mentioned in 1.1. However, Carter also includes (among different cases labelled by [A], [B(-)], etc.) metrics which, in fact, represent near-horizon geometries. The transition between the cases is discussed formally only, without a physical interpretation.

More recently, near-horizon geometries appeared in the discussion of extremal limits of black holes in grand canonical ensemble [87, 88] (cf. also [89]). In general, multiple procedures involving the near-horizon limit are possible with distinct interpretations related, for example, to the limiting behaviour of the Hawking temperature (see e.g. [90, 91]). In our work, we *start* with extremal MKN black holes with fixed physical parameters and use an arbitrary limiting parameter following the work by Bardeen and Horowitz [92] on the Kerr-Newman spacetime. We, however, start from spacetimes which are not included in Carter’s framework. That the near-horizon limit can be used beyond Kerr-family black holes has also been shown by Dias and Lemos in the case of accelerated black holes [93].

It is known that limiting metrics describing the near-horizon “throat” regions usually have AdS-like asymptotics. This property makes the near-horizon limit interesting in string theory and holographic duality (see [91, 92] and the living review by Compère [94]). The high symmetry of the near-horizon limiting spacetimes has been analysed by Kunduri and Lucietti [95, 96], emphasising that the picture is similar even beyond 4D

general relativity. In Appendix A we will give some explicit calculations that relate the well-known symmetry group  $\text{SO}(1, 2) \times \text{U}(1)$  generated by Killing vectors to the “Carter-type” symmetry studied in [4]. The fact that this kind of symmetry emerges in the near-horizon limit even when it is not present in the original spacetime will be useful to support our conclusions below.

We found that there are some missing terms in the expressions for electromagnetic potential in Carter’s fundamental work [4] (in subcases  $[\text{B}(\pm)]$ ). (This can also be seen by comparison with formulae for the  $B_{\pm}^0$  subcases restricted to  $f = 1$  in [97].) Krasinski noticed the problem when he was editing Carter’s later work [98] for its republication [99] in the “Golden Oldie” series in the GRG journal. However, he did not relate the error to its root in the earlier article [4]. Krasinski, in his editorial note [100], interpreted Carter’s derivation as a de facto near-horizon limit, but he did not find the correct remedy for the error (whereas Bardeen and Horowitz [92] did not discuss the behavior of the electromagnetic potential in the limit). In order to clarify these uncertainties, we rederive the process of the near-horizon limit step by step in Section 2.3. The general scheme was summarised by Compère [94].

The outline of the present chapter is as follows. In Section 2.2 we briefly review some features of black hole solutions in magnetic universes, including the three cases admitting degenerate horizons, going from simpler stationary Ernst solution [18], i.e. magnetised Reissner-Nordström black hole, to the Ernst-Wild solution [19], i.e. magnetised Kerr metric, and the general MKN black holes. We also mention possible gauges and the corresponding regularity of the electromagnetic potential at the axis – which appears to be unnoticed in the literature so far. In Section 2.3, we review the near-horizon geometries of extremal cases, which were previously studied in [101, 102]. (We were able to rearrange some of the expressions presented in 2.3 into simpler and shorter forms using the results of Section 2.4.)

It is known that the near-horizon geometry has four Killing vectors. In Appendix A we use them to construct a Killing tensor which is an element of symmetry related to the separability of the Hamilton-Jacobi (and the wave) equation. Since all the metrics admitting such symmetry were already derived by Carter, we conclude that there has to be some degeneracy and that it has to be possible to express the “new” solutions for near-horizon geometries of magnetised black holes using some simpler metrics with

less parameters. We discuss this point in Section 2.4 going from special cases that are easy to express to the general extremal case of MKN black holes. We find that the near-horizon metric of extremal MKN black holes coincides (up to rescaling of Killing vectors by a constant) with the near-horizon Kerr-Newman metric described using just two independent effective parameters ( $\hat{M}, \hat{a}, \hat{Q}$  minus the constraint of extremality) instead of three ( $B, M, a, Q$  minus the constraint of extremality); the parameter  $B$  characterising the strength of the external magnetic field enters expressions for  $\hat{a}$  and  $\hat{Q}$ . We can further reduce the number of parameters by excluding the physical scale and using dimensionless parameters. Then we end up with a graph of a plane with two parameters,  $BM$  and  $\gamma_{\text{KN}}$ , where  $\gamma_{\text{KN}}$  is the ‘‘Kerr-Newman mixing angle’’:  $a = M \cos \gamma_{\text{KN}}, Q = M \sin \gamma_{\text{KN}}$ . The plane is foliated by curves (classes of equivalence) labeled by just one parameter – the ‘‘effective Kerr-Newman mixing angle’’  $\hat{\gamma}_{\text{KN}}$ . We note that this parameter is related to the invariants like the curvature of the horizon.

We were led by the symmetry arguments given in Appendix A to conclude that the near-horizon description of any extremal MKN black hole is given by the near-horizon description of a corresponding extremal Kerr-Newman solution. However, this conclusion is also implied by the results of Lewandowski and Pawłowski [103], who used the theory of isolated horizons to prove that all the extremal axially symmetric electrovacuum horizons must be the Kerr-Newman ones (for generalisations of this statement in the framework of near-horizon description, see the living review by Kunduri and Lucietti [96]). In Section 2.4.4 we sketch how the approach of [103] can also be used to define the effective parameters.

Curiously enough, our expression for the product  $\hat{a}\hat{M}$  coincides precisely with the angular momentum of a MKN black hole derived from general principles in [28], when we restrict it to extremal cases. Our effective mass, however, does not match the one proposed in [28]. Booth *et al.* [29] recently inquired into (dis)agreements of various procedures of defining the mass of MKN black holes. One can see that our parameter  $\hat{M}$  coincides with ‘‘isolated horizon mass’’  $M_{\text{IH}}$  discussed in [29], when we evaluate it in the extremal case.

In Section 2.4 we also discuss the Meissner effect. The external magnetic field strength parameter  $B$  gets absorbed in the effective Kerr-Newman parameters. Hence, the magnetic flux coming through the degenerate horizon can be expressed without including  $B$ . Such flux is caused just by the physical charge on the black hole and its angular

momentum. The effect of the external magnetic field is just an “implicit” one.

## 2.2 Charged, rotating black holes in magnetic fields

As mentioned in the Introduction, application of the magnetising Harrison transformation (cf. Appendix B) on the Minkowski metric produces the Bonnor-Melvin universe (1.8), which is filled by a magnetic field pointing in the  $z$  direction (1.9). Analogically, the Harrison transformation can be used to generate what Ernst [18] called “black holes in a magnetic universe” from asymptotically flat black-hole models.

### 2.2.1 Stationary Ernst solution

By applying the Harrison transformation to the Reissner-Nordström solution (1.6) with mass  $M$  and charge  $Q$ , one obtains the stationary Ernst metric

$$\mathbf{g} = |\Lambda|^2 \left[ - \left( 1 - \frac{2M}{r} + \frac{Q^2}{r^2} \right) \mathbf{d}t^2 + \frac{1}{1 - \frac{2M}{r} + \frac{Q^2}{r^2}} \mathbf{d}r^2 + r^2 \mathbf{d}\vartheta^2 \right] + \frac{r^2 \sin^2 \vartheta}{|\Lambda|^2} (\mathbf{d}\varphi - \omega \mathbf{d}t)^2 . \quad (2.1)$$

The complex function  $\Lambda$  (cf. (B.18)), which carries the overall effect of the addition of the external magnetic field on the metric, is given by

$$\Lambda = 1 + \frac{1}{4} B^2 (r^2 \sin^2 \vartheta + Q^2 \cos^2 \vartheta) - i B Q \cos \vartheta , \quad (2.2)$$

where  $B$  parametrises the strength of the external field.

It is easy to see that if one superimposes a magnetic field pointing in the  $z$  direction onto the radial electric field of the Reissner-Nordström solution (1.7), the resulting electromagnetic field has a nonzero angular momentum. Such an angular momentum is the reason why the spacetime is not static and the following dragging potential arises:

$$\omega = -\frac{2BQ}{r} + B^3 Q r + \frac{B^3 Q^3}{2r} - \frac{B^3 Q}{2r} (r^2 - 2Mr + Q^2) \sin^2 \vartheta . \quad (2.3)$$

The actual electromagnetic field generated by the Harrison transformation is, however, much more involved than the simple combination we mentioned above. One can get the azimuthal component of the electromagnetic potential by means of the Harrison

transformation (see (B.3))

$$A_\varphi^{(1)} = \frac{1}{B|\Lambda|^2} [2 \operatorname{Re} \Lambda (\operatorname{Re} \Lambda - 1) + (\operatorname{Im} \Lambda)^2] . \quad (2.4)$$

However, the given gauge is not very convenient because  $A_\varphi^{(1)}$  has a nonzero value for  $\vartheta = 0$ . If we shift  $A_\varphi^{(1)}$  by a constant to remedy this problem, we obtain

$$A_\varphi = \frac{1}{B|\Lambda|^2} \left[ \frac{(2 + \frac{3}{2}B^2Q^2) (\operatorname{Re} \Lambda)^2 + (1 - \frac{1}{16}B^4Q^4) (\operatorname{Im} \Lambda)^2}{1 + \frac{3}{2}B^2Q^2 + \frac{1}{16}B^4Q^4} - 2 \operatorname{Re} \Lambda \right] . \quad (2.5)$$

This unique gauge, which corresponds to  $A_\mu$  being smooth on the axis, is important for the study of the particle motion within the Hamiltonian formalism (cf. 3.2), since there the electromagnetic potential becomes a physically relevant quantity. (For other physical arguments constraining the azimuthal component of the potential, see [94].)

Strength of the radial electric field in the locally non-rotating frame (cf. [45] and equations (2.29),(2.30)) is given by

$$F_{(r)(t)} = \frac{1}{|\Lambda|^4} \left\{ [(\operatorname{Re} \Lambda)^2 - (\operatorname{Im} \Lambda)^2] (2 - \operatorname{Re} \Lambda) \frac{Q}{r^2} + \frac{B}{2} \left( 1 - \frac{Q^2}{r^2} \right) \operatorname{Im} \Lambda [(\operatorname{Re} \Lambda)^2 - (\operatorname{Im} \Lambda)^2 - 4 \operatorname{Re} \Lambda] \cos \vartheta \right\} . \quad (2.6)$$

This quantity turns out to be important for the near-horizon limit.

## 2.2.2 Ernst-Wild solution and a general MKN black hole

The Ernst-Wild solution with metric

$$\mathbf{g} = |\Lambda|^2 \Sigma \left[ -\frac{\Delta}{\mathcal{A}} \mathbf{d}t^2 + \frac{\mathbf{d}r^2}{\Delta} + \mathbf{d}\vartheta^2 \right] + \frac{\mathcal{A}}{\Sigma |\Lambda|^2} \sin^2 \vartheta (\mathbf{d}\varphi - \omega \mathbf{d}t)^2 , \quad (2.7)$$

is generated by the Harrison transformation from the Kerr (uncharged) “seed” metric with rotation parameter  $a$  (cf. [19]). Here functions

$$\Sigma = r^2 + a^2 \cos^2 \vartheta , \quad \mathcal{A} = (r^2 + a^2)^2 - \Delta a^2 \sin^2 \vartheta , \quad \Delta = r^2 - 2Mr + a^2 \quad (2.8)$$

take the same form as in the Kerr solution. The complex function  $\Lambda$  reads

$$\Lambda = 1 + \frac{1}{4}B^2 \frac{\mathcal{A}}{\Sigma} \sin^2 \vartheta - \frac{i}{2}B^2 M a \cos \vartheta \left( 3 - \cos^2 \vartheta + \frac{a^2}{\Sigma} \sin^4 \vartheta \right). \quad (2.9)$$

The dragging potential

$$\begin{aligned} \omega = \frac{a}{r^2 + a^2} & \left\{ (1 - B^4 M^2 a^2) - \Delta \left[ \frac{\Sigma}{\mathcal{A}} + \frac{B^4}{16} \left( -8Mr \cos^2 \vartheta (3 - \cos^2 \vartheta) - \right. \right. \right. \\ & - 6Mr \sin^4 \vartheta + \frac{2Ma^2 \sin^6 \vartheta}{\mathcal{A}} [r(r^2 + a^2) + 2Ma^2] + \\ & \left. \left. \left. + \frac{4M^2 a^2 \cos^2 \vartheta}{\mathcal{A}} \left[ (r^2 + a^2) (3 - \cos^2 \vartheta)^2 - 4a^2 \sin^2 \vartheta \right] \right) \right] \right\}, \end{aligned} \quad (2.10)$$

differs from the one for the Kerr metric only by (complicated) contributions proportional to  $B^4$ . Although the components of the field strength tensor become even more involved than in the stationary Ernst case, the azimuthal component of the potential for the Ernst-Wild solution has a very simple form in the gauge implied directly by the Harrison transformation:

$$A_\varphi^{(1)} = \frac{2}{B} \left( 1 - \frac{\text{Re } \Lambda}{|\Lambda|^2} \right). \quad (2.11)$$

After subtracting its value at the axis to obtain a regular expression we have

$$A_\varphi = \frac{2}{B} \left( \frac{1}{1 + B^4 M^2 a^2} - \frac{\text{Re } \Lambda}{|\Lambda|^2} \right). \quad (2.12)$$

For the general MKN (magnetised Kerr-Newman) spacetime, the metric form is the same as for the Ernst-Wild solution (2.7), only with  $\Delta$  replaced by (as in the Kerr-Newman metric)

$$\Delta = r^2 - 2Mr + a^2 + Q^2. \quad (2.13)$$

The function  $\Lambda$  gets even more involved than in the previous case

$$\begin{aligned} \Lambda = 1 + \frac{1}{4}B^2 & \left( \frac{\mathcal{A} + a^2 Q^2 (1 + \cos^2 \vartheta)}{\Sigma} \sin^2 \vartheta + Q^2 \cos^2 \vartheta \right) + \\ & + \frac{BQ}{\Sigma} [ar \sin^2 \vartheta - i(r^2 + a^2) \cos \vartheta] - \\ & - \frac{i}{2}B^2 a \cos \vartheta \left[ M (3 - \cos^2 \vartheta) + \frac{Ma^2 \sin^2 \vartheta - Q^2 r}{\Sigma} \sin^2 \vartheta \right]. \end{aligned} \quad (2.14)$$

A full overview of expressions for  $\omega$  and for the electromagnetic potential in a general MKN spacetime is conveniently presented in [26], in equations (B.8)-(B.9) and (B.15)-(B.18), respectively.

### 2.2.3 Global properties of magnetised black holes

First, let us note that one can easily verify that the positions of the Killing horizons in the coordinate  $r$  are left in place by the Harrison transformation. They are still given by the roots of  $\Delta$ , i.e.  $r_{\pm} = M + \sqrt{M^2 - Q^2 - a^2}$ . The roots coincide for  $M^2 = Q^2 + a^2$ , which defines the extremal case; one can make sure that the surface gravity of the Killing horizon vanishes in this case. These facts were already noted e.g. in [27].

As we explained in the Introduction, the solutions generated by application of the Harrison transformation have pathological, non-flat asymptotic behaviour. Nevertheless, the asymptotic zone can be disregarded, if there at least exists a range of radii, for which the spacetime is approximately flat. As discussed by Bičák and Janiš [33], this is the case for values of  $r$  where  $|A|^2 \doteq 1$ , yet they are sufficiently outside the horizon, i.e. values satisfying

$$r_+ \ll r \ll 1/B . \quad (2.15)$$

This is well visualised by the embedding diagrams constructed in [104]. It is also noted in [33] that inequality (2.15) can be satisfied only when  $|BM| \ll 1$ , whereas for large values of dimensionless quantity  $BM$  the astrophysical relevance of magnetised black hole spacetimes is dubious.

Hiscock [25] noticed that MKN spacetimes contain a conical singularity along the axis of symmetry, which can be removed by modifying the range of the azimuthal coordinate to  $\varphi \in [0, \varphi_{\max})$ . Here  $\varphi_{\max}$  is obtained as follows:

$$\varphi_{\max} = 2\pi \lim_{\vartheta \rightarrow 0} \frac{\sqrt{g_{\vartheta\vartheta}(r, \vartheta)}}{\frac{\partial \sqrt{g_{\varphi\varphi}(r, \vartheta)}}{\partial \vartheta}} . \quad (2.16)$$

In case of a general MKN black hole we get

$$\varphi_{\max} = 2\pi \left[ 1 + \frac{3}{2}B^2Q^2 + 2B^3MQa + B^4 \left( \frac{1}{16}Q^4 + M^2a^2 \right) \right] . \quad (2.17)$$

Alternatively, one can define a new azimuthal coordinate  $\tilde{\varphi}$  with the standard range  $[0, 2\pi)$

by  $\tilde{\varphi} = (2\pi\varphi)/\varphi_{\max}$ . However, we shall follow most of the literature and use  $\varphi$  with (2.17).

## 2.3 The near-horizon description of extremal configurations

Let us now introduce the procedures used to find the near-horizon descriptions of extremal black holes (cf. also [92, 94]) and apply them to black holes in strong magnetic fields. In the case of the MKN black holes we impose the extremality condition  $M^2 = Q^2 + a^2$ .

### 2.3.1 General prescription

#### 2.3.1.1 The metric in the extremal case

The metric of an axisymmetric, stationary, electrovacuum black hole can be written as follows [105]:

$$\mathbf{g} = -N^2 \mathbf{d}t^2 + g_{\varphi\varphi} (\mathbf{d}\varphi - \omega \mathbf{d}t)^2 + g_{rr} \mathbf{d}r^2 + g_{\vartheta\vartheta} \mathbf{d}\vartheta^2 . \quad (2.18)$$

For an extremal black hole the metric can be cast into the form

$$\mathbf{g} = -(r - r_0)^2 \tilde{N}^2 \mathbf{d}t^2 + g_{\varphi\varphi} (\mathbf{d}\varphi - \omega \mathbf{d}t)^2 + \frac{\tilde{g}_{rr}}{(r - r_0)^2} \mathbf{d}r^2 + g_{\vartheta\vartheta} \mathbf{d}\vartheta^2 , \quad (2.19)$$

where the degenerate horizon is located at  $r = r_0$  and  $\tilde{N}$  and  $\tilde{g}_{rr}$  are regular and non-vanishing at the horizon.

To describe the “near-horizon” region, we introduce new time and spatial coordinates  $\tau$  and  $\chi$  by relations

$$r = r_0 + p\chi , \quad t = \frac{\tau}{p} , \quad (2.20)$$

where  $p$  is the limiting parameter. For any finite non-zero value of  $p$  the new coordinates cover the entire spacetime up to “standard” spatial infinity. However, in the extremal black-hole spacetimes, there exists yet another infinity: the proper radial distance between two points along  $t = \text{constant}$  diverges if one of the points approaches  $r_0$ . With parameter  $p$  in transformation (2.20) converging to zero, the metric (2.19) goes over to a new metric which describes the infinite region (“throat”) involving  $r = r_0$ . The standard spatial

infinity is “lost” in this limiting procedure.

A more complicated issue arises in describing the dragging in the near-horizon limit. To do this we first expand  $\omega$  around its value  $\omega_H$  at the horizon

$$\omega \doteq \omega_H + \left. \frac{\partial \omega}{\partial r} \right|_{r_0} (r - r_0) = \omega_H + \left. \frac{\partial \omega}{\partial r} \right|_{r_0} p\chi, \quad (2.21)$$

so that

$$\mathbf{d}\varphi - \omega \mathbf{d}t \doteq \mathbf{d}\varphi - \left( \omega_H + \left. \frac{\partial \omega}{\partial r} \right|_{r_0} p\chi \right) \frac{\mathbf{d}\tau}{p} = \mathbf{d}\varphi - \frac{\omega_H}{p} \mathbf{d}\tau - \left. \frac{\partial \omega}{\partial r} \right|_{r_0} \chi \mathbf{d}\tau. \quad (2.22)$$

Since as a consequence of the rigidity theorem (see Appendix B) the value  $\omega_H$  is constant, the transformation from  $\varphi$  to an “unwinded angle”  $\psi$  can be integrated

$$\varphi = \psi + \frac{\omega_H}{p} \tau. \quad (2.23)$$

With  $p \rightarrow 0$ , we obtain

$$\mathbf{d}\varphi - \omega \mathbf{d}t = \mathbf{d}\psi - \left. \frac{\partial \omega}{\partial r} \right|_{r_0} \chi \mathbf{d}\tau. \quad (2.24)$$

It is thus seen that the  $p \rightarrow 0$  limit replaces  $\omega$  by the linear-order term of its expansion at the horizon.

Following this procedure, we arrive at the near-horizon metric given in Appendix A, equation (A.3). In the specific case of the Kerr-Newman metric (1.1), we get

$$\begin{aligned} \mathbf{g} = & [Q^2 + a^2 (1 + \cos^2 \vartheta)] \left( -\frac{\chi^2}{(Q^2 + 2a^2)^2} \mathbf{d}\tau^2 + \frac{\mathbf{d}\chi^2}{\chi^2} + \mathbf{d}\vartheta^2 \right) + \\ & + \frac{(Q^2 + 2a^2)^2 \sin^2 \vartheta}{Q^2 + a^2 (1 + \cos^2 \vartheta)} \left( \mathbf{d}\psi + \frac{2a\sqrt{Q^2 + a^2}\chi}{(Q^2 + 2a^2)^2} \mathbf{d}\tau \right)^2, \end{aligned} \quad (2.25)$$

(cf. [98] and, in particular, [92], where the equation above with small rearrangements is formula (4.2)).

### 2.3.1.2 The electromagnetic field

As a consequence of the limiting procedure with  $p \rightarrow 0$ , components of some tensorial quantities may become singular, which is the case with the electromagnetic potential. However, the problem can be circumvented as we explain below. Defining the generalised

electrostatic potential by

$$\phi = -A_t - \omega A_\varphi, \quad (2.26)$$

and expanding the electromagnetic potential in  $r - r_0 = p\chi$  using equations (2.20), (2.23), we obtain

$$\begin{aligned} \mathbf{A} &= A_t \mathbf{d}t + A_\varphi \mathbf{d}\varphi \doteq \\ &\doteq \left( A_t|_{r_0} + \frac{\partial A_t}{\partial r} \Big|_{r_0} p\chi \right) \frac{\mathbf{d}\tau}{p} + \left( A_\varphi|_{r_0} + \frac{\partial A_\varphi}{\partial r} \Big|_{r_0} p\chi \right) \left( \mathbf{d}\psi + \frac{\omega_H}{p} \mathbf{d}\tau \right) \doteq \\ &\doteq (A_t|_{r_0} + \omega_H A_\varphi|_{r_0}) \frac{\mathbf{d}\tau}{p} + \left( \frac{\partial A_t}{\partial r} \Big|_{r_0} + \omega_H \frac{\partial A_\varphi}{\partial r} \Big|_{r_0} \right) \chi \mathbf{d}\tau + A_\varphi|_{r_0} \mathbf{d}\psi = \\ &= -\frac{\phi_H}{p} \mathbf{d}\tau + \left( \frac{\partial A_t}{\partial r} \Big|_{r_0} + \omega_H \frac{\partial A_\varphi}{\partial r} \Big|_{r_0} \right) \chi \mathbf{d}\tau + A_\varphi|_{r_0} \mathbf{d}\psi. \end{aligned} \quad (2.27)$$

Since  $\phi_H = \text{constant}$  (see Appendix B), the first term, which blows up, can be subtracted from the final limiting potential by a gauge transformation.

By applying the limiting procedure (including the gauge-fixing) to the electromagnetic potential of the Kerr-Newman solution (1.3), we obtain<sup>1</sup>

$$\mathbf{A} = \frac{Q}{Q^2 + a^2 (1 + \cos^2 \vartheta)} \left( \frac{Q^2 + a^2 \sin^2 \vartheta}{Q^2 + 2a^2} \chi \mathbf{d}\tau + a\sqrt{Q^2 + a^2 \sin^2 \vartheta} \mathbf{d}\psi \right). \quad (2.28)$$

Let us turn back to the general case of axially symmetric, stationary, electrovacuum black hole with metric (2.18) and electromagnetic potential (2.27). Introducing the frame vectors associated with metric (2.18)

$$\mathbf{e}_{(t)} = \frac{1}{N} \left( \frac{\partial}{\partial t} + \omega \frac{\partial}{\partial \varphi} \right), \quad \mathbf{e}_{(\varphi)} = \frac{1}{\sqrt{g_{\varphi\varphi}}} \frac{\partial}{\partial \varphi}, \quad (2.29)$$

$$\mathbf{e}_{(r)} = \frac{1}{\sqrt{g_{rr}}} \frac{\partial}{\partial r}, \quad \mathbf{e}_{(\vartheta)} = \frac{1}{\sqrt{g_{\vartheta\vartheta}}} \frac{\partial}{\partial \vartheta}, \quad (2.30)$$

---

<sup>1</sup>Bardeen and Horowitz [92] do not give the expression for the electromagnetic potential. Carter's potential (see equation (5.64) in the original version in [98]) does not satisfy Maxwell equations as noted in the "Editorial Note" [100]. Unfortunately, the potential given in the republication [99] of [98] is also not correct. The correct form of the potential, though given in an other rearrangement, is contained in equation (39) in [94].

we find that the frame component of the radial electric field strength reads

$$F_{(r)(t)} = \frac{1}{N\sqrt{g_{rr}}} \left( \frac{\partial A_t}{\partial r} + \omega \frac{\partial A_\varphi}{\partial r} \right) . \quad (2.31)$$

We shall note that for MKN black holes, it is possible to calculate this component straight from the relations of the Ernst formalism and of the Harrison transformation (cf. equation (B.26)), without reference to  $A_t$ . Regarding (2.27), the time component of the electromagnetic potential after  $p \rightarrow 0$  can be written as

$$A_\tau = \left( \tilde{N} \sqrt{\tilde{g}_{rr}} F_{(r)(t)} \right) \Big|_{r_0} \chi . \quad (2.32)$$

Now it is important to realise that on a degenerate horizon of any extremal MKN black hole (see Appendix B)

$$\tilde{\omega} \equiv \frac{\partial \omega}{\partial r} \Big|_{r=r_0} = \text{constant} , \quad \tilde{\phi} \equiv \frac{\partial \phi}{\partial r} \Big|_{r=r_0} = \text{constant} . \quad (2.33)$$

Combining equations (2.24), (2.27), (2.33) and realizing that the expression multiplying  $\chi$  in equation (2.32) is just a function of  $\vartheta$ , we see that in the near-horizon limit we can express

$$\omega = \tilde{\omega} \chi , \quad \phi = \tilde{\phi} \chi , \quad A_\tau = \tilde{A}_\tau(\vartheta) \chi . \quad (2.34)$$

Using also (2.26), we can write

$$\phi = -A_\tau - \omega A_\psi , \quad A_\psi(\vartheta) = \frac{1}{\tilde{\omega}} \left( -\tilde{\phi} - \tilde{A}_\tau(\vartheta) \right) , \quad (2.35)$$

where, observing (2.27), we put  $A_\psi = A_\varphi|_{r_0}$ . Since we demand the electromagnetic potential to be smooth, its azimuthal component must vanish at the axis, so

$$\phi = -A_\tau|_{\vartheta=0} , \quad A_\psi(\vartheta) = \frac{1}{\tilde{\omega}} \left( \tilde{A}_\tau(0) - \tilde{A}_\tau(\vartheta) \right) . \quad (2.36)$$

We conclude that we can determine the whole potential of the electromagnetic field in the near-horizon limit solely from the  $F_{(r)(t)}$  component of the electromagnetic field in the original spacetime by relations (2.32) and (2.36).

## 2.3.2 Near-horizon description of extremal black holes in strong magnetic fields

We shall now apply the above procedure to black holes in strong magnetic fields going from the simplest stationary Ernst solution to the MKN black holes.

### 2.3.2.1 Stationary Ernst solution

By taking the near-horizon limit of metric (2.1), we obtain

$$\begin{aligned} \mathbf{g} = & \left[ \left( 1 + \frac{1}{4} B^2 Q^2 \right)^2 + B^2 Q^2 \cos^2 \vartheta \right] \left( -\frac{\chi^2}{Q^2} \mathbf{d}\tau^2 + \frac{Q^2}{\chi^2} \mathbf{d}\chi^2 + Q^2 \mathbf{d}\vartheta^2 \right) + \\ & + \frac{Q^2 \sin^2 \vartheta}{\left( 1 + \frac{1}{4} B^2 Q^2 \right)^2 + B^2 Q^2 \cos^2 \vartheta} \left[ \mathbf{d}\psi - \frac{2B}{Q} \left( 1 + \frac{1}{4} B^2 Q^2 \right) \chi \mathbf{d}\tau \right]^2, \end{aligned} \quad (2.37)$$

which reduces to the well-known Robinson-Bertotti solution (also obtained by putting  $a = 0$  in (2.25)), if we set  $B = 0$ . Using the relations (2.32) and (2.36) with (2.6), we can express the the components of the electromagnetic potential as follows:

$$A_\tau = \frac{\chi}{Q} \frac{\left( 1 + \frac{1}{4} B^2 Q^2 \right)^2 - B^2 Q^2 \cos^2 \vartheta}{\left( 1 + \frac{1}{4} B^2 Q^2 \right)^2 + B^2 Q^2 \cos^2 \vartheta} \left( 1 - \frac{1}{4} B^2 Q^2 \right), \quad (2.38)$$

$$A_\psi = \frac{-BQ^2}{1 + \frac{3}{2} B^2 Q^2 + \frac{1}{16} B^4 Q^4} \frac{\left( 1 - \frac{1}{16} B^4 Q^4 \right) \sin^2 \vartheta}{\left( 1 + \frac{1}{4} B^2 Q^2 \right)^2 + B^2 Q^2 \cos^2 \vartheta}. \quad (2.39)$$

Let us note that this solution is contained in a wider class studied in [101].<sup>2</sup>

---

<sup>2</sup>In [101] generalisations of Reissner-Nordström and Robinson-Bertotti solutions with additional parameters are derived using Harrison transformation. Our expressions (2.37)-(2.39) can be obtained from equations (4.1)-(4.5) in [101], if we choose  $a = 1$ ,  $b = h = k = 0$ ,  $\alpha = 0$ ,  $\beta = 1$ , and rescale the metric by  $M^2$ ; from physical parameters in [101], we need to set  $g = B = 0$ , whereas  $e$  and  $E$  are equal to our  $Q/M$  and  $-BM/2$ ; coordinates  $\tau, q, p$ , and  $\sigma$ , respectively, correspond to our  $\tau/M, \chi/M, \cos \vartheta$ , and  $\psi$ , respectively. At the end of [101], a near horizon limit of “magnetic Reissner-Nordström” solution is shown to imply a “magnetised Robinson-Bertotti solution”.

### 2.3.2.2 Ernst-Wild solution

Application of the near-horizon limiting procedure to metric (2.7) leads to

$$\mathbf{g} = \left[ (1 + B^2 a^2)^2 + (1 - B^2 a^2)^2 \cos^2 \vartheta \right] \left( -\frac{\chi^2}{4a^2} \mathbf{d}\tau^2 + \frac{a^2}{\chi^2} \mathbf{d}\chi^2 + a^2 \mathbf{d}\vartheta^2 \right) + \frac{4a^2 \sin^2 \vartheta}{(1 + B^2 a^2)^2 + (1 - B^2 a^2)^2 \cos^2 \vartheta} \left[ \mathbf{d}\psi + \frac{\chi}{2a^2} (1 - B^4 a^4) \mathbf{d}\tau \right]^2. \quad (2.40)$$

Note the remarkable simplicity of  $\omega$  after the limit; this is because (2.10) contains only contributions proportional to  $B^4$ , and also because the terms multiplied by  $\Delta$  in (2.10) vanish in the limit. To calculate the electromagnetic potential, we again use the relations (2.32) and (2.36), together with  $F_{(r)(t)}$  expressed by (B.26), obtaining

$$A_\tau = -B\chi \left( 1 - \frac{2(1 + B^2 a^2)^2}{(1 + B^2 a^2)^2 + (1 - B^2 a^2)^2 \cos^2 \vartheta} \right), \quad (2.41)$$

$$A_\psi = \frac{1 - B^4 a^4}{1 + B^4 a^4} \frac{2Ba^2 \sin^2 \vartheta}{(1 + B^2 a^2)^2 + (1 - B^2 a^2)^2 \cos^2 \vartheta}. \quad (2.42)$$

### 2.3.2.3 A general MKN black hole

One can note that the marked difference in complexity of expressions between the stationary Ernst solution and the Ernst-Wild solution is not reflected in their near-horizon descriptions, which both turn out to be quite simple. Although the overall structure of the near-horizon metric does not change for a general MKN black hole (cf. also equation (A.4) in Appendix A)

$$\mathbf{g} = \underline{f}(\vartheta) \left( -\frac{\chi^2}{(Q^2 + 2a^2)^2} \mathbf{d}\tau^2 + \frac{\mathbf{d}\chi^2}{\chi^2} + \mathbf{d}\vartheta^2 \right) + \frac{(Q^2 + 2a^2)^2 \sin^2 \vartheta}{\underline{f}(\vartheta)} (\mathbf{d}\psi - \tilde{\omega}\chi \mathbf{d}\tau)^2, \quad (2.43)$$

the quantities entering it become much more complicated than in the previous cases. In particular, the dimensionful structural function  $\underline{f}(\vartheta)$  is obtained as

$$\underline{f}(\vartheta) = \left[ \sqrt{Q^2 + a^2} \left( 1 + \frac{1}{4} B^2 Q^2 + B^2 a^2 \right) + BQa \right]^2 + \left[ a \left( 1 - \frac{3}{4} B^2 Q^2 - B^2 a^2 \right) - BQ\sqrt{Q^2 + a^2} \right]^2 \cos^2 \vartheta, \quad (2.44)$$

whereas the dragging constant  $\tilde{\omega}$  can be evaluated using equation (B.22) in the following form:

$$\tilde{\omega} = -\frac{2}{(Q^2 + 2a^2)^2} \left[ \sqrt{Q^2 + a^2} \left( 1 + \frac{1}{4}B^2Q^2 + B^2a^2 \right) + \right. \\ \left. + BQa \right] \left[ a \left( 1 - \frac{3}{4}B^2Q^2 - B^2a^2 \right) - BQ\sqrt{Q^2 + a^2} \right]. \quad (2.45)$$

From relations (B.26) and (2.32) for the  $F_{(r)(t)}$  component we obtain:

$$A_r = \frac{1}{f(\vartheta)} \frac{\chi}{Q^2 + 2a^2} \left[ Q \left( 1 - \frac{1}{4}B^2Q^2 \right) + 2Ba\sqrt{Q^2 + a^2} \right] \left\{ \left[ Q \left( 1 - \frac{1}{4}B^2Q^2 \right) + \right. \right. \\ \left. \left. + 2Ba\sqrt{Q^2 + a^2} \right]^2 + \left[ a \left( 1 - \frac{3}{4}B^2Q^2 - B^2a^2 \right) - BQ\sqrt{Q^2 + a^2} \right]^2 \sin^2 \vartheta \right\}, \quad (2.46)$$

$$A_\psi = -\frac{\tilde{\omega}}{2f(\vartheta)} \frac{(Q^2 + 2a^2)^2 \left[ Q \left( 1 - \frac{1}{4}B^2Q^2 \right) + 2Ba\sqrt{Q^2 + a^2} \right] \sin^2 \vartheta}{1 + \frac{3}{2}B^2Q^2 + 2B^3Qa\sqrt{Q^2 + a^2} + B^4 \left( \frac{1}{16}Q^4 + Q^2a^2 + a^4 \right)}. \quad (2.47)$$

## 2.4 Near-horizon degeneracy of extremal cases of MKN solutions

### 2.4.1 Special cases

Let us start interpreting the results reviewed in the previous section by investigating important special cases. First, one can see that the near-horizon geometry of the Ernst-Wild solution (2.40) becomes static for  $Ba = 1$ , as the dragging parameter  $\tilde{\omega} = 0$ . Structural function  $f(\vartheta)$  turns to a constant,

$$f(\vartheta)|_{Ba=1} \equiv \left[ (1 + B^2a^2)^2 + (1 - B^2a^2)^2 \cos^2 \vartheta \right] \Big|_{Ba=1} = 4, \quad (2.48)$$

which results in a much simpler form of the metric. With some reshuffling of constants, it can be written as

$$\mathbf{g} = -\frac{\chi^2}{(2a)^2} (2 \mathbf{d}\tau)^2 + \frac{(2a)^2}{\chi^2} \mathbf{d}\chi^2 + (2a)^2 \mathbf{d}\vartheta^2 + (2a)^2 \sin^2 \vartheta \left( \frac{\mathbf{d}\psi}{2} \right)^2. \quad (2.49)$$

It is noteworthy that the magnetic field vanishes for  $Ba = 1$ , as the electromagnetic potential (given by (2.38) and (2.39)) reduces to the one of a constant electric field

$$\mathbf{A} = \frac{\chi}{2a} (2 \mathbf{d}\tau). \quad (2.50)$$

This special case is thus the Robinson-Bertotti solution with an electric field parameter  $2a$ , written in terms of rescaled temporal and azimuthal coordinate. (Note that the rescaled  $\psi/2 \in [0, 2\pi)$ , since the original  $\varphi \in [0, 4\pi)$  according to (2.17).)

One can also see that for  $Ba = -1$ , the outcome is the same as above, only with  $A_\mu$  exchanged by  $-A_\mu$ .

It can be readily shown that the geometry of the horizon (more precisely the embedding of its crosssection for  $t = \text{constant}$  or  $\tau = \text{constant}$ ) is the same for both the original spacetime and its near-horizon limit. Therefore, we see from the near-horizon metric (2.49) that the original Ernst-Wild solution with  $a = M, Ba = 1$  has a spherically symmetric horizon.

The general near-horizon metric (A.4) for the MKN solutions has a very simple form involving just one function  $f(\vartheta)$  and two constants  $K$  and  $\tilde{\omega}$ . Two still simpler cases are possible, in which one of the constants is either zero or directly related to the other. The Robinson-Bertotti solution with  $\tilde{\omega} = 0$  (and with  $f \equiv 1$ ) corresponds to the former possibility, whereas the latter arises for the near-horizon geometry of an extremal Kerr solution, in which  $\tilde{\omega} = -1/K^2$  (the minus sign means rotation in the sense of positive  $\psi$ ) and  $2f(\vartheta) = 1 + \cos^2 \vartheta$ . Expressing this case in the form (A.4), we get

$$\mathbf{g} = \frac{1 + \cos^2 \vartheta}{2} \left( -\frac{\chi^2}{2a^2} \mathbf{d}\tau^2 + \frac{2a^2}{\chi^2} \mathbf{d}\chi^2 + 2a^2 \mathbf{d}\vartheta^2 \right) + \frac{2a^2}{\frac{1}{2}(1 + \cos^2 \vartheta)} \sin^2 \vartheta \left( \mathbf{d}\psi + \frac{\chi}{2a^2} \mathbf{d}\tau \right)^2. \quad (2.51)$$

Remarkably, we arrive at the same metric starting from the special case of a stationary Ernst solution. Regarding (2.38) and (2.39), one easily sees that the potential vanishes if

we choose parameters  $B$  and  $Q$  such that  $BQ = 2$ . Function  $f(\vartheta)$  simplifies to

$$f(\vartheta)|_{BQ=2} = \left[ \left( 1 + \frac{1}{4} B^2 Q^2 \right)^2 + B^2 Q^2 \cos^2 \vartheta \right] \Big|_{BQ=2} = 4 (1 + \cos^2 \vartheta) , \quad (2.52)$$

and metric (2.37), after rearrangements, becomes

$$\begin{aligned} \mathbf{g} = & \frac{1 + \cos^2 \vartheta}{2} \left[ -\frac{\chi^2}{2(2Q)^2} (8 \mathbf{d}\tau)^2 + \frac{2(2Q)^2}{\chi^2} \mathbf{d}\chi^2 + 2(2Q)^2 \mathbf{d}\vartheta^2 \right] + \\ & + \frac{2(2Q)^2 \sin^2 \vartheta}{\frac{1}{2}(1 + \cos^2 \vartheta)} \left[ \frac{\mathbf{d}\psi}{8} + \frac{\chi}{2(2Q)^2} (8 \mathbf{d}\tau) \right]^2 . \end{aligned} \quad (2.53)$$

Hence, the near-horizon geometry for the stationary Ernst solution with  $BQ = 2$  goes over to the Kerr near-horizon form (2.51) with rotation parameter  $2Q$ . Notice that the relation  $\tilde{\omega} = -1/K^2$  appears only in appropriately rescaled coordinates; here again  $\psi/8 \in [0, 2\pi)$  similarly to (2.49).

In Section 2.4.3 we shall see that even a general MKN class admits special combinations of parameters  $Q, a, B$  for which either the dragging parameter  $\tilde{\omega}$  or electromagnetic potential vanish in the near-horizon limit. However, already from the simple examples above, we conclude that “bare” parameters  $Q, a, B$  do not describe properly physical properties of MKN black holes in the near-horizon limit. Since we do not observe any magnetic field in the near-horizon description in the special cases, we can be led to an idea that external axially symmetric stationary magnetic fields are expelled from degenerate horizons.

## 2.4.2 Effective parameters

It is known that near-horizon geometries exhibit high symmetry related to existence of four Killing vectors (cf. e.g. [94]). In Appendix A we show explicitly that it is possible to construct a “Carter-type” Killing tensor from these Killing vectors. Hence, the near-horizon spacetimes have to belong to the class of spacetimes studied by Carter [4, 98], even in the case when the original spacetime is outside this class. Therefore, it is natural to assume that the metrics (2.25) and (2.43) representing near-horizon limits of extremal Kerr-Newman and MKN black holes are equivalent in mathematical sense. It should be possible to describe the near-horizon limit of extremal black holes in magnetic fields char-

acterised by three parameters ( $M, a, Q, B$  minus the constraint of extremality) by just two effective ‘‘Kerr-Newman-like’’ parameters ( $\hat{M}, \hat{a}, \hat{Q}$  minus the constraint of extremality). However, metrics (2.25) and (2.43) cannot be compared directly, since their Killing vectors are scaled in a different way, as we observed in special cases already.

Now we shall rescale the coordinates in general MKN cases. It is convenient to redefine  $\varphi_{\max}$  in (2.17) by introducing  $\Xi = 2\pi/\varphi_{\max}$ , so that  $\psi \in [0, 2\pi/\Xi)$ . In the extremal case

$$\Xi = \frac{1}{1 + \frac{3}{2}B^2Q^2 + 2B^3Qa\sqrt{Q^2 + a^2} + B^4\left(\frac{1}{16}Q^4 + Q^2a^2 + a^4\right)}. \quad (2.54)$$

Next, by rearranging the constants in metric (2.43) in analogy with (2.49) and (2.53) we obtain

$$\mathbf{g} = \underline{f}(\vartheta) \left[ -\frac{\Xi^2\chi^2}{K^4} \left( \frac{\mathbf{d}\tau}{\Xi} \right)^2 + \frac{\mathbf{d}\chi^2}{\chi^2} + \mathbf{d}\vartheta^2 \right] + \frac{K^4 \sin^2 \vartheta}{\Xi^2 \underline{f}(\vartheta)} \left[ (\Xi \mathbf{d}\psi) - \Xi^2 \tilde{\omega} \chi \frac{\mathbf{d}\tau}{\Xi} \right]^2, \quad (2.55)$$

where ‘‘new’’ azimuthal coordinate  $\Xi\psi \in [0, 2\pi)$  and, correspondingly, the ‘‘new’’ time coordinate becomes  $\tau/\Xi$ . Similarly, for the electromagnetic potential we get

$$\mathbf{A} = \Xi A_\tau \frac{\mathbf{d}\tau}{\Xi} + \frac{A_\psi}{\Xi} (\Xi \mathbf{d}\psi). \quad (2.56)$$

Since the rescaling leaves function  $\underline{f}(\vartheta)$  in (2.44) unchanged, we can use it to establish the correspondence between the solutions. For the near-horizon geometry (2.25) of the Kerr-Newman black hole we have  $\underline{f}(\vartheta) = [Q^2 + a^2(1 + \cos^2 \vartheta)] = M^2 + a^2 \cos^2 \vartheta$ . If we express  $\underline{f}(\vartheta)$  for the near-horizon description in the same form (as we did in (2.44)), i.e.

$$\underline{f}(\vartheta) = \hat{M}^2 + \hat{a}^2 \cos^2 \vartheta, \quad (2.57)$$

we can obtain the effective parameters  $\hat{M}$  and  $\hat{a}$  as follows:

$$\hat{M} = \sqrt{Q^2 + a^2} \left( 1 + \frac{1}{4}B^2Q^2 + B^2a^2 \right) + BQa, \quad (2.58)$$

$$\hat{a} = a \left( 1 - \frac{3}{4}B^2Q^2 - B^2a^2 \right) - BQ\sqrt{Q^2 + a^2}. \quad (2.59)$$

In analogy with the extremal Kerr-Newman solution, we define the effective charge by

$\hat{Q}^2 = \hat{M}^2 - \hat{a}^2$ , which implies

$$\hat{Q} = Q \left( 1 - \frac{1}{4} B^2 Q^2 \right) + 2Ba\sqrt{Q^2 + a^2} . \quad (2.60)$$

It will be seen that  $\hat{Q}$  is a physical charge.

To demonstrate that the near-horizon descriptions of MKN black holes and of corresponding Kerr-Newman black holes are indeed equivalent, we need to prove that the limiting MKN metric (2.43) with coordinates rescaled according to the formula (2.55) equals to metric (2.25) with  $Q$  and  $a$  replaced by expressions for  $\hat{Q}, \hat{a}$  (2.60) and (2.59). Similarly, for the electromagnetic potential we need to compare (2.46) and (2.47) with appropriately rescaled coordinates (cf. (2.56)) with the two components of (2.28) with  $Q, a$  substituted by  $\hat{Q}, \hat{a}$ . When calculating (2.43), (2.46) and (2.47) from definition, such a comparison requires lengthy algebraic manipulations that are better done with assistance of a symbolic computation software. Nevertheless, once the equivalence is proven, we can express the near-horizon description of the extremal MKN solution in the simplest form, where the result is evident.

Regarding the expressions (2.58)-(2.60) for the effective parameters, it is of interest to notice that each of them contains the “bare” parameter multiplied by a “correction” involving  $B^2$  and an additional term linear in  $B$ . The extra term in the rotation parameter (2.59) is caused by the angular momentum of the electromagnetic field as can be seen from putting the bare rotation parameter  $a = 0$ . The extra term in charge (2.60) corresponds to the “Wald charge” in the weak-field limit (cf. [10]).

The effective parameters simplify considerably if one of the bare parameters  $Q$  or  $a$  is zero – they involve just one term. This is reflected in the fact that the near-horizon descriptions of the stationary Ernst solution (2.37) and of the Ernst-Wild solution (2.40) are much simpler than of a general MKN solution. For  $B = 0$ , the effective parameters are equal to the bare parameters. It is also worthwhile to notice that when one solves the equation  $\hat{M} = 0$  with respect to  $B$ , one finds that it has no real roots, so  $\hat{M}$  cannot be negative.

Concerning the effective charge, it can be shown that it is the physical charge integrated over the horizon. Indeed, Karas and Vokrouhlický [27] discuss various integral

quantities for a MKN black hole, including its physical charge

$$Q_{\text{H}} = \frac{1}{4\pi} \int_0^\pi \int_0^{\varphi_{\text{max}}} \star F_{\vartheta\varphi} d\varphi d\vartheta . \quad (2.61)$$

Using their formula (9) and evaluating the Ernst potentials (cf. Appendix B) for a *general* MKN black hole we obtain

$$Q_{\text{H}} = Q \left( 1 - \frac{1}{4} B^2 Q^2 \right) + 2BMa , \quad (2.62)$$

where  $M \geq \sqrt{Q^2 + a^2}$  (cf. also [26]). In the extremal case,  $M = \sqrt{Q^2 + a^2}$ , and it is seen explicitly from (2.60) that  $\hat{Q} = Q_{\text{H}}$ .

It is remarkable that when we define the angular momentum of extremal MKN black holes by  $\hat{J} = \hat{a}\hat{M}$ , i.e. in analogy with the standard case without magnetic field, we find that the result coincides precisely with the thermodynamic angular momentum given by Gibbons, Pang and Pope [28] in formula (5.11), when it is restricted to the extremal case. We already know that, in properly rescaled coordinates, the near-horizon limit of any extremal MKN black hole can be described just by effective parameters  $\hat{Q}, \hat{a}$ . We can substitute for  $\hat{a}$  using  $\hat{Q}, \hat{J}$  as follows:

$$\hat{a} = \frac{\text{sgn } \hat{J}}{\sqrt{2}} \sqrt{\sqrt{\hat{Q}^4 + 4\hat{J}^2} - \hat{Q}^2} . \quad (2.63)$$

Since  $\hat{Q}$  is a physical charge of the black hole and  $\hat{J}$  is derived in [28] as a meaningful angular momentum, we can conclude that the near-horizon limit of any extremal MKN black hole can be described by thermodynamic charges of the black hole.

However, a puzzle remains: whereas our “near-horizon mass”  $\hat{M} = \sqrt{\hat{Q}^2 + \hat{a}^2}$ , the thermodynamic mass evaluated in [28] by means of Kaluza-Klein reduction is found to be  $M/\varepsilon$  (with  $\varepsilon$  given by (2.54) in the external case) and, therefore, is a distinct parameter. The problem of (dis)agreements among different notions of mass in the MKN spacetimes has been recently discussed by Booth *et al.* [29]. By a closer inspection of their results, one can make sure that our  $\hat{M}$  coincides with the “isolated horizon mass”  $M_{\text{IH}}$  defined in [29], when we restrict it to the extremal case<sup>3</sup>.

---

<sup>3</sup>In [29] the authors claim that their  $M_{\text{IH}}$  is equal to the Komar mass of the MKN horizon. The Komar integrals for the MKN black holes were discussed also in [27] long time ago. The results disagree. This is

### 2.4.3 Dimensionless parameters

As a consequence of the extremality condition, one of three (bare) parameters  $M, a, Q$  is not independent.<sup>4</sup> Instead of choosing two of these as independent parameters, it is more convenient to introduce the ‘‘Kerr-Newman mixing angle’’  $\gamma_{\text{KN}}$  by relations

$$a = M \cos \gamma_{\text{KN}} , \quad Q = M \sin \gamma_{\text{KN}} . \quad (2.64)$$

Here  $\gamma_{\text{KN}}$  can be taken from the interval  $[-\pi/2, \pi/2]$ , if we restrict the rotation parameter to  $a > 0$ . Since the mass is just a scale, it is ignorable. As another dimensionless parameter we consider  $BM$ . These two parameters,  $\gamma_{\text{KN}}$  and  $BM$ , represent dimensionless quantities that define the parameter space. We now proceed to analyse its structure.

In Section 2.4.1 we considered a special case of the near-horizon description of Ernst-Wild solution for which the dragging parameter  $\tilde{\omega} = 0$ . During our proof of the equivalence of the near-horizon descriptions of a general extremal MKN black hole and the corresponding Kerr-Newman black hole (see the text below (2.60)) we found  $\tilde{\omega} \sim \hat{M}\hat{a}$ . From this it is evident that the case with  $\tilde{\omega} = 0$  within general extremal MKN black holes can be obtained just by putting  $\hat{a} = 0$  in (2.59). We find two branches of the solution with respect to  $B$  as follows:

$$B = \frac{-2Q\sqrt{Q^2 + a^2} \pm 2(Q^2 + 2a^2)}{a(3Q^2 + 4a^2)} . \quad (2.65)$$

From equation (2.57) it follows immediately that these two subclasses have the near-horizon geometry of the Robinson-Bertotti spacetime. Moreover, equations (2.46) and (2.47) indeed imply that  $A_\psi = 0$  and the component  $A_\tau$  yields constant electric field. In our dimensionless parameters the solutions (2.65) read

$$BM = \frac{-2 \sin \gamma_{\text{KN}} \pm 2(1 + \cos^2 \gamma_{\text{KN}})}{3 \cos \gamma_{\text{KN}} + \cos^3 \gamma_{\text{KN}}} . \quad (2.66)$$

Let us remark that in [27] Komar angular momentum for an extremal MKN black hole is evaluated; using our notation we see that it vanishes for  $\tilde{\omega} = 0$ . Our result (2.65) coincides with (12) in [27]. However, therein the results were derived differently – formula (2.65)

---

apparently caused by the fact that [29] uses different, more sophisticated forms of the Komar expressions.

<sup>4</sup>The same holds for the corresponding effective parameters.

was obtained by requiring the vanishing magnetic flux across an “upper hemisphere” of a horizon. We shall return to this Meissner-type effect below.

Let us turn to another special subclass of the MKN solutions. Since both components of the electromagnetic potential, (2.46) and (2.47), for the MKN solutions in the near-horizon limit are proportional to the parameter  $\hat{Q}$  given in (2.60), we can make them vanish by putting  $\hat{Q} = 0$ . This condition implies

$$B = \frac{4a\sqrt{Q^2 + a^2} \mp 2(Q^2 + 2a^2)}{Q^3} . \quad (2.67)$$

(The  $\mp$  sign corresponds to  $\tilde{\omega} = \mp 1/\varepsilon K^2$ .) In terms of dimensionless parameters we get

$$BM = \frac{4 \cos \gamma_{\text{KN}} \mp 2(1 + \cos^2 \gamma_{\text{KN}})}{\sin^3 \gamma_{\text{KN}}} . \quad (2.68)$$

Notice that in this case  $\hat{Q} = 0$  implies the physical charge (2.62) also vanishes. In fact, as demonstrated in [27], the physical charge  $Q_{\text{H}} = 0$  even for a non-extremal MKN black hole if  $B = 2Q^{-3} \left( 2Ma \pm \sqrt{4M^2 a^2 + Q^4} \right)$ . In the extremal case, this implies our result (2.67).

Regarding the parametrisation (2.64), we can view the special subclasses as curves in the parameter space of  $\gamma_{\text{KN}}$  and  $BM$  given by formulae (2.66) and (2.68) respectively. Moreover, we know that using the effective parameters  $\hat{M}, \hat{a}, \hat{Q}$  (see (2.58)-(2.60)) the near-horizon description of *any* extremal MKN black hole can be expressed as near-horizon description of the corresponding extremal Kerr-Newman solution (see the text below (2.60)). Therefore the entire parameter space can be foliated by curves which represent equivalent near-horizon geometries. This is illustrated in Figure 2.1. Four of such curves, representing special subclasses ( $\hat{a} = 0$  and  $\hat{Q} = 0$ ) analysed above, are given by four special values of dimensionless parameter  $\hat{\gamma}_{\text{KN}}$  introduced in analogy with (2.64) by

$$\hat{Q} = \hat{M} \sin \hat{\gamma}_{\text{KN}} . \quad (2.69)$$

Substituting for  $\hat{Q}$  and  $\hat{M}$  from (2.60) and (2.58) and using the previous relation to express  $B$  we obtain

$$B = \frac{4a\sqrt{Q^2 + a^2} - 2Qa \sin \hat{\gamma}_{\text{KN}} \mp 2(Q^2 + 2a^2) \cos \hat{\gamma}_{\text{KN}}}{Q^3 + (Q^2 + 4a^2) \sqrt{Q^2 + a^2} \sin \hat{\gamma}_{\text{KN}}} . \quad (2.70)$$

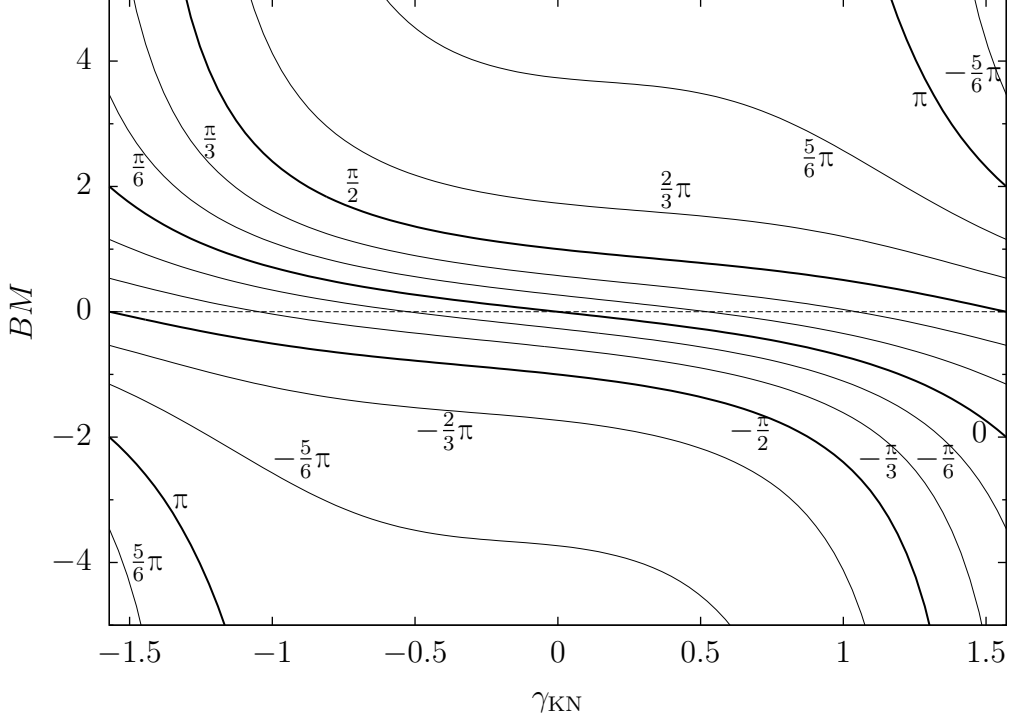


Figure 2.1: Near-horizon geometries of extremal MKN black holes illustrated in the dimensionless parameter space  $(\gamma_{\text{KN}}, BM)$ . Each curve describes geometries with fixed parameter  $\hat{\gamma}_{\text{KN}}$ , i.e. with fixed ratios  $\hat{Q}/\hat{M}$  and  $\hat{a}/\hat{M}$  (see equation (2.69)). Various regions in the plane correspond to different signs of parameters  $\hat{a}$ ,  $\hat{Q}$ , respectively. The boundaries between the regions are indicated by thick lines.

Equivalently, in terms of dimensionless  $\gamma_{\text{KN}}$  and  $BM$ ,

$$BM = \frac{4 \cos \gamma_{\text{KN}} - \sin 2\gamma_{\text{KN}} \sin \hat{\gamma}_{\text{KN}} \mp 2(1 + \cos^2 \gamma_{\text{KN}}) \cos \hat{\gamma}_{\text{KN}}}{\sin^3 \gamma_{\text{KN}} + (1 + 3 \cos^2 \gamma_{\text{KN}}) \sin \hat{\gamma}_{\text{KN}}}. \quad (2.71)$$

The  $\mp$  sign is not necessary if we extend the interval for  $\hat{\gamma}_{\text{KN}}$  to  $(-\pi, \pi]$ . Then the minus sign in front of the term with  $\cos \hat{\gamma}_{\text{KN}}$  guarantees that  $\hat{\gamma}_{\text{KN}} = 0$  implies  $\hat{a} = \hat{M}$ .

We can find an alternative form of equation (2.69) using the relation between  $\hat{a}$  and  $\hat{M}$ , i.e.  $\hat{a} = \hat{M} \cos \hat{\gamma}_{\text{KN}}$ . Then we obtain

$$B = \frac{-2Q\sqrt{Q^2 + a^2} - 2Qa \cos \hat{\gamma}_{\text{KN}} \pm 2(Q^2 + 2a^2) \sin \hat{\gamma}_{\text{KN}}}{a(3Q^2 + 4a^2) + (Q^2 + 4a^2)\sqrt{Q^2 + a^2} \cos \hat{\gamma}_{\text{KN}}}, \quad (2.72)$$

or

$$BM = \frac{-2 \sin \gamma_{\text{KN}} - \sin 2\gamma_{\text{KN}} \cos \hat{\gamma}_{\text{KN}} \pm 2(1 + \cos^2 \gamma_{\text{KN}}) \sin \hat{\gamma}_{\text{KN}}}{3 \cos \gamma_{\text{KN}} + \cos^3 \gamma_{\text{KN}} + (1 + 3 \cos^2 \gamma_{\text{KN}}) \cos \hat{\gamma}_{\text{KN}}}. \quad (2.73)$$

Karas and Vokrouhlický [27] found that in the two special cases with special relations among parameters  $B, Q, a$  given by expressions (2.65) and (2.67) the magnetic flux van-

ishes corresponding to the black hole Meissner effect discovered in the test-field limit. In these cases our results employing the near-horizon description support the conclusion given in [27], since the magnetic field is encoded in the component  $A_\psi$  of the electromagnetic potential, which is proportional to the product  $\hat{Q}\hat{a}$ . The two cases (2.65) and (2.67) correspond to  $\hat{a} = 0$  and  $\hat{Q} = 0$ , respectively. Hence  $A_\psi = 0$  and magnetic field necessarily vanishes.

For a general extremal MKN black hole the magnetic flux through the upper hemisphere of the horizon does not vanish. It can be expressed as follows:

$$\mathcal{F}_H = 2\pi \frac{A_\psi|_{\vartheta=\frac{\pi}{2}}}{\Xi} = 2\pi \frac{\hat{Q}\hat{a}}{\hat{M}} = \frac{4\pi\hat{Q}\hat{J}}{\hat{Q}^2 + \sqrt{\hat{Q}^4 + 4\hat{J}^2}} . \quad (2.74)$$

Since the structure of the azimuthal component of the electromagnetic potential in the near-horizon limit is identical (up to the rescaling) to the one of the Kerr-Newman black hole, the flux can be expressed using the Kerr-Newman-like effective parameters. As stated above, these parameters can be related to the thermodynamic charges of the black hole as derived in [28]. Therefore, we may conclude that the magnetic flux is intrinsic to the black hole configuration and there is no flux caused directly by the external magnetic field.

#### 2.4.4 Remark on invariants and uniqueness theorems

As we have seen, due to the ambiguity of the scaling of the Killing vectors in the MKN spacetime, we have to choose a particular rescaling in order to see that the near-horizon limit is given by a corresponding Kerr-Newman solution with effective parameters given above. However, invariants are unaffected by coordinate transformations of “*ignorable*” coordinates and, therefore, they can be in principle used to determine the effective parameters. For example, consider the invariant  $R_{2D} = 2/\rho_1\rho_2$ , where  $\rho_1, \rho_2$  are curvature radii of the (axially symmetric) degenerate horizon, given by the two-dimensional Ricci scalar

$$R_{2D} = \frac{2}{g_{\vartheta\vartheta}} \left[ \frac{g_{\vartheta\vartheta,\vartheta}g_{\varphi\varphi,\vartheta}}{4g_{\vartheta\vartheta}g_{\varphi\varphi}} - \frac{g_{\varphi\varphi,\vartheta\vartheta}}{2g_{\varphi\varphi}} + \frac{(g_{\varphi\varphi,\vartheta})^2}{4(g_{\varphi\varphi})^2} \right] \Bigg|_{r_0} . \quad (2.75)$$

In the near-horizon limit the angular metric functions have no spatial dependence, so

$$R_{2D} = \frac{2}{g_{\vartheta\vartheta}} \left[ \frac{g_{\vartheta\vartheta,\vartheta} g_{\psi\psi,\vartheta}}{4g_{\vartheta\vartheta} g_{\psi\psi}} - \frac{g_{\psi\psi,\vartheta\vartheta}}{2g_{\psi\psi}} + \frac{(g_{\psi\psi,\vartheta})^2}{4(g_{\psi\psi})^2} \right]. \quad (2.76)$$

It is explicitly seen that altering  $g_{\psi\psi}$  by a multiplicative factor (due to the linear rescaling of the coordinate  $\psi$ ) does not change the result.

For Kerr-Newman solution the invariant turns out to be

$$\frac{2}{R_{2D}} = \frac{[Q^2 + a^2 (1 + \cos^2 \vartheta)]^3}{(Q^2 + 2a^2) [Q^2 + a^2 (1 - 3 \cos^2 \vartheta)]}, \quad (2.77)$$

and hence for a MKN solution the form will be the same with  $\hat{Q}, \hat{a}$  in place of  $Q, a$ .

Although these expressions are not uniquely invertible, they show that there exists a connection between the effective parameters and the curvature invariants.

We used symmetry arguments stated in Appendix A to support the idea that the near-horizon geometry of any extremal MKN black hole can be described using near-horizon geometry of a corresponding Kerr-Newman solution. We should, however, note that Lewandowski and Pawłowski [103] conducted a sophisticated discussion of electrovacuum extremal horizons including uniqueness theorem from which the mentioned statement arises as a special case.<sup>5</sup> Namely they solved the constraint equations for all axially symmetrical extremal isolated horizons equipped with axially symmetrical electromagnetic field invariant with respect to the null flow (i.e. the field that is also in equilibrium). Having set the magnetic charge to zero they found out that their family of solutions has just two parameters, one of which is the area of the horizon and the other encodes the electric charge (they did not separate out the physical scale as we did in our subcase with the definition of  $\hat{\gamma}_{\text{KN}}$ ). Since there exists a Kerr-Newman extremal horizon for each pair of values of their parameters, Lewandowski and Pawłowski conclude that there are no other extremal isolated electrovacuum horizons than the Kerr-Newman ones (see also discussion of similar results including non-zero cosmological constant in the framework of near-horizon geometries given in [96]).

The area of the horizon  $\mathcal{S}_H$  used in [103] to parametrise their solutions is an integral invariant. Unlike the example of a differential invariant that we examined above, it can

---

<sup>5</sup>Indeed, in the recent preprint, [29] Booth *et al.*, led by the considerations in [103], give our formulae (2.58) and (2.59). Note that in [29] the effective parameters are defined by a formula analogous to our equation (2.57), rather than in the way suggested here in Section 2.4.4.

be used to give an alternative definition of the effective parameters, as we would like to sketch here. The area of the horizon of any MKN black hole is

$$\mathcal{S}_H = 4\pi \frac{r_+^2 + a^2}{\Xi}. \quad (2.78)$$

Therefore the magnetic field influences it just via factor  $\Xi$ , which assures the smoothness of the axis. In the extremal case  $r_+^2 + a^2 = Q^2 + 2a^2$  and  $\Xi$  is given by (2.54). From the fact that the area of the horizon of an extremal MKN black hole must be characterised by Kerr-Newman effective parameters, it follows the relation

$$\frac{Q^2 + 2a^2}{\Xi} = \hat{Q}^2 + 2\hat{a}^2, \quad (2.79)$$

which is also obtained when we directly compare the MKN near-horizon metric in the form (2.55) with the Kerr-Newman near-horizon metric in the form (A.4) with effective parameters plugged in. If we assume that the effective charge is the physical charge enclosed in the horizon  $\hat{Q} = Q_H$ , we can use formula (2.79) as a defining relation for  $\hat{a}$ . Finally, we can define  $\hat{M} = \sqrt{\hat{Q}^2 + \hat{a}^2}$ .

# Chapter 3

## Particle collisions in the equatorial plane: kinematic restrictions

### 3.1 Outline

In the Introduction, we have discussed that there exist two variants of the generalised BSW effect. One of them, let us call it “centrifugal”, requires particles with fine-tuned values of angular momentum orbiting around arbitrary rotating extremal black holes [53, 63]. The other, electrostatic variant requires particles with fine-tuned values of charge in maximally charged Reissner-Nordström spacetime. These two versions of the generalised BSW effect have so far been studied only separately. In the present chapter (accompanied by Appendix C), we unify the two variants and examine kinematic restrictions for the generalised BSW effect including effects of *both* dragging and electrostatic interaction. We base our study on the general metric form, which can include black holes with different types of (matter) fields, sometimes called “dirty” black holes, or black holes in spacetimes which are not asymptotically flat.

The generalised BSW effect always constitutes a “corner case” of the test-particle kinematics, and considering the setup with both charge and dragging requires a further increased rigour. Moreover, the notation and methods vary significantly among different authors. Thus, to be able to give a unified picture, in Section 3.2 we thoroughly go through methods of qualitative study of electrogeodesic motion, building up on classical works of Wilkins [6] and Bardeen [107]. Some further details are given in Appendix C.1.1.

In Section 3.3 we review how to take a horizon limit of the centre-of-mass collision

energy and the way to show that there are particles with distinct type of motion in a near-horizon zone, so-called critical particles, and that these particles cause the BSW singularity in the centre-of-mass collision energy. We present formulae for different types of collisions.

Section 3.4 contains the main results. We prove that the critical particles can approach the position of the horizon only if it is degenerate and their parameters satisfy certain restrictions. We discuss how these restrictions depend on the properties of the black hole and identify two cases corresponding to the original centrifugal and electrostatic mechanisms of the generalised BSW effect. Two other “mixed” cases are also seen to be possible.

In Section 3.5 we illustrate these results with the example of the extremal Kerr-Newman solution<sup>1</sup>, where just one of the mixed cases applies. Apart from the general restrictions on particles at *any* energy, we study what happens for the critical particles that are coming from rest at infinity or are bounded. We notice that, for a very small charge of the black hole, this kind of particle can reach the position of the degenerate horizon even with enormous values of angular momentum (and specific charge). Such a “mega-BSW” effect is possible neither in the vacuum case nor in the case with a large charge of the black hole.

## 3.2 Electrogeodesic motion in black-hole spacetimes

Let us consider an axially symmetric, stationary spacetime with the metric

$$\mathbf{g} = -N^2 dt^2 + g_{\varphi\varphi} (\mathbf{d}\varphi - \omega dt)^2 + g_{rr} dr^2 + g_{\vartheta\vartheta} d\vartheta^2, \quad (3.1)$$

which will serve as a model of an electrovacuum black hole. (The cosmological constant can also be included. For conditions on matter fields compatible with (3.1), see e.g. [105] and references therein.)

We assume the choice of coordinate  $r$  such that hypersurface  $r = r_+$  is the black-hole horizon, where  $N^2$  vanishes. If the black-hole horizon is degenerate (which will be denoted

---

<sup>1</sup>As discussed in Chapter 2, the near-horizon geometries of extremal magnetised Kerr-Newman black holes are equivalent to the ones of extremal Kerr-Newman black holes without the external field [106]. Therefore, it is justified to use the extremal Kerr-Newman solution as a surrogate for extremal black holes in strong magnetic fields with regard to processes near the horizon.

by  $r_0$ ), the following factorisation of (3.1) is useful (cf. (2.19)):

$$\mathbf{g} = -(r - r_0)^2 \tilde{N}^2 \mathbf{d}t^2 + g_{\varphi\varphi} (\mathbf{d}\varphi - \omega \mathbf{d}t)^2 + \frac{\tilde{g}_{rr}}{(r - r_0)^2} \mathbf{d}r^2 + g_{\vartheta\vartheta} \mathbf{d}\vartheta^2, \quad (3.2)$$

where  $\tilde{N}^2$  and  $\tilde{g}_{rr}$  are non-vanishing and finite at  $r = r_0$ .

Let us further require that the electromagnetic field accompanying (3.1) has the same symmetry as the metric, exhibited by the following choice of gauge:

$$\mathbf{A} = A_t \mathbf{d}t + A_\varphi \mathbf{d}\varphi = -\phi \mathbf{d}t + A_\varphi (\mathbf{d}\varphi - \omega \mathbf{d}t). \quad (3.3)$$

Here  $\phi = -A_t - \omega A_\varphi$  is called the generalised electrostatic potential. Recalling the locally non-rotating frame (cf. (2.29), (2.30) and [45]) associated with (3.1),

$$\mathbf{e}_{(t)} = \frac{1}{N} \left( \frac{\partial}{\partial t} + \omega \frac{\partial}{\partial \varphi} \right), \quad \mathbf{e}_{(\varphi)} = \frac{1}{\sqrt{g_{\varphi\varphi}}} \frac{\partial}{\partial \varphi}, \quad (3.4)$$

$$\mathbf{e}_{(r)} = \frac{1}{\sqrt{g_{rr}}} \frac{\partial}{\partial r}, \quad \mathbf{e}_{(\vartheta)} = \frac{1}{\sqrt{g_{\vartheta\vartheta}}} \frac{\partial}{\partial \vartheta}, \quad (3.5)$$

we see that  $\phi$  is proportional to  $A_{(t)}$ . Let us also consider an energy of a test particle locally measured in this frame given by  $\varepsilon_{\text{LNRF}} \equiv u^{(t)}$ .

Equations of motion for test particles (with rest mass  $m$  and charge  $q = \tilde{q}m$ ) influenced solely by the Lorentz force, i.e. of electrogeodesic motion, take the form

$$\frac{Dp^\alpha}{d\tau} \equiv m \frac{Du^\alpha}{d\tau} = q F^\alpha{}_\beta u^\beta. \quad (3.6)$$

They can be derived from the Lagrangian

$$\mathcal{L} = \frac{1}{2} m g_{\rho\sigma} u^\rho u^\sigma + q A_\rho u^\rho. \quad (3.7)$$

The corresponding canonical momentum is

$$\Pi_\mu = \frac{\partial \mathcal{L}}{\partial u^\mu} = p_\mu + q A_\mu. \quad (3.8)$$

Its projections on  $\partial/\partial t$ ,  $\partial/\partial \varphi$ , the two Killing vectors of (3.1), are conserved during the electrogeodesic motion. They can be interpreted as (minus) energy  $E$  and axial angular

momentum  $L_z$ . In our coordinates they read

$$-\Pi_t = -p_t - qA_t = E = \varepsilon m , \quad \Pi_\varphi = p_\varphi + qA_\varphi = L_z = lm . \quad (3.9)$$

Dividing by the mass  $m$  of the particle, we can get expressions for two contravariant components of the velocity,

$$u^t = \frac{\varepsilon - \omega l - \tilde{q}\phi}{N^2} , \quad u^\varphi = \frac{\omega}{N^2} (\varepsilon - \omega l - \tilde{q}\phi) + \frac{l - \tilde{q}A_\varphi}{g_{\varphi\varphi}} . \quad (3.10)$$

Assuming further that metric (3.1) is invariant under reflections  $\vartheta \rightarrow \pi - \vartheta$ , i.e. under “mirror symmetry” with respect to the equatorial “plane”, we can consider motion confined to this hypersurface (with conserved conditions  $\vartheta = \pi/2, u^\vartheta = 0$ ). The remaining component of the velocity then follows from its normalisation,

$$u^r = \pm \sqrt{\frac{1}{N^2 g_{rr}} \left[ (\varepsilon - \omega l - \tilde{q}\phi)^2 - N^2 \left( 1 + \frac{(l - \tilde{q}A_\varphi)^2}{g_{\varphi\varphi}} \right) \right]} . \quad (3.11)$$

Hence, we have a full set of the first-order equations of motion for an equatorial electrogeodesic test particle. (See [108] for references.)

There are some qualitative features of the motion that follow directly from the equations above. The motion of particles with some parameters may be forbidden in certain ranges of  $r$ . The first restriction comes from the conventional requirement (positivity of the locally measured energy  $\varepsilon_{\text{LNRF}}$ ) for motion “forward” in coordinate time  $t$ , which applies for  $r > r_+$  (or  $N^2 > 0$ ). From  $u^t$  in (3.10) we infer

$$\mathcal{X} \equiv \varepsilon - \omega l - \tilde{q}\phi > 0 . \quad (3.12)$$

(Later, we also consider the possibility  $\mathcal{X} \rightarrow 0$  for  $N \rightarrow 0$ .)

Another restriction is due to the square root in (3.11). If we assume that the metric determinant for (3.1), which is given by

$$\sqrt{-g} = N \sqrt{g_{rr} g_{\varphi\varphi} g_{\vartheta\vartheta}} , \quad (3.13)$$

is non-degenerate, the expression  $N^2 g_{rr}$  under the square root in (3.11) is non-vanishing

and positive. Therefore, the square root will be defined in real numbers if

$$W \equiv (\varepsilon - \omega l - \tilde{q}\phi)^2 - N^2 \left( 1 + \frac{(l - \tilde{q}A_\varphi)^2}{g_{\varphi\varphi}} \right) \geq 0. \quad (3.14)$$

Zeros of function  $W$  with respect to radius are turning points (because of that,  $W$  is often called effective potential). Stationary and inflection points of  $W$  with respect to  $r$  are used to find circular orbits and marginally stable circular orbits [45, 109] (see also C.1.1). However,  $W$  is not unique; for example, if we multiply it with a positive integer power of  $r$ , the results will be the same. This led to different conventions in literature [45, 109]. Nevertheless, we can define another effective potential which will be unique and also have other advantages.

First, for  $r \geq r_+$ , we can factorise  $W$  as

$$W = (\varepsilon - V_+) (\varepsilon - V_-), \quad (3.15)$$

where<sup>2</sup>

$$V_\pm = \omega l + \tilde{q}\phi \pm N \sqrt{1 + \frac{(l - \tilde{q}A_\varphi)^2}{g_{\varphi\varphi}}}. \quad (3.16)$$

Since  $V_+ \geq V_-$ , the condition  $W \geq 0$  is fulfilled whenever  $\varepsilon \geq V_+$  or  $\varepsilon \leq V_-$ . Considering  $l = 0, \tilde{q} = 0$  and comparing with (3.12), we can identify  $\varepsilon \leq V_-$  as the domain of unphysical particles moving “backwards in time”. (Conversely, we see that restriction  $\varepsilon \geq V_+$  is stronger than (3.12), so it ensures motion “forward in time”, and manifests (3.12) to be preserved during motion.)

Therefore, we can define  $V \equiv V_+$  and use  $\varepsilon \geq V$  as a condition for the motion to be allowed (in the  $r \geq r_+$ , or  $N^2 \geq 0$ , domain). In this sense,  $V$  is the best analogy of a classical effective potential. It is also called a “minimum energy” [107]. The ranges of radii where  $\varepsilon < V$  are referred to as “forbidden bands”, whereas the ones with  $\varepsilon > V$  are called “allowed bands”. Condition  $\varepsilon = V$  implies  $W = 0$  and thus corresponds to a turning point. For the convenience of the reader, in C.1.1 we derive relations between the derivatives of  $W$  and  $V$ .

---

<sup>2</sup>Note that we assume  $g_{\varphi\varphi} > 0$ , i.e. the absence of closed timelike curves.

### 3.3 Collision energy and critical particles

Let us consider two colliding (charged) particles in an arbitrary spacetime. The natural generalisation of the centre-of-mass frame from special relativity is a tetrad, where the total momentum of the colliding particles at the instant of collision has just the time component

$$(E_{\text{CM}}, 0, 0, 0) = m_1 \mathbf{u}_{(1)} + m_2 \mathbf{u}_{(2)} . \quad (3.17)$$

This tetrad component can be interpreted as the centre-of-mass collision energy. To get rid of the frame, we can take square of the above expression and define an invariant related to this quantity (cf. [57], for example)

$$\frac{E_{\text{CM}}^2}{2m_1 m_2} = \frac{m_1}{2m_2} + \frac{m_2}{2m_1} - g_{\mu\nu} u_{(1)}^\mu u_{(2)}^\nu . \quad (3.18)$$

Let us now investigate how this invariant behaves for collisions of electrogeodesic particles in black-hole spacetimes. Using the metric coefficients of (3.1), the expressions for components of particles' velocities given by first-order equations of equatorial electrogeodesic motion (3.10) and (3.11), and the definition (3.12) of “forwardness”  $\mathcal{X}$ , we obtain

$$\begin{aligned} \frac{E_{\text{CM}}^2}{2m_1 m_2} &= \frac{m_1}{2m_2} + \frac{m_2}{2m_1} - \frac{(l_1 - \tilde{q}_1 A_\varphi)(l_2 - \tilde{q}_2 A_\varphi)}{g_{\varphi\varphi}} + \frac{\mathcal{X}_1 \mathcal{X}_2}{N^2} \mp \\ &\mp \frac{1}{N^2} \sqrt{\mathcal{X}_1^2 - N^2 \left[ 1 + \frac{(l_1 - \tilde{q}_1 A_\varphi)^2}{g_{\varphi\varphi}} \right]} \sqrt{\mathcal{X}_2^2 - N^2 \left[ 1 + \frac{(l_2 - \tilde{q}_2 A_\varphi)^2}{g_{\varphi\varphi}} \right]} . \end{aligned} \quad (3.19)$$

The  $\mp$  sign before the last term corresponds to particles moving in the same or the opposite direction in  $r$ .

Now, let us consider the limit  $N \rightarrow 0$ . We need to Taylor expand the square roots  $\sqrt{W}$  coming from the radial components of the particles' velocities. For each of the colliding particles, there are two very different cases depending on the value  $\mathcal{X}_{\text{H}}$  of  $\mathcal{X}$  on the horizon. For a generic particle ( $\mathcal{X}_{\text{H}} > 0$ ), the expansion looks as follows:

$$\sqrt{W} \doteq \mathcal{X} - \frac{N^2}{2\mathcal{X}} \left[ 1 + \frac{(l - \tilde{q} A_\varphi)^2}{g_{\varphi\varphi}} \right] + \dots \quad (3.20)$$

If we consider two generic particles moving in the same direction (upper sign in (3.19)),

this behaviour leads to the cancellation of the terms that are singular in the limit  $N \rightarrow 0$ , and a finite limit arises,<sup>3</sup>

$$\begin{aligned} \frac{E_{\text{CM}}^2}{2m_1m_2} \Big|_{N=0} &= \frac{m_1}{2m_2} + \frac{m_2}{2m_1} - \frac{(l_1 - \tilde{q}_1 A_\varphi)(l_2 - \tilde{q}_2 A_\varphi)}{g_{\varphi\varphi}} \Big|_{N=0} + \\ &+ \frac{1}{2} \left[ 1 + \frac{(l_2 - \tilde{q}_2 A_\varphi)^2}{g_{\varphi\varphi}} \right] \Big|_{N=0} \frac{\mathcal{X}_1^{\text{H}}}{\mathcal{X}_2^{\text{H}}} + \frac{1}{2} \left[ 1 + \frac{(l_1 - \tilde{q}_1 A_\varphi)^2}{g_{\varphi\varphi}} \right] \Big|_{N=0} \frac{\mathcal{X}_2^{\text{H}}}{\mathcal{X}_1^{\text{H}}}. \end{aligned} \quad (3.21)$$

The presence of  $\mathcal{X}_{\text{H}}$  for both particles in the denominators suggests that for the so-called “critical particles” with  $\mathcal{X}_{\text{H}} = 0$  (so far excluded, see (3.12)) the limit may not be finite.

To verify this, let us first expand “forwardness”  $\mathcal{X}$  of a critical particle around  $r_+$ ,

$$\mathcal{X} \doteq - \left( \frac{\partial\omega}{\partial r} l + \tilde{q} \frac{\partial\phi}{\partial r} \right) \Big|_{r=r_+, \vartheta=\frac{\pi}{2}} (r - r_+) + \dots \quad (3.22)$$

Thus, for a critical particle,  $\mathcal{X}^2$  is proportional to  $(r - r_+)^2$  (with higher-order corrections). However, for a subextremal black hole, we expect  $N^2$  to be proportional just to  $r - r_+$ , so the positive term under the square root in  $\sqrt{W}$  will go to zero faster than the negative one. We thus anticipate that the motion of critical particles towards the horizon is forbidden for subextremal black holes. We return to these kinematic restrictions below.

In case of an extremal black hole (3.2) with  $N^2 = (r - r_0)^2 \tilde{N}^2$ , we get an expansion for  $\sqrt{W}$  of a critical particle very different from (3.20),

$$\sqrt{W} \Big|_{\mathcal{X}_{\text{H}}=0} \doteq (r - r_0) \sqrt{\left( \frac{\partial\omega}{\partial r} l + \tilde{q} \frac{\partial\phi}{\partial r} \right)^2 - \tilde{N}^2 \left[ 1 + \frac{(l - \tilde{q} A_\varphi)^2}{g_{\varphi\varphi}} \right]} \Big|_{r=r_0, \vartheta=\frac{\pi}{2}} + \dots \quad (3.23)$$

Now, if we again consider particles moving in the same direction, but assume that particle 1 is critical, whereas particle 2 is generic (usually referred to as “usual” in literature), we

---

<sup>3</sup>The case of the particles going in opposite directions, i.e. plus sign in (3.19), leads to the so-called Piran-Shaham effect (cf. the Introduction).

get the following leading-order behaviour in the limit  $r \rightarrow r_0$  (or  $N \rightarrow 0$ )

$$\begin{aligned} \frac{E_{\text{CM}}^2}{2m_1m_2} \approx & -\frac{\mathcal{X}_2^{\text{H}}}{r-r_0} \left\{ \frac{1}{\tilde{N}^2} \left[ \frac{\partial\omega}{\partial r} l_1 + \tilde{q}_1 \frac{\partial\phi}{\partial r} + \right. \right. \\ & \left. \left. + \sqrt{\left( \frac{\partial\omega}{\partial r} l_1 + \tilde{q}_1 \frac{\partial\phi}{\partial r} \right)^2 - \tilde{N}^2 \left[ 1 + \frac{(l_1 - \tilde{q}_1 A_\varphi)^2}{g_{\varphi\varphi}} \right]} \right] \right\} \Big|_{r=r_0, \vartheta=\frac{\pi}{2}}. \end{aligned} \quad (3.24)$$

The expression diverges like  $(r-r_0)^{-1}$ , so we confirmed that the different behaviour of  $\sqrt{W}$  for critical particles leads to singularity in the centre-of-mass collision energy invariant.

Since the divergent contribution is proportional to  $\mathcal{X}_H$  of the usual particle, we see that for a collision of two critical particles the limit is again finite, namely

$$\begin{aligned} \frac{E_{\text{CM}}^2}{2m_1m_2} \Big|_{N=0} = & \frac{m_1}{2m_2} + \frac{m_2}{2m_1} - \frac{(l_1 - \tilde{q}_1 A_\varphi)(l_2 - \tilde{q}_2 A_\varphi)}{g_{\varphi\varphi}} \Big|_{r=r_0, \vartheta=\frac{\pi}{2}} + \\ & + \left\{ \frac{1}{\tilde{N}^2} \left[ \left( \frac{\partial\omega}{\partial r} l_1 + \tilde{q}_1 \frac{\partial\phi}{\partial r} \right) \left( \frac{\partial\omega}{\partial r} l_2 + \tilde{q}_2 \frac{\partial\phi}{\partial r} \right) \mp \sqrt{\frac{1}{2} \frac{\partial^2 W_{(1)}}{\partial r^2}} \sqrt{\frac{1}{2} \frac{\partial^2 W_{(2)}}{\partial r^2}} \right] \right\} \Big|_{r=r_0, \vartheta=\frac{\pi}{2}}, \end{aligned} \quad (3.25)$$

where we observed

$$\frac{\partial^2 W}{\partial r^2} \Big|_{r=r_0, \mathcal{X}_H=0} = 2 \left\{ \left( \frac{\partial\omega}{\partial r} l + \tilde{q} \frac{\partial\phi}{\partial r} \right)^2 - \tilde{N}^2 \left[ 1 + \frac{(l - \tilde{q} A_\varphi)^2}{g_{\varphi\varphi}} \right] \right\} \Big|_{r=r_0, \vartheta=\frac{\pi}{2}}. \quad (3.26)$$

### 3.4 Kinematics of critical particles

We have seen that particles with zero forwardness  $\mathcal{X}$  at the horizon, i.e. critical particles, constitute a distinct kind of motion with a different behaviour of the radial velocity, leading to the singularity in the collision energy. The condition  $\mathcal{X}_H = 0$  can be formulated as a requirement for the particle's energy to have a critical value

$$\varepsilon_{\text{cr}} = l\omega_H + \tilde{q}\phi_H = V|_{r_+}, \quad (3.27)$$

which coincides with the value of effective potential (3.16) at the radius of the horizon. Thus if the minimum energy  $V$  grows for  $r > r_+$ , the motion of critical particles towards  $r_+$  is forbidden, since their energy will be lower than that allowed for  $r > r_+$ . On the other hand, if the effective potential decreases, the motion of critical particles towards  $r_+$  will be allowed. Thus, we have to look at the sign of the radial derivative of  $V$  to discriminate between the cases. For the geodesic ( $\tilde{q} = 0$ ) case, the discussion has already been carried out by Zaslavskii [63], who utilised rather mathematical considerations contained in [110].

### 3.4.1 Derivative of the effective potential

Taking the derivative of the effective potential (3.16), we obtain four terms

$$\frac{\partial V}{\partial r} = \frac{\partial \omega}{\partial r} l + \tilde{q} \frac{\partial \phi}{\partial r} + \frac{\partial N}{\partial r} \sqrt{1 + \frac{(l - \tilde{q} A_\varphi)^2}{g_{\varphi\varphi}}} + N \frac{\partial}{\partial r} \left( \sqrt{1 + \frac{(l - \tilde{q} A_\varphi)^2}{g_{\varphi\varphi}}} \right). \quad (3.28)$$

The fourth term is proportional to  $N$ , so we do not consider it in the limit  $N \rightarrow 0$ . The third term can be modified to the following form:

$$\lim_{N \rightarrow 0} \frac{\partial V}{\partial r} = \lim_{N \rightarrow 0} \left[ \frac{\partial \omega}{\partial r} l + \tilde{q} \frac{\partial \phi}{\partial r} + \frac{\partial(N^2)}{\partial r} \sqrt{1 + \frac{(l - \tilde{q} A_\varphi)^2}{g_{\varphi\varphi}}} \right] \Bigg|_{\vartheta = \frac{\pi}{2}}. \quad (3.29)$$

In subextremal cases the radial derivative of  $N^2$  is nonzero for  $N \rightarrow 0$ , i.e. the third term blows up in the limit that we wish to take. This term is manifestly positive in the near-horizon regime, so its domination means that no critical particles can approach  $r_+$  for subextremal black holes. Zaslavskii's result [63] is thus generalised to the  $\tilde{q} \neq 0$  case.

On the other hand, in the extremal case the radial derivative of  $N^2$  vanishes in the limit  $N \rightarrow 0$ . Using again the decomposition (3.2),  $N^2 = (r - r_0)^2 \tilde{N}^2$ , we get (for  $r \geq r_0$ )  $\partial N / \partial r = \tilde{N} + (r - r_0) \partial \tilde{N} / \partial r$ . This enables us to take the  $r \rightarrow r_0$  limit of the third term and to drop the contribution proportional to  $r - r_0$ ; thus,

$$\frac{\partial V}{\partial r} \Bigg|_{r=r_0} = \left( \frac{\partial \omega}{\partial r} l + \tilde{q} \frac{\partial \phi}{\partial r} + \tilde{N} \sqrt{1 + \frac{(l - \tilde{q} A_\varphi)^2}{g_{\varphi\varphi}}} \right) \Bigg|_{r=r_0, \vartheta = \frac{\pi}{2}}. \quad (3.30)$$

This final expression is indeed finite. However, it depends heavily on the parameters  $l, \tilde{q}$  of the particle as well on the properties of the black-hole model in question. Thus

(as already noted by Zaslavskii in [63] for the  $\tilde{q} = 0$  case) kinematic restrictions on the motion of critical particles towards  $r_0$  cannot be worked out in a model-independent way. However, one can qualitatively study the dependence of the kinematic restrictions on the features of a general model and then use these considerations to get quantitative results for particular models. This is our main aim in what follows.

### 3.4.2 Remarks on motion towards $r_0$

Before we analyse when the motion of critical particles towards  $r_0$  is allowed and when it is not, let us first elucidate some features that this motion has if it is allowed. First, let us note that, comparing the behaviour of  $\mathcal{X}$  (3.22) and  $N^2 = (r - r_0)^2 \tilde{N}^2$ , we see that  $u^t \rightarrow \infty$  with  $r \rightarrow r_0$  even for critical particles. For usual particles the locally measured energy  $\varepsilon_{\text{LNRF}}$  also blows up. However, the  $r \rightarrow r_0, r \geq r_0$  limit of  $\varepsilon_{\text{LNRF}}$  for the critical particles is finite, namely,

$$\varepsilon_{\text{LNRF}} \equiv u^{(t)} \doteq - \frac{\frac{\partial \omega}{\partial r} l + \tilde{q} \frac{\partial \phi}{\partial r}}{\tilde{N}} \Big|_{r=r_0, \vartheta=\frac{\pi}{2}} + \dots \quad (3.31)$$

This important distinction seems to have been noticed only lately [111] (for the  $\tilde{q} = 0$  case), although note it can be deduced from earlier calculations presented in [68]. There it is shown that critical particles have, unlike usual ones, a non-divergent redshift factor with respect to the stationary tetrad in the horizon limit. Therefore, although the BSW-type effects are often advertised as particle acceleration, they are in fact caused by “slowness” of the critical particles.

Let us illustrate this in yet another way. We have already noticed that  $\varepsilon = V$  at  $r_0$  for critical particles, which implies  $W = 0$ . Furthermore, it follows easily from (3.23) (or (C.1)) that

$$\frac{\partial W}{\partial r} \Big|_{r=r_0, \mathcal{X}_{\text{H}}=0} = 0 . \quad (3.32)$$

Concurrence of these conditions would seem to suggest that there is a circular orbit at  $r_0$  for parameters of each critical particle. However, there exist doubts about the properties of orbits in the  $r = r_0$  region (cf. [45, 112]). Regardless of these doubts, let us select an arbitrary radius  $r_{\text{orb}} \geq r_+$ , and see what it implies if we assume that  $W$  and its first

derivative are zero there. Expanding (3.11) around  $r_{\text{orb}}$  (for  $r \geq r_{\text{orb}}$ ), we get

$$u^r \equiv \frac{dr}{d\tau} \doteq \pm (r - r_{\text{orb}}) \sqrt{\left. \frac{1}{2\tilde{N}^2 \tilde{g}_{rr}} \frac{\partial^2 W}{\partial r^2} \right|_{r=r_{\text{orb}}}} + \dots \quad (3.33)$$

This equation has an asymptotic solution of the form

$$r \doteq r_{\text{orb}} \left[ 1 + \exp\left(\pm \frac{\tau}{\tau_{\text{relax}}}\right) \right] + \dots \quad \frac{1}{\tau_{\text{relax}}} = \sqrt{\left. \frac{1}{2\tilde{N}^2 \tilde{g}_{rr}} \frac{\partial^2 W}{\partial r^2} \right|_{r=r_{\text{orb}}}}, \quad (3.34)$$

which is valid for early proper times for outgoing particles (plus sign) and for late ones for incoming particles (minus sign). We can apply the result to critical particles by choosing the minus sign and  $r_{\text{orb}} = r_0$ . The result that critical particles only asymptotically approach the radius of the degenerate horizon and do not reach it in a finite proper time has already been derived in a slightly different way in various cases, see e.g. [62, 63]. Above, we have shown that it applies to the  $\tilde{q} \neq 0, \omega \neq 0$  case as well.

Let us yet mention that it follows from (3.23) (or (C.3)) that

$$\left. \frac{\partial^2 W}{\partial r^2} \right|_{r=r_0, \mathcal{L}_{\text{H}}=0} = 2 \left( \left. \frac{\partial V_+}{\partial r} \frac{\partial V_-}{\partial r} \right) \right|_{r=r_0}. \quad (3.35)$$

This interconnection between derivatives of  $W$  and  $V_{\pm}$  of different orders appears rather unusual regarding the general form of (C.3).

### 3.4.3 The hyperbola

As we have seen above, whether the motion of critical particles towards  $r_0$  is forbidden or not depends on whether the radial derivative of  $V$  at  $r = r_0$  is positive or not. To study the division between the critical particles that can approach  $r_0$  and those that cannot, we thus consider the condition

$$\left. \frac{\partial V}{\partial r} \right|_{r=r_0} = 0 \quad (3.36)$$

as a function of parameters  $\tilde{q}$  and  $l$  of the (critical) test particles. Regarding (3.30), one sees that it actually corresponds to a branch of a hyperbola in variables  $\tilde{q}$  and  $l$ . To study

its properties, we remove the square root in (3.30) and thus recover the second branch

$$\left[ \frac{\left( \frac{\partial \omega}{\partial r} l + \tilde{q} \frac{\partial \phi}{\partial r} \right)^2}{\tilde{N}^2} - \frac{(l - \tilde{q} A_\varphi)^2}{g_{\varphi\varphi}} \right] \Big|_{r=r_0, \vartheta=\frac{\pi}{2}} = 1 . \quad (3.37)$$

This equation corresponds in fact to

$$\frac{\partial^2 W}{\partial r^2} \Big|_{\mathcal{X}_H=0, r=r_0} = 0 . \quad (3.38)$$

Regarding (3.35) (cf. also the calculations leading to (3.30)), we find that the second branch corresponds to similar division for non-physical particles moving backwards in time.

We already observed that conditions (3.32) and  $W = 0$  always hold for critical particles at  $r_0$ : thus, the simultaneous validity of (3.38) signifies the usual requirement for a marginally stable circular orbit, often called innermost stable circular orbit (ISCO). Then, from (3.35) we see that the condition (3.36) also implies the ISCO in this sense (restricting to particles moving forward in time it is in fact equivalent to the requirement for ISCO).

The curve described by equation (3.37) is indeed a hyperbola, except for the case when the two squared expressions become proportional to each other. This would happen if

$$\left( \frac{\partial \phi}{\partial r} + \frac{\partial \omega}{\partial r} A_\varphi \right) \Big|_{r=r_0, \vartheta=\frac{\pi}{2}} = 0 . \quad (3.39)$$

Calculating the derivative of the generalised electrostatic potential (2.26),

$$\frac{\partial \phi}{\partial r} = -\frac{\partial A_t}{\partial r} - \omega \frac{\partial A_\varphi}{\partial r} - \frac{\partial \omega}{\partial r} A_\varphi , \quad (3.40)$$

and recalling the expression (2.31) for the radial electric field strength in the locally non-rotating frame (3.4), (3.5), which reads

$$F_{(r)(t)} = \frac{1}{N\sqrt{g_{rr}}} \left( \frac{\partial A_t}{\partial r} + \omega \frac{\partial A_\varphi}{\partial r} \right) , \quad (3.41)$$

we can write

$$\frac{\partial\phi}{\partial r} = -N\sqrt{g_{rr}}F_{(r)(t)} - \frac{\partial\omega}{\partial r}A_\varphi = -\tilde{N}\sqrt{\tilde{g}_{rr}}F_{(r)(t)} - \frac{\partial\omega}{\partial r}A_\varphi . \quad (3.42)$$

Since the product  $N^2g_{rr}$  is finite and non-vanishing (as manifested by passing to  $\tilde{N}^2$  and  $\tilde{g}_{rr}$  in extremal case, cf. (3.2)), the condition (3.39) reduces to

$$F_{(r)(t)}\Big|_{r=r_0, \vartheta=\frac{\pi}{2}} = 0 . \quad (3.43)$$

In this degenerate case equation (3.37) defines just a pair of straight lines in  $l\tilde{q}$  plane rather than a hyperbola.

The hyperbola (3.37) has asymptotes

$$l = -\tilde{q} \frac{\sqrt{g_{\varphi\varphi}}\frac{\partial\phi}{\partial r} \pm \tilde{N}A_\varphi}{\sqrt{g_{\varphi\varphi}}\frac{\partial\omega}{\partial r} \mp \tilde{N}} \Big|_{r=r_0, \vartheta=\frac{\pi}{2}} . \quad (3.44)$$

We can also rewrite (3.37) as

$$\left\{ l^2 \left[ \frac{\left(\frac{\partial\omega}{\partial r}\right)^2}{\tilde{N}^2} - \frac{1}{g_{\varphi\varphi}} \right] + \tilde{q}^2 \left[ \frac{\left(\frac{\partial\phi}{\partial r}\right)^2}{\tilde{N}^2} - \frac{A_\varphi^2}{g_{\varphi\varphi}} \right] + 2l\tilde{q} \left( \frac{\frac{\partial\omega}{\partial r}\frac{\partial\phi}{\partial r}}{\tilde{N}^2} + \frac{A_\varphi}{g_{\varphi\varphi}} \right) \right\} \Big|_{r=r_0, \vartheta=\frac{\pi}{2}} = 1 . \quad (3.45)$$

The coefficients in this form determine the orientation of the hyperbola with respect to axes  $\tilde{q}$  and  $l$ . We will distinguish several cases and denote them by numbers and letters (by which they are identified in figures in Section 3.5).

Case **1a**: If

$$\left[ g_{\varphi\varphi} \left( \frac{\partial\omega}{\partial r} \right)^2 - \tilde{N}^2 \right] \Big|_{r=r_0, \vartheta=\frac{\pi}{2}} > 0 , \quad (3.46)$$

(3.45) is valid for  $\tilde{q} = 0$ , which means that both branches exist for both signs of  $\tilde{q}$ , i.e. both cross the  $l$  axis.

Case **1b**: If, on the other hand,

$$\left[ g_{\varphi\varphi} \left( \frac{\partial\omega}{\partial r} \right)^2 - \tilde{N}^2 \right] \Big|_{r=r_0, \vartheta=\frac{\pi}{2}} < 0 , \quad (3.47)$$

(3.45) cannot be satisfied for  $\tilde{q} = 0$ , so the branches are separated by the  $l$  axis and each

of them corresponds to different sign of  $\tilde{q}$ . The marginal case **1c** occurs when in (3.45)

$$\left[ g_{\varphi\varphi} \left( \frac{\partial\omega}{\partial r} \right)^2 - \tilde{N}^2 \right] \Big|_{r=r_0, \vartheta=\frac{\pi}{2}} = 0 , \quad (3.48)$$

i.e. the coefficient multiplying  $l^2$  vanishes. Comparing with (3.44), we see that this corresponds to one of the asymptotes having infinite slope, thus coinciding with the  $l$  axis.

A similar discussion applies to the coefficient of  $\tilde{q}^2$ .

Case **2a**: If

$$\left[ g_{\varphi\varphi} \left( \frac{\partial\phi}{\partial r} \right)^2 - \tilde{N}^2 A_\varphi^2 \right] \Big|_{r=r_0, \vartheta=\frac{\pi}{2}} > 0 , \quad (3.49)$$

both branches of the hyperbola cross the  $\tilde{q}$  axis and exist for both signs of  $l$ .

Case **2b**: The opposite inequality,

$$\left[ g_{\varphi\varphi} \left( \frac{\partial\phi}{\partial r} \right)^2 - \tilde{N}^2 A_\varphi^2 \right] \Big|_{r=r_0, \vartheta=\frac{\pi}{2}} < 0 , \quad (3.50)$$

means that the branches are separated by the  $\tilde{q}$  axis and each of them has different sign of  $l$ .

Case **2c**: If

$$\left[ g_{\varphi\varphi} \left( \frac{\partial\phi}{\partial r} \right)^2 - \tilde{N}^2 A_\varphi^2 \right] \Big|_{r=r_0, \vartheta=\frac{\pi}{2}} = 0 , \quad (3.51)$$

one can see again from (3.44) that this means that (at least) one of the asymptotes has zero slope, i.e. it coincides with the  $\tilde{q}$  axis.

Case **3**: If

$$\left( g_{\varphi\varphi} \frac{\partial\omega}{\partial r} \frac{\partial\phi}{\partial r} + \tilde{N}^2 A_\varphi \right) \Big|_{r=r_0, \vartheta=\frac{\pi}{2}} = 0 , \quad (3.52)$$

the coefficient multiplying  $l\tilde{q}$  vanishes. In that case, the hyperbola is symmetrical with respect to the inversions  $l \rightarrow -l$  and  $\tilde{q} \rightarrow -\tilde{q}$ . Since we are interested in just one of the branches, only one of the symmetries matters.

Let us note that when the electromagnetic field vanishes, the conditions (3.39), (3.51) and (3.52) are satisfied simultaneously – the charge of the particle loses any effect on kinematics.

Turning back to (3.30) in general, it is obvious that the radial derivative of the effective

potential at  $r_0$  will be positive for  $l = 0, \tilde{q} = 0$ . Therefore, the “admissible region” in the  $l\tilde{q}$  plane will be “behind” the hyperbola branch given by (3.36) with (3.30). If the branches are separated by one of the axes, critical particles must have a specific sign of one of the parameters to possibly reach  $r_0$ . Therefore, the difference among the **a** and **b** subcases of **1** and **2** is essential.

It is even more important to look at combinations of these subcases. There are two generic possibilities, when one of the two BSW mechanisms prevails: the combination **1a2b**, when only the sign of  $l$  is restricted, corresponds to the “classical” centrifugal mechanism of BSW effect (first described in [53] and generalised in [63]). On the other hand, the variant **1b2a** with a restriction on the sign of  $\tilde{q}$  signifies the dominance of the electrostatic analogy of the BSW effect (conceived in [66]).

However, in the  $\omega \neq 0, \tilde{q} \neq 0$  case, another two (more unusual) combinations can possibly occur. Scenario **1a2a** means that the sign of neither  $l$  nor  $\tilde{q}$  is restricted. In this case, there will be critical particles with both signs of  $l$  and with both signs of  $\tilde{q}$  that can approach  $r_0$ . Just *one* combination of signs of both parameters will be excluded. In contrast, the possibility **1b2b** would mean that signs of both  $l$  and  $\tilde{q}$  are restricted, i.e. that only critical particles with just one combination of signs of  $l$  and  $\tilde{q}$  can approach  $r_0$ . Curiously enough, for the extremal Kerr-Newman solution (see below), of those two, only the **1a2a** case can occur. However, the **1b2b** variant could possibly be realised in more general black-hole models.

As the **c** cases represent transitions between different combinations described above, the corresponding conditions (3.48) and (3.51) have particular physical significance; it is of primary interest, if these conditions can be satisfied for some black-hole solution and for which values of its parameters.

Finally, let us note that the condition (3.27) for critical particles can be used to define a system of parallel lines (labeled by different values of  $\varepsilon_{\text{cr}}$ ) in the  $l\tilde{q}$  plane.<sup>4</sup> Apart from the orientation of the hyperbola, it is also of interest to examine how the branch defined by (3.36) with (3.30) intersects these critical energy lines and which critical energies belong to the the admissible region.

---

<sup>4</sup>Alternatively, one can also interpret (3.27) as an equation of a single plane in  $\varepsilon l\tilde{q}$  space.

### 3.4.4 Parametric solution

There are many possible parametrisations for branch(es) of a hyperbola. We will derive a particular parametrisation of the hyperbola branch given by (3.36) with (3.30), which is simple and which can also be used to describe curves given by analogues of (3.36) with higher derivatives.<sup>5</sup>

Namely, let us make the following change of variables (assuming  $A_\varphi|_{r=r_0, \vartheta=\pi/2} \neq 0$ ):

$$l = \tilde{\lambda} \tilde{\eta} , \quad \tilde{q} A_\varphi|_{r=r_0, \vartheta=\frac{\pi}{2}} = \tilde{\lambda} (\tilde{\eta} - 1) , \quad (3.53)$$

under which (3.36) with (3.30) becomes

$$\left( \frac{\partial \omega}{\partial r} \tilde{\lambda} \tilde{\eta} + \frac{\tilde{\lambda}}{A_\varphi} (\tilde{\eta} - 1) \frac{\partial \phi}{\partial r} + \tilde{N} \sqrt{1 + \frac{\tilde{\lambda}^2}{g_{\varphi\varphi}}} \right) \Big|_{r=r_0, \vartheta=\frac{\pi}{2}} = 0 . \quad (3.54)$$

Expressing  $\tilde{\eta}$  as

$$\tilde{\eta} = \frac{\tilde{\lambda} \frac{\partial \phi}{\partial r} - \tilde{N} A_\varphi \sqrt{1 + \frac{\tilde{\lambda}^2}{g_{\varphi\varphi}}}}{\tilde{\lambda} \left( \frac{\partial \phi}{\partial r} + \frac{\partial \omega}{\partial r} A_\varphi \right)} \Big|_{r=r_0, \vartheta=\frac{\pi}{2}} = \frac{-\tilde{\lambda} \frac{\partial \phi}{\partial r} + \tilde{N} A_\varphi \sqrt{1 + \frac{\tilde{\lambda}^2}{g_{\varphi\varphi}}}}{\tilde{\lambda} \tilde{N} \sqrt{\tilde{g}_{rr}} F_{(r)}(t)} \Big|_{r=r_0, \vartheta=\frac{\pi}{2}} , \quad (3.55)$$

and plugging back into (3.53), we get parametric equations for  $l, \tilde{q}$  as functions of  $\tilde{\lambda}$

$$l = \frac{\tilde{\lambda} \frac{\partial \phi}{\partial r} - \tilde{N} A_\varphi \sqrt{1 + \frac{\tilde{\lambda}^2}{g_{\varphi\varphi}}}}{\frac{\partial \phi}{\partial r} + \frac{\partial \omega}{\partial r} A_\varphi} \Big|_{r=r_0, \vartheta=\frac{\pi}{2}} = \frac{-\tilde{\lambda} \frac{\partial \phi}{\partial r} + \tilde{N} A_\varphi \sqrt{1 + \frac{\tilde{\lambda}^2}{g_{\varphi\varphi}}}}{\tilde{N} \sqrt{\tilde{g}_{rr}} F_{(r)}(t)} \Big|_{r=r_0, \vartheta=\frac{\pi}{2}} , \quad (3.56)$$

and

$$\tilde{q} = - \frac{\tilde{\lambda} \frac{\partial \omega}{\partial r} + \tilde{N} \sqrt{1 + \frac{\tilde{\lambda}^2}{g_{\varphi\varphi}}}}{\frac{\partial \phi}{\partial r} + \frac{\partial \omega}{\partial r} A_\varphi} \Big|_{r=r_0, \vartheta=\frac{\pi}{2}} = \frac{\tilde{\lambda} \frac{\partial \omega}{\partial r} + \tilde{N} \sqrt{1 + \frac{\tilde{\lambda}^2}{g_{\varphi\varphi}}}}{\tilde{N} \sqrt{\tilde{g}_{rr}} F_{(r)}(t)} \Big|_{r=r_0, \vartheta=\frac{\pi}{2}} . \quad (3.57)$$

---

<sup>5</sup>In order to match the formalism developed in Chapter 5 for energy extraction, the prescription (3.53) is slightly modified in the present text as compared to [113]. The variables  $\tilde{\lambda}, \tilde{\eta}$  here are related to  $\lambda, \eta$  in [113] by  $\tilde{\lambda} = -\lambda A_\varphi|_{r=r_0, \vartheta=\pi/2}, \tilde{\eta} = -\eta$ .

If  $A_\varphi|_{r=r_0, \vartheta=\pi/2} = 0$ , (3.36) with (3.30) is just linear in  $\tilde{q}$ , so we can solve for it directly,

$$\tilde{q} = - \left. \frac{\frac{\partial \omega}{\partial r} l + \tilde{N} \sqrt{1 + \frac{l^2}{g_{\varphi\varphi}}}}{\frac{\partial \phi}{\partial r}} \right|_{r=r_0, \vartheta=\frac{\pi}{2}}. \quad (3.58)$$

### 3.4.5 Remarks on class II critical particles

One of the least studied aspects of the BSW-like phenomena is what happens when relaxation time  $\tau_{\text{relax}}$  in (3.34) is infinite, i.e when the leading order of the expansion of  $W$  in  $r - r_0$  for a critical particle is the third one instead of the second. Comparing with (3.35) and (3.36), we can make sure that this is the case for particles on the border of the admissible region.

Let us note that in [69] (cf. Table I therein), Harada and Kimura propose a classification (for nonequatorial critical particles in the Kerr field) somewhat similar to our discussion based on  $\partial V / \partial r|_{r_0}$ . In particular, class I critical particles correspond to those inside our admissible region, class II to those on the border and class III to the ones outside of it.

For the class II critical particles the expansion of the radial equation of motion (3.11) at  $r_0$  turns to

$$u^r \equiv \frac{dr}{d\tau} \doteq - (r - r_0)^{\frac{3}{2}} \left. \sqrt{\frac{1}{6\tilde{N}^2 \tilde{g}_{rr}} \frac{\partial^3 W}{\partial r^3}} \right|_{r=r_0} + \dots \quad (3.59)$$

This leads to the following approximate solution (which describes outgoing critical particles for  $\tau \rightarrow -\infty$  and ingoing ones for  $\tau \rightarrow \infty$ ):

$$r = r_0 + \frac{1}{\tau^2} \left. \left( \frac{24\tilde{N}^2 \tilde{g}_{rr}}{\partial^3 W} \right) \right|_{r=r_0} + \dots \quad (3.60)$$

This type of trajectory was previously considered in the equatorial geodesic case in [115] (be aware of typographic errors in equation (91) therein). Because of their inverse power-law behaviour, class II critical particles approach  $r_0$  much more slowly than class I critical particles with their exponential approach.

### 3.4.6 The second derivative

In order for the critical particles to approach  $r = r_0$ , their parameters  $\tilde{q}, l$  must lie in the admissible region. This region in the  $\tilde{q}l$  plane is delimited by the hyperbola branch given by the requirement of zero first derivative of the effective potential  $V$  at  $r_0$ , which corresponds to class II critical particles, as noted above. For class II critical particles the second derivative of  $V$  at  $r = r_0$  clearly has to be negative in order for them to be able to approach  $r_0$  (compare (3.59) with (C.10)). There are, however, more subtle aspects. First, for critical particles with parameters located *almost* at the border of the admissible region, i.e. parameters corresponding to almost zero first derivative of  $V$  at  $r = r_0$ , the second derivative of  $V$  also determines the trend of the effective potential  $V$  and the admissibility of motion.

Furthermore, one should distinguish between the conditions suitable for “black hole particle supercollider experiment”, where the motion towards  $r = r_0$  should be allowed to start from some radius well above  $r_0$  (if not from infinity of the spacetime, like in [53]), and a situation, when the allowed band outside  $r_0$  is tiny.<sup>6</sup> If we do not make assumptions about asymptotics of the effective potential  $V$  (or of the spacetime itself), this distinction also depends on the second derivative of  $V$  at  $r = r_0$ . There are multiple possibilities inside the admissible region. If the first derivative of  $V$  at  $r = r_0$  is negative but very small, whereas the second one is positive,  $V$  will reach a minimum and start to increase for some radii not much higher than  $r_0$ . Thus, the motion of the corresponding critical particle will be allowed only in a modest range of  $r$ . On the other hand, if both the first and the second derivative of  $V$  at  $r = r_0$  are negative, they will not be outweighed by higher Taylor orders until radii of multiples of  $r_0$ , so the motion can start well outside of the black hole. (See the Kerr-Newman example below, cf. Figure 3.1.) The higher derivatives can make a difference, even at radii very close to  $r_0$ , only in the (uncommon) case when both the first and the second derivative of  $V$  at  $r = r_0$  will be very small.

Focusing here on the second derivative of  $V$  at  $r = r_0$  for an extremal black hole (3.2), let us proceed analogously to what we described for the first derivative, namely, observing

---

<sup>6</sup>These other cases may be compatible with the particle starting to plunge after moving on a non-geodesic trajectory due to viscous losses inside an accretion disc. Such a process was discussed by Harada and Kimura in a slightly different context [114].

$\partial^2 N/\partial r^2 = 2\partial\tilde{N}/\partial r + (r - r_0) \partial^2\tilde{N}/\partial r^2$ . The result is

$$\begin{aligned} \left. \frac{\partial^2 V}{\partial r^2} \right|_{r=r_0} = & \left[ \frac{\partial^2 \omega}{\partial r^2} l + \tilde{q} \frac{\partial^2 \phi}{\partial r^2} + \left( 2 \frac{\partial \tilde{N}}{\partial r} - \frac{\tilde{N}}{g_{\varphi\varphi}} \frac{\partial g_{\varphi\varphi}}{\partial r} \right) \sqrt{1 + \frac{(l - \tilde{q} A_\varphi)^2}{g_{\varphi\varphi}}} + \right. \\ & \left. + \frac{\tilde{N}}{g_{\varphi\varphi}} \left( \frac{\partial g_{\varphi\varphi}}{\partial r} - 2\tilde{q} (l - \tilde{q} A_\varphi) \frac{\partial A_\varphi}{\partial r} \right) \frac{1}{\sqrt{1 + \frac{(l - \tilde{q} A_\varphi)^2}{g_{\varphi\varphi}}} \right] \Bigg|_{r=r_0, \vartheta=\frac{\pi}{2}} \end{aligned} \quad (3.61)$$

Again, we will consider the condition

$$\left. \frac{\partial^2 V}{\partial r^2} \right|_{r=r_0} = 0 \quad (3.62)$$

as a prescription of a curve in variables  $\tilde{q}$  and  $l$ . First, one can deduce its asymptotes,

$$l = -\tilde{q} \frac{\frac{\partial^2 \phi}{\partial r^2} \pm \frac{1}{\sqrt{g_{\varphi\varphi}}} \left[ \left( 2 \frac{\partial \tilde{N}}{\partial r} - \frac{\tilde{N}}{g_{\varphi\varphi}} \frac{\partial g_{\varphi\varphi}}{\partial r} \right) A_\varphi + 2\tilde{N} \frac{\partial A_\varphi}{\partial r} \right]}{\frac{\partial^2 \omega}{\partial r^2} \mp \frac{1}{\sqrt{g_{\varphi\varphi}}} \left( 2 \frac{\partial \tilde{N}}{\partial r} - \frac{\tilde{N}}{g_{\varphi\varphi}} \frac{\partial g_{\varphi\varphi}}{\partial r} \right)} \Bigg|_{r=r_0, \vartheta=\frac{\pi}{2}} \quad (3.63)$$

However, since (3.62) leads to much more complicated curve than a branch of a hyperbola, the asymptotes do not provide good information. (In fact, for the Kerr-Newman solution it can be seen that in some cases the curve approaches the asymptotes very slowly and that it may also cross them.)

Nevertheless, we can use change of variables (3.53) to obtain a parametric solution in the form

$$l = \frac{\tilde{\lambda} \frac{\partial^2 \phi}{\partial r^2} \sqrt{1 + \frac{\tilde{\lambda}^2}{g_{\varphi\varphi}}} - 2 \frac{\partial \tilde{N}}{\partial r} A_\varphi - \left[ \left( 2 \frac{\partial \tilde{N}}{\partial r} - \frac{\tilde{N}}{g_{\varphi\varphi}} \frac{\partial g_{\varphi\varphi}}{\partial r} \right) A_\varphi + 2\tilde{N} \frac{\partial A_\varphi}{\partial r} \right] \frac{\tilde{\lambda}^2}{g_{\varphi\varphi}}}{\left( \frac{\partial^2 \omega}{\partial r^2} A_\varphi + \frac{\partial^2 \phi}{\partial r^2} \right) \sqrt{1 + \frac{\tilde{\lambda}^2}{g_{\varphi\varphi}}} - \frac{2\tilde{N}}{g_{\varphi\varphi}} \tilde{\lambda} \frac{\partial A_\varphi}{\partial r}} \Bigg|_{r=r_0, \vartheta=\frac{\pi}{2}} \quad (3.64)$$

and

$$\tilde{q} = - \frac{\tilde{\lambda} \frac{\partial^2 \omega}{\partial r^2} \sqrt{1 + \frac{\tilde{\lambda}^2}{g_{\varphi\varphi}}} + 2 \frac{\partial \tilde{N}}{\partial r} + \left( 2 \frac{\partial \tilde{N}}{\partial r} - \frac{\tilde{N}}{g_{\varphi\varphi}} \frac{\partial g_{\varphi\varphi}}{\partial r} \right) \frac{\tilde{\lambda}^2}{g_{\varphi\varphi}}}{\left( \frac{\partial^2 \omega}{\partial r^2} A_\varphi + \frac{\partial^2 \phi}{\partial r^2} \right) \sqrt{1 + \frac{\tilde{\lambda}^2}{g_{\varphi\varphi}}} - \frac{2\tilde{N}}{g_{\varphi\varphi}} \tilde{\lambda} \frac{\partial A_\varphi}{\partial r}} \Bigg|_{r=r_0, \vartheta=\frac{\pi}{2}} \quad (3.65)$$

Once more, when  $A_\varphi|_{r=r_0, \vartheta=\pi/2} = 0$  and (3.53) does not work, we can solve (3.62) directly

for  $\tilde{q}$ , obtaining

$$\tilde{q} = - \frac{\frac{\partial^2 \omega}{\partial r^2} l \sqrt{1 + \frac{l^2}{g_{\varphi\varphi}} + 2 \frac{\partial \tilde{N}}{\partial r} + \left(2 \frac{\partial \tilde{N}}{\partial r} - \frac{\tilde{N}}{g_{\varphi\varphi}} \frac{\partial g_{\varphi\varphi}}{\partial r}\right) \frac{l^2}{g_{\varphi\varphi}}}}{\frac{\partial^2 \phi}{\partial r^2} \sqrt{1 + \frac{l^2}{g_{\varphi\varphi}} - \frac{2\tilde{N}}{g_{\varphi\varphi}} l \frac{\partial A_\varphi}{\partial r}}} \Bigg|_{r=r_0, \vartheta=\frac{\pi}{2}} . \quad (3.66)$$

The details of the behaviour of the curve (3.62) are in general not quite simple, since the curve can have two branches separated by a “third asymptote”. This is manifested by the fact that denominators of (3.64) and (3.65) can go to zero for a finite value of parameter  $\tilde{\lambda}$ . One can verify that for real  $\tilde{\lambda}$  the only such value can be

$$\tilde{\lambda}_0 = \left[ \operatorname{sgn} \left( \frac{\partial A_\varphi}{\partial r} \right) \frac{\frac{\partial^2 \omega}{\partial r^2} A_\varphi + \frac{\partial^2 \phi}{\partial r^2}}{\sqrt{4\tilde{N}^2 \left( \frac{\partial A_\varphi}{\partial r} \right)^2 - g_{\varphi\varphi} \left( \frac{\partial^2 \omega}{\partial r^2} A_\varphi + \frac{\partial^2 \phi}{\partial r^2} \right)^2}} \right] \Bigg|_{r=r_0, \vartheta=\frac{\pi}{2}} . \quad (3.67)$$

Taking the limit  $\tilde{\lambda} \rightarrow \tilde{\lambda}_0$  of the ratio of (3.64) and (3.65), we find the third asymptote to be the line  $l = \tilde{q} A_\varphi|_{r=r_0, \vartheta=\pi/2}$ . Since the values of  $l$  and  $\tilde{q}$  given by (3.64) and (3.65) for  $\tilde{\lambda} = 0$  lie on this line, we see that the curve (3.62) necessarily crosses this third asymptote.

In order for the branch separation to occur,  $\tilde{\lambda}_0$  must be a real number. Therefore, if it holds that

$$\left[ \frac{4\tilde{N}^2}{g_{\varphi\varphi}} \left( \frac{\partial A_\varphi}{\partial r} \right)^2 - \left( \frac{\partial^2 \omega}{\partial r^2} A_\varphi + \frac{\partial^2 \phi}{\partial r^2} \right)^2 \right] \Bigg|_{r=r_0, \vartheta=\frac{\pi}{2}} > 0 , \quad (3.68)$$

the curve (3.62) will indeed have two branches, whereas for

$$\left[ \frac{4\tilde{N}^2}{g_{\varphi\varphi}} \left( \frac{\partial A_\varphi}{\partial r} \right)^2 - \left( \frac{\partial^2 \omega}{\partial r^2} A_\varphi + \frac{\partial^2 \phi}{\partial r^2} \right)^2 \right] \Bigg|_{r=r_0, \vartheta=\frac{\pi}{2}} < 0 , \quad (3.69)$$

there will be only one branch. Interestingly, in the marginal case,

$$\left[ \frac{4\tilde{N}^2}{g_{\varphi\varphi}} \left( \frac{\partial A_\varphi}{\partial r} \right)^2 - \left( \frac{\partial^2 \omega}{\partial r^2} A_\varphi + \frac{\partial^2 \phi}{\partial r^2} \right)^2 \right] \Bigg|_{r=r_0, \vartheta=\frac{\pi}{2}} = 0 ; \quad (3.70)$$

one can verify that the line  $l = \tilde{q} A_\varphi|_{r=r_0, \vartheta=\pi/2}$  coincides with one of the asymptotes (3.63).

The formulae (3.64) and (3.65) can be decomposed into two contributions

$$l(\tilde{\lambda}) = l_{\text{reg}}(\tilde{\lambda}) + l_{\text{sing}}(\tilde{\lambda}) , \quad \tilde{q}(\tilde{\lambda}) = \tilde{q}_{\text{reg}}(\tilde{\lambda}) + \tilde{q}_{\text{sing}}(\tilde{\lambda}) . \quad (3.71)$$

Here  $l_{\text{reg}}$  and  $\tilde{q}_{\text{reg}}$  are finite for  $\tilde{\lambda} \rightarrow \tilde{\lambda}_0$ , whereas  $l_{\text{sing}}$  and  $\tilde{q}_{\text{sing}}$  are given by expressions (3.64) and (3.65) with their numerators evaluated at  $\tilde{\lambda}_0$ . One can show that  $l_{\text{reg}}, \tilde{q}_{\text{reg}}$  alone form a parametric expression of a branch of a hyperbola with asymptotes (3.63), whereas  $l_{\text{sing}}, \tilde{q}_{\text{sing}}$  parametrise the line  $l = \tilde{q} A_\varphi|_{r=r_0, \vartheta=\pi/2}$ . Unfortunately, the resulting expressions are not so “practical” in general (see C.2), but they become shorter for the Kerr-Newman case (cf. (3.90), (3.91), (3.92), (3.93)).

Leaving aside the technical details, let us note that it is of interest to study the intersections of curve (3.64), (3.65) with the border (3.56), (3.57) of the admissible region. If there is a part of the border that lies inside the region where the second derivative of  $V$  at  $r_0$  is positive, the cases described at the beginning of this section will arise. In the figures in the next section, these “problematic” parts of the border will be plotted **in red**.

### 3.5 Results for the Kerr-Newman solution

For the Kerr-Newman solution (1.1) with mass  $M$ , angular momentum  $aM$  ( $a \geq 0$ ), and charge  $Q$ , the metric in the form (3.1) reads

$$\mathbf{g} = -\frac{\Delta\Sigma}{\mathcal{A}} \mathbf{d}t^2 + \frac{\mathcal{A}}{\Sigma} \sin^2 \vartheta \left[ \mathbf{d}\varphi - \frac{a}{\mathcal{A}} (2Mr - Q^2) \mathbf{d}t \right]^2 + \frac{\Sigma}{\Delta} \mathbf{d}r^2 + \Sigma \mathbf{d}\vartheta^2, \quad (3.72)$$

where

$$\Delta = r^2 - 2Mr + a^2 + Q^2, \quad \Sigma = r^2 + a^2 \cos^2 \vartheta, \quad \mathcal{A} = (r^2 + a^2)^2 - \Delta a^2 \sin^2 \vartheta. \quad (3.73)$$

In the extremal case,  $M^2 = Q^2 + a^2$  and  $\Delta = (r - M)^2$ , so  $\Delta$  plays the role of expression  $(r - r_0)^2$  factored out in (3.2) with  $r_0 = M$ . It is obvious that one of the parameters, say  $M$ , constitutes just a scale; only ratios of the other two parameters with respect to it imply properties of the solution. Thus, the extremal case is effectively a one-parameter class (cf. (2.64)).

The electromagnetic potential for the Kerr-Newman solution (1.3) reads

$$\mathbf{A} = -\frac{Qr}{\Sigma} (\mathbf{d}t - a \sin^2 \vartheta \mathbf{d}\varphi), \quad (3.74)$$

which implies the generalised electrostatic potential,

$$\phi = \frac{Qr}{\mathcal{A}} (r^2 + a^2) . \quad (3.75)$$

Substituting (3.72), (3.74) and (3.75) into (3.16), we get the effective potential for equatorial electrogeodesic motion (cf. [107])

$$V = \frac{1}{\mathcal{A}_{\text{eq}}} \left\{ (2Mr - Q^2) al + \tilde{q}Qr (r^2 + a^2) + r\sqrt{\Delta [\mathcal{A}_{\text{eq}} + (lr - \tilde{q}Qa)^2]} \right\} , \quad (3.76)$$

where  $\mathcal{A}_{\text{eq}}$  stands for  $\mathcal{A}|_{\vartheta=\pi/2}$ . It is interesting to note that in the extremal case, for particles with special values of parameters

$$l = a , \quad \tilde{q} = \frac{\sqrt{Q^2 + a^2}}{Q} , \quad (3.77)$$

it holds that  $V \equiv 1$ .

### 3.5.1 The hyperbola

Critical particles with given values of  $\tilde{q}$  and  $l$  must have the energy defined by

$$\varepsilon_{\text{cr}} = \frac{al}{Q^2 + 2a^2} + \frac{\tilde{q}Q\sqrt{Q^2 + a^2}}{Q^2 + 2a^2} . \quad (3.78)$$

Kinematic restrictions on their motion towards  $r = M$  are expressed by the branch of the hyperbola defined by equation (3.36) with (3.30), which for the extremal Kerr-Newman solution takes the form (when multiplied by common denominator  $(Q^2 + 2a^2)^2$ )

$$-2al\sqrt{Q^2 + a^2} - \tilde{q}Q^3 + \sqrt{Q^2 + a^2}\sqrt{(Q^2 + 2a^2)^2 + (l\sqrt{Q^2 + a^2} - \tilde{q}Qa)^2} = 0 . \quad (3.79)$$

If we turn to the whole hyperbola in the form (3.37), we get

$$\frac{(2al\sqrt{Q^2 + a^2} + \tilde{q}Q^3)^2}{(Q^2 + a^2)(Q^2 + 2a^2)^2} - \frac{(l\sqrt{Q^2 + a^2} - \tilde{q}Qa)^2}{(Q^2 + 2a^2)^2} = 1 . \quad (3.80)$$

In the form (3.45), it reads

$$l^2 \frac{3a^2 - Q^2}{(Q^2 + 2a^2)^2} + \tilde{q}^2 \frac{Q^2 (Q^4 - Q^2 a^2 - a^4)}{(Q^2 + a^2) (Q^2 + 2a^2)^2} + 2l\tilde{q} \frac{Qa (3Q^2 + a^2)}{\sqrt{Q^2 + a^2} (Q^2 + 2a^2)^2} = 1. \quad (3.81)$$

Equation (3.44) for the asymptotes of the hyperbola reduces to

$$l = \tilde{q} \frac{Q}{\sqrt{Q^2 + a^2}} \frac{-Q^2 \pm a\sqrt{Q^2 + a^2}}{2a \pm \sqrt{Q^2 + a^2}}. \quad (3.82)$$

The parametric solution for (3.79) given in general by (3.56) and (3.57) turns out to be

$$l = \frac{\tilde{\lambda} Q^2 + a\sqrt{(Q^2 + 2a^2)^2 + \tilde{\lambda}^2 (Q^2 + a^2)}}{Q^2 + 2a^2}, \quad (3.83)$$

$$\tilde{q} = \frac{\sqrt{Q^2 + a^2}}{Q(Q^2 + 2a^2)} \left[ -2\tilde{\lambda}a + \sqrt{(Q^2 + 2a^2)^2 + \tilde{\lambda}^2 (Q^2 + a^2)} \right]. \quad (3.84)$$

### 3.5.2 The second derivative

Regarding (3.61), we find for the value of the second derivative of  $V$  at  $r = M$

$$\begin{aligned} \frac{\partial^2 V}{\partial r^2} \Big|_{r=M} &= \frac{1}{(Q^2 + 2a^2)^3} \left[ 2a (2Q^2 + a^2) l + 2Q\sqrt{Q^2 + a^2} (Q^2 - a^2) \tilde{q} - \right. \\ &\quad \left. - 4Q^2 \sqrt{(Q^2 + 2a^2)^2 + (l\sqrt{Q^2 + a^2} - \tilde{q}Qa)^2} \right] + \\ &\quad + \frac{2}{(Q^2 + 2a^2)^2} \frac{Q^4 + 2Q^2 a^2 + \tilde{q}Qa (l\sqrt{Q^2 + a^2} - \tilde{q}Qa)}{\sqrt{(Q^2 + 2a^2)^2 + (l\sqrt{Q^2 + a^2} - \tilde{q}Qa)^2}}. \end{aligned} \quad (3.85)$$

One can check that for  $\tilde{q} = 0, l = 0$  this expression reduces to

$$\frac{\partial^2 V}{\partial r^2} \Big|_{r=M} = -\frac{2Q^2}{(Q^2 + 2a^2)^2}, \quad (3.86)$$

so that the region of  $\partial^2 V / \partial r^2|_{r_0} > 0$  will lie “behind” the curve (3.62). The parametric equations (3.64) and (3.65) for this curve become

$$l = \frac{1}{\tilde{\lambda} a (Q^2 + a^2) + Q^2 \sqrt{(Q^2 + 2a^2)^2 + (Q^2 + a^2) \tilde{\lambda}^2}} \left\{ a (Q^4 + 2Q^2 a^2) + \right. \\ \left. + \frac{1}{Q^2 + 2a^2} \left[ \tilde{\lambda} (Q^4 - a^4) \sqrt{(Q^2 + 2a^2)^2 + (Q^2 + a^2) \tilde{\lambda}^2} + (3Q^2 + 2a^2) (Q^2 + a^2) \tilde{\lambda}^2 \right] \right\}, \quad (3.87)$$

$$\tilde{q} = \frac{1}{\tilde{\lambda} Q a \sqrt{Q^2 + a^2} + \frac{Q^3}{\sqrt{Q^2 + a^2}} \sqrt{(Q^2 + 2a^2)^2 + (Q^2 + a^2) \tilde{\lambda}^2}} \left\{ Q^4 + 2Q^2 a^2 + \right. \\ \left. + \frac{1}{Q^2 + 2a^2} \left[ -\tilde{\lambda} a (2Q^2 + a^2) \sqrt{(Q^2 + 2a^2)^2 + (Q^2 + a^2) \tilde{\lambda}^2} + 2Q^2 (Q^2 + a^2) \tilde{\lambda}^2 \right] \right\}. \quad (3.88)$$

The value  $\tilde{\lambda}_0$ , for which the denominators of (3.87) and (3.88) vanish, is

$$\tilde{\lambda}_0 = -\frac{Q^2}{\sqrt{Q^2 + a^2}} \frac{Q^2 + 2a^2}{\sqrt{a^4 + a^2 Q^2 - Q^4}}. \quad (3.89)$$

Performing the decomposition (3.71), we find that finite part of (3.87) is

$$l_{\text{reg}} = \frac{1}{(Q^2 + 2a^2) (Q^4 - Q^2 a^2 - a^4)} \left[ (Q^2 + a^2) (Q^4 - 4Q^2 a^2 - 2a^4) \tilde{\lambda} + \right. \\ \left. + a (2Q^4 + 2Q^2 a^2 + a^4) \sqrt{(Q^2 + 2a^2)^2 + (Q^2 + a^2) \tilde{\lambda}^2} \right], \quad (3.90)$$

whereas for (3.88) the finite part (C.14) goes over to

$$\tilde{q}_{\text{reg}} = \sqrt{Q^2 + a^2} \frac{-a (4Q^4 + 3Q^2 a^2) \tilde{\lambda} + (2Q^4 + 2Q^2 a^2 + a^4) \sqrt{(Q^2 + 2a^2)^2 + (Q^2 + a^2) \tilde{\lambda}^2}}{Q (Q^2 + 2a^2) (Q^4 - Q^2 a^2 - a^4)}. \quad (3.91)$$

The contributions (C.16) and (C.15) that blow up for  $\tilde{\lambda} \rightarrow \tilde{\lambda}_0$  are given by<sup>7</sup>

$$l_{\text{sing}} = -\frac{Q^2 a (Q^2 + a^2)}{Q^4 - Q^2 a^2 - a^4} \frac{(Q^2 + 2a^2)^2}{\tilde{\lambda} a (Q^2 + a^2) + Q^2 \sqrt{(Q^2 + 2a^2)^2 + (Q^2 + a^2) \tilde{\lambda}^2}}, \quad (3.92)$$

$$\tilde{q}_{\text{sing}} = l_{\text{sing}} \frac{\sqrt{Q^2 + a^2}}{Qa}. \quad (3.93)$$

The curves (3.83), (3.84) and (3.87), (3.88) have two intersections. Naturally, one of them coincides with (3.77). This corresponds to  $V \equiv 1$ , as we stated before; thus, all the derivatives of  $V$  at all radii will be zero for these values of  $\tilde{q}$  and  $l$ . One can check that the point (3.77) corresponds to  $\tilde{\lambda} = 0$  in (3.83), (3.84) and (3.87), (3.88). The other intersection lies at

$$l = \frac{a}{|Q|} \frac{2Q^2 + a^2}{\sqrt{Q^2 + a^2}}, \quad \tilde{q} = \frac{1}{|Q|} \frac{Q^2 - a^2}{Q}, \quad (3.94)$$

and corresponds to

$$\tilde{\lambda} = \frac{a}{|Q|} \frac{Q^2 + 2a^2}{\sqrt{Q^2 + a^2}}. \quad (3.95)$$

One can make sure that the second derivative of  $V$  at  $r = M$  is positive on a finite stretch of the curve (3.83), (3.84), which lies in between these intersections. This part of the curve (plotted **in red** in the corresponding figures) corresponds to class II critical particles that cannot approach  $r = M$ . For parameters on the rest of the border (3.83), (3.84), the approach of class II critical particles towards  $r = M$  is allowed.

### 3.5.3 Important special cases

Let us now examine kinematic restrictions coming from the equations above for some specific cases of the extremal Kerr-Newman solution.

#### 3.5.3.1 Extremal Kerr solution

The condition (3.39) for the hyperbola branch (3.79) to degenerate into straight line corresponds to

$$\frac{Q}{Q^2 + 2a^2} = 0 \quad (3.96)$$

---

<sup>7</sup>Interestingly, all the resulting formulae work well even for the case when real  $\lambda_0$  does not exist (3.69). They are not defined in the marginal case (3.70).

for the extremal Kerr-Newman solution. We see that this can be satisfied only by setting  $Q = 0$ , i.e. for the extremal Kerr solution. Regarding (3.81), the conditions (3.51) and (3.52) (case **2c3**) are also satisfied for  $Q = 0$ , which we anticipated for a case without an electromagnetic field.

Equation (3.79) is satisfied for  $l/M \equiv l/a = 2/\sqrt{3}$ . Therefore, critical particles can approach  $r = M$  for angular momenta  $l/M > 2/\sqrt{3}$  in this case, which corresponds to energies  $\varepsilon_{\text{cr}} > 1/\sqrt{3}$ , as seen from (3.78). However, the expression (3.85) becomes

$$\left. \frac{\partial^2 V}{\partial r^2} \right|_{r=M} = \frac{l}{4a^3}, \quad (3.97)$$

so the second derivative of  $V$  at  $r = M$  will be positive for all those particles. Thus, the bounded particles with  $l/M = 2/\sqrt{3}$ , i.e. class II critical particles, cannot approach  $r = M$  in the extremal Kerr spacetime. Moreover, for particles with parameters close to  $l/M = 2/\sqrt{3}$ , their motion will be allowed only for a short range of radii.

Let us yet note that the parameters  $l/M = 2/\sqrt{3}, \varepsilon = 1/\sqrt{3}$  mentioned above are those of the marginally stable circular orbit in the extremal Kerr limit, as given in [45]. Furthermore, the other special circular orbits considered in [45], i.e. the marginally bound orbit and the photon orbit (with  $\varepsilon \rightarrow \infty, l \rightarrow 2M\varepsilon$ ), also correspond to critical particles in the extremal Kerr limit.

### 3.5.3.2 “Sixty-degree” black hole

Turning again to (3.81), we find that condition (3.48) (case **1c**) can be satisfied if and only if  $3a^2 = Q^2$ . This corresponds to  $a/M = 1/2$  and  $|Q|/M = \sqrt{3}/2$ , respectively.<sup>8</sup> The special alignment of the hyperbola branch (3.79) and the critical energy lines in the admissible region in this case can be seen in Figure 3.2.

In order to explore the significance of the sign of  $\partial^2 V / \partial r^2|_{r_0}$ , we plotted  $V$  for several particles on the “border” (with  $\partial V / \partial r|_{r_0}$ ) in Figure 3.1. With  $\partial^2 V / \partial r^2|_{r_0} < 0$ , even the bounded particle shown (with  $\tilde{q} = 0.5$ ) has a reasonable allowed band.

---

<sup>8</sup>If we express the parameters of the extremal Kerr-Newman black hole by a “mixing angle” defined by  $a = M \cos \gamma_{\text{KN}}, Q = M \sin \gamma_{\text{KN}}$  (cf. (2.64)),  $a/M = 1/2$  corresponds to its value of sixty degrees, hence the name for this case.

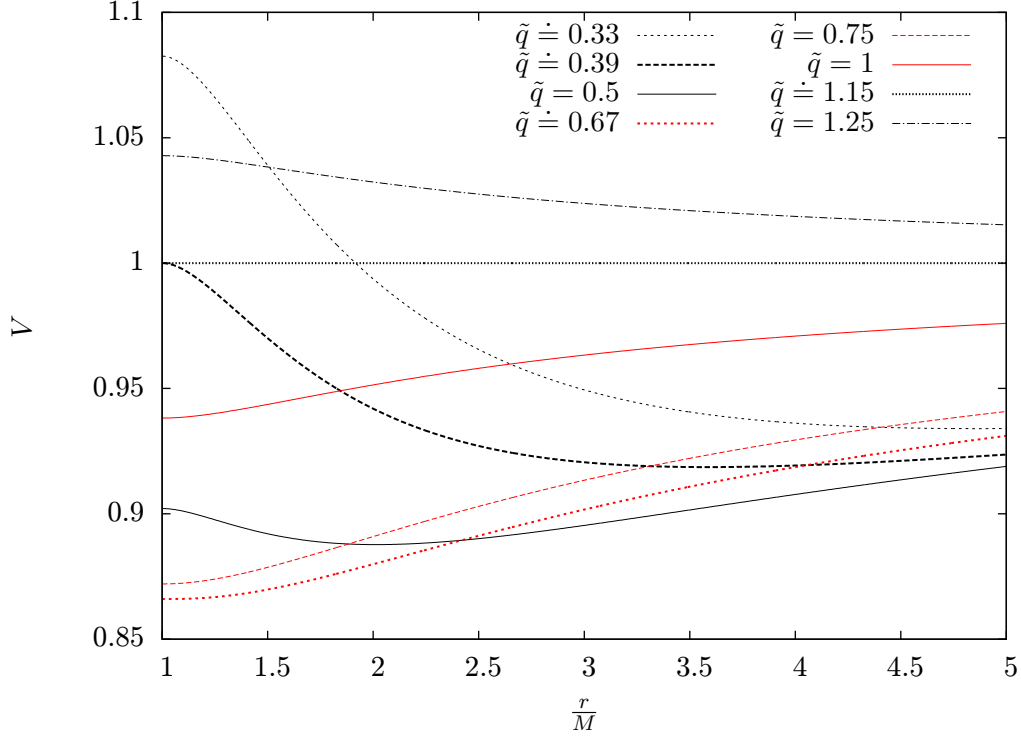


Figure 3.1: Effective potential  $V$  for several particles with  $\partial V/\partial r|_{r=r_0} = 0$  moving around the extremal Kerr-Newman black hole with  $a/M = 1/2$ . For  $2/3 < \tilde{q} < 2/\sqrt{3}$  (in red), the effect of the positive second derivative of  $V$  at  $r_0$  is clearly visible.

### 3.5.3.3 “Golden” black hole

Apart from the degenerate Kerr case, condition (3.51) (case **2c**) will be also satisfied if  $Q^4 - Q^2 a^2 - a^4 = 0$ , as follows from (3.81). This equation has one positive root, which corresponds to  $Q^2/a^2 = (\sqrt{5}+1)/2$ . This is the “golden ratio” number.<sup>9</sup> Since the golden ratio plus one equals the golden ratio squared, we get  $M/a = (\sqrt{5}+1)/2$  and  $M^2/Q^2 = (\sqrt{5}+1)/2$ . And, by definition, one over the golden ratio is the golden ratio minus one, so it holds that, e.g.  $a/M = (\sqrt{5}-1)/2$ . The plot of the hyperbola branch (3.79) in this case can be seen in Figure 3.3.

Curiously enough, the condition (3.70) also corresponds to  $Q^4 - Q^2 a^2 - a^4 = 0$ , as seen from (3.89). Thus, for  $a/M > (\sqrt{5}-1)/2$  there will be two branches of the curve (3.87), (3.88). However, it turns out that only one of the branches will intersect the admissible region. This follows from the fact that one of the intersections with its border, curve (3.79), lies at  $\tilde{\lambda} = 0$  and the position in  $\tilde{\lambda}$  (cf. (3.95)) of the other has always the opposite sign compared to  $\tilde{\lambda}_0$  (see (3.89)), where the branch cut occurs.

<sup>9</sup>F. H. thanks Miguel Coelho Ferreira for kindly pointing this out.

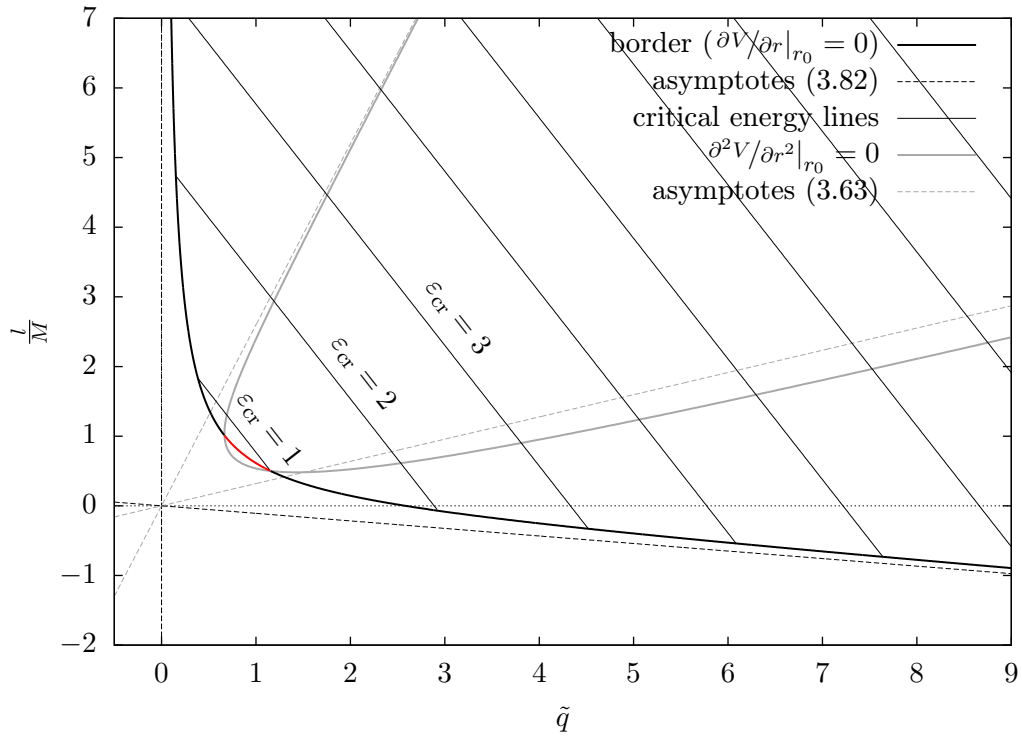


Figure 3.2: Case **1c2a**: Kinematic restrictions for critical particles in the case of the extremal Kerr-Newman black hole with  $a/M = 1/2$ . The hyperbola branch forms a border between the critical particles that can approach  $r = M$  and those that cannot. In the admissible region the lines of constant critical energy are plotted. We considered  $Q > 0$ ; the figure for  $Q < 0$  can be obtained by the inversion  $\tilde{q} \rightarrow -\tilde{q}$ . Note that one of the asymptotes coincides with the  $l$  axis.

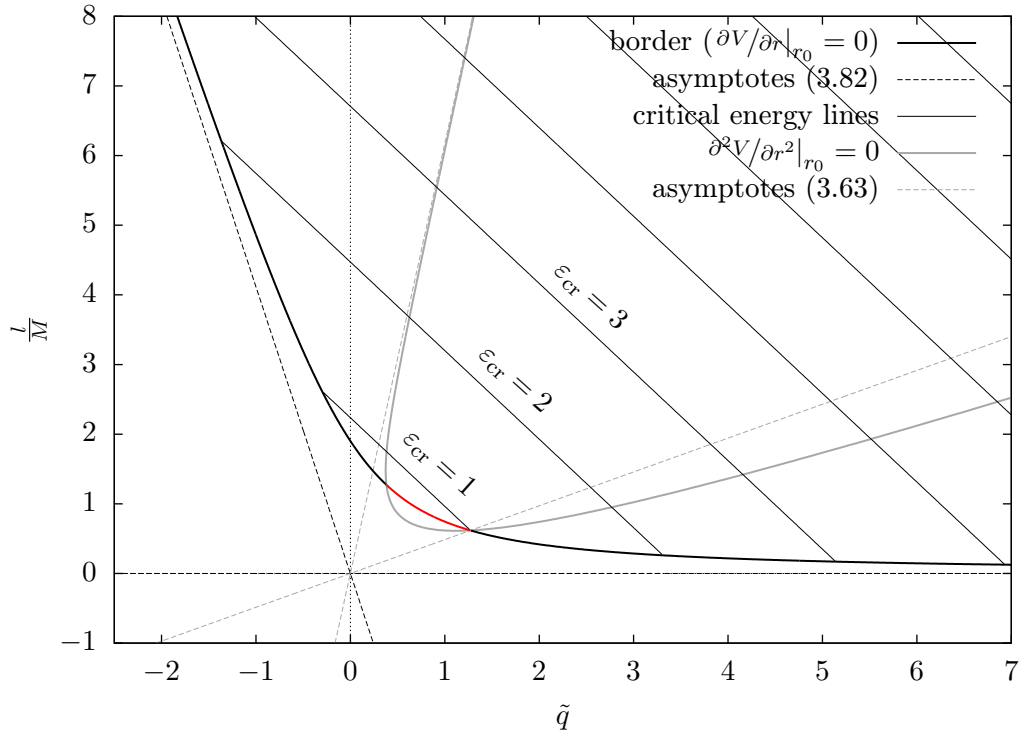


Figure 3.3: Case **1a2c**: Kinematic restrictions for critical particles in the case of the extremal Kerr-Newman black hole with  $a/M = (\sqrt{5}-1)/2$  (golden black hole). The hyperbola branch forms a border between the critical particles that can approach  $r = M$  and those that cannot. In the admissible region the lines of constant critical energy are plotted. We considered  $Q > 0$ ; the figure for  $Q < 0$  can be obtained by the inversion  $\tilde{q} \rightarrow -\tilde{q}$ . Note that one of the asymptotes coincides with the  $\tilde{q}$  axis.

We have exhausted all cases when conditions (3.48) and (3.51) can be satisfied. Now let us look at the signs of the coefficients multiplying  $l^2$  and  $\tilde{q}^2$  terms in (3.81) on the intervals delimited by these special cases. For  $a/M > (\sqrt{5}-1)/2 \doteq 0.618$ , the coefficient of  $l^2$  is positive and the coefficient of  $\tilde{q}^2$  is negative (case **1a2b**). Thus, the critical particles need to be corotating in order to approach  $r = M$ , but they can have both signs of charge (or be uncharged). The “centrifugal mechanism” prevails in this interval. On the other hand, for  $a/M < 1/2$  the coefficient of  $l^2$  is negative and the coefficient of  $\tilde{q}^2$  is positive (case **1b2a**). Therefore, critical particles can be radially moving, counterrotating, or corotating, but they must have the same sign of charge as the black hole. In particular, they cannot be uncharged (cf. [65]). Thus, in this interval the “electrostatic mechanism” prevails. However, for  $(\sqrt{5}-1)/2 > a/M > 1/2$ , both coefficients are positive (case **1a2a**, so inequalities (3.46) and (3.49) hold simultaneously). In this interval one can choose between the mechanisms; the critical particles need to either be corotating or have the same sign of charge as the black hole in order to approach  $r = M$ .

### 3.5.3.4 Extremal Reissner-Nordström solution

Again, in addition to the Kerr case, condition (3.52) (case **3**) can also be satisfied for  $a = 0$ , as we see from (3.81). As this case of the extremal Reissner-Nordström black hole is non-rotating, particle kinematics cannot depend on the change  $l \rightarrow -l$ . This is reflected in the symmetry of the hyperbola branch (3.79) with respect to  $\tilde{q}$  axis, see Figure 3.4.

Since  $A_\varphi \equiv 0$  for  $a = 0$ , one should use solution (3.58) for the hyperbola branch (3.79), which reads

$$\tilde{q} = \frac{1}{Q} \sqrt{Q^2 + l^2}, \quad (3.98)$$

and the solution (3.66) for (3.62), which becomes

$$\tilde{q} = \frac{2l^2 + Q^2}{Q\sqrt{Q^2 + l^2}}. \quad (3.99)$$

These curves touch at  $l = 0, \tilde{q} = \text{sgn} Q$ . Let us note that radial critical particles were previously studied by Zaslavskii in [66].

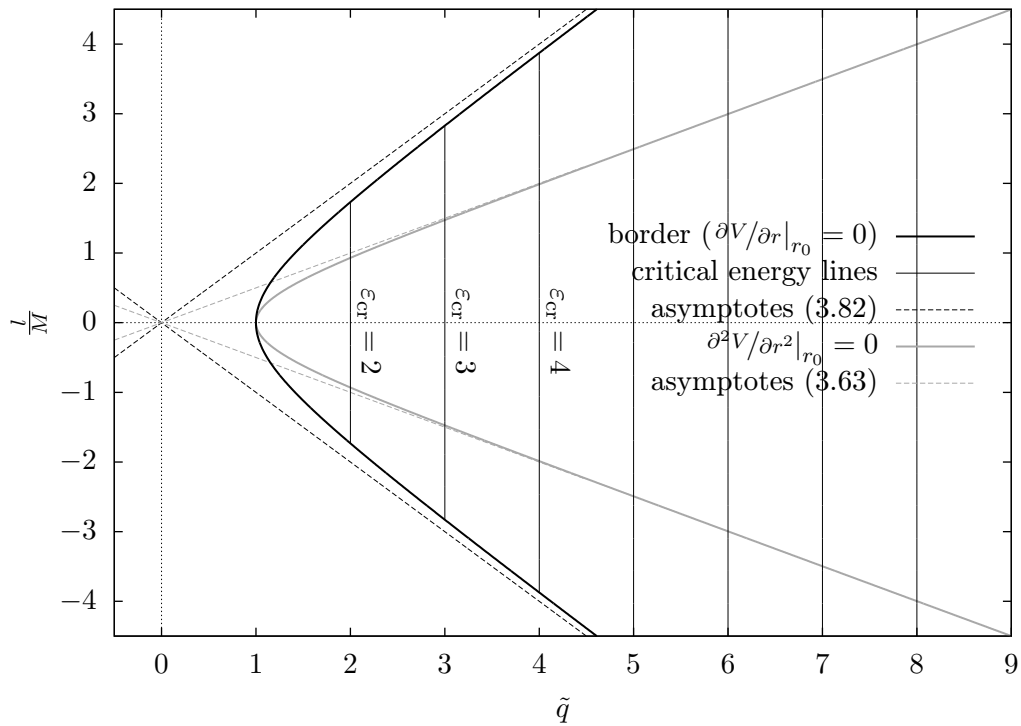


Figure 3.4: Case **1b2a3**: Kinematic restrictions for critical particles in the case of the extremal Reissner-Nordström black hole ( $a = 0$ ). The hyperbola branch forms a border between the critical particles that can approach  $r = M$  and those that cannot. In the admissible region the lines of constant critical energy are plotted. We considered  $Q > 0$ ; the figure for  $Q < 0$  can be obtained by the inversion  $\tilde{q} \rightarrow -\tilde{q}$ . Note the symmetry with respect to the  $\tilde{q}$  axis.

### 3.5.4 Energy considerations

As mentioned above, it is also of interest to study the intersections of the hyperbola branch (3.79) with critical energy lines. Since the Kerr-Newman solution is asymptotically flat, we focus on energy line with  $\varepsilon_{\text{cr}} = 1$ , which corresponds to critical particles coming from rest at infinity. Solving for intersections of (3.78) for  $\varepsilon_{\text{cr}} = 1$  with (3.79), we find that one is at the point (3.77), where  $V \equiv 1$  (all radial derivatives vanish for these parameters), and the other one occurs for

$$l = a \frac{3Q^2 + 2a^2}{Q^2}, \quad \tilde{q} = \frac{\sqrt{Q^2 + a^2}}{Q^3} (Q^2 - 2a^2). \quad (3.100)$$

Both intersections coincide for  $a = 0$ , when they reduce to  $l = 0, \tilde{q} = \text{sgn } Q$  and lie on the  $\tilde{q}$  axis. Apart from this case, both intersections occur for positive  $l$ , so critical particles with  $\varepsilon_{\text{cr}} \leq 1$  must be always corotating for  $a \neq 0$ . Only the second intersection can lie on the  $l$  axis, which happens for  $Q^2 = 2a^2$ . This condition corresponds to  $a/M = 1/\sqrt{3}, |Q|/M = \sqrt{2/3}$ . Thus, we reproduced the result of [64] that uncharged critical particles with  $\varepsilon_{\text{cr}} = 1$  cannot approach  $r = M$  for an extremal Kerr-Newman black hole with  $a/M < 1/\sqrt{3}$ . The hyperbola branch (3.79) for this case is plotted in Figure 3.5. For  $Q \rightarrow 0$ , the expressions (3.77) and (3.100) break down, because for the  $Q = 0$  (Kerr) case there is no dependence of the particle kinematics on  $\tilde{q}$ . In that case both (3.79) and (3.78) reduce just to (non-intersecting) lines of constant  $l$ .

Another interesting question is to find the “energy vertex” of the hyperbola branch, i.e. what is the minimal value of the critical energy on curve (3.79). One finds that it lies at the point (3.94), with the corresponding critical energy being

$$\varepsilon_{\text{cr}} = \frac{|Q|}{\sqrt{Q^2 + a^2}}. \quad (3.101)$$

This vertex energy will always be smaller than 1, except for the  $a = 0$  (Reissner-Nordström) case, when the vertex coincides with the intersections with the  $\varepsilon_{\text{cr}} = 1$  line ((3.77) and (3.100)) and lies on the  $\tilde{q}$  axis. The vertex can cross the  $l$  axis, which occurs if  $Q^2 = a^2$ . That corresponds to  $a/M = |Q|/M = 1/\sqrt{2}$  (see Figure 3.6).

Let us note that although the expressions (3.94) break down for  $Q \rightarrow 0$ , the corresponding critical energy (3.101) is regular. However, it does not have the correct limit for  $Q \rightarrow 0$ , since it goes to zero, whereas the lowest energy required for critical particles in

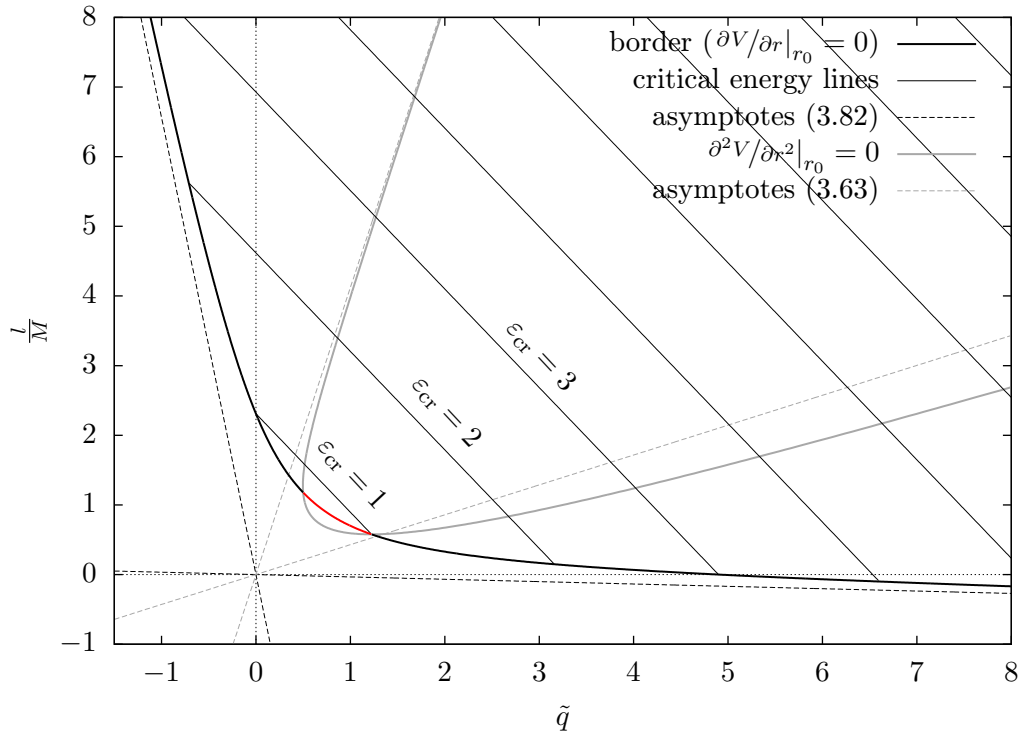


Figure 3.5: Case **1a2a**: Kinematic restrictions for critical particles in the case of the extremal Kerr-Newman black hole with  $a/M = 1/\sqrt{3}$ . The hyperbola branch forms a border between the critical particles that can approach  $r = M$  and those that cannot. In the admissible region the lines of constant critical energy are plotted. We considered  $Q > 0$ ; the figure for  $Q < 0$  can be obtained by the inversion  $\tilde{q} \rightarrow -\tilde{q}$ . Note that the  $\varepsilon_{\text{cr}} = 1$  intersects with the border at the  $l$  axis.

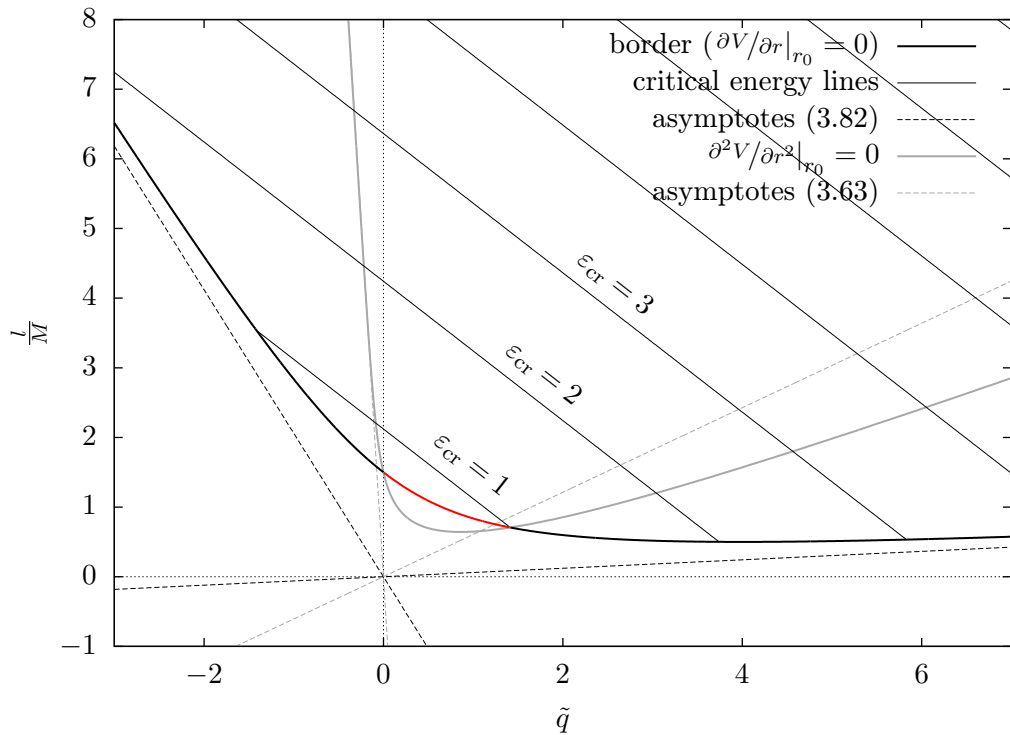


Figure 3.6: Case **1a2b**: Kinematic restrictions for critical particles in the case of the extremal Kerr-Newman black hole with  $a/M = 1/\sqrt{2}$ . The hyperbola branch forms a border between the critical particles that can approach  $r = M$  and those that cannot. In the admissible region the lines of constant critical energy are plotted. We considered  $Q > 0$ ; the figure for  $Q < 0$  can be obtained by the inversion  $\tilde{q} \rightarrow -\tilde{q}$ .

the extremal Kerr solution in order to approach  $r = M$  is  $1/\sqrt{3}$ , as noted above. This is an example of a “discontinuous” behaviour of the kinematic restrictions in the limit  $Q \rightarrow 0$ ; it has further manifestations that we discuss below.

### 3.5.5 The mega-BSW phenomena

If  $Q$  is small but nonzero, however tiny it may be, one can still maintain the magnitude of electrostatic force carried to a particular test particle if it has accordingly high  $\tilde{q}$ . This can be related to the divergent behaviour that we noticed in the expressions for positions of special points (all of them corresponding to  $\varepsilon_{\text{cr}} \leq 1$ ) (3.77), (3.94) and (3.100) in the  $l\tilde{q}$  plane. These features still occur regardless of how small the charge  $Q$  is, but at higher and higher values of  $\tilde{q}$ . We can see that in all these cases it holds that  $|l| \doteq |Q\tilde{q}|$  if we consider  $Q$  very small ( $|Q| \ll M$ ). However, the divergences in the expressions are of different orders, which has interesting consequences.

Though the position of the intersection (3.77) in  $l$  approaches a constant for  $Q \rightarrow 0$  and just the position in  $\tilde{q}$  diverges, for the other two points even the position in  $l$  diverges for  $Q \rightarrow 0$ . Thus, for very small  $Q$ , we can have charged critical particles that have  $\varepsilon_{\text{cr}} \leq 1$ , yet possess enormous values of angular momentum, and which still can approach  $r = M$  (hence the mega-BSW effect). Such a thing is not possible in either the  $|Q| \approx a$  or  $Q = 0$  regimes.

To examine this effect in more detail, let us assume that there is some value  $\tilde{q}_{\text{max}} \gg 1$  that acts as an upper bound for specific charge of the particles,  $|\tilde{q}| \leq \tilde{q}_{\text{max}}$ . Then we can find a value  $\tilde{Q}_{\text{min}}$  of black hole’s specific charge  $\tilde{Q} \equiv Q/M$  such that for  $|\tilde{Q}| \geq \tilde{Q}_{\text{min}}$  some of the special points ((3.77), (3.94), or (3.100)) will fit in the interval  $[-\tilde{q}_{\text{max}}, \tilde{q}_{\text{max}}]$ . The  $Q \rightarrow 0$  behaviour will be parametrised by  $\tilde{q}_{\text{max}} \rightarrow \infty$  asymptotics. Furthermore, we can define  $\tilde{l}_{\text{max}}$  such that the position of a selected special point ((3.77), (3.94), or (3.100)) will be  $|l| \doteq M\tilde{l}_{\text{max}}$  for  $|\tilde{Q}| = \tilde{Q}_{\text{min}}$ . Since  $\tilde{Q}_{\text{min}}$  will be small, we can use approximations and then observe the asymptotics for the three special points, which are summarised in Table 3.1.

These asymptotics tell us how small is the value of  $Q$ , for which we can still fit one of the special points into the bounded range of values of charge  $\tilde{q}$ , and how large angular momentum  $l$  the particles corresponding to this point can have for that value of  $Q$ .

This effect can also be relevant for considering BSW-type effects as an edge case

Table 3.1: The mega-BSW effect illustrated (see text for details).

Point	$\tilde{Q}_{\min}$	$\tilde{l}_{\max}$
(3.77)	$(\tilde{q}_{\max})^{-1}$	1
(3.94)	$(\tilde{q}_{\max})^{-\frac{1}{2}}$	$(\tilde{q}_{\max})^{\frac{1}{2}}$
(3.100)	$2^{\frac{1}{3}} (\tilde{q}_{\max})^{-\frac{1}{3}}$	$2^{\frac{1}{3}} (\tilde{q}_{\max})^{\frac{2}{3}}$

for possible astrophysical particle collision processes. Let us again stress that there are calculations, first using Wald’s approximate (test-field) solution [10] and later an exact Ernst-Wild solution [25], showing that a black hole can maintain a small, non-zero charge in the presence of an external magnetic field. Furthermore, considering elementary particles, an electron gives us  $\tilde{q}_{\max} > 10^{20}$ . However, the practical viability of the generalised BSW effect is in any case put in question by the unlikely existence of extremal black holes, the validity of the test-particle approximation and complications with energy extraction (cf. the Introduction). A more detailed assessment of such problems in the present setup (and a partial resolution of some of them) is given in 5.6.

### 3.6 Summary

We have studied the kinematics of critical particles moving around axially symmetric stationary extremal black holes, focusing on the case when *both* rotation and electromagnetic interaction are present. In the discussion, we used the minimum energy  $V$  (equation (3.16)), which is an analogy of a classical potential. Whether a critical particle can approach the position of the degenerate horizon or not depends heavily on properties of the black hole as well as on the parameters of the particle. If we treat the black hole as fixed, we can visualise the restrictions in the space of the parameters  $l$  and  $\tilde{q}$  (specific axial angular momentum and charge) of the particle.

To do so, we derived expressions for curves  $\partial V/\partial r|_{r_0} = 0$ , see (3.56), (3.57), and  $\partial^2 V/\partial r^2|_{r_0} = 0$ , cf. (3.64), (3.65), in this parameter space. The first is just a branch of a hyperbola, whereas the second is technically complicated and can split into two branches. These curves divide the parameter space into different regions. Critical particles with parameters in the  $\partial V/\partial r|_{r_0} < 0$  part (the admissible region) can approach  $r_0$ . However, the interval of  $r$  for which the motion is allowed may be short, if they fall into the part, where  $\partial^2 V/\partial r^2|_{r_0} > 0$ .

We then studied the dependence of the restrictions on the properties of the black hole. The relevant question is how many quadrants of the  $l\tilde{q}$  plane are intersected by the hyperbola branch (forming the border of the admissible region). As the admissible region is “behind” the hyperbola branch, it lies in the same quadrants as its border. In general cases it passes through two quadrants. In the case that we denoted as **1a2b**, critical particles must have a specific sign of angular momentum in order to approach  $r = r_0$ , but can have either sign of charge. Specially, they can be uncharged, but cannot move purely radially. This means the dominance of the centrifugal type of generalised BSW effect. On the other hand, in case **1b2a** the particles must have a specific sign of charge to approach  $r = r_0$ , but they can have either sign of angular momentum. This corresponds to the electrostatic type of generalised BSW effect.

Furthermore, we found that two mixed cases are also possible. In case **1a2a**, the hyperbola branch passes through three quadrants, so that the signs of the charge and angular momentum of the critical particles are not restricted in order to approach  $r = r_0$ . Just one combination of the signs is forbidden. In contrast, in case **1b2b**, the signs of both charge and angular momentum of the critical particle approaching  $r = r_0$  are restricted. We denoted the special limiting cases between **a** and **b** as **c** (see also Table 3.2). Another special situation is case **3**, when the border (and therefore the whole admissible region) has the symmetry with respect to one of the inversions  $l \rightarrow -l$  or  $\tilde{q} \rightarrow -\tilde{q}$ . The hyperbola branch may also degenerate into a straight line. We noted that this naturally happens for a vacuum black hole, together with conditions **2c3**.

We applied and illustrated the general discussion summarised above on the one-parameter class of extremal Kerr-Newman solutions. From the mixed cases, only **1a2a** is realised in this class. Apart from general kinematic restrictions (embodied in the position of the hyperbola branch enclosing the whole admissible region), we also investigated a subset of critical particles with energies corresponding to coming from rest at infinity or lower,  $\varepsilon_{\text{cr}} \leq 1$ , i.e. marginally bound and bound particles. We found that for  $a/M > 1/\sqrt{3}$  these particles can have either sign of charge, but must be corotating to approach  $r = M$ , whereas for  $a/M < 1/\sqrt{3}$  they must be both corotating and have the same sign of the charge as the black hole in order to approach  $r = M$ . The restrictions for particles with  $\varepsilon_{\text{cr}} \leq 1$  are thus more stringent. The main results for restrictions on the parameters of critical particles in order to approach  $r = M$  for extremal Kerr-Newman black holes are

summarised in Table 3.2.<sup>10</sup>

As a last point, we discussed unusual behaviour in the  $Q \rightarrow 0$  limit, when one can maintain the magnitude of electrostatic force by considering very large  $|\tilde{q}|$ . We found that for very small  $Q$ , critical particles with  $\varepsilon_{\text{cr}} \leq 1$  can have enormous values not only of specific charge, but also of angular momentum, and still be able to approach  $r = M$ . This is not possible for the cases  $Q = 0$  or  $Q \approx a$ . We discussed that this mega-BSW effect could have some significance in astrophysics because black holes can maintain a small charge due to interaction with external fields (see Section 1.2 and [10, 25]).

---

<sup>10</sup>For convenience, apart from the ratios  $a/M, |Q|/M$ , we used also the Kerr-Newman mixing angle ( $Q = M \sin \gamma_{\text{KN}}, a = M \cos \gamma_{\text{KN}}$ , cf. (2.64)) to parametrise the class.

Table 3.2: Restrictions on signs of  $l, \tilde{q}$  for critical particles that can approach  $r = M$  in an extremal Kerr-Newman spacetime. Special positions of special points in their parameter space are also indicated. (Note that (3.94) is the point with smallest  $\varepsilon_{\text{cr}}$  in the admissible region, whereas (3.100) and (3.77) are special points on its border, curve  $\partial V/\partial r|_{r_0} = 0$ , with  $\varepsilon_{\text{cr}} = 1$ . In the  $a = 0$  case, all three points coincide.)

Kerr-Newman black-hole parameters				Restrictions		Notes
$ \gamma_{\text{KN}} $	$\frac{a}{M}$	$\frac{ Q }{M}$	General case	For $\varepsilon_{\text{cr}} \leq 1$		
$0^\circ$	1	0	Vacuum			
$0^\circ <  \gamma_{\text{KN}}  < 45^\circ$	$1 > \frac{a}{M} > \frac{1}{\sqrt{2}}$	$0 < \frac{ Q }{M} < \frac{1}{\sqrt{2}}$				
$45^\circ$	$\frac{1}{\sqrt{2}}$	$\frac{1}{\sqrt{2}}$	<b>1a2b</b>			(3.94) at $\tilde{q} = 0$
$45^\circ <  \gamma_{\text{KN}}  < 51.8^\circ$	$\frac{1}{\sqrt{2}} > \frac{a}{M} > \frac{\sqrt{5}-1}{2}$	$\frac{1}{\sqrt{2}} < \frac{ Q }{M} < \sqrt{\frac{\sqrt{5}-1}{2}}$			$l > 0$	
$ \gamma_{\text{KN}}  \doteq 51.8^\circ$	$\frac{\sqrt{5}-1}{2}$	$\sqrt{\frac{\sqrt{5}-1}{2}}$	<b>1a2c</b>			
$51.8^\circ <  \gamma_{\text{KN}}  < 54.7^\circ$	$\frac{\sqrt{5}-1}{2} > \frac{a}{M} > \frac{1}{\sqrt{3}}$	$\sqrt{\frac{\sqrt{5}-1}{2}} < \frac{ Q }{M} < \sqrt{\frac{2}{3}}$				
$ \gamma_{\text{KN}}  \doteq 54.7^\circ$	$\frac{1}{\sqrt{3}}$	$\sqrt{\frac{2}{3}}$	<b>1a2a</b>		$l > 0, \tilde{q}Q \geq 0$	(3.100) at $\tilde{q} = 0$
$54.7^\circ <  \gamma_{\text{KN}}  < 60^\circ$	$\frac{1}{\sqrt{3}} > \frac{a}{M} > \frac{1}{2}$	$\sqrt{\frac{2}{3}} < \frac{ Q }{M} < \frac{\sqrt{3}}{2}$				
$60^\circ$	$\frac{1}{2}$	$\frac{\sqrt{3}}{2}$	<b>1c2a</b>		$l > 0, \tilde{q}Q > 0$	
$60^\circ <  \gamma_{\text{KN}}  < 90^\circ$	$\frac{1}{2} > \frac{a}{M} > 0$	$\frac{\sqrt{3}}{2} < \frac{ Q }{M} < 1$	<b>1b2a</b>			
$90^\circ$	0	1	<b>1b2a3</b>		$l = 0, \tilde{q}Q > 0$	(3.100), (3.94), (3.77) at $l = 0$



# Chapter 4

## Particle collisions along the axis of symmetry: kinematic restrictions and energy extraction

### 4.1 Outline and summary

An effect of electrostatic origin analogous to the BSW effect is possible for radially moving charged particles in the extremal Reissner-Nordström spacetime [66], as we have discussed in the Introduction. For this effect it turned out that, in the test particle approximation, there is no bound on the mass and the energy of an escaping particle produced in the collision [80]. This is in sharp contrast to the original “centrifugal” BSW effect, where unconditional bounds exist [72] (cf. also [71, 73]).

There are two natural ways of generalisation of this effect to more realistic black holes with a smaller charge than in the extremal Reissner-Nordström case. First, one can include effects of angular momentum of the particles and of the dragging from the rotation of the black hole and study overlapping and transition between the electrostatic and the centrifugal BSW-type effect. Concerning only the approach phase of the process, we have analysed this way of generalisation in detail in Chapter 3. On the other hand, one can keep the restriction to “purely radial” motion, which is possible in any axially symmetric spacetime for particles moving along the axis of symmetry. In the present chapter, we study this case and show that the interesting results for the extremal Reissner-Nordström black hole can be replicated even in models closer to astrophysical situations.

The chapter is organised as follows. In Section 4.2, we review the basic features of electrogeodesic motion along the axis of symmetry of a general stationary axially symmetric black-hole spacetime, including the local definition of the critical particles. We review why they cannot approach the horizon for subextremal black holes and how they cause the divergent behaviour of the centre-of-mass energy in the limit of the collision point approaching the horizon radius. In 4.2.3 we recall that the trajectory of a critical particle is approximated by an exponential relaxation towards the horizon radius. Because of this, any collision event involving a critical particle must always happen at a radius greater than the horizon radius. Therefore it makes sense to consider also particles that behave approximately as critical at a given collision radius (so-called nearly critical particles). We also recall that doubly fine-tuned critical particles with infinite relaxation time exhibit an inverse power-law behaviour and thus approach the horizon radius much more slowly, as we have previously shown in 3.4.5.

In Section 4.3 we study restrictions on the values of energy and charge of critical particles in order for them to be able to approach the radius of the degenerate horizon. Our discussion is based, similarly to Chapter 3, on derivatives of a certain effective potential. In Appendix C.1.2 we show how this approach can be rigorously related to the expansion coefficients of the radial equation of motion (including the relaxation time). In 4.3.2 we give particular results for the extremal Kerr-Newman spacetime, which show that for small values of the black hole charge the critical particles must be highly relativistic in order to be able to approach the horizon radius.

In Section 4.4 we deal with the energy extraction. First, we briefly review how to rearrange the conservation laws to prove that, for a  $2 \rightarrow 2$  process, a collision of a critical particle with an incoming “usual” (i.e. not fine-tuned) particle necessarily leads to the production of a nearly critical particle and an incoming usual particle. Then we study whether the produced nearly critical particle can escape and extract energy. We find that there are two threshold values, one for mass and one for energy. If the nearly critical particle is produced below/above the mass threshold, it is initially outgoing/incoming. Below the energy threshold the particle must be produced with such a value of charge that the corresponding critical energy will be lower than the actual energy, whereas above the threshold the critical energy corresponding to the charge is above the actual energy. These results qualitatively agree with the special case [80]. Here we focus on comparing

the BSW-type process (collision with an incoming critical particle) and the Schnittman process (collision with an outgoing, reflected critical particle). For instance, a particle that is initially incoming with energy above the critical energy will fall into a black hole. Therefore, a particle that is produced with mass above the threshold must have the energy also above the respective threshold in order to avoid this. In 4.4.3 we show that this may not be generally possible by considering a toy model of interactions of microscopic particles (cf. the “neutral mass” problem). However, this problem occurs only for the BSW-type kinematics. Thus, the Schnittman variant again fares better. The problem is actually related to other two caveats for microscopic particles spotted earlier [80, 81]. As the energy of (nearly) critical particles is proportional to their charge, the (nearly) critical microscopic particles need to be highly relativistic (i.e. the “energy feeding” problem), and also the produced particle must have a higher charge than the initial one, which limits the efficiency. Finally, we show that the energy feeding problem for microscopic particles may be reduced by six orders of magnitude if we go from the maximal value of the black hole charge for the Reissner-Nordström solution to some minimal value required for the processes to be possible. Despite this, the critical microscopic particles would still have to be highly relativistic, which is in sharp contrast to the behaviour for a small black hole charge (“mega-BSW effect”) seen for the equatorial electrogeodesic case in 3.5.5.

## 4.2 Motion and collisions of test particles along the axis

Let us again start from a general axially symmetric stationary metric (2.18) in the form

$$\mathbf{g} = -N^2 \mathbf{d}t^2 + g_{\varphi\varphi} (\mathbf{d}\varphi - \omega \mathbf{d}t)^2 + g_{rr} \mathbf{d}r^2 + g_{\vartheta\vartheta} \mathbf{d}\vartheta^2 . \quad (4.1)$$

The metric components  $g_{\varphi\varphi}, g_{rr}, g_{\vartheta\vartheta}$  and functions  $N, \omega$  are independent of  $t$  and  $\varphi$ ; the metric is suitable to describe an equilibrium state of a black hole. We consider also an electromagnetic field with potential in the form

$$\mathbf{A} = A_t \mathbf{d}t + A_\varphi \mathbf{d}\varphi , \quad (4.2)$$

with  $A_t, A_\varphi$  independent of  $t$  and  $\varphi$ . We assume that the outer black-hole horizon (where  $N = 0$ ) corresponds to  $r = r_+$ . For extremal black holes, we denote the position of their degenerate horizon by  $r = r_0$ .

### 4.2.1 Equations of motion and effective potential

Let us consider the motion of charged test particles along the axis of symmetry. The (semi)axis forms a two-dimensional submanifold. We can use two integrals of motion therein, which are related to the Killing vector  $\partial/\partial t$  and to the normalisation of the momentum. The axial motion is thus fully integrable. The first-order equations of motion for a particle with rest mass  $m$  and charge  $q$  read

$$p^t = \frac{E + qA_t}{N^2}, \quad p^r = \sigma \sqrt{\frac{1}{N^2 g_{rr}} [(E + qA_t)^2 - m^2 N^2]}. \quad (4.3)$$

Here  $E$  has the interpretation of the energy of the particle and  $\sigma = \pm 1$  distinguishes the outward/inward radial motion.

The motion can be forbidden in some intervals of  $r$  due to the presence of the square root in the expression for  $p^r$ ; we require  $(p^r)^2 > 0$ . Let us assume that the product  $N^2 g_{rr}$  (which is equal to the volume element at the axis) is finite and non-vanishing at the axis, even for  $N \rightarrow 0$ . For photons, we put  $m = q = 0$ , and their kinematics is thus described by only one parameter  $E$ . Their motion is allowed for any  $E \neq 0$ . In order to have  $p^t > 0$ , we restrict to  $E > 0$ .

On the other hand, the kinematics of massive particles is characterised by two parameters  $\varepsilon \equiv E/m$  and  $\tilde{q} \equiv q/m$  (specific energy and specific charge). Denoting

$$W = (\varepsilon + \tilde{q}A_t)^2 - N^2, \quad (4.4)$$

the condition for the motion to be allowed can be stated as  $W \geq 0$ . Furthermore, since  $N^2 \geq 0$  outside of the black hole, we can (analogously to (3.15)) prescribe the decomposition of  $W$ ,

$$W = (\varepsilon - V_+) (\varepsilon - V_-), \quad (4.5)$$

in terms of  $V_\pm$  that read

$$V_\pm = -\tilde{q}A_t \pm N. \quad (4.6)$$

In order for  $W$  to be non-negative, it must hold either  $\varepsilon \geq V_+$  or  $\varepsilon \leq V_-$ . However, only the first variant is consistent with  $p^t > 0$ . Thus, we define  $V \equiv V_+$  and consider only  $\varepsilon \geq V$  as the condition for the motion to be allowed.  $\varepsilon = V$  is the condition for a turning point.

## 4.2.2 Critical particles and collision energy

Conditions  $(p^r)^2 > 0$  and  $p^t > 0$  noted above have further implications. Particles with  $E + qA_t^H > 0$  ( $A_t^H$  denotes  $A_t$  at  $r_+$ ) can fall into the black hole. For photons, this is the sole option as they have  $E > 0$ ,  $q = 0$ . Thus, unlike in the equatorial case (see e.g. [72, 74]), photons along the axis are not so interesting. Turning to massive, charged particles, there is also a possibility for  $\varepsilon + \tilde{q}A_t^H < 0$ , which corresponds to particles that cannot get close to the black hole, so it is also uninteresting for a generalised BSW effect. However, we can consider massive, charged particles with  $\varepsilon + \tilde{q}A_t^H = 0$ . These are on the verge between the previous cases, and hence they are usually called critical particles.<sup>1</sup> (To complement, particles that are not critical are called usual in the literature.) Critical particles appear to have a turning point at the horizon radius, as seen e.g. through the fact that their specific energy,  $\varepsilon_{\text{cr}}$ , is equal to the value of the effective potential at the horizon (cf. also (3.27))

$$\varepsilon_{\text{cr}} = -\tilde{q} A_t|_{r=r_+} = V|_{r=r_+} . \quad (4.7)$$

Nevertheless, their trajectories actually do not reach a turning point, which we discuss in the next section. Why are the critical particles interesting for collision processes close to the horizon?

The formula for centre-of-mass collision energy reads (see e.g. [57] for more details)

$$E_{\text{CM}}^2 = m_1^2 + m_2^2 - 2g_{\alpha\beta}p_{(1)}^\alpha p_{(2)}^\beta . \quad (4.8)$$

---

<sup>1</sup>Some authors (see e.g. [53]) define the critical particles in a different way, such that they are on the brink of being able to reach the black hole *from infinity*. In the present thesis, we follow the *local* definition (cf. [63]), which is more general. Both notions become compatible for extremal, asymptotically flat black hole spacetimes.

Plugging in the equations of axial motion (4.3), we get

$$E_{\text{CM}}^2 = m_1^2 + m_2^2 + 2 \frac{(E_1 + q_1 A_t)(E_2 + q_2 A_t)}{N^2} - \sigma_1 \sigma_2 \frac{2}{N^2} \sqrt{(E_1 + q_1 A_t)^2 - m_1^2 N^2} \sqrt{(E_2 + q_2 A_t)^2 - m_2^2 N^2} . \quad (4.9)$$

In order to consider the  $N \rightarrow 0$  limit (i.e. the collision point arbitrarily close to the horizon radius) in the case of a collision involving a critical particle, we examine the expansion of  $W$  around  $r_+$  with  $\varepsilon + \tilde{q}A_t^{\text{H}} = 0$ :

$$W \doteq - \left. \frac{\partial(N^2)}{\partial r} \right|_{r=r_+} (r - r_+) + \left[ \tilde{q}^2 \left( \frac{\partial A_t}{\partial r} \right)^2 - \frac{1}{2} \frac{\partial^2(N^2)}{\partial r^2} \right] \Big|_{r=r_+} (r - r_+)^2 + \dots \quad (4.10)$$

The first radial derivative of  $N^2$  at the horizon is proportional to surface gravity of the horizon and is non-negative. Let us first consider a generic, subextremal black hole (with non-zero surface gravity). We see from (4.10) that for some  $r$  sufficiently close to  $r_+$ , expression  $W$  will become negative due to the linear term and, therefore, critical particles cannot approach  $r_+$  for subextremal black holes (note that  $W$  appears under the square root in (4.3); cf. (4.4)). In order to consider collisions with (precisely) critical particles arbitrarily close to the horizon radius, we thus have to turn to extremal black holes (see e.g. [62, 63, 113] for more detailed analysis). Then we can use  $N^2 = (r - r_0)^2 \tilde{N}^2$ , where  $\tilde{N}^2$  can be (at least formally) defined as

$$\tilde{N}^2 \equiv \sum_{n=2}^{\infty} \frac{1}{n!} \frac{\partial^n(N^2)}{\partial r^n} (r - r_0)^{n-2} . \quad (4.11)$$

Evaluating (4.9) for a collision of a critical particle 1 and a usual particle 2, we find that the leading order behavior in the  $r \rightarrow r_0$  limit is

$$E_{\text{CM}}^2 \approx \frac{2}{r - r_0} \left\{ \frac{E_2 + q_2 A_t}{\tilde{N}^2} \left[ q_1 \frac{\partial A_t}{\partial r} \mp \sqrt{q_1^2 \left( \frac{\partial A_t}{\partial r} \right)^2 - m_1^2 \tilde{N}^2} \right] \right\} \Big|_{r=r_0, \vartheta=0} . \quad (4.12)$$

The  $\mp$  sign corresponds to  $\sigma_1 \sigma_2 = \pm 1$ . However, for the usual particle one should consider only  $\sigma_2 = -1$  (cf. [79] for detailed reasoning). With this restriction, the  $\mp$  sign means just  $\sigma_1 = \mp 1$ . The scenario with incoming particle 1 (upper sign,  $\sigma_1 = -1$ ) was first described by Bañados, Silk and West for the extremal Kerr case in [53] and was generalised to

charged particles in [66]. The collision process with an outgoing critical particle ( $\sigma_1 = +1$ ) was introduced by Schnittman [74] in a numerical study focused again on uncharged particles in the extremal Kerr spacetime. (Analytical treatment of the Schnittman process was considered e.g. in [75, 76].)

### 4.2.3 Motion towards $r_0$ , nearly critical particles and class II critical particles

We have seen that for critical particles the centre-of-mass collision energy with an usual particle diverges in the limit  $r \rightarrow r_0$ . However, the energy attainable in such a thought experiment is always finite, although unbounded, because critical particles are not able to reach  $r_0$  in a finite proper time. To demonstrate this, let us expand the equation of radial motion (4.3) near the radius of the degenerate horizon,

$$\frac{p^r}{m} \equiv \frac{dr}{d\tau} \doteq - (r - r_0) \sqrt{\frac{1}{2\tilde{N}^2 \tilde{g}_{rr}} \frac{\partial^2 W}{\partial r^2}} \Big|_{r=r_0} + \dots \quad (4.13)$$

We denoted (cf. (2.19))

$$\tilde{g}_{rr} \equiv \frac{N^2 g_{rr}}{\tilde{N}^2} . \quad (4.14)$$

Then the approximate solution valid for late proper times is an exponential “relaxation” towards  $r_0$

$$r \doteq r_0 \left[ 1 + \exp\left(-\frac{\tau}{\tau_{\text{relax}}}\right) \right] + \dots \quad (4.15)$$

$$\frac{1}{\tau_{\text{relax}}} \equiv \sqrt{\frac{1}{2\tilde{N}^2 \tilde{g}_{rr}} \frac{\partial^2 W}{\partial r^2}} \Big|_{r=r_0} . \quad (4.16)$$

Note that this result has the same form that follows from (3.34) for charged critical particles moving in the equatorial plane. The agreement is due to the fact that in both cases we can write

$$\frac{dr}{d\tau} = \sigma \sqrt{\frac{W}{\tilde{N}^2 \tilde{g}_{rr}}} . \quad (4.17)$$

(Here  $W$  is given by (3.14) in the equatorial case and by (4.4) in the axial case.)

Since no critical particle can ever reach  $r_0$ , the collision with another particle can only happen at some radius  $r_C > r_0$ . Because of this, the difference between usual and critical

particles gets blurred. Indeed, a usual particle with energy very close to the critical energy will effectively behave as a critical particle at some radius  $r_C$  close to  $r_0$  provided that

$$\left|1 - \frac{\varepsilon}{\varepsilon_{\text{cr}}}\right| \sim \left(\frac{r_C}{r_0} - 1\right). \quad (4.18)$$

Such particles are called nearly critical.

Nearly critical particles with  $\varepsilon < \varepsilon_{\text{cr}}$  cannot fall into the black hole, and they have a turning point at some radius smaller than  $r_C$ . Thus, it makes sense to consider also the outgoing nearly critical particles. Furthermore, if the turning point is much closer to  $r_0$  than the desired collision point  $r_C$  or, more precisely, if

$$0 < \left(1 - \frac{\varepsilon}{\varepsilon_{\text{cr}}}\right) \ll \left(\frac{r_C}{r_0} - 1\right), \quad (4.19)$$

such *outgoing* nearly critical particles effectively behave as precisely critical at  $r_C$ . This is the motivation behind including outgoing critical particles in the Schnittman process.

Let us recall that the relaxation time  $\tau_{\text{relax}}$  in (4.16) can turn out to be infinite, and then the leading order of the expansion of  $W$  in  $r - r_0$  for a critical particle is the third one instead of the second. The critical particles with this property are called the “class II” critical particles by Harada and Kimura [69] (“class I” standing for the generic critical particles with finite  $\tau_{\text{relax}}$ ). Since the equation (4.17) takes the same form (in terms of appropriate  $W$ ) for both equatorial and axial motion, the general results for class II critical particles presented in 3.4.5 are relevant also for the present discussion.

## 4.3 Kinematic restrictions

### 4.3.1 General formulae for critical particles

Critical particles can, in principle, approach the horizon radius only for extremal black holes. Whether their motion towards  $r_0$  is really allowed will depend on their values of charge  $\tilde{q}$  as well as on the properties of a particular extremal black hole spacetime.

One way to figure out the conditions for the approach to be allowed is to look at the expansions of the radial equation of motion. For class I critical particles the relaxation time  $\tau_{\text{relax}}$  in (4.16) must be a real number, and for class II critical particles the square root on the right-hand side of (3.59) must also be real.

The other way is to consider the  $\varepsilon \geq V$  condition, similarly as we did in 3.4.1 and 3.4.3. Let us recall that the energy  $\varepsilon_{\text{cr}}$  of a critical particle is equal to the value of  $V$  at  $r_0$  (4.7). Therefore, if the effective potential  $V$  grows for  $r > r_0$ , we will get  $\varepsilon_{\text{cr}} < V$ , and the motion of the critical particle towards  $r_0$  is forbidden. Thus, to see whether a critical particle can approach  $r_0$ , we need to check whether the first radial derivative of  $V$  at  $r_0$  is negative. Furthermore, we should also look at the second derivative of  $V$  at  $r_0$ , since it will determine the trend of  $V$ , if the first one is zero (cf. 3.4.6).

However, both approaches are equivalent. For critical particles with  $p^t > 0$ , it can be shown (see Appendix C.1.2) that

$$\text{sgn} \left. \frac{\partial^2 W}{\partial r^2} \right|_{r=r_0} = - \text{sgn} \left. \frac{\partial V}{\partial r} \right|_{r=r_0} . \quad (4.20)$$

An analogous statement (cf. (C.10)) can be made for class II critical particles, and for our present setup, it actually holds that

$$\left. \frac{\partial^3 W}{\partial r^3} \right|_{r=r_0, \vartheta=0} = -6 \left( \tilde{N} \left. \frac{\partial^2 V}{\partial r^2} \right) \right|_{r=r_0, \vartheta=0} . \quad (4.21)$$

Let us proceed with the analysis based on  $V$ . For an extremal black hole, it is possible to write down an arbitrary ( $n$ -th) order derivative of  $V$  with respect to  $r$  as follows:

$$\frac{\partial^n V}{\partial r^n} = -\tilde{q} \frac{\partial^n A_t}{\partial r^n} + n \frac{\partial^{n-1} \tilde{N}}{\partial r^{n-1}} + (r - r_0) \frac{\partial^n \tilde{N}}{\partial r^n} . \quad (4.22)$$

At  $r_0$ , this simplifies to

$$\left. \frac{\partial^n V}{\partial r^n} \right|_{r=r_0} = \left( -\tilde{q} \frac{\partial^n A_t}{\partial r^n} + n \frac{\partial^{n-1} \tilde{N}}{\partial r^{n-1}} \right) \Big|_{r=r_0, \vartheta=0} . \quad (4.23)$$

It is possible to solve for the value of  $\tilde{q}$ , for which this expression becomes zero, and evaluate also the corresponding energy of the critical particle using (4.7). In particular, for  $n = 1$ , we get

$$\tilde{q}_{\text{II}} = \left. \frac{\tilde{N}}{\frac{\partial A_t}{\partial r}} \right|_{r=r_0, \vartheta=0} , \quad (4.24)$$

and

$$\varepsilon_{\text{II}} = - \left. \frac{\tilde{N} A_t}{\frac{\partial A_t}{\partial r}} \right|_{r=r_0, \vartheta=0} . \quad (4.25)$$

If we denote

$$\alpha \equiv - \left. \frac{\frac{\partial A_t}{\partial r}}{\tilde{N} A_t} \right|_{r=r_0, \vartheta=0}, \quad (4.26)$$

and assume  $\alpha > 0$  (this corresponds to a plausible choice of gauge constant for  $A_t$ ), we can state that class I critical particles are allowed to approach  $r_0$ , whenever  $\alpha\varepsilon > 1$ . For class II critical particles, it holds  $\alpha\varepsilon = 1$ . Plugging (4.24) into (4.23) with  $n = 2$ , we obtain

$$\left. \frac{\partial^2 V}{\partial r^2} \right|_{r=r_0} = \left( -\tilde{N} \frac{\frac{\partial^2 A_t}{\partial r^2}}{\frac{\partial A_t}{\partial r}} + 2 \frac{\partial \tilde{N}}{\partial r} \right) \Big|_{r=r_0, \vartheta=0}. \quad (4.27)$$

Class II critical particles are allowed to approach  $r_0$  if this expression is, for a given spacetime, negative.

Let us note that for a particle of any kind moving at a radius  $r_C$  close to  $r_0$ , the expansion of  $V$  to linear order can be expressed as

$$V = \varepsilon_{\text{cr}} + \tilde{N}_{\text{H}} (1 - \alpha\varepsilon_{\text{cr}}) (r_C - r_0) + \dots \quad (4.28)$$

Here  $\varepsilon_{\text{cr}}(\tilde{q})$  is given by (4.7); if  $\alpha\varepsilon_{\text{cr}}(\tilde{q}) > 1$ , the linear coefficient is negative. However, for particles that behave as nearly critical around  $r_C$ , their actual energy  $\varepsilon$  is by definition (4.18) close to the critical one. Therefore, we can use  $\alpha\varepsilon > 1$  also as a condition for the existence of escape trajectories of nearly critical particles (unless  $\alpha\varepsilon$  is very close to 1), which is discussed in 4.4.2.

### 4.3.2 Results for the Kerr-Newman solution

Let us again consider the Kerr-Newman solution (1.1) with mass  $M$ , angular momentum  $aM$  (convention  $a \geq 0$ ), and charge  $Q$ , with the metric in the form (4.1), i.e.

$$\mathbf{g} = -\frac{\Delta\Sigma}{\mathcal{A}} \mathbf{d}t^2 + \frac{\mathcal{A}}{\Sigma} \sin^2 \vartheta \left[ \mathbf{d}\varphi - \frac{a}{\mathcal{A}} (2Mr - Q^2) \mathbf{d}t \right]^2 + \frac{\Sigma}{\Delta} \mathbf{d}r^2 + \Sigma \mathbf{d}\vartheta^2, \quad (4.29)$$

where

$$\begin{aligned}
\Delta &= r^2 - 2Mr + a^2 + Q^2 , \\
\Sigma &= r^2 + a^2 \cos^2 \vartheta , \\
\mathcal{A} &= (r^2 + a^2)^2 - \Delta a^2 \sin^2 \vartheta .
\end{aligned} \tag{4.30}$$

In the extremal case  $M^2 = Q^2 + a^2$ , so  $\Delta$  has a double root at  $r_0 \equiv M$ . The electromagnetic potential is

$$\mathbf{A} = -\frac{Qr}{\Sigma} (\mathbf{d}t - a \sin^2 \vartheta \mathbf{d}\varphi) . \tag{4.31}$$

The effective potential for axial electrogeodesic motion (as given in (4.7) in [116]) reads

$$V = \frac{\tilde{q}Qr}{r^2 + a^2} + \sqrt{\frac{\Delta}{r^2 + a^2}} . \tag{4.32}$$

Let us note that for  $a = 0$ ,  $Q^2 = M^2$  and  $\tilde{q} = \text{sgn } Q$  we get  $V \equiv 1$ .

Particles moving along the axis of an extremal Kerr-Newman black hole are critical if their specific energy and charge are related by

$$\varepsilon_{\text{cr}} = \frac{\tilde{q}Q\sqrt{Q^2 + a^2}}{Q^2 + 2a^2} . \tag{4.33}$$

In general, the first radial derivative of  $V$  at the degenerate horizon is

$$\left. \frac{\partial V}{\partial r} \right|_{r=M} = -\tilde{q} \frac{Q^3}{(Q^2 + 2a^2)^2} + \frac{1}{\sqrt{Q^2 + 2a^2}} . \tag{4.34}$$

It becomes zero for particles with the specific charge given by

$$\tilde{q}_{\text{II}} = \frac{(Q^2 + 2a^2)^{\frac{3}{2}}}{Q^3} , \tag{4.35}$$

and if these particles are critical, their specific energy is

$$\varepsilon_{\text{II}} \equiv \frac{1}{\alpha} = \frac{\sqrt{(Q^2 + a^2)(Q^2 + 2a^2)}}{Q^2} . \tag{4.36}$$

Class I critical particles are allowed to approach  $r = M$ , whenever  $\alpha\varepsilon > 1$ . For class II critical particles  $\alpha\varepsilon = 1$ . Let us note that  $\alpha \leq 1$  for any  $Q$  and  $a$ . Therefore the condition

$\alpha\varepsilon > 1$  implies  $\varepsilon > 1$  (i.e.  $E > m$ ). No bound critical particles can approach  $r = M$  along the axis of the extremal Kerr-Newman spacetime.<sup>2</sup> Furthermore, we can see that  $\alpha \sim Q^2$ . Thus, for  $Q$  very small, only highly relativistic critical particles ( $\varepsilon \gg 1$ ) can approach  $r = M$  along the axis.<sup>3</sup>

The second derivative of  $V$  at  $r = M$  is

$$\left. \frac{\partial^2 V}{\partial r^2} \right|_{r=M} = 2\tilde{q}Q\sqrt{Q^2 + a^2} \frac{Q^2 - 2a^2}{(Q^2 + 2a^2)^3} - \frac{2\sqrt{Q^2 + a^2}}{(Q^2 + 2a^2)^{\frac{3}{2}}}. \quad (4.37)$$

Inserting (4.35), or evaluating (4.27), we get

$$\left. \frac{\partial^2 V}{\partial r^2} \right|_{r=M} = -\frac{4a^2\sqrt{Q^2 + a^2}}{Q^2(Q^2 + 2a^2)^{\frac{3}{2}}}. \quad (4.38)$$

This quantity is negative for  $a \neq 0$ , and it blows up for  $Q \rightarrow 0$ . Thus, class II critical particles are allowed to approach  $r = M$  along the axis, except for the cases of the extremal Kerr solution (where there are no critical particles moving along the axis whatsoever) and of the extremal Reissner-Nordström solution (where  $V$  becomes constant for  $\alpha\varepsilon = 1$ ).

## 4.4 Energy extraction

### 4.4.1 Application of conservation laws

Let us now explore, in a simple setup, the possibility of energy extraction from black holes either by a BSW-type process occurring between particles moving along the axis, or by its Schnittman variant. We shall consider a scenario in which a (nearly) critical particle 1 collides with an incoming usual particle 2 close to the horizon radius  $r_0$ , they interact, and two new particles, 3 and 4, are produced. We impose the conservation of charge,

$$q_1 + q_2 = q_3 + q_4, \quad (4.39)$$

---

<sup>2</sup>This differs from the equatorial case; see 3.5.4, in particular (3.101).

<sup>3</sup>Similarly, looking at the boundary value for charge  $\tilde{q}_{\text{II}}$  (4.35), we see that only critical particles with  $|\tilde{q}| > 1$  can approach  $r = M$ . And due to  $Q^{-3}$  dependence in (4.35), for  $|Q| \ll M$ , only critical particles with  $|\tilde{q}| \gg \varepsilon \gg 1$  can approach  $r = M$ .

and the conservation of (both components of) momentum at the point of collision. The time component gives us the conservation of energy

$$E_1 + E_2 = E_3 + E_4 . \quad (4.40)$$

In order to make the best use of the conservation of radial momentum, we shall note that for usual particles near the horizon, the following combination of the momentum components cancels up to the first order in  $r - r_0$ :

$$N^2 p^t - \sigma N \sqrt{g_{rr}} p^r \sim (r - r_0)^2 , \quad (4.41)$$

whereas with the opposite sign

$$N^2 p^t + \sigma N \sqrt{g_{rr}} p^r \doteq 2 (E + q A_t^H) + \dots \quad (4.42)$$

contributes to the zeroth order. In contrast, for the critical particles, or particles that behave as nearly critical around a desired collision radius  $r_C$ , both expressions are of the first order in  $r_C - r_0$ ,

$$N^2 p^t \pm N \sqrt{g_{rr}} p^r \sim (r_C - r_0) . \quad (4.43)$$

To account consistently (at each order) for the effect of a particle labeled  $i$ , which is not precisely critical, yet nearly critical, we define a formal expansion:

$$E_{\text{cr}} - E_i = C_{(i,1)} (r_C - r_0) + C_{(i,2)} (r_C - r_0)^2 + \dots \quad (4.44)$$

Now, let us sum the conservation laws for the time and radial components of the momenta as follows:

$$N^2 (p_{(1)}^t + p_{(2)}^t) + N \sqrt{g_{rr}} (p_{(1)}^r + p_{(2)}^r) = N^2 (p_{(3)}^t + p_{(4)}^t) + N \sqrt{g_{rr}} (p_{(3)}^r + p_{(4)}^r) . \quad (4.45)$$

Considering expansion of this formula in  $r_C - r_0$  and using (4.41),(4.42) and (4.43), we reach a conclusion (analogously to [72, 80]) that collision between a (nearly) critical particle 1 and an incoming ( $\sigma_2 = -1$ ) usual particle 2 at a radius  $r_C$  close to  $r_0$  must necessarily lead to the production of an incoming<sup>4</sup> usual particle, to be denoted 4, and a

---

<sup>4</sup>See also [79] for a more detailed discussion on why it is impossible to produce outgoing usual particles

nearly critical particle, which we will label as 3.

Then, the leading (first) order of (4.45), divided by  $\tilde{N}_H$ , implies

$$\alpha E_1 + \sigma_1 \sqrt{\alpha^2 E_1^2 - m_1^2} = \alpha E_3 - \tilde{C}_3 + \sigma_3 \sqrt{(\alpha E_3 - \tilde{C}_3)^2 - m_3^2}. \quad (4.46)$$

Here again  $\sigma_1 = -1$  corresponds to the BSW-type process, whereas  $\sigma_1 = +1$  to the Schnittman variant (and  $\sigma_3 = \pm 1$  to outgoing/incoming particle 3). Above we introduced

$$\tilde{C}_3 \equiv \frac{C_{(3,1)}}{\tilde{N}_H}, \quad (4.47)$$

and, for simplification, we chose the particle 1 precisely critical ( $E_1 = E_{\text{cr}}$ , and hence  $\tilde{C}_1 = 0$ ), which means that we are using the approximation (4.19) for the Schnittman process.

All the information about the spacetime coming into (4.46) is carried by the parameter  $\alpha$  (defined in (4.26)). Furthermore, if we denote the whole left-hand side of (4.46) as a new parameter<sup>5</sup>

$$A_1 \equiv \alpha E_1 + \sigma_1 \sqrt{\alpha^2 E_1^2 - m_1^2}, \quad (4.48)$$

this parameter will express all the dependence on the properties of particle 1. Since we assumed  $p^t > 0$  and particle 1 cannot be massless, we can make sure that  $A_1 > 0$ .

Because we absorbed the difference between the BSW-type process and the Schnittman variant into the definition of the parameter  $A_1$ , the discussion of kinematic regimes in the next section is the same for both. However, if we consider a particular model process, a significant distinction may appear, as we discuss in 4.4.3.

## 4.4.2 Kinematic regimes

Equation (4.46) enables us to determine whether and under which circumstances particle 3 can escape and extract energy from a black hole. Particle 4 necessarily falls into the black hole, which is the essence of a Penrose process. Let us note that particle 3 can actually be produced in four different kinematic regimes, depending on the combination

---

near the horizon.

<sup>5</sup>In order to keep the same letter for this quantity (introduced in [72] for the vacuum case, and followed e.g. by [73, 80]), we use a different font to distinguish it from the components of the electromagnetic potential.

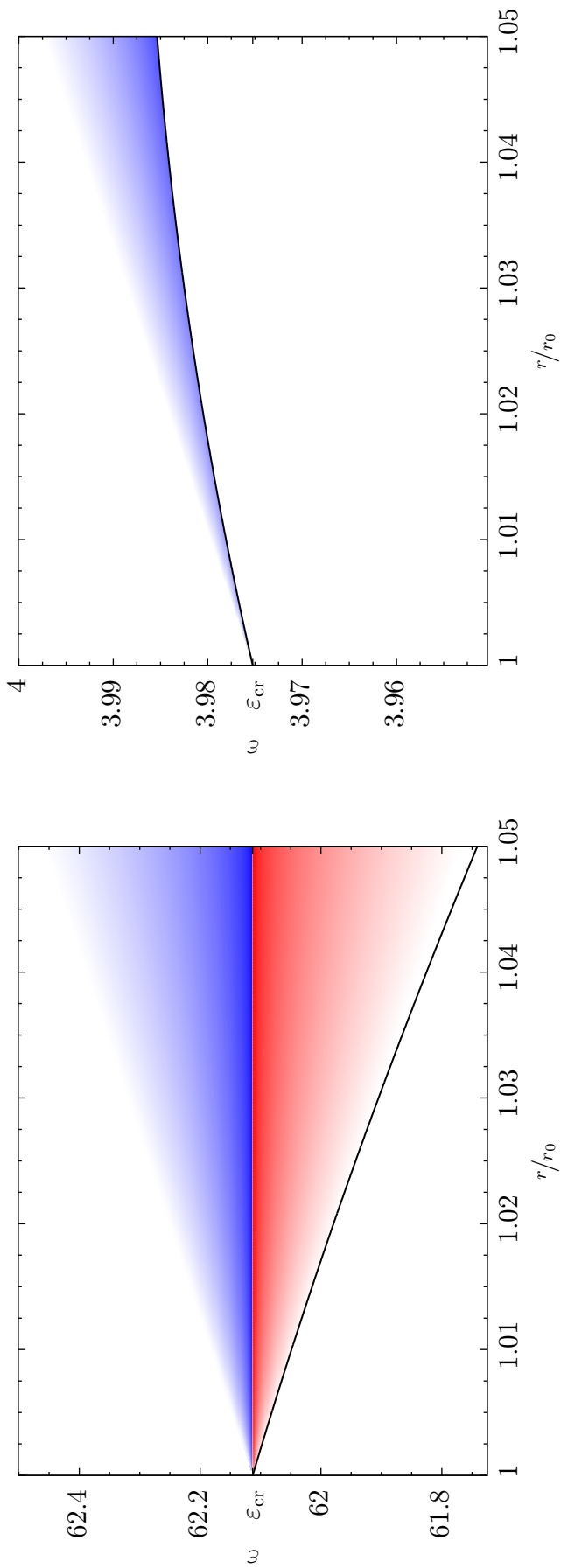


Figure 4.1: Effective potential  $V$  near the horizon radius  $r_0 = M$  of the extremal Kerr-Newman black hole with  $Q/M = 1/\sqrt{5}$ ,  $a/M = 2/\sqrt{5}$ . The shading represents nearly critical particles; the varying height of the shaded areas illustrates the varying range of energies of particles that behave as nearly critical at a given  $r$ . The red color corresponds to “+” ( $\tilde{C} > 0$ ), blue to “-” ( $\tilde{C} < 0$ ). (See (4.44) and (4.47) for the definition of  $\tilde{C}$ .) **Left:** For particles with  $\tilde{q} = 250$ ,  $V$  is decreasing, and thus both signs of  $\tilde{C}$  are allowed. **Right:** For  $\tilde{q} = 16$ ,  $V$  is increasing, and thus nearly critical particles can exist only with  $\tilde{C} < 0$ . It can be seen that particles that behave as nearly critical at lower values of  $r$  will get reflected by  $V$  at some higher values of  $r$ , and thus they cannot escape.

of the sign of  $\tilde{C}_3$  and the sign variable  $\sigma_3$ . Following the classification in [80], we will refer to the regimes with  $C_3 > 0$  as “+”,  $C_3 < 0$  as “-”,  $\sigma_3 = +1$  as “OUT” and  $\sigma_3 = -1$  as “IN”.

We analyse the different kinematic regimes from several points of view. First, we should understand which combinations are compatible with particle 3 escaping from the vicinity of the black hole (see Figure 4.1 for illustration). For simplicity, let us assume a situation when effective potential  $V$  for particle 3 is well approximated by a linear function around  $r_C$  (i.e. that  $\alpha\varepsilon_3$  is not very close to 1).

By definition,  $\tilde{C}_3 > 0$  implies  $\varepsilon_3 < \varepsilon_{\text{cr}}$ , and hence  $\varepsilon_3 < V$  (forbidden motion) at the horizon. Therefore, a particle produced with  $\tilde{C}_3 > 0$  cannot fall into the black hole, and even if it is initially incoming, it must reach a turning point and turn to outgoing. Moreover, since it must hold that  $\varepsilon_3 > V$  at the radius  $r_C$  where the particle is produced, for such a particle the effective potential  $V$  must be decreasing at  $r_0$  (i.e.  $\alpha\varepsilon_3 > 1$ ). Thus, we see that in kinematic regimes OUT+ and IN+ the local escape condition is satisfied automatically.

On the other hand, particle 3 with  $\tilde{C}_3 < 0$  will have  $\varepsilon_3 > V$  both at the horizon and at the point where it is produced (and also in between these points due to the assumption of  $V$  being well approximated by a linear function). Thus, if a particle 3 with  $\tilde{C}_3 < 0$  is not produced as outgoing, it will fall into the black hole. Furthermore, if the effective potential  $V$  is growing at  $r_0$ , i.e.  $\alpha\varepsilon_3 < 1$ , particle 3 will have a turning point at some radius greater than  $r_C$  and it will not be able to escape even if it is produced as outgoing. Therefore, in the IN- regime the escape is impossible and for OUT- it depends on the trend of the effective potential  $V$ . (These findings are summarised in Table 4.1.)

Second, we should determine to what ranges of parameters of particle 3 do the different kinematic regimes correspond. Then we can infer, whether the impossibility of escape in the IN- regime leads to some bounds on parameters of the escaping particles, and more specifically, whether it does limit the efficiency of the collisional Penrose process, which is defined as

$$\eta = \frac{E_3}{E_1 + E_2} . \quad (4.49)$$

Table 4.1: The four kinematic regimes for production of particle 3.

	$\sigma_3 = +1$	$\sigma_3 = -1$
$\tilde{C}_3 > 0$	OUT+ $m_3 < A_1, E_3 > \mu$ Guaranteed to escape	IN+ $m_3 > A_1, E_3 > \mu$ Guaranteed to escape
$\tilde{C}_3 \leq 0$	OUT- $m_3 < A_1, E_3 \leq \mu$ Escapes if $\alpha E_3 > m_3$	IN- $m_3 > A_1, E_3 \leq \mu$ Falls inside the black hole

Solving (4.46) to express  $\tilde{C}_3$  and  $\sigma_3$ , we get

$$\tilde{C}_3 = \alpha E_3 - \frac{1}{2} \left( A_1 + \frac{m_3^2}{A_1} \right), \quad (4.50)$$

$$\sigma_3 = \text{sgn} \left( A_1 - \frac{m_3^2}{A_1} \right) \equiv \text{sgn}(A_1 - m_3). \quad (4.51)$$

From the second equation we see that the value of parameter  $A_1$  forms a threshold for  $m_3$ . If the interaction produces particle 3 with a mass above the threshold, the particle must be incoming, if its mass is below the threshold, it must be outgoing.

Turning to parameter  $\tilde{C}_3$  note that the solution (4.50) satisfies the inequality

$$\tilde{C}_3 \leq \alpha E_3 - m_3. \quad (4.52)$$

Therefore, if  $\tilde{C}_3 > 0$ , we must have  $\alpha \varepsilon_3 > 1$ , as we anticipated because particles with  $\varepsilon < \varepsilon_{\text{cr}}$  can be produced only if effective potential  $V$  is decreasing at  $r_0$ . (In general, one can see from (4.28), (4.44) and (4.47) that (4.52) is actually the linear order of the expansion in  $r_C - r_0$  of the condition  $\varepsilon \geq V$ .)

Let us denote the value of  $E_3$  for which  $\tilde{C}_3 = 0$  as  $\mu$ :

$$\mu = \frac{1}{2\alpha} \left( A_1 + \frac{m_3^2}{A_1} \right). \quad (4.53)$$

This quantity again represents a threshold. If particle 3 is produced with  $E_3 > \mu$ , it must have such a value of charge that  $E_{\text{cr}}(q_3) > E_3$ ; if  $E_3 < \mu$ , it must hold that  $E_{\text{cr}}(q_3) < E_3$ . (Here  $E_{\text{cr}}(q_3) \equiv m_3 \varepsilon_{\text{cr}}(q_3)$ ; cf. (4.7).)

A summary of the results about the four kinematic regimes is given in Table 4.1. Let us note that these results resemble those for the special case of the Reissner-Nordström

solution studied in [80]. In particular, there is still no unconditional upper bound on the energy or mass of particle 3, in contrast with the geodesic (equatorial) case [72, 73]. (Such a possibility is often called the super-Penrose process.) However, the impossibility of escape in the IN– regime means that whenever particle 3 is produced with the mass above the threshold  $A_1$ , its energy also must be above the threshold  $\mu$  (which therefore acts as a lower bound on  $E_3$  in this case). Conversely, whenever particle 3 is produced with  $E_3 \leq \mu$ , it must also have  $m_3 < A_1$ , otherwise it falls into the black hole. These requirements may not be compatible with the properties of a particular type of interaction that is responsible for producing particle 3. This is the third aspect of the kinematic regimes that needs to be examined. In 4.4.3 we consider a toy model, where this limitation gets highlighted (the “neutral mass” problem).

Before carrying out this discussion, let us further note one interesting property of the OUT– regime. Condition  $m_3 < A_1$  (OUT) implies

$$\alpha\mu < A_1 \tag{4.54}$$

due to (4.53). From definition (4.48), we can derive an upper bound on  $A_1$ . For the BSW-type process ( $\sigma_1 = -1$ ), we get  $A_1 < \alpha E_1$ , whereas for the Schnittman variant ( $\sigma_1 = 1$ ), it is  $A_1 < 2\alpha E_1$ . Combining with (4.54), we get  $\mu < E_1$  for the BSW-type effect and  $\mu < 2E_1$  for the Schnittman one. Using also the “–” condition  $E_3 \leq \mu$ , we get  $E_3 < E_1$  and  $E_3 < 2E_1$ , respectively. Therefore, we see that  $E_3$  can never exceed  $E_1$  in the OUT– regime for the BSW-type process (preventing net energy extraction), whereas for the Schnittman variant  $E_3 > E_1$  is possible in this regime.

### 4.4.3 Discussion of caveats

#### 4.4.3.1 Energy feeding problem

High efficiency  $\eta$  of the collisional Penrose process means by definition (4.49) that we can gain much more energy than we invest. However, despite a high value of  $\eta$  the process may be “inefficient” if the invested energy itself needs to be high in order for the process to occur. We call this the “energy feeding” problem. There are two different sources of this problem for particles moving along the axis. One of them was already mentioned in the discussion below equation (4.36): for the extremal Kerr-Newman spacetime with a

small value of charge ( $|Q| \ll M$ ), only highly relativistic critical particles can approach  $r = M$  along the axis. This does not depend on the nature of the particles.

In contrast, the second source of the energy feeding problem comes into play only if we consider specifically processes involving microscopic particles that exhibit charge quantisation. For all those particles (known in nature) their specific charge  $|\tilde{q}| \gg 1$ . However, the specific energy of (nearly) critical particles is proportional to their specific charge (approximately) through relation (4.7), or, in particular, by relation (4.33) for Kerr-Newman black holes. Therefore, such microscopic particles need to be highly relativistic ( $\varepsilon \gg 1$ , i.e.  $E \gg m$ ) in order to be (nearly) critical. Since the elementary charge is just one order of magnitude short of the Planck mass, they would actually have to be *extremely* relativistic. This issue was previously noted in [81], and it led the authors to introduce macroscopic objects acting as critical particles, which would make  $\varepsilon \sim 1$  possible (note  $\varepsilon > 1$  due to (4.36)).

#### 4.4.3.2 Neutral mass problem

Although energy extraction by processes involving critical microscopic particles is already unfeasible due to the severe energy feeding problem, there are even further restrictions due to particle physics. Since the energy of a (nearly) critical particle is proportional to its charge, we need  $|q_3| > |q_1|$  in order to have  $E_3 > E_1$ . For microscopic particles, this means that we need to turn to interactions involving atomic nuclei. (Let us note that such processes would actually *not* benefit from high  $E_{\text{CM}}$  due to a relatively low binding energy of nuclei, but here we focus on kinematic aspects.) One of the further problems was noted previously in [80]; stable nuclei have values of charge in a range that spans just two orders of magnitude. Thus,  $E_3$  cannot exceed  $E_1$  by more than a factor of  $10^2$ . However, the problems become much deeper, if we focus specifically on the BSW-type mechanism. The mass of stable nuclei generally increases faster than their charge due to an increasing share of neutrons (hence “neutral mass”). Thus, for our model process with  $q_3 > q_1 > 0$  and  $m_3 > m_1$ , it will also be more common than the opposite to have<sup>6</sup>

$$\frac{q_3}{q_1} < \frac{m_3}{m_1} < \frac{m_3^2}{m_1^2}. \quad (4.55)$$

---

<sup>6</sup>Inequality (4.55) could be the “rule of thumb” even for macroscopic particles, as it is harder to hold together larger amounts of charge.

Now we should check whether this inequality is consistent with particle 3 escaping. The problem again stems from the fact that critical microscopic particles are to be immensely relativistic. (At this point we exclude the possibility  $Q \ll M$ , i. e.  $\alpha \ll 1$ , which is revisited in 4.4.3.3.)

Namely, for  $E_1 \gg m_1$  and  $\sigma_1 = -1$  parameter  $A_1$  (4.48) will be very small; it can be approximated as

$$A_1 \doteq \frac{m_1^2}{2\alpha E_1} + \dots \quad (4.56)$$

Given this, parameter  $\mu$  (4.53) gets large, and it is approximated as

$$\mu \approx E_1 \frac{m_3^2}{m_1^2} + \dots \quad (4.57)$$

Since certainly  $A_1 < m_1$  and we assumed  $m_1 < m_3$ , it will hold that  $m_3 > A_1$ . Thus, our nuclear reaction will occur in the IN regime. Condition  $E_3 > \mu$ , which is required for the escape of particle 3 in this regime (cf. Table 4.1), due to (4.57) means

$$\frac{E_3}{E_1} > \frac{m_3^2}{m_1^2}. \quad (4.58)$$

As both energies are (approximately) proportional to the respective charges by the same factor, this translates to the relation

$$\frac{q_3}{q_1} > \frac{m_3^2}{m_1^2}. \quad (4.59)$$

However, this is the inequality opposite to (4.55). Therefore, we conclude that in our “common nuclear process”, particle 3 will be produced in the IN– regime ( $E_3 < \mu$ ) and it will fall into the black hole. Condition (4.59) can be satisfied, e.g. with specific reactions with  $q_3 > q_1 > 0$ ,  $m_3 < m_1$ , which are in principle also possible. Nevertheless, we see that there is a strong limitation on the BSW-type processes with microscopic particles.

However, if we turn to the Schnittman-type kinematics, the neutral mass problem is circumvented. In particular, for  $E_1 \gg m_1$  and  $\sigma_1 = +1$ , parameter  $A_1$  is large, namely

$$A_1 \approx 2\alpha E_1 + \dots \quad (4.60)$$

Hence we infer  $m_3 < A_1$  and particle 3 to be produced in the OUT regime. Parameter  $\mu$

will be large again, but this time dominated by the other term than before, i.e.

$$\mu \approx E_1 + \dots \quad (4.61)$$

Since we assumed  $q_3 > q_1 > 0$ , and hence  $E_3 > E_1$ , particle 3 will be produced in the OUT+ regime and will indeed escape.

#### 4.4.3.3 Specific charge cutoff

The problems arising from the fact that critical microscopic particles have to be immensely relativistic can be reduced for the extremal Kerr-Newman solution if we consider  $Q$  very small ( $|Q| \ll M$ ). However, we cannot decrease the required energy arbitrarily, because we run into the other source of the energy feeding problem, which is the proportionality  $\alpha \sim Q^2$ . Specific charges for all nuclei are roughly the same (of the same order), say  $\tilde{q}_{\text{nucl}}$ . Because of the critical condition (4.33), all critical nuclei will also have values of specific energy of the same order. Thus, there will be a distinct transition.

Let us first consider a general value of  $\tilde{q}$ . Using (4.35) we can define a value  $\tilde{Q}_{\text{min}}$  of the specific charge of the black hole  $\tilde{Q} \equiv Q/M$ , such that for  $\tilde{Q} \text{sgn } \tilde{q} < \tilde{Q}_{\text{min}}$  all the critical particles with the given value of  $\tilde{q}$  would be forbidden to approach  $r = M$ . Using (4.33) or (4.36) we can also evaluate a corresponding specific energy  $\varepsilon_{\text{min}}$ . We obtain

$$\tilde{Q}_{\text{min}} = \sqrt{\frac{2}{1 + |\tilde{q}|^{\frac{2}{3}}}}, \quad \varepsilon_{\text{min}} = \frac{|\tilde{q}|^{\frac{1}{3}}}{\sqrt{2}} \sqrt{1 + |\tilde{q}|^{\frac{2}{3}}}. \quad (4.62)$$

However, for critical nuclei with  $\tilde{q}_{\text{nucl}} \gg 1$ , we can use approximate expressions

$$\tilde{Q}_{\text{min}} \doteq \frac{\sqrt{2}}{\sqrt[3]{\tilde{q}_{\text{nucl}}}}, \quad \varepsilon_{\text{min}} \approx \frac{(\tilde{q}_{\text{nucl}})^{\frac{2}{3}}}{\sqrt{2}}. \quad (4.63)$$

Since  $\tilde{q}_{\text{nucl}}$  is around  $5 \cdot 10^{17}$ , we get  $\tilde{Q}_{\text{min}}$  of order  $10^{-6}$  and  $\varepsilon_{\text{min}}$  around  $5 \cdot 10^{11}$ . Therefore, for extremal Kerr-Newman black holes with  $\tilde{Q} = \tilde{Q}_{\text{min}}$ , the energy feeding problem for microscopic particles is reduced by six orders of magnitude as compared with the extremal Reissner-Nordström case (where  $\varepsilon_{\text{cr}} = \tilde{q}_{\text{nucl}}$ ). Nevertheless,  $\varepsilon_{\text{min}} \gg 1$  in any case. Thus, we can never have non-relativistic critical microscopic particles approaching  $r = M$  along the axis of an extremal Kerr-Newman black hole. This is very different from the “mega-BSW” effect described in Section 3.5.5 for equatorial charged critical particles.



# Chapter 5

## Particle collisions in the equatorial plane: energy extraction

### 5.1 Outline and summary

In Chapter 3, we generalised the BSW effect for charged particles moving in the equatorial plane of an extremal rotating electrovacuum black hole. Now we shall examine the possibilities of energy extraction through this kind of process, including also the Schnittman variant.

In the following, we use the leading-order approximation of momentum conservation law (unlike in Chapter 3, where we studied derivatives of the effective potential of both first and second order). This allows us to use a simplified, robust formalism, which is introduced in Section 5.2. In Section 5.3, we revisit the kinematic restrictions on motion of critical particles studied in Chapter 3, and we calculate precise bounds on the values of angular momentum and charge in the admissible region in the parameter space of critical particles.

We proceed to the energy extraction in Section 5.4. We review the different kinematic regimes, in which nearly critical particle 3 can be produced. Section 5.4.2 contains the main results. We identify the regions in parameter space of nearly critical particles corresponding to the different kinematic regimes and we determine bounds on parameters of particle 3 in those regimes, which allow it to escape. It turns out that there is no upper bound on the energy of escaping particle 3 in general. In addition, we show that several new possibilities open due to the larger dimensionality of the parameter space. In 5.4.3,

we discuss how to recover the special limiting cases, in particular how the bounds on extracted energy appear for geodesic (uncharged) particles and for vacuum spacetimes.

We illustrate these results on the example of extremal Kerr-Newman black holes in Section 5.5, and in Section 5.6 we discuss limitations of the results. Although the energy feeding problem for microscopic particles is also an issue, similarly to the axial case [120], we show that in equatorial case there are multiple ways to mitigate it, most of which do still allow significant energy extraction (cf. Table 5.2).

## 5.2 Motion and collisions of charged test particles

We shall consider a general stationary, axially symmetric spacetime with metric

$$\mathbf{g} = -N^2 dt^2 + g_{\varphi\varphi} (d\varphi - \omega dt)^2 + g_{rr} dr^2 + g_{\vartheta\vartheta} d\vartheta^2 \quad (5.1)$$

as a model of an isolated black hole (cf. (2.18)). Here  $N^2$  is the lapse function and  $\omega$  is the dragging potential.

Let us further assume that our spacetime contains a Maxwell field that obeys the same symmetry as the metric (5.1), which is manifested by the following choice of gauge for its potential:

$$\mathbf{A} = A_t dt + A_\varphi d\varphi = -\phi dt + A_\varphi (d\varphi - \omega dt) . \quad (5.2)$$

The component  $\phi$  is called the generalised electrostatic potential.

### 5.2.1 General equations of equatorial motion

Let us now consider motion of electrogeodesic test particles (i.e. particles influenced solely by Lorentz force) with rest mass  $m$  and charge  $q \equiv \tilde{q}m$  in the spacetime (5.1). Because of the two symmetries that we assumed, there exist two quantities that are conserved during the electrogeodesic motion, as we explained in Section 3.2. They can be interpreted as energy  $E$  and axial angular momentum  $L_z$ :

$$E = -p_t - qA_t , \quad L_z = p_\varphi + qA_\varphi . \quad (5.3)$$

We also assume that the metric (5.1) and the electromagnetic field are symmetric with respect to reflections  $\vartheta \rightarrow \pi - \vartheta$ . Then we can consider motion confined to the invariant hypersurface  $\vartheta = \pi/2$ , called equatorial “plane”. (For equatorial particles,  $L_z$  is the total angular momentum, hence we can drop the subscript;  $L \equiv L_z$ .)

If we define two auxiliary functions  $\mathcal{X}$  and  $\mathcal{Z}$ ,

$$\mathcal{X} = E - \omega L - q\phi, \quad \mathcal{Z} = \sqrt{\mathcal{X}^2 - N^2 \left[ m^2 + \frac{(L - qA_\varphi)^2}{g_{\varphi\varphi}} \right]}, \quad (5.4)$$

we can write the contravariant components of the particle’s momentum in a compact form

$$p^t = \frac{\mathcal{X}}{N^2}, \quad p^\varphi = \frac{\omega\mathcal{X}}{N^2} + \frac{L - qA_\varphi}{g_{\varphi\varphi}}, \quad p^r = \frac{\sigma\mathcal{Z}}{N\sqrt{g_{rr}}}. \quad (5.5)$$

The parameter  $\sigma = \pm 1$  determines the direction of the radial motion. In order for the motion to be allowed, the quantity  $\mathcal{Z}$  has to be real.

Outside of the black hole, where  $N^2 > 0$ , the condition  $\mathcal{Z}^2 > 0$  can be equivalently<sup>1</sup> stated as

$$|\mathcal{X}| \geq N \sqrt{m^2 + \frac{(L - qA_\varphi)^2}{g_{\varphi\varphi}}}. \quad (5.6)$$

It can be seen that there are two disjoint realms of allowed motion, one with  $\mathcal{X} > 0$  and the other with  $\mathcal{X} < 0$ . (They “touch” for  $N \rightarrow 0$ , where  $\mathcal{X} \rightarrow 0$  becomes possible.) However, to preserve causality, we need to enforce  $p^t > 0$ , and thus we restrict to the  $\mathcal{X} > 0$  variant. Then the requirement for the motion to be allowed becomes

$$\mathcal{X} \geq N \sqrt{m^2 + \frac{(L - qA_\varphi)^2}{g_{\varphi\varphi}}}. \quad (5.7)$$

The equality

$$\mathcal{X} = N \sqrt{m^2 + \frac{(L - qA_\varphi)^2}{g_{\varphi\varphi}}} \quad (5.8)$$

is the condition for a turning point.

The number of relevant parameters can be reduced depending on whether the particle in question is massive or massless. Kinematics of massive particles is determined by three parameters: specific energy  $\varepsilon \equiv E/m$ , specific angular momentum  $l \equiv L/m$  and specific

---

<sup>1</sup>We assumed  $g_{\varphi\varphi} > 0$ , and also that the product  $N\sqrt{g_{rr}} > 0$  is finite and non-vanishing even for  $N \rightarrow 0$ .

charge  $\tilde{q} \equiv q/m$ . On the other hand, for photons we put  $m = 0$  and  $q = 0$ , and thus their kinematics is characterised by just one parameter  $b \equiv L/E$ , called the impact parameter.

Based on this distinction, additional features of the motion like the existence of (circular) orbits can be deduced. Effective potentials are frequently employed, both for massive particles (cf. Section 3.2 and references therein) and for photons (see e.g. [117–119] for various uses).

### 5.2.2 Near-horizon expansions and (nearly) critical particles

We wish to study collisions of particles near the black hole horizon, where  $N \rightarrow 0$ . Let us denote the values of various quantities on the (outer) black hole horizon by subscript or superscript H; e.g.  $\omega_{\text{H}}$  is the value of  $\omega$  on the black hole horizon. (As we consider solely equatorial motion, all quantities in the following are understood to be evaluated at  $\vartheta = \pi/2$ , which will not be marked explicitly for brevity. For example, by  $A_{\varphi}^{\text{H}}$  we mean the value of  $A_{\varphi}$  on the horizon at  $\vartheta = \pi/2$ .)

Focusing on the vicinity of the horizon allows us to use expansions and approximations. We are interested in extremal black holes, which we emphasise by labeling the radius of their degenerate horizon as  $r_0$ . Let us invoke symbols  $\tilde{\omega}, \tilde{\phi}$  for first-order expansion coefficients of the dragging potential and of the generalised electrostatic potential (cf. (2.33))

$$\tilde{\omega} = \left. \frac{\partial \omega}{\partial r} \right|_{r=r_0}, \quad \tilde{\phi} = \left. \frac{\partial \phi}{\partial r} \right|_{r=r_0}. \quad (5.9)$$

For extremal black holes, we can also decompose the lapse function as  $N^2 = (r - r_0)^2 \tilde{N}^2$ , which leads, in particular, to

$$\tilde{N}_{\text{H}}^2 = \left. \frac{1}{2} \frac{\partial^2 N^2}{\partial r^2} \right|_{r=r_0}. \quad (5.10)$$

Finally, let us introduce a new set of “constants of motion”  $\mathcal{X}_{\text{H}}, x, \lambda$  useful to describe the kinematics of particles close to  $r_0$ . They are defined (in terms of  $E, L, q$ ) as follows:<sup>2</sup>

$$\mathcal{X}_{\text{H}} = E - \omega_{\text{H}} L - q \phi_{\text{H}}, \quad x = -\tilde{\omega} L - q \tilde{\phi}, \quad \lambda \equiv p_{\varphi}^{\text{H}} = L - q A_{\varphi}^{\text{H}}. \quad (5.11)$$

---

<sup>2</sup>In the present text, parameter  $\lambda$  is defined in a slightly different way than in [113]. The formulae given here can be recast into the convention used in [113] by putting  $\lambda \rightarrow -m\lambda A_{\varphi}^{\text{H}}$ . Let us also note that in Chapter 3, we used  $\tilde{\lambda}$ , which is related to  $\lambda$  in the present chapter by  $\lambda = m\tilde{\lambda}$ .

Two of the new parameters are expansion coefficients of the forwardness function  $\mathcal{X}$

$$\mathcal{X} \doteq \mathcal{X}_H + x(r - r_0) + \dots \quad (5.12)$$

Parameters  $E, L, q$  can be expressed in terms of the new ones through inverse relations

$$E = \mathcal{X}_H + \frac{(\omega_H \tilde{\phi} - \tilde{\omega} \phi_H) \lambda + x A_t^H}{\tilde{\phi} + \tilde{\omega} A_\varphi^H}, \quad L = \frac{\tilde{\phi} \lambda - x A_\varphi^H}{\tilde{\phi} + \tilde{\omega} A_\varphi^H}, \quad q = -\frac{\tilde{\omega} \lambda + x}{\tilde{\phi} + \tilde{\omega} A_\varphi^H} \quad (5.13)$$

All of them contain the same expression in the denominator, hence, it is clear that a problem occurs when it vanishes, i.e.

$$\tilde{\phi} + \tilde{\omega} A_\varphi^H = 0. \quad (5.14)$$

Indeed, in such a case  $x$  and  $\lambda$  become proportional to each other ( $x = -\tilde{\omega} \lambda$ ), and thus the variables  $\mathcal{X}_H, x, \lambda$  no longer span the whole parameter space. When this degeneracy happens, we can use  $\mathcal{X}_H, \lambda, q$  as our alternative set of parameters. Then the inverse relations to express  $E, L$  become

$$E = \mathcal{X}_H + \omega_H \lambda - q A_t^H \quad L = \lambda + q A_\varphi^H. \quad (5.15)$$

Let us also note that the condition (5.14) is equivalent to equation (3.43), as we have shown in 3.4.3.

The behaviour of particles close to the horizon radius  $r_0$  depends significantly on the value of  $\mathcal{X}_H$ . For particles with  $\mathcal{X}_H < 0$ , the condition (5.7) is necessarily violated near the horizon, and thus they can not get arbitrarily close to  $r_0$ .

### 5.2.2.1 Usual (subcritical) particles

On the other hand, particles with  $\mathcal{X}_H > 0$  are bound to fall into the black hole if they move inwards and get near the horizon. In our discussion, we will refer to those particles as usual. Let us emphasise that we will not consider *outgoing* usual particles in the vicinity of  $r_0$ , since it has been shown that such particles can not be produced in (generic) near-horizon collisions (cf. [79]).<sup>3</sup>

---

<sup>3</sup>Considering an astrophysical setup, we exclude the “white hole” region, from which outgoing usual particles could naturally emerge.

For usual particles moving close to  $r_0$ , the function  $\mathcal{Z}$  can be expanded in terms of  $N^2$  (and, consequently, of  $\mathcal{X}$ ) as follows:

$$\mathcal{Z} \doteq \mathcal{X} - \frac{N^2}{2\mathcal{X}} \left[ m^2 + \frac{(L - qA_\varphi)^2}{g_{\varphi\varphi}} \right] + \dots \quad (5.16)$$

### 5.2.2.2 Critical particles

We can also consider particles with  $\mathcal{X}_H = 0$ , which are called critical. They are fine-tuned to be on the verge between not being able to reach the horizon and falling into the black hole.<sup>4</sup> By definition (5.11), condition  $\mathcal{X}_H = 0$  can be understood also as a constraint for parameters  $E, L, q$ :

$$E - \omega_H L - q\phi_H = 0. \quad (5.17)$$

The expansion of  $\mathcal{Z}$  around  $r_0$  looks rather different for critical particles

$$\mathcal{Z} \doteq \sqrt{x^2 - \tilde{N}_H^2 \left( m^2 + \frac{\lambda^2}{g_{\varphi\varphi}^H} \right)} (r - r_0) + \dots \quad (5.18)$$

Let us emphasise that with  $\mathcal{X}_H = 0$  the causality condition  $p^t > 0$  necessarily implies  $x > 0$ .

It can be shown that critical particles cannot approach the horizon unless the black hole is extremal (see e.g. [63, 113] for discussion). Harada and Kimura [69] distinguished several subtypes of critical particles, out of which we consider chiefly so-called class I critical particles. The approximate trajectory of incoming class I critical particles near  $r_0$  has the form  $r = r_0 [1 + \exp(-\tau/\tau_{\text{relax}})]$ , where  $\tau$  is the proper time and  $\tau_{\text{relax}}$  is a positive constant (cf. 3.4.2, in particular (3.34), and also 4.2.3 and (4.16)). Since critical particles of any type can never reach  $r_0$ , any collisional process involving them will thus happen at some radius  $r_C > r_0$ . Therefore, it makes sense to consider particles that behave approximately as critical at a given radius.

---

<sup>4</sup>Let us again note that in the present thesis we use the *local* notion of critical particles. For asymptotically flat spacetimes, it is also possible to define the critical particles globally, such that they are on the edge of being able to approach the horizon *from infinity* (cf. [53]).

### 5.2.2.3 Nearly critical particles

A particle will behave approximately as critical at a radius  $r_C$ , if the zeroth order in the expansion of  $\mathcal{X}$  is of comparable magnitude as the first one. To quantify this, let us define a formal expansion (note the conventional minus sign)

$$\mathcal{X}_H \doteq -C_{(1)}(r_C - r_0) - C_{(2)}(r_C - r_0)^2 + \dots \quad (5.19)$$

The higher-order coefficients are needed for consistency of expansion of momentum conservation law. However, here we are interested only in the first order, and so we put  $C \equiv C_{(1)}$ .

For nearly critical particles, the expansion (5.12) evaluated at  $r_C$  can be recast as follows:

$$\mathcal{X} \doteq (x - C)(r_C - r_0) + \dots \quad (5.20)$$

Analogously, the expansion of  $\mathcal{Z}$  reads for them

$$\mathcal{Z} \doteq \sqrt{(x - C)^2 - \tilde{N}_H^2 \left( m^2 + \frac{\lambda^2}{g_{\varphi\varphi}^H} \right)} (r_C - r_0) + \dots \quad (5.21)$$

Nearly critical particles with  $C > 0$  cannot fall into the black hole and they must have a turning point at some radius smaller than  $r_C$ . Therefore, it makes sense to study collisional processes near the horizon involving also outgoing nearly critical particles. Furthermore, for particles with

$$x \gg C > 0, \quad (5.22)$$

we can neglect  $C$  and treat them as precisely critical around  $r_C$ . Thus, we can consider outgoing critical particles, too.

### 5.2.2.4 Class II (nearly) critical particles

There exist values of parameters of (nearly) critical particles, for which the leading order coefficient in the expansion (5.18) (or (5.21)) vanishes. The new leading order then becomes

$$\mathcal{Z} \sim (r_C - r_0)^{\frac{3}{2}} \quad (5.23)$$

or higher. Such (nearly) critical particles are called class II.

Kinematics of class II critical particles (cf. 3.4.5 and 3.4.6) represents an interesting theoretical issue, which, however, involves technical complications (see Appendix C.2). Moreover, since class II critical particles require fine-tuning of not just one, but two parameters, they are much less important for practical considerations. Thus, to simplify the matter, we will mostly omit details regarding class II critical particles in the following.

### 5.2.3 BSW effect and its Schnittman variant

We have seen that in the near-horizon region of an extremal black hole, two distinct types of motion do coexist. Whereas usual particles with  $\mathcal{X}_H > 0$  cross  $r_0$  and fall into the black hole, critical particles with  $\mathcal{X}_H = 0$  can only approach  $r_0$  asymptotically. This leads to divergent relative velocity between the two types of motion.

Hence, for near-horizon collisions between critical and usual particles, the collision energy scalar (cf. Section 3.3 for a derivation)

$$E_{\text{CM}}^2 = m_1^2 + m_2^2 - 2g_{\mu\nu}p_{(1)}^\mu p_{(2)}^\nu, \quad (5.24)$$

will be dominated by the scalar-product term. In particular, if we label the critical particle as 1 and the usual one as 2, the leading order contribution is

$$E_{\text{CM}}^2 \approx \frac{\mathcal{X}_2^H}{r_C - r_0} \left\{ \frac{2}{\tilde{N}_H^2} \left[ x_1 + \sigma_1 \sqrt{x_1^2 - \tilde{N}_H^2 \left( m_1^2 + \frac{\lambda_1^2}{g_{\varphi\varphi}^H} \right)} \right] \right\}. \quad (5.25)$$

A process with incoming critical particle ( $\sigma_1 = -1$ ) is called BSW-type after Bañados, Silk and West [53], whereas the one with reflected (nearly) critical particle ( $\sigma_1 = +1$ ) is called Schnittman-type [74]. (Note that the usual particle is always incoming, i.e.  $\sigma_2 = -1$ . We used the approximation (5.22) for the Schnittman process.)

## 5.3 Approach phase

Critical particles are the key ingredient of certain high-energy collisional processes in extremal black hole spacetimes. Nevertheless, parameters of critical particles that can act in such processes are restricted, since the requirement (5.7) must be fulfilled all the way from the point of inception to the point of collision.

### 5.3.1 Admissible region in the parameter space

Let us disregard the concern about where the critical particle originated and focus instead on the point of collision at radius  $r_C$ . Since we want  $r_C$  very close to  $r_0$ , the minimum requirement is that there must be some neighborhood of  $r_0$ , where condition (5.7) is satisfied. Using linear approximation in  $r - r_0$ , we get

$$x > \tilde{N}_H \sqrt{m^2 + \frac{\lambda^2}{g_{\varphi\varphi}^H}}. \quad (5.26)$$

Conversely, for parameters satisfying the inequality opposite to (5.26), condition (5.7) will be violated in some neighborhood of  $r_0$ . The equality

$$x = \tilde{N}_H \sqrt{m^2 + \frac{\lambda^2}{g_{\varphi\varphi}^H}}, \quad (5.27)$$

corresponds to the breakdown of the linear approximation of (5.7). Comparing with (5.18), we see that (5.27) also implies the critical particles to be class II. Higher-order expansion terms are needed to decide, whether motion of class II critical particles is allowed close to  $r_0$  (cf. 3.4.5 and 3.4.6).

Now, let us consider physical interpretation of the “admissible region” of parameters, which is defined by (5.26). In particular, we would like to distinguish different variants of the collisional processes corresponding to the previously known limiting cases. For extremal vacuum black holes, only critical particles corotating with the black hole can participate in the high-energy collisions, whereas for the non-rotating extremal black holes, the critical particles need to have the same sign of charge as the black hole. In order to identify counterparts of these limiting variants, which we will call “centrifugal mechanism” and “electrostatic mechanism”, we need to assess how to define the direction in which a (charged) particle orbits.

The momentum component  $p_\varphi$  determines the direction of motion in  $\varphi$  with respect to a locally non-rotating observer (cf. [45]). For uncharged particles,  $p_\varphi \equiv L$  is constant, and thus the distinction is universal and unambiguous.<sup>5</sup> Nevertheless, for charged particles  $p_\varphi$

---

<sup>5</sup>Note that  $p^\varphi$  is not proportional to  $p_\varphi$  in general, and thus the direction of orbiting with respect to a locally non-rotating observer is not straightforwardly related to properties of particle’s trajectory. A prominent example is the ergoregion, where it holds  $\text{sgn } p^\varphi = \text{sgn } \omega$ . Hence trajectories with constant  $\varphi$  are not possible in the ergoregion, although sign of  $p_\varphi$  is unrestricted therein.

depends on  $r$  through the  $qA_\varphi$  term. Therefore, we essentially need to compare values of  $p_\varphi$  at some reference radius. A straightforward choice would be to use  $\lambda \equiv p_\varphi^H$ . However, it is clear from (5.27) that one can find points with any value of  $\lambda$  in the admissible region (whereas values of  $x$  in the admissible region are bounded from below by  $x \geq \tilde{N}_H m$ ). Apart from the degenerate case (5.14), no kinematic restriction on  $\lambda$  is thus possible. Hence, basing the definition of the centrifugal mechanism on  $\lambda$  would lead to a trivial result.

What is the justification to use  $L$  instead? We shall consider a region of our spacetime, where the influence of the dragging and of the magnetic field is insignificant, for example a far zone of an asymptotically flat spacetime. More precisely, let us consider a region where  $\omega, A_\varphi$  are negligible, and thus  $p_\varphi \doteq p^\varphi g_{\varphi\varphi} \doteq L$ . Then it readily follows that in such a region particles with  $L = 0$  move along trajectories of (approximately) constant  $\varphi$  and, conversely, particles with different signs of  $L$  orbit in different directions therein. Hence, we can say that  $L$  uniquely distinguishes the direction of motion in  $\varphi$  of a particle before it came under the influence of the dragging and of the magnetic field near the black hole.

We conclude that we need to view the admissible region through parameters  $L, q$  for physical interpretation. Similarly to 3.4.3, let us focus on the equation (5.27) of the “border” of the admissible region. Substituting for  $x, \lambda$  in (5.27) from definition (5.11) does not generally lead to a single-valued functional dependence between  $q, L$ . We circumvent this issue by plugging the condition (5.27) into relations (5.13), which yields parametric expressions for the border:<sup>6</sup>

$$q = -\frac{\tilde{\omega}\lambda + \tilde{N}_H \sqrt{m^2 + \frac{\lambda^2}{g_{\varphi\varphi}^H}}}{\tilde{\phi} + \tilde{\omega}A_\varphi^H} \quad (5.28)$$

$$L = \frac{\tilde{\phi}\lambda - \tilde{N}_H A_\varphi^H \sqrt{m^2 + \frac{\lambda^2}{g_{\varphi\varphi}^H}}}{\tilde{\phi} + \tilde{\omega}A_\varphi^H} \quad (5.29)$$

$$E = \frac{(\omega_H \tilde{\phi} - \tilde{\omega} \phi_H) \lambda + \tilde{N}_H A_t^H \sqrt{m^2 + \frac{\lambda^2}{g_{\varphi\varphi}^H}}}{\tilde{\phi} + \tilde{\omega}A_\varphi^H} \quad (5.30)$$

In 3.4.3 we identified different variants, like the centrifugal and electrostatic mechanism, by studying restrictions on signs of parameters  $L, q$  in the admissible region. Here we revisit these results and complement and deepen them by determining the precise bounds

---

<sup>6</sup>Since we are dealing with critical particles, the three expressions are not independent.

on  $L, q$  (and  $E$ ).

### 5.3.1.1 Bounds on parameters

Bounds on values of  $q, L$  and  $E$  in the admissible region will appear as extrema of expressions (5.28)-(5.30) with respect to  $\lambda$ . Starting with (5.28), we find that a stationary point can occur at the following value of  $\lambda$ :

$$\lambda = -m \frac{g_{\varphi\varphi}^{\text{H}} \tilde{\omega}}{\sqrt{\tilde{N}_{\text{H}}^2 - g_{\varphi\varphi}^{\text{H}} \tilde{\omega}^2}} \quad (5.31)$$

Due to the square root in the denominator, we need to distinguish three possibilities.

Case **1a**: If (5.31) is imaginary, (5.28) will take all real values, and hence there is no bound on  $q$ .

Case **1b**: If (5.31) is real, it will correspond to an extremum of (5.28) with value

$$q_{\text{b}} = -\frac{m}{\tilde{\phi} + \tilde{\omega} A_{\varphi}^{\text{H}}} \sqrt{\tilde{N}_{\text{H}}^2 - g_{\varphi\varphi}^{\text{H}} \tilde{\omega}^2}, \quad (5.32)$$

and to the following values of the other parameters on the border:

$$L = -\frac{m}{\tilde{\phi} + \tilde{\omega} A_{\varphi}^{\text{H}}} \frac{\tilde{N}_{\text{H}}^2 A_{\varphi}^{\text{H}} + g_{\varphi\varphi}^{\text{H}} \tilde{\omega} \tilde{\phi}}{\sqrt{\tilde{N}_{\text{H}}^2 - g_{\varphi\varphi}^{\text{H}} \tilde{\omega}^2}}, \quad (5.33)$$

$$E = \frac{m}{\tilde{\phi} + \tilde{\omega} A_{\varphi}^{\text{H}}} \frac{\tilde{N}_{\text{H}}^2 A_{\varphi}^{\text{H}} - g_{\varphi\varphi}^{\text{H}} \tilde{\omega} (\omega_{\text{H}} \tilde{\phi} - \tilde{\omega} \phi_{\text{H}})}{\sqrt{\tilde{N}_{\text{H}}^2 - g_{\varphi\varphi}^{\text{H}} \tilde{\omega}^2}}. \quad (5.34)$$

Looking at  $|\lambda| \rightarrow \infty$  behaviour of (5.28), one can deduce when

$$\tilde{\phi} + \tilde{\omega} A_{\varphi}^{\text{H}} < 0, \quad (5.35)$$

then (5.32) will be a lower bound, whereas if the opposite inequality is satisfied, (5.32) will be an upper bound.

Case **1c**: If the expression under the square root in (5.31) is zero (and (5.31) is thus an invalid expression), the values of charge in the admissible region will be bounded by  $q_{\text{b}} = 0$ . However,  $q = 0$  can not be attained for any finite value of other parameters on the border.

Turning to (5.29), we find that a value of  $\lambda$  for a candidate stationary point is

$$\lambda = m \frac{g_{\varphi\varphi}^{\text{H}} \tilde{\phi} \operatorname{sgn} A_{\varphi}^{\text{H}}}{\sqrt{\tilde{N}_{\text{H}}^2 (A_{\varphi}^{\text{H}})^2 - g_{\varphi\varphi}^{\text{H}} \tilde{\phi}^2}} . \quad (5.36)$$

Again, there are three possible cases.

Case **2a**: If (5.36) is imaginary, there is no bound on  $L$  in the admissible region.

Case **2b**: If (5.36) is real, it will correspond to an extremum of (5.29) with value

$$L_{\text{b}} = -\frac{m \operatorname{sgn} A_{\varphi}^{\text{H}}}{\tilde{\phi} + \tilde{\omega} A_{\varphi}^{\text{H}}} \sqrt{\tilde{N}_{\text{H}}^2 (A_{\varphi}^{\text{H}})^2 - g_{\varphi\varphi}^{\text{H}} \tilde{\phi}^2} , \quad (5.37)$$

and to the following values of the other parameters:

$$q = -\frac{m \operatorname{sgn} A_{\varphi}^{\text{H}}}{\tilde{\phi} + \tilde{\omega} A_{\varphi}^{\text{H}}} \frac{\tilde{N}_{\text{H}}^2 A_{\varphi}^{\text{H}} + g_{\varphi\varphi}^{\text{H}} \tilde{\omega} \tilde{\phi}}{\sqrt{\tilde{N}_{\text{H}}^2 (A_{\varphi}^{\text{H}})^2 - g_{\varphi\varphi}^{\text{H}} \tilde{\phi}^2}} \quad (5.38)$$

$$E = \frac{m \operatorname{sgn} A_{\varphi}^{\text{H}}}{\tilde{\phi} + \tilde{\omega} A_{\varphi}^{\text{H}}} \frac{\tilde{N}_{\text{H}}^2 A_{\varphi}^{\text{H}} A_{\varphi}^{\text{H}} + g_{\varphi\varphi}^{\text{H}} \tilde{\phi} (\omega_{\text{H}} \tilde{\phi} - \tilde{\omega} \phi_{\text{H}})}{\sqrt{\tilde{N}_{\text{H}}^2 (A_{\varphi}^{\text{H}})^2 - g_{\varphi\varphi}^{\text{H}} \tilde{\phi}^2}} . \quad (5.39)$$

From the  $|\lambda| \rightarrow \infty$  behaviour of (5.29), we can infer that (5.37) is a lower bound, if

$$\frac{A_{\varphi}^{\text{H}}}{\tilde{\phi} + \tilde{\omega} A_{\varphi}^{\text{H}}} < 0 . \quad (5.40)$$

When the opposite inequality is satisfied, (5.37) is an upper bound.

Case **2c**: If (5.36) is undefined, values of  $L$  in the admissible region will be bounded by  $L_{\text{b}} = 0$ , and this value can not be reached for a finite value of other parameters on the border.

Combining the possibilities together, we can conclude that cases **1a2b** and **1a2c** correspond to the centrifugal mechanism, whereas variants **1b2a** and **1c2a** correspond to the electrostatic mechanism. Case **1a2a** signifies the coexistence of both. (Note that the combination of signs of  $L, q$  leading to  $x < 0$  is excluded in any case.) The other possible combinations, i.e. **1b2b** and **1c2c**, do not correspond to any simpler limiting cases.

Let us now finish the discussion of bounds on parameters by looking at a possible

stationary point of (5.30). The corresponding value of  $\lambda$ ,

$$\lambda = -m \frac{g_{\varphi\varphi}^{\text{H}} \left( \omega_{\text{H}} \tilde{\phi} - \tilde{\omega} \phi_{\text{H}} \right) \text{sgn } A_t^{\text{H}}}{\sqrt{\tilde{N}_{\text{H}}^2 (A_t^{\text{H}})^2 - g_{\varphi\varphi}^{\text{H}} \left( \omega_{\text{H}} \tilde{\phi} - \tilde{\omega} \phi_{\text{H}} \right)^2}}, \quad (5.41)$$

can be adjusted using the available gauge freedom, unlike in the previous cases. Therefore, we can choose  $\lambda$  to be real. Furthermore, it turns out that we can also choose the corresponding stationary point of (5.30) to be a minimum. Its value is

$$E_{\min} = \frac{m \text{sgn } A_t^{\text{H}}}{\tilde{\phi} + \tilde{\omega} A_{\varphi}^{\text{H}}} \sqrt{\tilde{N}_{\text{H}}^2 (A_t^{\text{H}})^2 - g_{\varphi\varphi}^{\text{H}} \left( \omega_{\text{H}} \tilde{\phi} - \tilde{\omega} \phi_{\text{H}} \right)^2}, \quad (5.42)$$

whereas the values of the other parameters on the border implied by (5.41) are

$$q = -\frac{m \text{sgn } A_t^{\text{H}}}{\tilde{\phi} + \tilde{\omega} A_{\varphi}^{\text{H}}} \frac{\tilde{N}_{\text{H}}^2 A_t^{\text{H}} - g_{\varphi\varphi}^{\text{H}} \tilde{\omega} \left( \omega_{\text{H}} \tilde{\phi} - \tilde{\omega} \phi_{\text{H}} \right)}{\sqrt{\tilde{N}_{\text{H}}^2 (A_t^{\text{H}})^2 - g_{\varphi\varphi}^{\text{H}} \left( \omega_{\text{H}} \tilde{\phi} - \tilde{\omega} \phi_{\text{H}} \right)^2}}, \quad (5.43)$$

$$L = -\frac{m \text{sgn } A_t^{\text{H}}}{\tilde{\phi} + \tilde{\omega} A_{\varphi}^{\text{H}}} \frac{\tilde{N}_{\text{H}}^2 A_t^{\text{H}} A_{\varphi}^{\text{H}} + g_{\varphi\varphi}^{\text{H}} \tilde{\phi} \left( \omega_{\text{H}} \tilde{\phi} - \tilde{\omega} \phi_{\text{H}} \right)}{\sqrt{\tilde{N}_{\text{H}}^2 (A_t^{\text{H}})^2 - g_{\varphi\varphi}^{\text{H}} \left( \omega_{\text{H}} \tilde{\phi} - \tilde{\omega} \phi_{\text{H}} \right)^2}}. \quad (5.44)$$

### 5.3.1.2 Gauge conditions

What are the requirements in order to have a lower bound on  $E$  in the admissible region and is it always possible to make them satisfied simultaneously? First, we have to impose the condition

$$\tilde{N}_{\text{H}}^2 (A_t^{\text{H}})^2 - g_{\varphi\varphi}^{\text{H}} \left( \omega_{\text{H}} \tilde{\phi} - \tilde{\omega} \phi_{\text{H}} \right)^2 > 0 \quad (5.45)$$

to make (5.41) real. By checking the  $|\lambda| \rightarrow \infty$  behaviour of (5.30), we can see that we must also require

$$\frac{A_t^{\text{H}}}{\tilde{\phi} + \tilde{\omega} A_{\varphi}^{\text{H}}} > 0 \quad (5.46)$$

in order for (5.42) to be a lower bound. Next, one can observe that combinations  $A_t^{\text{H}} \equiv -\varphi_{\text{H}} - \omega_{\text{H}} A_{\varphi}^{\text{H}}$  and  $\omega_{\text{H}} \tilde{\phi} - \tilde{\omega} \phi_{\text{H}}$  are linearly independent (except for the degenerate case when (5.14) holds, which has to be treated separately anyway). Therefore, there is always a way to choose values of  $\phi_{\text{H}}$  and  $\omega_{\text{H}}$  that make any of the conditions (5.45) and (5.46) satisfied (or violated).

### 5.3.1.3 Additional remarks

Above, we have identified points on the border of the admissible region where a minimal or maximal value of one of the parameters  $q, L, E$  is reached. Values of all the parameters at such points are proportional to the particle's mass. This illustrates the fact that only a reduced set of parameters is needed to describe particles' kinematics. In particular, for massive critical particles, two parameters are sufficient. These can be either  $\tilde{x} = x/m$  and  $\tilde{\lambda} = \lambda/m$ , or any two of  $\tilde{q}, l, \varepsilon$ .

In this sense, we can understand the admissible region (5.26) as an area in a two-dimensional parameter space. Its border (5.27) can be viewed as a curve therein, namely a branch of a hyperbola with axes  $\tilde{x} = 0$  and  $\tilde{\lambda} = 0$ , and with its vertex on  $\tilde{\lambda} = 0$ .

Considering the parameters normalized to unit rest mass excludes critical photons. However, this is not a big issue, since they have trivial kinematics. Indeed, all critical photons share the same single value of impact parameter  $b_{\text{cr}} = 1/\omega_{\text{H}}$ . Therefore, parameter space of critical photons is effectively zero-dimensional, and their kinematics depends only on the properties of the spacetime itself.

When are the critical photons able to approach  $r_0$ ? The expansion (5.18) reads for them

$$\mathcal{Z} \doteq |L| \sqrt{\tilde{\omega}^2 - \frac{\tilde{N}_{\text{H}}^2}{g_{\varphi\varphi}^{\text{H}}}(r - r_0) + \dots} \quad (5.47)$$

Here the expression under the square root is proportional to the one in (5.31) with a negative factor. Therefore, critical photons can be involved in the high-energy collision processes close to  $r_0$  only in the case **1a**.

Finally, let us clarify the link between bounds on  $q, L, E$  and restrictions on signs of those parameters. Starting with  $q$ , we can observe that condition (5.35) also determines the sign of (5.32). Thus, if (5.32) is a lower bound, its value is positive, whereas if it is an upper bound, its value is negative. Therefore, whenever values of  $q$  in the admissible region are bounded by (5.32), they must also have all the same sign. The identical relation holds between (5.40) and (5.37). Last, the gauge condition (5.46), which we use to enforce a lower bound on energy, also implies that this bound (5.42) has a positive value.

Hence, dividing by  $m$  and rearranging the sign factors, we can express the (possible)

bounds on values of  $\tilde{q}, l, \varepsilon$  in the admissible region as follows:

$$-\tilde{q} \operatorname{sgn}(\tilde{\phi} + \tilde{\omega} A_\varphi^{\text{H}}) > \frac{1}{|\tilde{\phi} + \tilde{\omega} A_\varphi^{\text{H}}|} \sqrt{\tilde{N}_{\text{H}}^2 - g_{\varphi\varphi}^{\text{H}} \tilde{\omega}^2}, \quad (5.48)$$

$$-l \operatorname{sgn}\left[\left(\tilde{\phi} + \tilde{\omega} A_\varphi^{\text{H}}\right) A_\varphi^{\text{H}}\right] > \frac{1}{|\tilde{\phi} + \tilde{\omega} A_\varphi^{\text{H}}|} \sqrt{\tilde{N}_{\text{H}}^2 (A_\varphi^{\text{H}})^2 - g_{\varphi\varphi}^{\text{H}} \tilde{\phi}^2}, \quad (5.49)$$

$$\varepsilon > \frac{1}{|\tilde{\phi} + \tilde{\omega} A_\varphi^{\text{H}}|} \sqrt{\tilde{N}_{\text{H}}^2 (A_t^{\text{H}})^2 - g_{\varphi\varphi}^{\text{H}} (\omega_{\text{H}} \tilde{\phi} - \tilde{\omega} \phi_{\text{H}})^2}. \quad (5.50)$$

### 5.3.2 Degenerate case

Let us now explore the (previously excluded) case when the degeneracy condition (5.14) is satisfied. As we noted in 5.2.2, this means that variables  $x$  and  $\lambda$  become proportional, namely  $x = -\tilde{\omega}\lambda$ . Because of this, (5.27) with (5.14) degenerates into an algebraic equation (for one variable), which has a single solution

$$\lambda = -\frac{m \operatorname{sgn} \tilde{\omega}}{\sqrt{\frac{\tilde{\omega}^2}{\tilde{N}^2} - \frac{1}{g_{\varphi\varphi}^{\text{H}}}}}. \quad (5.51)$$

One can see that the expressions under the square roots in the denominators of (5.51) and (5.31) are related by a negative factor. Therefore, (5.51) is defined in real numbers in case **1a**. On the other hand, in cases **1b** and **1c**, there is no real solution of (5.27) with (5.14), and thus the collisional processes studied here are impossible for critical particles with any value of  $\lambda$ .<sup>7</sup> (Note that  $\lambda \operatorname{sgn} \tilde{\omega} > 0$  certainly violates (5.27) with (5.14).)

Let us consider physical interpretation of (5.51). Using (5.15), it can be expressed as

$$L = -\frac{m \operatorname{sgn} \tilde{\omega}}{\sqrt{\frac{\tilde{\omega}^2}{\tilde{N}^2} - \frac{1}{g_{\varphi\varphi}^{\text{H}}}} + q A_\varphi^{\text{H}}, \quad (5.52)$$

$$E = -\frac{m \omega_{\text{H}} \operatorname{sgn} \tilde{\omega}}{\sqrt{\frac{\tilde{\omega}^2}{\tilde{N}^2} - \frac{1}{g_{\varphi\varphi}^{\text{H}}}} - q A_t^{\text{H}}. \quad (5.53)$$

The charge of the particle plays a role of a free variable; there can never be a bound on

---

<sup>7</sup>We are unaware of a black-hole spacetime where this would occur in the equatorial plane. However, similar thing happens around the poles of the Kerr solution, as demonstrated by [69].

the values of  $q$  in the admissible region in the degenerate case. However, if  $A_\varphi^H = 0$ , (5.52) will correspond to single value of  $L$ , which will constitute a bound on  $L$ . For (5.14) with  $A_\varphi^H = 0$ , it holds  $-\text{sgn}(\tilde{\omega}L) = \text{sgn } x > 0$ , and therefore we can infer

$$-l \text{sgn } \tilde{\omega} > \frac{1}{\sqrt{\frac{\tilde{\omega}^2}{N^2} - \frac{1}{g_{\varphi\varphi}^H}}} . \quad (5.54)$$

(Note that (5.14) with  $A_\varphi^H = 0$  implies  $\tilde{\phi} = 0$ , and hence case **2c**, although the bound has a non-zero value.)

We want a lower bound on  $E$  in the admissible region, and therefore we impose gauge conditions  $A_t^H = 0$  and  $\omega_H \text{sgn } \tilde{\omega} < 0$ . Then it holds

$$\varepsilon > \frac{|\omega_H|}{\sqrt{\frac{\tilde{\omega}^2}{N^2} - \frac{1}{g_{\varphi\varphi}^H}}} . \quad (5.55)$$

## 5.4 Energy extraction

Now we shall discuss properties of particles than can be produced in the high-energy collisional processes described in 5.2.3 and, in particular, how much energy can such particles extract from a black hole.

### 5.4.1 Conservation laws and kinematic regimes

Let us consider a simple setup in which a (nearly) critical particle 1 and an incoming usual particle 2 collide close to the horizon radius  $r_0$ , and their interaction leads to production of just two new particles, 3 and 4. We assume the conservation of charge

$$q_1 + q_2 = q_3 + q_4 \quad (5.56)$$

and also the conservation of (all components of) momentum at the point of collision. From the azimuthal component, we infer the conservation of angular momentum

$$L_1 + L_2 = L_3 + L_4 . \quad (5.57)$$

The conservation law for the time component of momentum can be used to derive the conservation of energy

$$E_1 + E_2 = E_3 + E_4 , \quad (5.58)$$

or combined together with the conservation law for the radial component. This is advantageous, because summing the components with appropriate coefficients gives us combinations of functions  $\mathcal{X}$  and  $\mathcal{Z}$

$$N^2 p^t \mp N \sqrt{g_{rr}} p^r \equiv \mathcal{X} \mp \sigma \mathcal{Z} . \quad (5.59)$$

Since we assumed that particle 2 is incoming ( $\sigma_2 = -1$ ), the summation of the conservation laws leads to following two equations:

$$\mathcal{X}_1 \mp \sigma_1 \mathcal{Z}_1 + \mathcal{X}_2 \pm \mathcal{Z}_2 = \mathcal{X}_3 \mp \sigma_3 \mathcal{Z}_3 + \mathcal{X}_4 \mp \sigma_4 \mathcal{Z}_4 . \quad (5.60)$$

For usual particles,  $\mathcal{X}$  and  $\mathcal{Z}$  differ by a term proportional to  $N^2$ , so their combinations with different signs have different leading orders in expansion around  $r_0$

$$\mathcal{X} - \mathcal{Z} \sim (r - r_0) , \quad \mathcal{X} + \mathcal{Z} \doteq 2\mathcal{X}_H . \quad (5.61)$$

On the other hand, in the case of (nearly) critical particles, the leading order of expansion in  $r_C - r_0$  for both combinations is the first one

$$\mathcal{X} \mp \mathcal{Z} \sim (r_C - r_0) . \quad (5.62)$$

Now let us look at (5.60) with the upper sign. We assumed particle 2 to be usual, and thus the leading order is the zeroth one

$$2\mathcal{X}_2^H = \mathcal{X}_3^H - \sigma_3 \mathcal{Z}_3^H + \mathcal{X}_4^H - \sigma_4 \mathcal{Z}_4^H . \quad (5.63)$$

This equation can be satisfied only when one of the final particles, say 4, is usual and incoming, i.e.  $\mathcal{X}_4^H > 0$ ,  $\sigma_4 = -1$ . Turning to the lower sign of (5.60), we see that usual incoming particles 2 and 4 will make no contribution to zeroth and first order. On the other hand, critical particle 1 will contribute to the first order and this contribution will dominate the left-hand side. Therefore, the expansion of right-hand side must also be

dominated by a first-order contribution, which means that particle 3 has to be (nearly) critical. The leading order of (5.60) with the lower sign thus becomes

$$x_1 + \sigma_1 \sqrt{x_1^2 - \tilde{N}_H^2 \left( m_1^2 + \frac{\lambda_1^2}{g_{\varphi\varphi}^H} \right)} = x_3 - C_3 + \sigma_3 \sqrt{(x_3 - C_3)^2 - \tilde{N}_H^2 \left( m_3^2 + \frac{\lambda_3^2}{g_{\varphi\varphi}^H} \right)} \quad (5.64)$$

Here  $C_3 \equiv C_{(3,1)}$  parametrises deviation of particle 3 from criticality according to (5.19). We put  $C_1 = 0$  for simplicity. One can denote the whole left-hand side of (5.64) as a new parameter

$$\tilde{N}_H A_1 \equiv x_1 + \sigma_1 \sqrt{x_1^2 - \tilde{N}_H^2 \left( m_1^2 + \frac{\lambda_1^2}{g_{\varphi\varphi}^H} \right)} , \quad (5.65)$$

which will carry all the information about particle 1. Since  $x_1 > 0$ , we can make sure that  $A_1 \geq 0$ . The difference between BSW-type processes ( $\sigma_1 = -1$ ) and Schnittman-type processes ( $\sigma_1 = +1$ ) is absorbed into the definition of  $A_1$ , and thus the results expressed using  $A_1$  hereafter will be the same for both.

For a Penrose process, one of the particles must fall inside the black hole; and we can make sure that particle 4 is bound to do so. On the other hand, particle 3 can be produced in four distinct kinematic regimes, based on the combination of sign of  $C_3$  and the sign variable  $\sigma_3$ . In accordance with [80], let us denote the regimes with  $C_3 > 0$  as “+”,  $C_3 < 0$  as “-”,  $\sigma_3 = +1$  as “OUT” and  $\sigma_3 = -1$  as “IN”.

There are important differences among the four kinematic regimes in several regards. First, we should determine which ones allow particle 3 to escape from the vicinity of the black hole. For simplicity, let us assume a situation when condition (5.7) is well approximated by linear expansion terms. In such a case, there can be at most one turning point near  $r_0$ . The radius  $r_T$  of this turning point is defined by the condition

$$x_3 (r_T - r_0) - C_3 (r_C - r_0) = \tilde{N}_H \sqrt{m_3^2 + \frac{\lambda_3^2}{g_{\varphi\varphi}^H}} (r_T - r_0) , \quad (5.66)$$

which can be rearranged as follows

$$r_C - r_T = (r_C - r_0) \frac{x_3 - C_3 - \tilde{N}_H \sqrt{m_3^2 + \frac{\lambda_3^2}{g_{\varphi\varphi}^H}}}{x_3 - \tilde{N}_H \sqrt{m_3^2 + \frac{\lambda_3^2}{g_{\varphi\varphi}^H}}} . \quad (5.67)$$

(Note that (5.67) may imply  $r_T < r_0$ , and hence no turning point in the region of our

interest.) The motion of particle 3 must be allowed at  $r_C$ , where it is produced, hence

$$x_3 - C_3 - \tilde{N}_H \sqrt{m_3^2 + \frac{\lambda_3^2}{g_{\varphi\varphi}^H}} > 0 . \quad (5.68)$$

Therefore, the numerator of the fraction in (5.67) is positive and since  $r_C > r_0$  by definition, recalling (5.26), we can conclude that  $r_T < r_C$  for particles produced with parameters in the admissible region, whereas  $r_T > r_C$  for the ones outside of it. However, if  $r_T > r_C$ , particle 3 produced at  $r_C$  can never escape. Therefore, in order for particle 3 to escape, it must be produced with parameters in the admissible region.

Particles with  $C_3 > 0$  can not fall into the black hole by definition, and thus they must have a turning point at a radius  $r_0 < r_T < r_C$ . Therefore, in regimes OUT+ and IN+, particle 3 can be produced *only* with parameters in the admissible region, and it is automatically guaranteed to escape.

On the other hand, particles with  $C_3 < 0$  can cross the horizon; their motion is allowed both at  $r_0$  and at  $r_C$ . Hence, there must be an even number of turning points between  $r_0$  and  $r_C$ . However, we assumed the existence of at most one turning point, and thus there can be none. Incoming particle 3 produced with  $C_3 < 0$  therefore has to fall into the black hole; i.e. escape in the IN– regime is impossible. Last, in the OUT– regime, particle 3 can either escape or be reflected and fall into the black hole, based on whether its parameters lie in the admissible region or not.

The way in which parameters  $C_3$  and  $\sigma_3$  determine escape possibilities of particle 3 is actually independent of the particular system in question. (This can be seen e.g. through comparison with Section 4.4.2, where we considered particles moving along the symmetry axis.) However, despite being so universal and so important for escape of particle 3, parameters  $C_3$  and  $\sigma_3$  are quite irrelevant for all other purposes. Indeed, if particle 3 escapes,  $\sigma_3$  must eventually flip to +1, whereas  $C_3$  encodes only a small deviation from fine-tuning of parameters of particle 3.

Hence, we shall now solve (5.64) for  $C_3$  and  $\sigma_3$ , in order to view the different kinematic regimes in terms of the other parameters, i.e.  $x_3, \lambda_3, m_3$  and  $A_1$ . First, we can observe from (5.64) that

$$\sigma_3 = \text{sgn}\left(\tilde{N}_H A_1 - x_3 + C_3\right) . \quad (5.69)$$

Expressing  $C_3$  from (5.64) and then substituting it back into (5.69), we obtain the solutions

as follows:

$$C_3 = x_3 - \frac{\tilde{N}_H}{2} \left[ A_1 + \frac{1}{A_1} \left( m_3^2 + \frac{\lambda_3^2}{g_{\varphi\varphi}^H} \right) \right], \quad (5.70)$$

$$\sigma_3 = \text{sgn} \left[ A_1^2 - \left( m_3^2 + \frac{\lambda_3^2}{g_{\varphi\varphi}^H} \right) \right]. \quad (5.71)$$

Since we are interested only in the sign of  $C_3$ , and  $\sigma_3$  is a sign variable per se, only ratios among the four parameters on the right-hand sides matter to us. Therefore, we have a considerable freedom in choosing the relevant (three) variables. Nevertheless, we have seen above that we also need to consider the admissible region, for which the relevant parameters are  $\tilde{x}, \tilde{\lambda}$ . Thus, it is natural to understand (5.70) and (5.71) as depending on  $\tilde{x}_3, \tilde{\lambda}_3$  and on the ratio between  $A_1$  and  $m_3$ .

The third “parameter”, i.e. ratio between  $A_1$  and  $m_3$ , clearly stands out; it tracks a comparison between properties of two particles, and it is irrelevant for the admissible region of particle 3. Therefore, we find it natural to visualise the different kinematic regimes as regions in the same two-dimensional parameter space as the admissible region, with the ratio between  $A_1$  and  $m_3$  serving as an “external parameter”. (However, since we are interested in physical interpretation, namely in energy extraction, we will keep  $A_1$  and  $m_3$  separate in the equations and we will not explicitly pass to the parameters normalized to unit rest mass.)

If we treat the ratio between  $A_1$  and  $m_3$  as an external parameter, there are just two main possibilities.

“Heavy regime”: If  $m_3 > A_1$ , the right-hand side of (5.71) is negative for any  $\tilde{\lambda}_3$ , and hence the IN region covers the whole parameter space.

“Light regime”: On the other hand, if  $m_3 < A_1$ , the parameter space is divided into IN and OUT regions.

## 5.4.2 Structure of the parameter space

Now we should understand how are the regions of parameters corresponding to different kinematic regimes distributed across our parameter space. Let us start with the distinction between “+” and “−” regimes, which is always present. From the solution (5.70), we see

that  $C_3 > 0$  implies

$$x_3 > \frac{\tilde{N}_H}{2} \left[ A_1 + \frac{1}{A_1} \left( m_3^2 + \frac{\lambda_3^2}{g_{\varphi\varphi}^H} \right) \right]. \quad (5.72)$$

Conversely, the inequality opposite to (5.72) entails  $C_3 < 0$ . The equality

$$x_3 = \frac{\tilde{N}_H}{2} \left[ A_1 + \frac{1}{A_1} \left( m_3^2 + \frac{\lambda_3^2}{g_{\varphi\varphi}^H} \right) \right] \quad (5.73)$$

defines the border between the regions, and it corresponds to  $C_3 = 0$ , i.e. to particle 3 being produced as precisely critical. In  $\tilde{x}_3, \tilde{\lambda}_3$  parameter space, (5.73) represents a parabola with axis  $\tilde{\lambda}_3 = 0$ .

For physical interpretation, let us substitute (5.73) into (5.13) to obtain parametric expressions for the border as follows:

$$q_3 = -\frac{1}{\tilde{\phi} + \tilde{\omega}A_\varphi^H} \left\{ \tilde{\omega}\lambda_3 + \frac{\tilde{N}_H}{2} \left[ A_1 + \frac{1}{A_1} \left( m_3^2 + \frac{\lambda_3^2}{g_{\varphi\varphi}^H} \right) \right] \right\} \quad (5.74)$$

$$L_3 = \frac{1}{\tilde{\phi} + \tilde{\omega}A_\varphi^H} \left\{ \tilde{\phi}\lambda_3 - \frac{\tilde{N}_H A_\varphi^H}{2} \left[ A_1 + \frac{1}{A_1} \left( m_3^2 + \frac{\lambda_3^2}{g_{\varphi\varphi}^H} \right) \right] \right\} \quad (5.75)$$

$$E_3 = \frac{1}{\tilde{\phi} + \tilde{\omega}A_\varphi^H} \left\{ \left( \omega_H \tilde{\phi} - \tilde{\omega} \phi_H \right) \lambda_3 + \frac{\tilde{N}_H A_t^H}{2} \left[ A_1 + \frac{1}{A_1} \left( m_3^2 + \frac{\lambda_3^2}{g_{\varphi\varphi}^H} \right) \right] \right\} \quad (5.76)$$

Recalling the gauge condition (5.46), we can make sure that (5.76) leads to  $E_3 \rightarrow \infty$  for  $|\lambda_3| \rightarrow \infty$ . Therefore, we see that values of  $E_3$  in neither “+” nor “-” region are bounded from above. This was not possible in the previously known special cases. Since the escape of particle 3 is guaranteed in the “+” regime, we can also conclude that there is no upper bound on the energy extracted from the black hole. (Such a possibility is often called the super-Penrose process.) Furthermore, as the “+” region exists for any value of  $m_3$ , we see that there is no bound on the mass of escaping particles as well.

Now let us turn to the distinction between IN and OUT regimes. From (5.71) we can see that parameters in the IN region must satisfy the condition

$$|\lambda_3| > \sqrt{g_{\varphi\varphi}^H (A_1^2 - m_3^2)}, \quad (5.77)$$

whereas the opposite inequality holds for parameters in the OUT region. The two values

of  $\lambda_3$  that separate the regions, i.e.

$$\lambda_3 = \pm \sqrt{g_{\varphi\varphi}^{\text{H}} (A_1^2 - m_3^2)}, \quad (5.78)$$

correspond to a situation when our leading-order approximation (5.64) breaks down, since we cannot consistently assign a value to  $\sigma_3$ . This indicates that particle 3 with those values of  $\lambda_3$  will be produced as class II nearly critical, and a different expansion would be needed to determine its initial direction of motion.

Let us note that particle 3 can be produced in the IN+ regime (i.e. with  $x_3, \lambda_3$  satisfying both (5.72) and (5.77)) for any value of the ratio between  $m_3$  and  $A_1$ . This is another thing that was not possible in the previously studied special cases.

#### 5.4.2.1 Osculation points

Having derived borders that divide the  $\tilde{x}_3, \tilde{\lambda}_3$  parameter space according to various criteria, we shall now consider the “corners” where the borders meet. We can get insight into this issue from the physical interpretation of the borders; (5.27) is a set of parameters for which precisely critical particles are of class II, (5.73) corresponds to particle 3 being produced as precisely critical and (5.78) corresponds to particle 3 being produced as class II (nearly) critical. If any two of those eventualities happen together, the third one follows automatically. Therefore, all three borders must meet in the same points of the parameter space. Indeed, substituting (5.78) into both (5.27) and (5.73) leads to  $x_3 = \tilde{N}_{\text{H}} A_1$ . Conversely, in the “heavy regime”  $m_3 > A_1$ , in which (5.78) is absent, the remaining borders (5.27) and (5.73) cannot meet at any point.<sup>8</sup>

We have also seen that particle 3 can be produced with  $C_3 > 0$  only when its other parameters satisfy the condition (5.26). Therefore, the “+” region must lie inside the admissible region in the parameter space and their borders can only osculate. (One can make sure that this is indeed the case by comparing the limiting behaviour of (5.27) and (5.73) for  $|\lambda_3| \rightarrow \infty$  and their values at  $\lambda_3 = 0$ , i.e. in between (5.78).)

---

<sup>8</sup>Note that in the  $m_3 = A_1$  case, (5.27) and (5.73) touch at  $\lambda_3 = 0$ .

By plugging (5.78) into (5.74)-(5.76) (or into (5.28)-(5.30)), we obtain

$$q = \frac{1}{\tilde{\phi} + \tilde{\omega} A_\varphi^H} \left[ \mp \tilde{\omega} \sqrt{g_{\varphi\varphi}^H (A_1^2 - m_3^2)} - \tilde{N}_H A_1 \right] , \quad (5.79)$$

$$L = \frac{1}{\tilde{\phi} + \tilde{\omega} A_\varphi^H} \left[ \pm \tilde{\phi} \sqrt{g_{\varphi\varphi}^H (A_1^2 - m_3^2)} - \tilde{N}_H A_\varphi^H A_1 \right] , \quad (5.80)$$

$$E = \frac{1}{\tilde{\phi} + \tilde{\omega} A_\varphi^H} \left[ \pm \left( \omega_H \tilde{\phi} - \tilde{\omega} \phi_H \right) \sqrt{g_{\varphi\varphi}^H (A_1^2 - m_3^2)} + \tilde{N}_H A_t^H A_1 \right] . \quad (5.81)$$

#### 5.4.2.2 Bounds on parameters (general considerations)

We have seen that there is no upper bound on energy  $E_3$  in the regions of parameter space, which correspond to particle 3 being able to escape. Let us now search for other bounds on parameters of particle 3 in these regions.

There are multiple possibilities, depending on the ratio between  $A_1$  and  $m_3$ . As a first step, let us consider a hypothetical interaction, for which this ratio can take any value. More precisely, we shall consider an idealised scenario, in which it is possible to produce particle 3 with any value of  $m_3$  in processes with the same fixed value of  $A_1$ .<sup>9</sup> Now let us look at the union of all the “+” regions corresponding to all the possible values of  $m_3$ . Since the osculation points (5.78) can occur at any value of  $\tilde{\lambda}_3$ , we see that this union will fill the whole admissible region in  $\tilde{x}_3, \tilde{\lambda}_3$  space. Therefore, the (possible) bounds (5.48)-(5.50) on  $\tilde{q}, l, \varepsilon$  in the admissible region will also serve as bounds on  $\tilde{q}_3, l_3, \varepsilon_3$  of particles produced by our hypothetical interaction.

Second, let us consider a more realistic scenario, in which only some values of the ratio between  $m_3$  and  $A_1$  are possible. In such a case, we can search for bounds on parameters in the “+” region for given values of  $m_3$  and  $A_1$ . Since parametric expressions (5.74)-(5.76) are mere quadratic functions of  $\lambda_3$ , they will always reach an extremum, and therefore there will always be bounds on values of  $q_3, L_3, E_3$  in the “+” region.

Starting with  $q_3$ , we find that for

$$\lambda_3 = -\frac{g_{\varphi\varphi}^H \tilde{\omega}}{\tilde{N}_H} A_1 , \quad (5.82)$$

---

<sup>9</sup>Keeping  $A_1$  fixed is motivated by existence of upper bounds on  $A_1$  in terms of  $E_1$ ; cf. (5.96), (5.92). Moreover, one can also find a lower bound on  $A_1$  in a similar manner for  $\sigma_1 = +1$ .

expression (5.74) reaches an extremum with value

$$q_3^b = -\frac{1}{2(\tilde{\phi} + \tilde{\omega}A_\varphi^H)} \left[ \tilde{N}_H \left( A_1 + \frac{m_3^2}{A_1} \right) - \frac{g_{\varphi\varphi}^H \tilde{\omega}^2 A_1}{\tilde{N}_H} \right]. \quad (5.83)$$

Turning to  $L_3$ , we can infer that for

$$\lambda_3 = \frac{g_{\varphi\varphi}^H \tilde{\phi}}{\tilde{N}_H A_\varphi^H} A_1, \quad (5.84)$$

expression (5.75) reaches an extremum with value

$$L_3^b = -\frac{1}{2(\tilde{\phi} + \tilde{\omega}A_\varphi^H)} \left[ \tilde{N}_H A_\varphi^H \left( A_1 + \frac{m_3^2}{A_1} \right) - \frac{g_{\varphi\varphi}^H \tilde{\phi}^2 A_1}{\tilde{N}_H A_\varphi^H} \right]. \quad (5.85)$$

For  $E_3$ , the situation is again different due to dependence on gauge. Looking at the  $|\lambda_3| \rightarrow \infty$  behaviour of (5.76), we can make sure that the condition (5.46) implies that (5.76) will reach a minimum. It occurs for

$$\lambda_3 = -\frac{g_{\varphi\varphi}^H A_1}{\tilde{N}_H A_t^H} \left( \omega_H \tilde{\phi} - \tilde{\omega} \phi_H \right), \quad (5.86)$$

and its value is

$$E_3^{\min} = \frac{1}{2(\tilde{\phi} + \tilde{\omega}A_\varphi^H)} \left[ \tilde{N}_H A_t^H \left( A_1 + \frac{m_3^2}{A_1} \right) - \frac{g_{\varphi\varphi}^H A_1}{\tilde{N}_H A_t^H} \left( \omega_H \tilde{\phi} - \tilde{\omega} \phi_H \right)^2 \right]. \quad (5.87)$$

#### 5.4.2.3 Additional remarks on OUT– region

The discussion above can be extended by analysing bounds on parameters in further, special regions in the parameter space. OUT– is particularly interesting in this regard, since there is an upper bound on the values of energy  $E_3$  in this region. As we noted in 4.4.2, this can be used to illustrate the difference between the BSW-type and Schnittman-type collisional process. Let us extend this argument to our more complicated case of equatorial charged particles.

Expression (5.76) can not have a maximum due to (5.46), and thus the upper bound on  $E_3$  in the OUT– region must be its value for one of the osculation points. Picking the

higher of the values (5.81), we can write the bound as follows:

$$E_3 < \left| \frac{\omega_H \tilde{\phi} - \tilde{\omega} \phi_H}{\tilde{\phi} + \tilde{\omega} A_\varphi^H} \right| \sqrt{g_{\varphi\varphi}^H (A_1^2 - m_3^2)} + \frac{\tilde{N}_H A_t^H A_1}{\tilde{\phi} + \tilde{\omega} A_\varphi^H}. \quad (5.88)$$

We shall maximise the bound with respect to all possible parameters in order to derive an unconditional bound in terms of  $E_1$ . First, we consider  $m_3 \ll A_1$ , which also allows us to factorize out  $A_1$

$$E_3 < \left( \left| \frac{\omega_H \tilde{\phi} - \tilde{\omega} \phi_H}{\tilde{\phi} + \tilde{\omega} A_\varphi^H} \right| \sqrt{g_{\varphi\varphi}^H} + \frac{\tilde{N}_H A_t^H}{\tilde{\phi} + \tilde{\omega} A_\varphi^H} \right) A_1. \quad (5.89)$$

Second, we shall express  $A_1$  using  $E_1$  and maximise it with respect to other parameters of particle 1. The easiest way is to rewrite  $x_1$  in terms of  $E_1$  and  $\lambda_1$ ,

$$x_1 = E_1 \frac{\tilde{\phi} + \tilde{\omega} A_\varphi^H}{A_t^H} - \lambda_1 \frac{\omega_H \tilde{\phi} - \tilde{\omega} \phi_H}{A_t^H}. \quad (5.90)$$

(Note that gauge condition (5.46) implies that the coefficient multiplying  $E_1$  is positive.)

Looking at the leading order of  $A_1$  (5.65) with (5.90) in the  $|\lambda_1| \rightarrow \infty$  limit (for fixed  $E_1$ ),

$$A_1 \approx -\lambda_1 \frac{\omega_H \tilde{\phi} - \tilde{\omega} \phi_H}{\tilde{N}_H A_t^H} + \sigma_1 |\lambda_1| \sqrt{\left( \frac{\omega_H \tilde{\phi} - \tilde{\omega} \phi_H}{\tilde{N}_H A_t^H} \right)^2 - \frac{1}{g_{\varphi\varphi}^H}}, \quad (5.91)$$

one can see that it is not real due to (5.45). Therefore, for a given  $E_1$ , parameter  $A_1$  will lie in the in real numbers only for a finite interval of values of  $\lambda_1$  and  $\partial A_1 / \partial \lambda_1$  will blow up with opposite signs at the opposite ends of that interval. Thus, there will always be an extremum with respect to  $\lambda_1$ . In particular, for Schnittman-type process ( $\sigma_1 = +1$ ), there will be a maximum. We can also see that we need to put  $m_1 = 0$  to maximise  $A_1$  with  $\sigma_1 = +1$ . Then we can find the maximum with respect to  $\lambda_1$  and derive the unconditional bound on  $A_1$

$$A_1 \leq 2E_1 \frac{\tilde{N}_H \left( \tilde{\phi} + \tilde{\omega} A_\varphi^H \right) A_t^H}{\tilde{N}_H^2 (A_t^H)^2 - g_{\varphi\varphi}^H \left( \omega_H \tilde{\phi} - \tilde{\omega} \phi_H \right)^2}. \quad (5.92)$$

Combining with (5.89), we conclude that the unconditional upper bound on energy  $E_3$  of

a particle produced in OUT– regime in the Schnittman-type process is

$$E_3 < 2E_1 \frac{\tilde{N}_H |A_t^H|}{\tilde{N}_H |A_t^H| - \sqrt{g_{\varphi\varphi}^H} |\omega_H \tilde{\phi} - \tilde{\omega} \phi_H|} . \quad (5.93)$$

On the other hand, for the BSW-type process, we shall start with the following inequality:

$$\tilde{N}_H A_1(E_1, \lambda_1, m_1) \leq x(E_1, \lambda_1) . \quad (5.94)$$

In order to maximise  $x(E_1, \lambda_1)$ , we need to look at values of  $\lambda_1$  that satisfy

$$\tilde{N}_H A_1(E_1, \lambda_1, m_1) = x(E_1, \lambda_1) , \quad (5.95)$$

i.e. the ends of the interval mentioned above, and on their dependence on  $m_1$ . The resulting unconditional bound on  $A_1$  with  $\sigma_1 = -1$  is

$$A_1 \leq E_1 \frac{|\tilde{\phi} + \tilde{\omega} A_\varphi^H|}{\tilde{N}_H |A_t^H| - \sqrt{g_{\varphi\varphi}^H} |\omega_H \tilde{\phi} - \tilde{\omega} \phi_H|} . \quad (5.96)$$

In combination with (5.89), it gives us the unconditional upper bound on energy  $E_3$  of a particle produced in OUT– regime in the BSW-type process as follows:

$$E_3 < E_1 \frac{\tilde{N}_H |A_t^H| + \sqrt{g_{\varphi\varphi}^H} |\omega_H \tilde{\phi} - \tilde{\omega} \phi_H|}{\tilde{N}_H |A_t^H| - \sqrt{g_{\varphi\varphi}^H} |\omega_H \tilde{\phi} - \tilde{\omega} \phi_H|} . \quad (5.97)$$

Let us note that for  $\omega \equiv 0$ , the above results reduce to the ones we derived in 4.4.2, i.e.  $E_3 < E_1$  for BSW-type process and  $E_3 < 2E_1$  for Schnittman-type process. The bound for Schnittman-type process is higher than for BSW-type process even in the general case, due to (5.45). On the other hand, also due to (5.45), we can see that  $E_3 > E_1$  is generally not prevented for the BSW-type process, unlike in the  $\omega \equiv 0$  case. However, the biggest difference is that in the general case the gauge-dependent factors do not cancel, and thus the bounds need to be interpreted more carefully.

### 5.4.3 Special cases and the degenerate case

We have seen that the collisional processes analysed above have some features that were absent in the previously studied special cases. Thus, now we shall discuss how the special cases follow from the general results.

#### 5.4.3.1 (Quasi)radial limit

First, let us investigate how to recover the results for radially moving particles [80]. The key feature we want to reproduce is the existence of a threshold value  $\mu$ , such that  $E_3 > \mu$  corresponds to “+” regime and  $E_3 < \mu$  to “-” regime. Similarly as in 5.3.1, we can choose to consider either particles that move radially with respect to a locally non-rotating observer very close to the horizon ( $\lambda_3 = 0$ ), or particles that would move radially in a region devoid of the influence of dragging and of magnetic field ( $L_3 = 0$ ). However, both choices lead to a trivial transition, unlike in 5.3.1. Considering particles with fixed value of  $\lambda_3$ , the condition  $C_3 > 0$  can be restated as follows

$$E_3 > \frac{1}{\tilde{\phi} + \tilde{\omega} A_\varphi^H} \left\{ \left( \omega_H \tilde{\phi} - \tilde{\omega} \phi_H \right) \lambda_3 + \frac{\tilde{N}_H A_t^H}{2} \left[ A_1 + \frac{1}{A_1} \left( m_3^2 + \frac{\lambda_3^2}{g_{\varphi\varphi}^H} \right) \right] \right\}. \quad (5.98)$$

Therefore, by setting  $\lambda_3 = 0$ , we get the threshold value anticipated above

$$\mu \equiv \frac{\tilde{N}_H A_t^H}{2 \left( \tilde{\phi} + \tilde{\omega} A_\varphi^H \right)} \left( A_1 + \frac{m_3^2}{A_1} \right). \quad (5.99)$$

Moreover,  $\lambda_3 = 0$  lies in the OUT region whenever it exists. Thus we can also see that for  $\lambda_3 = 0$  the “heavy regime”  $m_3 > A_1$  coincides with the IN regime and the “light regime”  $m_3 < A_1$  with the OUT regime. This also replicates the results of [80].

#### 5.4.3.2 Geodesic limit

Next we shall discuss the transition to geodesic particles ( $q_3 = 0$ ). In this case, it should be possible to produce particles with high values of  $E_3$  or  $m_3$  only in the IN- regime (which prevents their escape).

Let us start by rewriting  $C_3$  in terms of  $E_3$  and  $q_3$

$$C_3 = -\frac{1}{\omega_H} \left[ \tilde{\omega} E_3 + q_3 \left( \omega_H \tilde{\phi} - \tilde{\omega} \phi_H \right) \right] - \frac{\tilde{N}_H}{2} \left[ A_1 + \frac{1}{A_1} \left( m_3^2 + \frac{(E_3 + q_3 A_t^H)^2}{g_{\varphi\varphi}^H \omega_H^2} \right) \right] \quad (5.100)$$

The resulting expression admits a factorisation,

$$C_3 = -\frac{\tilde{N}_H}{2g_{\varphi\varphi}^H \omega_H^2 A_1} (E - R_+) (E - R_-) , \quad (5.101)$$

where  $R_{\pm}$  stand for

$$R_{\pm} = -q_3 A_t^H - \frac{g_{\varphi\varphi}^H A_1}{\tilde{N}_H} \left[ \omega_H \tilde{\omega} \mp |\omega_H| \sqrt{\tilde{\omega}^2 - \frac{2q_3 \tilde{N}_H}{g_{\varphi\varphi}^H A_1} \left( \tilde{\phi} + \tilde{\omega} A_{\varphi}^H \right) - \frac{\tilde{N}_H^2}{g_{\varphi\varphi}^H} \left( 1 + \frac{m_3^2}{A_1^2} \right)} \right] . \quad (5.102)$$

Since  $R_+ > R_-$ , the “+” regime corresponds to  $R_- < E_3 < R_+$  for a fixed value of  $q_3$ .

We can also express (5.71) using  $E_3$  and  $q_3$

$$\sigma_3 = \text{sgn} \left[ A_1^2 - \left( m_3^2 + \frac{(E_3 + q_3 A_t^H)^2}{g_{\varphi\varphi}^H \omega_H^2} \right) \right] . \quad (5.103)$$

The result again admits a factorisation,

$$\sigma_3 = -\text{sgn}[(E_3 - S_+) (E_3 - S_-)] \quad (5.104)$$

where  $S_{\pm}$  are

$$S_{\pm} = -q_3 A_t^H \pm |\omega_H| \sqrt{g_{\varphi\varphi}^H (A_1^2 - m_3^2)} . \quad (5.105)$$

As  $S_+ > S_-$ , the OUT regime corresponds to  $S_- < E_3 < S_+$  for a fixed value of  $q_3$ .

Now, let us put  $q_3 = 0$  and denote the resulting values of  $R_{\pm}$  as  $R_{\pm}^g$

$$R_{\pm}^g = \frac{g_{\varphi\varphi}^H A_1}{\tilde{N}_H} \left[ -\omega_H \tilde{\omega} \pm |\omega_H| \sqrt{\tilde{\omega}^2 - \frac{\tilde{N}_H^2}{g_{\varphi\varphi}^H} \left( 1 + \frac{m_3^2}{A_1^2} \right)} \right] . \quad (5.106)$$

Since  $S_-$  becomes negative for  $q_3 = 0$  and  $E_3 > 0$ , we need to consider only  $S_+^g$ , which reads

$$S_+^g = |\omega_H| \sqrt{g_{\varphi\varphi}^H (A_1^2 - m_3^2)} . \quad (5.107)$$

If a geodesic particle 3 has sufficiently high energy, such that it satisfies both  $E_3 > R_+^g$  and  $E_3 > S_+^g$ , it will be produced in the IN– regime and fall into the black hole. Conversely, we can see that  $R_{\pm}^g$  and  $S_{\pm}^g$  all become imaginary for  $m_3 \gg A_1$ , and thus IN– is the only possible regime in that case. Hence, we reproduced the results of [72, 73] that the mass and energy of escaping geodesic particles is bounded.<sup>10</sup>

### 5.4.3.3 The degenerate case

Let us now return to the degenerate case (5.14), which was so far excluded from our discussion of energy extraction. We shall use the same parametrisation as in the geodesic case. If we apply (5.14) to  $R_{\pm}$  (5.102), they go over to  $R_{\pm}^d$ , which read

$$R_{\pm}^d = -q_3 A_t^H - \frac{g_{\varphi\varphi}^H A_1}{\tilde{N}_H} \left[ \omega_H \tilde{\omega} \mp |\omega_H| \sqrt{\tilde{\omega}^2 - \frac{\tilde{N}_H^2}{g_{\varphi\varphi}^H} \left( 1 + \frac{m_3^2}{A_1^2} \right)} \right]. \quad (5.108)$$

We have determined in 5.3.2 that we need to impose gauge condition  $A_t^H = 0$  in the degenerate case. However, with this condition it holds  $R_{\pm}^d = R_{\pm}^g$ . Furthermore, putting  $A_t^H = 0$  has the same effect on  $S_{\pm}$  (5.105) as putting  $q_3 = 0$ . Thus we see that upon the gauge condition  $A_t^H = 0$ , the degenerate case completely coincides with the geodesic case. Therefore, the degenerate case corresponds to a situation when the spacetime behaves locally as vacuum close to  $r_0$ . However, it can be shown that the spacetime does not need to be globally vacuum in order for (5.14) to be satisfied.

## 5.5 Results for Kerr-Newman solution

Let us now return to the Kerr-Newman solution (1.1) with mass  $M$ , angular momentum  $aM$ , and charge  $Q$  (allowing also negative values of  $a$  this time). In the form (5.1), the metric is given by

$$\mathbf{g} = -\frac{\Delta\Sigma}{\mathcal{A}} dt^2 + \frac{\mathcal{A}}{\Sigma} \sin^2 \vartheta \left[ d\varphi - \frac{a}{\mathcal{A}} (2Mr - Q^2) dt \right]^2 + \frac{\Sigma}{\Delta} dr^2 + \Sigma d\vartheta^2, \quad (5.109)$$

<sup>10</sup>Note that in [72, 73] symbols  $\lambda_{\pm}$  were used for  $R_{\pm}^g$  and  $\lambda_0$  for  $S_{\pm}^g$ .

where

$$\Delta = r^2 - 2Mr + a^2 + Q^2, \quad \Sigma = r^2 + a^2 \cos^2 \vartheta, \quad \mathcal{A} = (r^2 + a^2)^2 - \Delta a^2 \sin^2 \vartheta. \quad (5.110)$$

The electromagnetic potential (cf. (1.3)) is

$$\mathbf{A} = -\frac{Qr}{\Sigma} (\mathbf{d}t - a \sin^2 \vartheta \mathbf{d}\varphi). \quad (5.111)$$

Let us also recall the relation between the energy  $E_{\text{cr}}$  of critical particles and their angular momentum and charge (cf. (5.17), (3.78))

$$E_{\text{cr}} = \frac{aL + qQ\sqrt{Q^2 + a^2}}{Q^2 + 2a^2}. \quad (5.112)$$

### 5.5.1 Admissible region in the parameter space

Critical particles can approach  $r = M$ , whenever their parameters lie inside the admissible region in the parameter space. In the case of the extremal Kerr-Newman solution, the expressions (5.28)-(5.30) for the border of the admissible region go over to (see also (3.83), (3.84))

$$q = \frac{\sqrt{Q^2 + a^2}}{Q(Q^2 + 2a^2)} \left[ -2a\lambda + \sqrt{(Q^2 + 2a^2)^2 m^2 + (Q^2 + a^2) \lambda^2} \right], \quad (5.113)$$

$$L = \frac{Q^2 \lambda + a \sqrt{(Q^2 + 2a^2)^2 m^2 + (Q^2 + a^2) \lambda^2}}{Q^2 + 2a^2}, \quad (5.114)$$

$$E = \frac{-a\lambda + \sqrt{(Q^2 + 2a^2)^2 m^2 + (Q^2 + a^2) \lambda^2}}{Q^2 + 2a^2}. \quad (5.115)$$

#### 5.5.1.1 Bounds on parameters

As we discussed in 5.3.1.1, bounds on values of  $q$ ,  $L$  and  $E$  in the admissible region are given by extrema of expressions (5.113)-(5.115) as functions of  $\lambda$ . If  $|a|/M < 1/2$ , then (5.113) reaches an extremum, which has a value (5.32)

$$q_{\text{b}} = m \frac{\sqrt{Q^2 - 3a^2}}{Q}, \quad (5.116)$$

and which corresponds to the following values of the other parameters on the border:

$$L = \frac{ma}{\sqrt{Q^2 + a^2}} \frac{3Q^2 + a^2}{\sqrt{Q^2 - 3a^2}}, \quad E = \frac{m}{\sqrt{Q^2 + a^2}} \frac{Q^2 - a^2}{\sqrt{Q^2 - 3a^2}}. \quad (5.117)$$

For  $|a|/M > (\sqrt{5}-1)/2$ , there exists an extremum of (5.114), which has a value (5.37)

$$L_b = m \operatorname{sgn} a \frac{\sqrt{a^4 + Q^2 a^2 - Q^4}}{\sqrt{Q^2 + a^2}}, \quad (5.118)$$

and which corresponds to the following values of the other parameters on the border:

$$q = m \frac{|a|}{Q} \frac{3Q^2 + a^2}{\sqrt{a^4 + Q^2 a^2 - Q^4}}, \quad E = \frac{m |a|}{\sqrt{Q^2 + a^2}} \frac{2Q^2 + a^2}{\sqrt{a^4 + Q^2 a^2 - Q^4}}. \quad (5.119)$$

In the standard gauge vanishing at spatial infinity, the dragging potential of (5.109) and the electromagnetic potential (5.111) satisfy the conditions (5.45), (5.46). Therefore, (5.115) always has a minimum (cf. (5.42), (3.101), (3.94))

$$E_{\min} = \frac{m |Q|}{\sqrt{Q^2 + a^2}}, \quad (5.120)$$

which corresponds to the following values of the other parameters on the border:

$$q = \frac{m}{|Q|} \frac{Q^2 - a^2}{Q}, \quad L = \frac{ma}{|Q|} \frac{2Q^2 + a^2}{\sqrt{Q^2 + a^2}}. \quad (5.121)$$

Let us note that  $E \geq m$  for the the values of energy (5.117), (5.119), whereas  $E_{\min} \leq m$ .

The degenerate case (5.14) corresponds to the extremal Kerr solution, which we studied in 3.5.3.1. Summary of the bounds on parameters in the admissible region for the extremal Kerr-Newman solutions is given in Table 5.1.

## 5.5.2 Structure of the parameter space with regard to energy extraction

As we examined in 5.4.2, the parameter space of nearly critical particles can be divided into various regions corresponding to different kinematic regimes, in which particle 3 can be produced in our collisional process. In extremal Kerr-Newman spacetime, the

Table 5.1: Bounds on parameters  $l$ ,  $\tilde{q}$  and  $\varepsilon_{\text{cr}}$  of critical particles that can approach  $r = M$  in an extremal Kerr-Newman spacetime. The general case can be inferred from equations (5.48)-(5.50), whereas the vacuum extremal Kerr case from (5.54), (5.55) (see also 3.5.3.1). The placement of non-strict inequalities is based on the information about class II critical particles obtained in 3.5.2. (The present table expands the conclusions about restrictions on signs of  $l$ ,  $\tilde{q}$  in Table 3.2.)

Kerr-Newman black-hole parameters		Restrictions				
$ \gamma_{\text{KN}} $	$\frac{ a }{M}$	$\frac{ Q }{M}$	General case	Bounds on $l$	Bounds on $\tilde{q}$	Bounds on $\varepsilon$
$0^\circ$	1	0	Vacuum	$l \operatorname{sgn} a > \frac{2 a }{\sqrt{3}}$		$\varepsilon > \frac{1}{\sqrt{3}}$
$0^\circ <  \gamma_{\text{KN}}  < 51.8^\circ$	$1 > \frac{ a }{M} > \frac{\sqrt{5}-1}{2}$	$0 < \frac{ Q }{M} < \sqrt{\frac{\sqrt{5}-1}{2}}$	<b>1a2b</b>	$l \operatorname{sgn} a \geq \frac{\sqrt{a^4+Q^2a^2-Q^4}}{\sqrt{Q^2+a^2}}$		
$ \gamma_{\text{KN}}  \doteq 51.8^\circ$	$\frac{\sqrt{5}-1}{2}$	$\sqrt{\frac{\sqrt{5}-1}{2}}$	<b>1a2c</b>	$l \operatorname{sgn} a > 0$		$\varepsilon > \frac{ Q }{\sqrt{Q^2+a^2}}$
$51.8^\circ <  \gamma_{\text{KN}}  < 60^\circ$	$\frac{\sqrt{5}-1}{2} > \frac{ a }{M} > \frac{1}{2}$	$\sqrt{\frac{\sqrt{5}-1}{2}} < \frac{ Q }{M} < \frac{\sqrt{3}}{2}$	<b>1a2a</b>			
$60^\circ$	$\frac{1}{2}$	$\frac{\sqrt{3}}{2}$	<b>1c2a</b>			
$60^\circ <  \gamma_{\text{KN}}  < 90^\circ$	$\frac{1}{2} > \frac{ a }{M} > 0$	$\frac{\sqrt{3}}{2} < \frac{ Q }{M} < 1$	<b>1b2a</b>		$\tilde{q} \operatorname{sgn} Q \geq \frac{\sqrt{Q^2-3a^2}}{ Q }$	
$90^\circ$	0	1	<b>1b2a3</b>		$\tilde{q} \operatorname{sgn} Q > 1$	

expressions (5.74)-(5.76) for the border separating the “+” and “-” regions become

$$q_3 = \frac{\sqrt{Q^2 + a^2}}{Q} \left\{ -\frac{2a\lambda_3}{Q^2 + 2a^2} + \frac{1}{2} \left[ A_1 + \frac{1}{A_1} \left( m_3^2 + \frac{(Q^2 + a^2)\lambda_3^2}{(Q^2 + 2a^2)^2} \right) \right] \right\}, \quad (5.122)$$

$$L_3 = \frac{Q^2\lambda_3}{Q^2 + 2a^2} + \frac{a}{2} \left[ A_1 + \frac{1}{A_1} \left( m_3^2 + \frac{(Q^2 + a^2)\lambda_3^2}{(Q^2 + 2a^2)^2} \right) \right], \quad (5.123)$$

$$E_3 = -\frac{a\lambda_3}{Q^2 + 2a^2} + \frac{1}{2} \left[ A_1 + \frac{1}{A_1} \left( m_3^2 + \frac{(Q^2 + a^2)\lambda_3^2}{(Q^2 + 2a^2)^2} \right) \right]. \quad (5.124)$$

The two values of  $\lambda_3$  that separate IN and OUT regions (5.78) are

$$\lambda_3 = \pm \frac{Q^2 + 2a^2}{\sqrt{Q^2 + a^2}} \sqrt{A_1^2 - m_3^2}. \quad (5.125)$$

The structure of the parameter space is visualised for  $A_1 < m_3$  in Figure 5.1 and for  $A_1 > m_3$  in Figure 5.2, where it is also shown how special limiting cases discussed in 5.4.3 correspond to different sections of the parameter space.

### 5.5.2.1 Osculation points

The expressions (5.79)-(5.81) for the osculation points, where curves (3.84)-(5.115) and (5.122)-(5.124) touch, turn out to be

$$q_3 = \frac{1}{Q} \left[ \sqrt{Q^2 + a^2} A_1 \mp 2a \sqrt{A_1^2 - m_3^2} \right], \quad (5.126)$$

$$L_3 = aA_1 \pm Q^2 \frac{\sqrt{A_1^2 - m_3^2}}{\sqrt{Q^2 + a^2}}, \quad (5.127)$$

$$E_3 = A_1 \mp a \frac{\sqrt{A_1^2 - m_3^2}}{\sqrt{Q^2 + a^2}}. \quad (5.128)$$

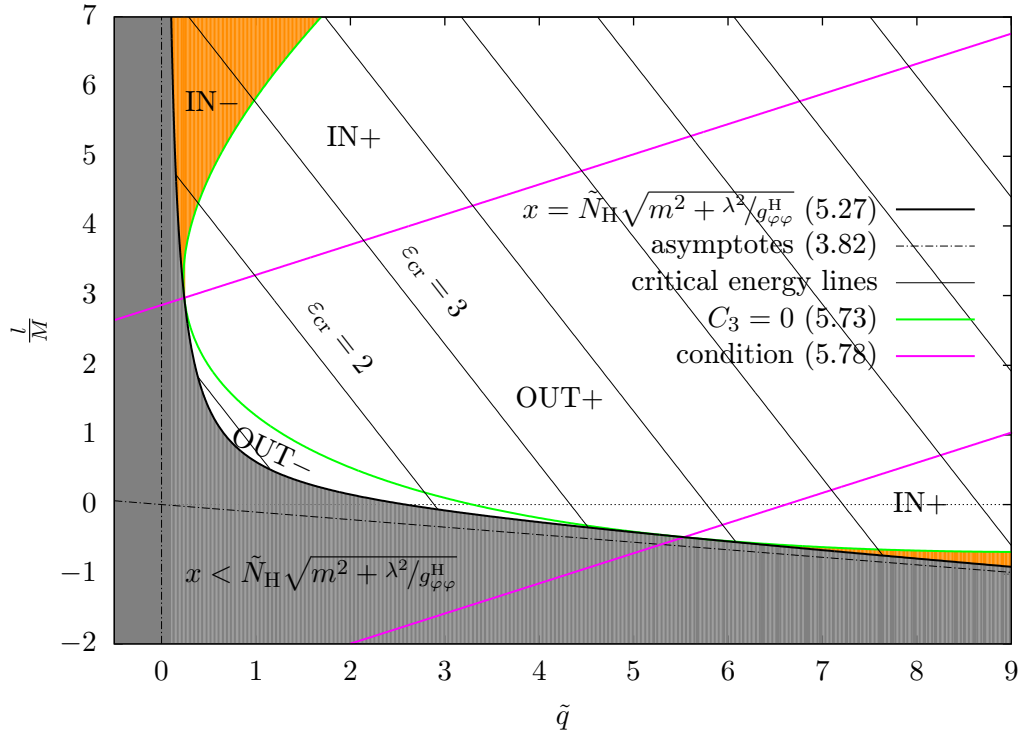


Figure 5.1: Parameter space of (nearly) critical particles for extremal Kerr-Newman black hole with  $a/M = 1/2$ . The part shaded in grey is outside the admissible region, critical particles with those parameters can not approach  $r = M$ , and nearly critical particles produced with those parameters in the vicinity of  $r = M$  cannot escape. The regions corresponding to different kinematic regimes of production of particle 3 are plotted for a process with  $A_1 = 2.5m_3$ . Region IN–, which corresponds to particle 3 falling into the black hole is shaded in orange.

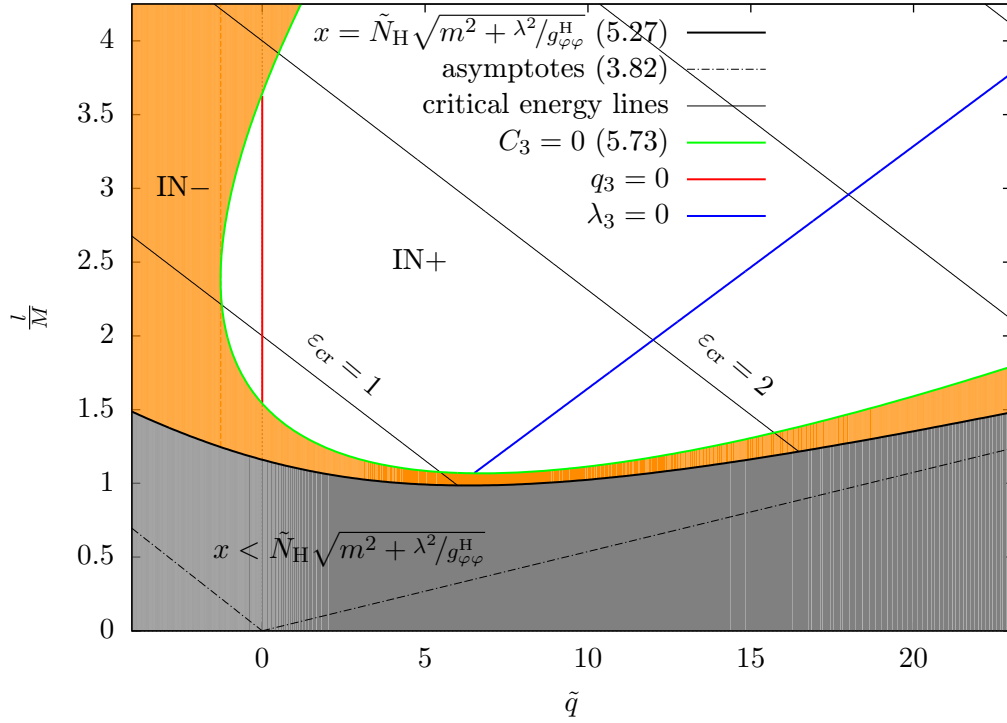


Figure 5.2: Parameter space of (nearly) critical particles for extremal Kerr-Newman black hole with  $a/M = \sqrt{35}/6$ . The part shaded in grey is outside the admissible region, critical particles with those parameters can not approach  $r = M$ , and nearly critical particles produced with those parameters in the vicinity of  $r = M$  cannot escape. The regions corresponding to different kinematic regimes of production of particle 3 are plotted for a process with  $3A_1 = 2m_3$ . Region IN $-$ , which corresponds to particle 3 falling into the black hole is shaded in orange.

### 5.5.2.2 Bounds on parameters

As we noted in 5.4.2.2, values of  $q_3$ ,  $L_3$  and  $E_3$  in the “+” region are always bounded. The expressions (5.83), (5.85), (5.87) for bounds on these parameters go over to

$$q_3^b = \frac{1}{2Q} \left[ \frac{Q^2 - 3a^2}{\sqrt{Q^2 + a^2}} A_1 + \sqrt{Q^2 + a^2} \frac{m_3^2}{A_1} \right], \quad (5.129)$$

$$L_3^b = \frac{1}{2} \left[ \frac{a^4 + Q^2 a^2 - Q^4}{a(Q^2 + a^2)} A_1 + a \frac{m_3^2}{A_1} \right], \quad (5.130)$$

$$E_3^{\min} = \frac{1}{2} \left[ \frac{Q^2}{Q^2 + a^2} A_1 + \frac{m_3^2}{A_1} \right]. \quad (5.131)$$

## 5.6 Discussion of caveats

We have concluded that there are no upper bounds on the energy or the mass of particles that can escape from the vicinity of the horizon after being produced in the collisional processes studied above. Now we shall discuss limitations of these results, from both theoretical and practical standpoint.

First, we should be aware of the simplifying assumptions involved. In particular, caution is needed regarding the parts of the parameter space where our leading-order approximation breaks down. These comprise the border of the admissible region (5.27), the two lines of constant  $\lambda_3$  separating the IN and OUT regions (5.78), and the corresponding osculation points. (For the approach phase, we studied the higher-order effects, which may arise, in 3.4.6 and 3.5.2.) Furthermore, we should also note that for charged particles, the electromagnetic self-force (cf. [121]) will become significant in addition to the gravitational backreaction.

Second, as we have seen in 4.4.3 on the example of particle collisions along the axis of symmetry, problems may arise even when all the simplifying assumptions are satisfied. Let us now check, whether the issues identified in 4.4.3 are present in the case of charged particle collisions in the equatorial plane.

We have noted above that it always holds  $E_{\min} \leq m$  for the lowest energy (5.120) required for the critical particles in the extremal Kerr-Newman spacetime in order to approach  $r = M$ . Therefore, unlike in the case of collisions along the axis, there is no general need for the critical particles involved in collisions in the vicinity of  $r = M$  to be

relativistic.

On the other hand, for all microscopic particles (known in nature), it holds  $|q| \gg m$ . Therefore, the critical condition (5.112) will generally imply  $E \gg m$  for such particles, and we see that the second type of “energy feeding problem” identified in 4.4.3 arises also in the equatorial case. In the following, we shall discuss ways how to remedy this issue.

### 5.6.1 Restrictions on processes with (marginally) bound microscopic particles

First of all, we can avoid the energy feeding problem by considering the initial critical particle 1 to be either an uncharged massive particle or a photon. We can see from Table 3.2 that this is possible for charge-to-mass ratio of the black hole smaller than  $\sqrt{2/3}$  in the case of the massive uncharged particle, or (recalling 5.3.1.3) smaller than  $\sqrt{3}/2$  for the photon.

If we want particle 1 to be charged, we can look for ways to “compensate” the effect of  $|q| \gg m$  in (5.112). It can be canceled either additively by considering particles with  $|L| \gg mM$ , or multiplicatively by restricting to black holes with  $|Q| \ll M$ . However, we have discussed in 3.5.5 that critical particles with  $|L| \gg mM$  and  $E_{\text{cr}} \sim m$  can approach  $r = M$  only for Kerr-Newman black holes with  $|Q| \ll M$ . Therefore, we need to assume this for both ways of compensation of the energy feeding problem.

As noted above, the points with the lowest or highest values of  $q$  and  $L$  in the admissible region always have  $E \geq m$  (cf. (5.117), (5.119)). Hence, the expressions (5.113) and (5.114) for values of  $q$  and  $L$  on the border (5.27) of the admissible region are monotonic along the part of the border corresponding to  $E_{\text{cr}} \leq m$ . The range of values of  $q$  and  $L$  in the part of the admissible region with  $E_{\text{cr}} \leq m$  is thus delimited by the points on (5.27) with  $E_{\text{cr}} = m$ , i.e. (3.100) and (3.77).

For simplicity, let us consider only particles that all have the same magnitude of their charge-to-mass ratio  $\tilde{q}$  (for example electrons and positrons), i.e.  $|\tilde{q}| = \tilde{q}_{\text{max}}$ . Let us also assume  $\tilde{q}_{\text{max}} \gg 1$ . We always want  $\text{sgn } q_3 = \text{sgn } Q$ , so that the electrostatic repulsion by the black-hole charge helps eject particle 3. Then we are left with two possibilities, either  $\text{sgn } q_1 = -\text{sgn } Q$  or  $\text{sgn } q_1 = \text{sgn } Q$ . One can check that (3.100) corresponds to  $\text{sgn } q_1 = -\text{sgn } Q$  for  $|Q| \ll M$ , whereas (3.77) implies  $\text{sgn } q_1 = \text{sgn } Q$ . For either of these variants, there exists a value  $\tilde{Q}_{\text{max}}$  of the charge-to-mass ratio  $\tilde{Q} \equiv Q/M$  of the black hole,

such that for  $|\tilde{Q}| < \tilde{Q}_{\max}$  the particle 1 with given sign of  $q_1$  can approach  $r = M$ , whilst having  $E_{\text{cr}} \leq m$ . These values are given in Table 3.1. We can also conclude from the values of  $\tilde{l}_{\max}$  in Table 3.1 that the  $\text{sgn } q_1 = -\text{sgn } Q$  variant implies the cancellation of energy feeding problem by  $|L| \gg mM$ , whereas  $L \sim mM$  for the  $\text{sgn } q_1 = \text{sgn } Q$  variant.

Now we shall examine, whether the cancellation of the energy feeding problem for black holes with  $|Q| \ll M$  hinders the energy extraction. The highest energy of an escaping particle 3 with a fixed value of charge is given by  $R_+$  (5.102), which for extremal Kerr-Newman solution turns to

$$R_+ = \frac{q_3 Q}{\sqrt{Q^2 + a^2}} + \frac{A_1}{Q^2 + a^2} \left[ 2a^2 + |a| \sqrt{3a^2 - Q^2 + \frac{2q_3 Q \sqrt{Q^2 + a^2}}{A_1} - (Q^2 + a^2) \frac{m_3^2}{A_1^2}} \right]. \quad (5.132)$$

Let us determine the values of  $A_1$  for the points (3.100) and (3.77) of the parameter space of particle 1 in  $|Q| \ll M$  approximation. For (3.100) we obtain

$$A_1 \approx \frac{2m_1}{\tilde{Q}^2}, \quad (5.133)$$

whereas for (3.77) we find

$$A_1 = m_1. \quad (5.134)$$

By inserting these values into (5.132) and using the corresponding expressions for  $\tilde{Q}_{\max}$ , we can estimate the highest achievable extracted energy for the  $\text{sgn } q_1 = -\text{sgn } Q$  variant as

$$R_+ \approx 2^{\frac{1}{3}} (\tilde{q}_{\max})^{\frac{2}{3}} \left[ m_3 + m_1 \left( 2 + \sqrt{3 + 2 \frac{m_3}{m_1}} \right) \right], \quad (5.135)$$

whereas for the  $\text{sgn } q_1 = \text{sgn } Q$  variant we get

$$R_+ = m_3 + m_1 \left( 2 + \sqrt{3 + 2 \frac{m_3}{m_1} - \frac{m_3^2}{m_1^2}} \right). \quad (5.136)$$

If we put  $m_1 = m_3$ , (5.135) simplifies to

$$R_+ \approx 2^{\frac{1}{3}} (\tilde{q}_{\max})^{\frac{2}{3}} (3 + \sqrt{5}) m_3, \quad (5.137)$$

and (5.136) to

$$R_+ = 5m_3. \quad (5.138)$$

Table 5.2: The four ways to remedy the energy feeding problem (see text for details).

Particle 1	$\tilde{Q}_{\max}$	$\varepsilon_3^{\max}$
$m_1 = 0, q_1 = 0$	$\frac{\sqrt{3}}{2}$	$\frac{\sqrt{3}}{2} \tilde{q}_{\max}$
$\varepsilon_1 \leq 1, \tilde{q}_1 = 0$	$\sqrt{\frac{2}{3}}$	$\sqrt{\frac{2}{3}} \tilde{q}_{\max}$
$\varepsilon_1 \leq 1, \tilde{q}_1 = -\tilde{q}_{\max} \operatorname{sgn} Q$	$2^{\frac{1}{3}} (\tilde{q}_{\max})^{-\frac{1}{3}}$	$2^{\frac{1}{3}} (\tilde{q}_{\max})^{\frac{2}{3}} (3 + \sqrt{5})$
$\varepsilon_1 \leq 1, \tilde{q}_1 = \tilde{q}_{\max} \operatorname{sgn} Q$	$(\tilde{q}_{\max})^{-1}$	5

Therefore, we can conclude that with  $q_1 \neq 0$ , only the  $\operatorname{sgn} q_1 = -\operatorname{sgn} Q$  variant of cancellation of the energy feeding problem allows for significant energy extraction. Summary of results for all the remedies to the energy feeding problem that we discussed is given in Table 5.2.



# Chapter 6

## Conclusions

In the present thesis, we have studied energetics of extremal rotating electrovacuum black holes with regard to energy extraction through charged generalisations of the BSW effect (cf. Section 1.4 for reference).

Since the inclusion of black-hole charge is primarily motivated by interaction of black holes with external magnetic fields (see Section 1.2), we first focused on this issue. In Chapter 2 we considered magnetised Kerr-Newman (MKN) solutions and studied the near-horizon geometries of their extremal cases. We have found in Section 2.4 that there exists a correspondence map between the MKN near-horizon geometries and the near-horizon geometries of extremal Kerr-Newman black holes without the external field. This fact can be linked to other interesting issues like the Meissner effect of expulsion of external fields from extremal black holes, as we have discussed in 2.4.3. If we consider extremal black holes as an approximation for fast-spinning astrophysical black holes, the correspondence also gives us justification to use Kerr-Newman black holes as surrogates for magnetised black holes with regard to processes happening near the horizon.

In the rest of the thesis, we analysed the generalised BSW effect. In Chapter 3, we considered collisions of charged particles moving in the equatorial plane of extremal rotating electrovacuum black holes. In this way we unified the two versions (centrifugal and electrostatic) of the generalised BSW effect that have been so far studied only separately. In 3.4.3, we have studied the restrictions that the angular momentum and the charge of the critical particles must satisfy in order for the generalised BSW effect to be possible, and how these restrictions depend on the properties of the black hole. In particular, we have identified in 3.5.3 the ranges of parameters of the extremal Kerr-Newman solution,

in which different variants of the generalised BSW effect are possible (cf. Table 3.2, and also Table 5.1).

In 3.5.5 we studied the physically most relevant case of very small value of black-hole charge (i.e. the  $Q \rightarrow 0$  limit). We have found that only in this case the critical particles approaching the horizon radius can simultaneously have non-relativistic energies and enormous-charge-to-mass ratios. This is very useful with regard to microscopic particles. We call this phenomenon “mega-BSW effect”.

In Chapter 4, we turned to collisions of charged particles moving along the axis of symmetry of extremal rotating electrovacuum black holes. In this simpler setup, we proceeded to analyse the possibilities of energy extraction, also including the Schnittman-type process. We have found in 4.4.2 that the results for the maximally charged black hole can be replicated for black holes with arbitrarily small value of charge, i.e. that no restrictions on the extracted energy appear. However, in 4.4.3 we identified numerous caveats that can make the energy extraction unfeasible despite the lack of unconditional kinematic bounds. Such problems stem mostly from properties of microscopic particles, in particular the enormous magnitudes of their charge-to-mass ratios.

In Chapter 5, we have extended the discussion of energy extraction also to the more complicated case of charged particles moving in the equatorial plane. We analysed the parameter space of nearly critical particles in 5.4.2 and identified its regions that correspond to different kinematic regimes of production of particle 3. It turned out that due to increased dimensionality of the parameter space with respect to previously studied cases, several new possibilities open. We have also discussed in 5.4.3 how to recover the simpler limiting cases as different sections of the enlarged parameter space. Nevertheless, the most important result is that there are no bounds on the extracted energy whenever both the black hole and the escaping particle 3 are charged, regardless of the magnitude of the black-hole charge.

Furthermore, we have shown in 5.6.1 that the limitations for microscopic particles, revealed on the example of collisions along the axis of symmetry, can be circumvented for collisions in the equatorial plane by suitable processes. One possibility is to consider a setup, in which the colliding particles are electrically neutral, and only the final particles produced in the collision are charged. Another variant is a process, in which the initial critical particle 1 has the opposite sign of charge than the black hole, whereas the final

particle 3 has the same sign of charge as the black hole. This other option can be realised with microscopic particles only for very small values of the black-hole charge, since it relies on the “mega-BSW effect” (cf. Table 5.2, and also Table 3.1).



# Appendix A

## Killing vectors and tensors in the near-horizon spacetimes

If one applies the general recipe for the near-horizon limit (cf. 2.3.1) to the metric (2.19), the result is

$$\mathbf{g} = -\chi^2 \tilde{N}^2 \Big|_{r_0}(\vartheta) \mathbf{d}\tau^2 + g_{\varphi\varphi}|_{r_0}(\vartheta) (\mathbf{d}\psi - \tilde{\omega}\chi \mathbf{d}\tau)^2 + \frac{\tilde{g}_{rr}|_{r_0}(\vartheta)}{\chi^2} \mathbf{d}\chi^2 + g_{\vartheta\vartheta}|_{r_0}(\vartheta) \mathbf{d}\vartheta^2 . \quad (\text{A.1})$$

Here the metric “functions” come from the original spacetime. In the models we analyse it is easy to see that

$$\frac{\tilde{g}_{rr}}{\tilde{N}^2} \Big|_{r_0} = K^4 \quad (\text{A.2})$$

does not depend on  $\vartheta$ . Hence the metric (A.1) can be written as follows:

$$\mathbf{g} = f(\vartheta) \left( -\frac{\chi^2}{K^2} \mathbf{d}\tau^2 + \frac{K^2}{\chi^2} \mathbf{d}\chi^2 \right) + g_{\varphi\varphi}|_{r_0}(\vartheta) (\mathbf{d}\psi - \tilde{\omega}\chi \mathbf{d}\tau)^2 + g_{\vartheta\vartheta}|_{r_0}(\vartheta) \mathbf{d}\vartheta^2 , \quad (\text{A.3})$$

where we choose the structural function  $f(\vartheta)$  non-negative. Comparing with (2.43), we find for the near-horizon geometries of the MKN class

$$\mathbf{g} = f(\vartheta) \left( -\frac{\chi^2}{K^2} \mathbf{d}\tau^2 + \frac{K^2}{\chi^2} \mathbf{d}\chi^2 + K^2 \mathbf{d}\vartheta^2 \right) + \frac{K^2 \sin^2 \vartheta}{f(\vartheta)} (\mathbf{d}\psi - \tilde{\omega}\chi \mathbf{d}\tau)^2 . \quad (\text{A.4})$$

The near-horizon geometry (A.1) is stationary and axially symmetric just like the original metric (2.19), and so it has the Killing vectors  $\boldsymbol{\xi}_{(1)} = \partial/\partial\tau$  and  $\boldsymbol{\xi}_{(4)} = \partial/\partial\psi$ . Additionally, regarding the Killing equation for (A.1), one finds the Killing vector of

“anti-de Sitter type” (cf. [92])

$$\xi_{(2)} = \tau \frac{\partial}{\partial \tau} - \chi \frac{\partial}{\partial \chi}, \quad (\text{A.5})$$

and another Killing vector of anti-de Sitter type,

$$\xi_{(3)} = \left( \frac{K^4}{2\chi^2} + \frac{\tau^2}{2} \right) \frac{\partial}{\partial \tau} - \tau \chi \frac{\partial}{\partial \chi} + \tilde{\omega} \frac{K^4}{\chi} \frac{\partial}{\partial \psi}, \quad (\text{A.6})$$

which involves constant  $K$  (A.2). Therefore, the general near-horizon geometry (A.3) exhibits all the Killing vectors found in the near-horizon limit of the Kerr black hole [92, 94]. We give the expressions (A.5),(A.6) explicitly here to use them to construct Killing tensors.

The increased symmetry resembling the Kerr case poses naturally the question, whether the “Carter-type” constant of motion<sup>1</sup> yielding the complete separability of geodesic equations exists in the near-horizon spacetimes. Let us prove this by constructing the Killing tensor which is related to the separation constant  $\tilde{\mathcal{K}}$ .

We start from the well-known fact that a symmetrised tensor product of two Killing vectors produces a Killing tensor. By adding such products of the available Killing vectors, we find a Killing tensor with time-independent components

$$\zeta_{(0)}^{\iota\kappa} = \xi_{(1)}^{\iota} \xi_{(3)}^{\kappa} + \xi_{(3)}^{\iota} \xi_{(1)}^{\kappa} - \xi_{(2)}^{\iota} \xi_{(2)}^{\kappa}, \quad (\text{A.7})$$

$$\zeta_{(0)}^{\alpha\beta} \frac{\partial}{\partial x^{\alpha}} \frac{\partial}{\partial x^{\beta}} = \frac{K^4}{\chi^2} \left( \frac{\partial}{\partial \tau} \right)^2 - \chi^2 \left( \frac{\partial}{\partial \chi} \right)^2 + \tilde{\omega} \frac{K^4}{\chi} \left( \frac{\partial}{\partial \tau} \frac{\partial}{\partial \psi} + \frac{\partial}{\partial \psi} \frac{\partial}{\partial \tau} \right). \quad (\text{A.8})$$

Covariant components of this Killing tensor can be simplified by adding the tensor product of the axial Killing vector with itself:

$$\zeta_{\mu\nu}^{(1)} = \xi_{\mu}^{(1)} \xi_{\nu}^{(3)} + \xi_{\mu}^{(3)} \xi_{\nu}^{(1)} - \xi_{\mu}^{(2)} \xi_{\nu}^{(2)} + \tilde{\omega}^2 K^4 \xi_{\mu}^{(4)} \xi_{\nu}^{(4)}, \quad (\text{A.9})$$

$$\zeta_{\kappa\lambda}^{(1)} \mathbf{d}x^{\kappa} \mathbf{d}x^{\lambda} = f^2(\vartheta) \left( \chi^2 \mathbf{d}\tau^2 - \frac{K^4}{\chi^2} \mathbf{d}\chi^2 \right). \quad (\text{A.10})$$

Assuming the decomposition  $f(\vartheta) = f_{(0)} + f_{(1)}(\vartheta)$  with  $f_{(0)} = \text{constant}$ , and recalling that

---

<sup>1</sup>Note that the linear constants of motion related to Killing vectors  $\xi_{(2)}^{\mu}$  and  $\xi_{(3)}^{\mu}$  do not comply with the stationarity of the equations of motion. This is due to the fact that components of  $\xi_{(2)}^{\mu}$  and  $\xi_{(3)}^{\mu}$  depend on  $\tau$ .

the metric is also a Killing tensor, we arrive at the final Killing tensor

$$\zeta_{\mu\nu}^{(2)} = \xi_{\mu}^{(1)}\xi_{\nu}^{(3)} + \xi_{\mu}^{(3)}\xi_{\nu}^{(1)} - \xi_{\mu}^{(2)}\xi_{\nu}^{(2)} + \tilde{\omega}^2 K^4 \xi_{\mu}^{(4)}\xi_{\nu}^{(4)} + f_{(0)} K^2 g_{\mu\nu} , \quad (\text{A.11})$$

which satisfies

$$\zeta_{\alpha\beta}^{(2)} u^{\alpha} u^{\beta} = \mathcal{H} . \quad (\text{A.12})$$

Last, let us recall that there exists a Killing tensor  $\zeta_{\iota\kappa}^{\text{C}}$  in the Kerr-Newman spacetime, which is related to the Carter constant (cf. [98, 109]). One can make sure that the Killing tensor  $\zeta_{\iota\kappa}^{(2)}$  defined above arises as a near-horizon limit of  $\zeta_{\iota\kappa}^{\text{C}}$  (see [122–124]).



# Appendix B

## Harrison transformation

Here we briefly review the essential knowledge regarding the use of the Harrison transformation to generate the MKN solution. Starting from an overview of the Ernst formalism (according to the general formulation given in Chapters 18 and 34 in [15]), we focus on the particular case of Ernst potentials based on  $\partial/\partial\varphi$ . Then we discuss how these potentials can be utilised in the magnetising Harrison transformation (cf. [17–19]), and how the “magnetised” solution is “reconstructed” from the transformed potentials. We finish by demonstrating that  $\omega$  and  $\phi$  in the MKN spacetime satisfy certain properties (including the rigidity theorems) thanks to preservation of these properties by the Harrison transformation (see also [102]).

### B.1 Ernst formalism

Assuming  $\xi^\iota$  is a Killing vector, we can define a corresponding twist vector  $w^\kappa$  as follows:

$$w^\alpha = \varepsilon^{\alpha\beta\gamma\delta} \xi_\beta \xi_{\gamma;\delta} . \quad (\text{B.1})$$

Combining the electromagnetic field strength tensor and its Hodge dual, one can construct a complex-valued self-dual field strength tensor

$$F_{\mu\nu}^{\text{sd}} = F_{\mu\nu} + \frac{i}{2} \varepsilon_{\mu\nu\rho\sigma} F^{\rho\sigma} . \quad (\text{B.2})$$

Then the complex Ernst potential for the electromagnetic field  $\Phi$  and the complex Ernst gravitational potential  $\mathcal{E}$  are defined by the following differential equations:

$$\Phi_{,\kappa} = F_{\kappa\lambda}^{\text{sd}} \xi^\lambda , \quad (\text{B.3})$$

$$\mathcal{E}_{,\rho} = -(\xi_\sigma \xi^\sigma)_{,\rho} + i w_\rho - 2\bar{\Phi}\Phi_{,\rho} . \quad (\text{B.4})$$

If we observe that

$$2\bar{\Phi}\Phi_{,\mu} = (|\Phi|^2)_{,\mu} + \bar{\Phi}\Phi_{,\mu} - \bar{\Phi}_{,\mu}\Phi = (|\Phi|^2)_{,\mu} + 2i \left[ \text{Re } \Phi (\text{Im } \Phi)_{,\mu} - (\text{Re } \Phi)_{,\mu} \text{Im } \Phi \right] , \quad (\text{B.5})$$

we can separate the real and imaginary parts of  $\mathcal{E}$ , obtaining

$$\text{Re } \mathcal{E} = -\xi_\iota \xi^\iota - |\Phi|^2 , \quad (\text{B.6})$$

$$(\text{Im } \mathcal{E})_{,\alpha} = w_\alpha + i (\bar{\Phi}\Phi_{,\alpha} - \bar{\Phi}_{,\alpha}\Phi) . \quad (\text{B.7})$$

The set of orbits of the Killing vector  $\xi^\rho$  can be understood as a quotient manifold. We can define a conformally rescaled metric  $\gamma$  on this manifold by relation

$$\gamma_{\mu\nu} = |\xi^2| \left( g_{\mu\nu} - \frac{1}{\xi^2} \xi_\mu \xi_\nu \right) . \quad (\text{B.8})$$

Quantities  $\Phi$ ,  $\mathcal{E}$ ,  $\gamma$  represent a solution of Einstein-Maxwell system in the Ernst framework.

Let us now apply this formalism to metric (2.18) and its Killing vector  $\partial/\partial\varphi$ . Calculating the twist vector (B.1) for  $\partial/\partial\varphi$ , we see that it contains derivatives of the dragging potential

$$w_\mu \mathbf{d}x^\mu = -\frac{(g_{\varphi\varphi})^2}{\sqrt{-g}} \left( g_{rr} \frac{\partial\omega}{\partial\vartheta} \mathbf{d}r - g_{\vartheta\vartheta} \frac{\partial\omega}{\partial r} \mathbf{d}\vartheta \right) . \quad (\text{B.9})$$

If we separate the real and imaginary parts of  $\Phi$  (B.3), we can see that the real part is given just by

$$\text{Re } \Phi = A_\varphi , \quad (\text{B.10})$$

whereas the imaginary part satisfies differential equations

$$\frac{\partial \text{Im } \Phi}{\partial r} = -\frac{\sqrt{-g}}{N^2 g_{\vartheta\vartheta}} \left( \frac{\partial A_t}{\partial\vartheta} + \omega \frac{\partial A_\varphi}{\partial\vartheta} \right) , \quad \frac{\partial \text{Im } \Phi}{\partial\vartheta} = \frac{\sqrt{-g}}{N^2 g_{rr}} \left( \frac{\partial A_t}{\partial r} + \omega \frac{\partial A_\varphi}{\partial r} \right) . \quad (\text{B.11})$$

Regarding the Ernst gravitational potential, (B.6) turns to

$$\operatorname{Re} \mathcal{E} = -g_{\varphi\varphi} - |\Phi|^2 . \quad (\text{B.12})$$

whereas (B.7) can be rewritten as

$$\frac{\partial \operatorname{Im} \mathcal{E}}{\partial r} = -\frac{g_{rr} (g_{\varphi\varphi})^2}{\sqrt{-g}} \frac{\partial \omega}{\partial \vartheta} - 2 \left( \operatorname{Re} \Phi \frac{\partial \operatorname{Im} \Phi}{\partial r} - \frac{\partial \operatorname{Re} \Phi}{\partial r} \operatorname{Im} \Phi \right) , \quad (\text{B.13})$$

$$\frac{\partial \operatorname{Im} \mathcal{E}}{\partial \vartheta} = \frac{g_{\vartheta\vartheta} (g_{\varphi\varphi})^2}{\sqrt{-g}} \frac{\partial \omega}{\partial r} - 2 \left( \operatorname{Re} \Phi \frac{\partial \operatorname{Im} \Phi}{\partial \vartheta} - \frac{\partial \operatorname{Re} \Phi}{\partial \vartheta} \operatorname{Im} \Phi \right) . \quad (\text{B.14})$$

Last, the metric (B.8) on the quotient manifold becomes

$$\gamma = g_{\varphi\varphi} \left( -N^2 \mathbf{d}t^2 + g_{rr} \mathbf{d}r^2 + g_{\vartheta\vartheta} \mathbf{d}\vartheta^2 \right) . \quad (\text{B.15})$$

When used with the Kerr-Newman solution (1.1), (1.3), the relations (B.12)-(B.14) for the Ernst gravitational potential lead to (cf. [18])

$$\mathcal{E} = - \left( r^2 + a^2 - a \frac{2Ma + i(2Mr - Q^2) \cos \vartheta}{r + ia \cos \vartheta} \right) \sin^2 \vartheta - (4Ma^2 + iQ^2 \cos \vartheta) \frac{a - ir \cos \vartheta}{r + ia \cos \vartheta} . \quad (\text{B.16})$$

Employing (B.10) and (B.11) with (1.3), the Ernst potential for the electromagnetic field in the Kerr-Newman spacetime is obtained as

$$\Phi = Q \frac{a - ir \cos \vartheta}{r + ia \cos \vartheta} . \quad (\text{B.17})$$

## B.2 Generating “magnetised” solutions

In order to perform the Harrison transformation, we first define a complex function  $\Lambda$  involving the potentials  $\mathcal{E}$ ,  $\Phi$  of the “seed” solution

$$\Lambda = 1 + B\Phi - \frac{1}{4}B^2\mathcal{E} . \quad (\text{B.18})$$

Here  $B$  is the real continuous parameter. The transformation consists in the transition from  $\mathcal{E}$ ,  $\Phi$  to the new potentials  $\mathcal{E}'$ ,  $\Phi'$  (representing a new solution). It has the following

form:

$$\mathcal{E}' = \frac{\mathcal{E}}{\Lambda}, \quad \Phi' = \frac{\Phi - \frac{1}{2}B\mathcal{E}}{\Lambda}. \quad (\text{B.19})$$

The new solution needs to be “reconstructed” from its Ernst potentials. First, one can use relation (B.12) for “primed” quantities to determine the effect of the transformation (B.19) on the norm of the Killing vector  $\partial/\partial\varphi$

$$g'_{\varphi\varphi} = - \left( \text{Re } \mathcal{E}' + |\Phi'|^2 \right) = - \frac{\text{Re } \mathcal{E} + |\Phi|^2}{|\Lambda|^2} = \frac{g_{\varphi\varphi}}{|\Lambda|^2}. \quad (\text{B.20})$$

The metric  $\gamma$  on the quotient manifold remains unchanged by the transformation. Nevertheless, when we invert the relation (B.15) for the new solution, the change from  $g_{\varphi\varphi}$  to  $g'_{\varphi\varphi}$  leads to the following form of the whole transformed metric:

$$\mathbf{g}' = |\Lambda|^2 \left( -N^2 \mathbf{d}t^2 + g_{rr} \mathbf{d}r^2 + g_{\vartheta\vartheta} \mathbf{d}\vartheta^2 \right) + \frac{g_{\varphi\varphi}}{|\Lambda|^2} (\mathbf{d}\varphi - \omega' \mathbf{d}t)^2. \quad (\text{B.21})$$

The new dragging potential  $\omega'$  (again a real quantity) is specified by two real partial differential equations

$$\frac{\partial\omega'}{\partial r} = |\Lambda|^2 \frac{\partial\omega}{\partial r} + \frac{2\sqrt{-g}}{g_{\varphi\varphi}g_{\vartheta\vartheta}} \left( \text{Re } \Lambda \frac{\partial \text{Im } \Lambda}{\partial\vartheta} - \frac{\partial \text{Re } \Lambda}{\partial\vartheta} \text{Im } \Lambda \right), \quad (\text{B.22})$$

$$\frac{\partial\omega'}{\partial\vartheta} = |\Lambda|^2 \frac{\partial\omega}{\partial\vartheta} - \frac{2\sqrt{-g}}{g_{\varphi\varphi}g_{rr}} \left( \text{Re } \Lambda \frac{\partial \text{Im } \Lambda}{\partial r} - \frac{\partial \text{Re } \Lambda}{\partial r} \text{Im } \Lambda \right) = \quad (\text{B.23})$$

$$= |\Lambda|^2 \frac{\partial\omega}{\partial\vartheta} - 2 \frac{N\sqrt{g_{\vartheta\vartheta}}}{\sqrt{g_{\varphi\varphi}g_{rr}}} \left( \text{Re } \Lambda \frac{\partial \text{Im } \Lambda}{\partial r} - \frac{\partial \text{Re } \Lambda}{\partial r} \text{Im } \Lambda \right), \quad (\text{B.24})$$

which can be derived from relations (B.13) and (B.14) for “primed” quantities.

The differential equations (B.11) determining the imaginary part of  $\Phi$  can be rewritten using the components of the electromagnetic field strength tensor in the locally non-rotating frame (2.29), (2.30) as follows:

$$\frac{\partial \text{Im } \Phi}{\partial r} = -\sqrt{g_{\varphi\varphi}g_{rr}} F_{(\vartheta)(t)}, \quad \frac{\partial \text{Im } \Phi}{\partial\vartheta} = \sqrt{g_{\varphi\varphi}g_{\vartheta\vartheta}} F_{(r)(t)}. \quad (\text{B.25})$$

(These relations together with (B.10) hold both for the original and transformed, “primed” quantities. Note that under the Harrison transformation the products  $g_{\varphi\varphi}g_{rr}$  and  $g_{\varphi\varphi}g_{\vartheta\vartheta}$

do not change, as seen from (B.21).) If we substitute for  $\Phi'$  from (B.19), equation (B.25) then implies

$$F'_{(r)(t)} = \frac{1}{\sqrt{g_{\varphi\varphi}g_{\vartheta\vartheta}}} \frac{\partial}{\partial\vartheta} \left[ \frac{1}{|\Lambda|^2} \left( -\text{Im } \Lambda \text{Re } \Phi + \frac{1}{2} B \text{Im } \Lambda \text{Re } \mathcal{E} + \right. \right. \\ \left. \left. + \text{Re } \Lambda \text{Im } \Phi - \frac{1}{2} B \text{Re } \Lambda \text{Im } \mathcal{E} \right) \right]. \quad (\text{B.26})$$

### B.3 Remark on rigidity theorems

Now let us show that the dragging potential and the generalised electrostatic potential in the MKN spacetime satisfy rigidity theorems, and also the relations (2.33), as a consequence of preservation of these properties by the Harrison transformation. From equation (B.24) it follows directly

$$\left. \frac{\partial\omega}{\partial\vartheta} \right|_{N=0} = 0 \quad \Longrightarrow \quad \left. \frac{\partial\omega'}{\partial\vartheta} \right|_{N'=0} = 0; \quad (\text{B.27})$$

so the validity of the the rigidity theorem for  $\omega$  in the MKN spacetime is implied by its validity for the Kerr-Newman solution.

Regarding the generalised electrostatic potential  $\phi'$ , we shall first take the derivative with respect to  $\vartheta$  of the relation (2.26),

$$\frac{\partial\phi'}{\partial\vartheta} = -\frac{\partial A'_t}{\partial\vartheta} - \omega' \frac{\partial A'_\varphi}{\partial\vartheta} - \frac{\partial\omega'}{\partial\vartheta} A'_\varphi. \quad (\text{B.28})$$

Now we can observe that the first two terms are proportional to the tetrad component  $F'_{(\vartheta)(t)}$  and use (B.25) to obtain

$$\frac{\partial\phi'}{\partial\vartheta} = \frac{N\sqrt{g_{\vartheta\vartheta}}}{\sqrt{g_{\varphi\varphi}g_{rr}}} \frac{\partial\Phi'}{\partial r} - \frac{\partial\omega'}{\partial\vartheta} A'_\varphi, \quad (\text{B.29})$$

where  $\Phi'$  is given by (B.19).

Therefore

$$\left. \frac{\partial\omega'}{\partial\vartheta} \right|_{N'=0} = 0 \quad \Longrightarrow \quad \left. \frac{\partial\phi'}{\partial\vartheta} \right|_{N'=0} = 0; \quad (\text{B.30})$$

i.e. the validity of the rigidity theorem for  $\phi$  in the MKN spacetime is dictated by the validity of the one for  $\omega$ .

We shall further calculate the radial derivative of the equation (B.24)

$$\begin{aligned}
\frac{\partial^2 \omega'}{\partial r \partial \vartheta} &= \frac{\partial}{\partial r} (|A|^2) \frac{\partial \omega}{\partial \vartheta} + |A|^2 \frac{\partial^2 \omega}{\partial r \partial \vartheta} - \\
&- \frac{\partial}{\partial r} (N^2) \frac{2}{N \sqrt{g_{rr}}} \sqrt{\frac{g_{\vartheta\vartheta}}{g_{\varphi\varphi}}} \left( \operatorname{Re} \Lambda \frac{\partial \operatorname{Im} \Lambda}{\partial r} - \operatorname{Im} \Lambda \frac{\partial \operatorname{Re} \Lambda}{\partial r} \right) - \\
&- N^2 \frac{\partial}{\partial r} \left[ \frac{2}{N \sqrt{g_{rr}}} \sqrt{\frac{g_{\vartheta\vartheta}}{g_{\varphi\varphi}}} \left( \operatorname{Re} \Lambda \frac{\partial \operatorname{Im} \Lambda}{\partial r} - \operatorname{Im} \Lambda \frac{\partial \operatorname{Re} \Lambda}{\partial r} \right) \right].
\end{aligned} \tag{B.31}$$

Note that the product  $N \sqrt{g_{rr}}$  must be finite and non-zero for  $\sqrt{-g}$  non-degenerate. Restricting (B.31) to  $N = 0$  with regard to (B.27), we arrive at

$$\begin{aligned}
\left. \frac{\partial^2 \omega'}{\partial r \partial \vartheta} \right|_{N'=0} &= \left( |A|^2 \frac{\partial^2 \omega}{\partial r \partial \vartheta} \right) \Big|_{N=0} - \\
&- \left[ \frac{\partial}{\partial r} (N^2) \frac{2}{N \sqrt{g_{rr}}} \sqrt{\frac{g_{\vartheta\vartheta}}{g_{\varphi\varphi}}} \left( \operatorname{Re} \Lambda \frac{\partial \operatorname{Im} \Lambda}{\partial r} - \operatorname{Im} \Lambda \frac{\partial \operatorname{Re} \Lambda}{\partial r} \right) \right] \Big|_{N=0}.
\end{aligned} \tag{B.32}$$

The radial derivative of  $N^2$  is proportional to surface gravity  $\varkappa$ , which vanishes for the degenerate horizon, so we can state

$$\left. \frac{\partial^2 \omega}{\partial r \partial \vartheta} \right|_{N=0, \varkappa=0} = 0 \quad \Longrightarrow \quad \left. \frac{\partial^2 \omega'}{\partial r \partial \vartheta} \right|_{N'=0, \varkappa=0} = 0. \tag{B.33}$$

Thus, we reach another desired conclusion: The radial derivative of  $\omega$  is constant over the horizon of the extremal MKN black hole, since the same is true for the extremal Kerr-Newman solution.

Similarly, we can calculate the radial derivative of equation (B.28) to get

$$\begin{aligned}
\frac{\partial^2 \phi'}{\partial r \partial \vartheta} &= \frac{\partial}{\partial r} (N^2) \frac{1}{N \sqrt{g_{rr}}} \sqrt{\frac{g_{\vartheta\vartheta}}{g_{\varphi\varphi}}} \frac{\partial \operatorname{Im} \Phi'}{\partial r} + N^2 \frac{\partial}{\partial r} \left( \frac{1}{N \sqrt{g_{rr}}} \sqrt{\frac{g_{\vartheta\vartheta}}{g_{\varphi\varphi}}} \frac{\partial \operatorname{Im} \Phi'}{\partial r} \right) - \\
&- \frac{\partial^2 \omega'}{\partial r \partial \vartheta} A'_\varphi - \frac{\partial \omega'}{\partial \vartheta} \frac{\partial A'_\varphi}{\partial r}.
\end{aligned} \tag{B.34}$$

If we evaluate this equation at  $N = 0$  and consider (B.27), we obtain

$$\left. \frac{\partial^2 \phi'}{\partial r \partial \vartheta} \right|_{N'=0} = \left( \frac{\partial}{\partial r} (N^2) \frac{1}{N \sqrt{g_{rr}}} \sqrt{\frac{g_{\vartheta\vartheta}}{g_{\varphi\varphi}}} \frac{\partial \operatorname{Im} \Phi'}{\partial r} \right) \Big|_{N=0} - \left( \frac{\partial^2 \omega'}{\partial r \partial \vartheta} A'_\varphi \right) \Big|_{N'=0}. \tag{B.35}$$

For the extremal case, this leads to

$$\left. \frac{\partial^2 \omega'}{\partial r \partial \vartheta} \right|_{N'=0, \varkappa=0} = 0 \quad \Longrightarrow \quad \left. \frac{\partial^2 \phi'}{\partial r \partial \vartheta} \right|_{N'=0, \varkappa=0} = 0 . \quad (\text{B.36})$$

Therefore, the radial derivative of  $\phi$  does not depend on  $\vartheta$  on the degenerate horizon of an extremal MKN black hole.



# Appendix C

## Auxiliary calculations

### C.1 Derivatives of effective potentials

#### C.1.1 Conditions for circular orbits

The turning point, which is also a stationary point of an effective potential, corresponds to a circular orbit. The effective potential in question may be either  $W$  [45, 109] or  $V$  [107] (see equations (3.14) to (3.16)). Let us examine the correspondence between the conditions, which holds for  $r > r_+$  (or  $N^2 > 0$ , more precisely). Taking the radial derivative of (3.15), we see

$$\frac{\partial W}{\partial r} = -\frac{\partial V_+}{\partial r}(\varepsilon - V_-) - (\varepsilon - V_+) \frac{\partial V_-}{\partial r} . \quad (\text{C.1})$$

Indeed, all radial turning points indicated by  $W$ , which are also radial stationary points of  $W$ , are radial stationary points of either  $V_+$  or  $V_-$  as well,

$$W = 0 \ \& \ \frac{\partial W}{\partial r} = 0 \iff \left( \varepsilon = V_+ \ \& \ \frac{\partial V_+}{\partial r} = 0 \right) \text{ or } \left( \varepsilon = V_- \ \& \ \frac{\partial V_-}{\partial r} = 0 \right) . \quad (\text{C.2})$$

Thus, under restriction to the motion forward in time (3.12),  $W$  and  $V \equiv V_+$  are interchangeable for finding orbits.

The circular orbit, which is also an inflection point of an effective potential, is marginally stable. To see that  $W$  and  $V$  are interchangeable in this regard as well (cf. [45, 107, 109]),

let us take another radial derivative of (3.15),

$$\frac{\partial^2 W}{\partial r^2} = -\frac{\partial^2 V_+}{\partial r^2} (\varepsilon - V_-) + 2\frac{\partial V_+}{\partial r} \frac{\partial V_-}{\partial r} - (\varepsilon - V_+) \frac{\partial^2 V_-}{\partial r^2}, \quad (\text{C.3})$$

which leads to the desired conclusion

$$W = 0 \ \& \ \frac{\partial W}{\partial r} = 0 \ \& \ \frac{\partial^2 W}{\partial r^2} = 0 \iff \left( \varepsilon = V_+ \ \& \ \frac{\partial V_+}{\partial r} = 0 \ \& \ \frac{\partial^2 V_+}{\partial r^2} = 0 \right) \text{ or} \quad (\text{C.4}) \\ \left( \varepsilon = V_- \ \& \ \frac{\partial V_-}{\partial r} = 0 \ \& \ \frac{\partial^2 V_-}{\partial r^2} = 0 \right).$$

However, the most important result is an insight on how these results break down for  $r \rightarrow r_+$ , where  $V_+ \rightarrow V_-$  and derivatives of  $V_{\pm}$  generally may not be finite (so  $W$  may seem favourable). Nonetheless, for critical particles in extremal black hole spacetimes, a different form of correspondence emerges, and since (the radial derivative of)  $V$  still embodies information about motion forward in time, it becomes preferable.

### C.1.2 Relations for critical particles

Taking the third radial derivative of (3.15), we get

$$\frac{\partial^3 W}{\partial r^3} = -\frac{\partial^3 V_+}{\partial r^3} (\varepsilon - V_-) + 3\frac{\partial^2 V_+}{\partial r^2} \frac{\partial V_-}{\partial r} + 3\frac{\partial V_+}{\partial r} \frac{\partial^2 V_-}{\partial r^2} - (\varepsilon - V_+) \frac{\partial^3 V_-}{\partial r^3}. \quad (\text{C.5})$$

If we evaluate this relation for critical particles ( $\varepsilon = \varepsilon_{\text{cr}}$ ) at the radius of the degenerate horizon (where  $V_+ = V_- = \varepsilon_{\text{cr}}$ ), it simplifies to

$$\frac{\partial^3 W}{\partial r^3} \Big|_{r=r_0, \varepsilon=\varepsilon_{\text{cr}}} = 3 \left( \frac{\partial^2 V_+}{\partial r^2} \frac{\partial V_-}{\partial r} + \frac{\partial V_+}{\partial r} \frac{\partial^2 V_-}{\partial r^2} \right) \Big|_{r=r_0}. \quad (\text{C.6})$$

The relation (4.5) among  $W$  and  $V_{\pm}$  for the axial motion is the same as the one for the equatorial motion, i.e. (3.15). Hence, equations (3.35) and (C.6) have implications valid for both the equatorial and the axial motion, some of which can be further simplified in the axial case.

### C.1.2.1 General case

Because  $V_+ > V_-$  outside the horizon, though  $V_+ = V_-$  on the horizon, it must hold that

$$\left. \frac{\partial V_+}{\partial r} \right|_{r=r_0} > \left. \frac{\partial V_-}{\partial r} \right|_{r=r_0} . \quad (\text{C.7})$$

Using this with (3.35), we arrive at the following two logical statements:

$$\left. \frac{\partial^2 W}{\partial r^2} \right|_{r=r_0, \varepsilon=\varepsilon_{\text{cr}}} < 0 \iff \left( \left. \frac{\partial V_+}{\partial r} \right|_{r=r_0} > 0 \right) \& \left( \left. \frac{\partial V_-}{\partial r} \right|_{r=r_0} < 0 \right) , \quad (\text{C.8})$$

$$\left. \frac{\partial^2 W}{\partial r^2} \right|_{r=r_0, \varepsilon=\varepsilon_{\text{cr}}} > 0 \iff \left( \left. \frac{\partial V_+}{\partial r} \right|_{r=r_0} < 0 \right) \text{ or } \left( \left. \frac{\partial V_-}{\partial r} \right|_{r=r_0} > 0 \right) . \quad (\text{C.9})$$

It is easy to check that the two variants in the second statement correspond to the critical particle having  $p^t > 0$  or  $p^t < 0$ , respectively.<sup>1</sup> Thus, with restriction to  $p^t > 0$ , equation (4.20) follows.

Using (C.7) also with (C.6), we get a statement analogous to (4.20) for class II critical particles:

$$\varepsilon = \varepsilon_{\text{cr}} \& \left. \frac{\partial V_+}{\partial r} \right|_{r=r_0} = 0 \implies \left( \left. \frac{\partial^2 W}{\partial r^2} \right|_{r=r_0} = 0 \right) \& \left( \text{sgn} \left. \frac{\partial^3 W}{\partial r^3} \right|_{r=r_0} = - \text{sgn} \left. \frac{\partial^2 V_+}{\partial r^2} \right|_{r=r_0} \right) . \quad (\text{C.10})$$

### C.1.2.2 Axial case

For motion along the axis (C.10) can be further refined. From definition (4.6), we can calculate

$$\left. \frac{\partial V_-}{\partial r} \right|_{r=r_0, \vartheta=0} = - \left( \tilde{q} \frac{\partial A_t}{\partial r} + \tilde{N} \right) \Big|_{r=r_0, \vartheta=0} . \quad (\text{C.11})$$

Using the value of  $\tilde{q}$  for class II critical particles (4.24), we get

$$\left. \frac{\partial V_-}{\partial r} \right|_{r=r_0, \vartheta=0} = -2 \tilde{N} \Big|_{r=r_0, \vartheta=0} , \quad (\text{C.12})$$

and if we plug the result into (C.6), we arrive at (4.21).

---

<sup>1</sup>Note that  $p_t > 0$  corresponds to  $\varepsilon \geq V_+$  and  $p_t < 0$  to  $\varepsilon \leq V_-$ , and for critical particles their energy  $\varepsilon_{\text{cr}} = V_+|_{r_0} = V_-|_{r_0}$ . Thus  $\partial V_+/\partial r|_{r_0} < 0$  corresponds to critical particles with  $p_t > 0$  and  $\partial V_-/\partial r|_{r_0} > 0$  to those with  $p_t < 0$ .

## C.2 The decomposition (3.71)

Now let us present the general form of the contributions to (3.64) and (3.65) according to the decomposition (3.71). Introducing the abbreviations

$$\mathcal{W} = \frac{\partial^2 \omega}{\partial r^2} A_\varphi + \frac{\partial^2 \phi}{\partial r^2}, \quad \mathcal{N} = 2 \frac{\partial \tilde{N}}{\partial r} - \frac{\tilde{N}}{g_{\varphi\varphi}} \frac{\partial g_{\varphi\varphi}}{\partial r}, \quad (\text{C.13})$$

the finite and the singular part of (3.65) can be written as

$$\tilde{q}_{\text{reg}} = \frac{\left( \mathcal{W} \frac{\partial^2 \omega}{\partial r^2} + 2 \mathcal{N} \frac{\tilde{N}}{g_{\varphi\varphi}} \frac{\partial A_\varphi}{\partial r} \right) \tilde{\lambda} + \left( \mathcal{W} \mathcal{N} + 2 \tilde{N} \frac{\partial^2 \omega}{\partial r^2} \frac{\partial A_\varphi}{\partial r} \right) \sqrt{1 + \frac{\tilde{\lambda}^2}{g_{\varphi\varphi}}}}{\frac{4 \tilde{N}^2}{g_{\varphi\varphi}} \left( \frac{\partial A_\varphi}{\partial r} \right)^2 - \mathcal{W}^2} \Bigg|_{r=r_0, \vartheta=\frac{\pi}{2}}, \quad (\text{C.14})$$

and

$$\tilde{q}_{\text{sing}} = - \frac{2 \mathcal{W} \tilde{N} \frac{\partial^2 \omega}{\partial r^2} \frac{\partial A_\varphi}{\partial r} - \mathcal{W}^2 \frac{\tilde{N}}{g_{\varphi\varphi}} \frac{\partial g_{\varphi\varphi}}{\partial r} + \frac{8 \tilde{N}^2}{g_{\varphi\varphi}} \frac{\partial \tilde{N}}{\partial r} \left( \frac{\partial A_\varphi}{\partial r} \right)^2}{\left[ \frac{4 \tilde{N}^2}{g_{\varphi\varphi}} \left( \frac{\partial A_\varphi}{\partial r} \right)^2 - \mathcal{W}^2 \right] \left( \mathcal{W} \sqrt{1 + \frac{\tilde{\lambda}^2}{g_{\varphi\varphi}}} - \frac{2 \tilde{N}}{g_{\varphi\varphi}} \tilde{\lambda} \frac{\partial A_\varphi}{\partial r} \right)} \Bigg|_{r=r_0, \vartheta=\frac{\pi}{2}}. \quad (\text{C.15})$$

Then, the expressions for contributions to (3.64) are closely related to the above,

$$l_{\text{reg}} = \tilde{\lambda} + \tilde{q}_{\text{reg}} A_\varphi \Big|_{r=r_0, \vartheta=\frac{\pi}{2}}, \quad l_{\text{sing}} = \tilde{q}_{\text{sing}} A_\varphi \Big|_{r=r_0, \vartheta=\frac{\pi}{2}}. \quad (\text{C.16})$$

# Bibliography

- [1] C. W. Misner, K. S. Thorne, J. A. Wheeler, *Gravitation*. (W. H. Freeman and company, San Francisco, 1973).
- [2] R. P. Kerr, Gravitational Field of a Spinning Mass as an Example of Algebraically Special Metrics, *Phys. Rev. Lett.* **11**, 237–238 (1963).
- [3] B. Carter, Global Structure of the Kerr Family of Gravitational Fields, *Phys. Rev.* **174**, 1559-1571 (1968).
- [4] B. Carter, Hamilton-Jacobi and Schrödinger separable solutions of Einstein's equations *Commun. Math. Phys.* **10**, 280–310 (1968).
- [5] E. T. Newman, E. Couch, K. Chinnapared, A. Exton, A. Prakash, R. Torrence, Metric of a Rotating, Charged Mass, *J. Math. Phys.* **6**, 918-919 (1965).
- [6] D. C. Wilkins, Bound Geodesics in the Kerr Metric, *Phys. Rev. D* **5**, 814-822 (1972).
- [7] E. Hackmann, H. Xu, Charged particle motion in Kerr-Newmann space-times, *Phys. Rev. D* **87**, 124030 (2013), 21 pages, arXiv:1304.2142 [gr-qc].
- [8] M. R. Anderson, J. P. S. Lemos, Viscous shear in the Kerr metric *Mon. Not. R. Astron. Soc.* **233**, 489–502 (1988).
- [9] E. Barausse, V. Cardoso, P. Pani, Can environmental effects spoil precision gravitational-wave astrophysics? *Phys. Rev. D* **89**, 104059 (2014), 60 pages, arXiv:1404.7149 [gr-qc].
- [10] R. M. Wald, Black hole in a uniform magnetic field, *Phys. Rev. D* **10**, 1680-1685 (1974).

- [11] W. B. Bonnor, Static Magnetic Fields in General Relativity, P. Phys. Soc. Lond. A **67**, 225-232 (1954).
- [12] M. A. Melvin, Pure magnetic and electric geons, Phys. Lett. **8**, 65-68 (1964).
- [13] F. J. Ernst, New Formulation of the Axially Symmetric Gravitational Field Problem, Phys. Rev. **167**, 1175-1178 (1968).
- [14] F. J. Ernst, New Formulation of the Axially Symmetric Gravitational Field Problem, Phys. Rev. **168**, 1415-1417 (1968).
- [15] H. Stephani, D. Kramer, M. MacCallum, C. Hoenselaers, E. Herlt, *Exact Solutions of Einstein's Field Equations*, Second Edition (Cambridge Univ. Press, Cambridge, 2003).
- [16] W. Kinnersley, Generation of stationary Einstein-Maxwell fields, J. Math. Phys. **14**, 651-653 (1973).
- [17] B. K. Harrison, New Solutions of the Einstein-Maxwell Equations from Old, J. Math. Phys. **9**, 1744-1752 (1968).
- [18] F. J. Ernst, Black holes in a magnetic universe, J. Math. Phys. **17**, 54-56 (1976).
- [19] F. J. Ernst, W. J. Wild, Kerr black holes in a magnetic universe, J. Math. Phys. **17**, 182-184 (1976).
- [20] A. García Díaz, Magnetic generalization of the Kerr–Newman metric, J. Math. Phys. **26**, 155-156 (1985).
- [21] F. J. Ernst, Removal of the nodal singularity of the  $C$ -metric, J. Math. Phys. **17**, 515-516 (1976).
- [22] J. Bičák, The Motion of a Charged Black Hole in an Electromagnetic Field, P. Roy. Soc. A-Math. Phys. **371**, 429-438 (1980).
- [23] N. Bretón Baez, A. García Díaz, The most general magnetized Kerr-Newman metric, J. Math. Phys. **27**, 562-563 (1986).
- [24] A. García Díaz, N. Bretón Baez, The gravitational field of a charged, magnetized, accelerating, and rotating mass, J. Math. Phys. **26**, 465-466 (1985).

- [25] W. A. Hiscock, On black holes in magnetic universes, *J. Math. Phys.* **22**, 1828-1833 (1981).
- [26] G. W. Gibbons, A. H. Mujtaba, C. N. Pope, Ergoregions in Magnetized Black Hole Spacetimes, *Classical Quant. Grav.* **30**, 125008 (2013), 23 pages, arXiv:1301.3927 [gr-qc].
- [27] V. Karas, D. Vokrouhlický, On interpretation of the magnetized Kerr-Newman black hole, *J. Math. Phys.* **32**, 714-716 (1991).
- [28] G. W. Gibbons, Yi Pang, C. N. Pope, Thermodynamics of magnetized Kerr-Newman black holes, *Phys. Rev. D* **89**, 044029 (2014), 14 pages, arXiv:1310.3286 [hep-th].
- [29] I. Booth, M. Hunt, A. Palomo-Lozano, H. K. Kunduri, Insights from Melvin-Kerr-Newman spacetimes, (*version 2*), arXiv:1502.07388v2 [gr-qc].
- [30] I. Booth, M. Hunt, A. Palomo-Lozano, H. K. Kunduri, Insights from Melvin-Kerr-Newman spacetimes, *Classical Quant. Grav.* **32**, 235025 (2015), 23 pages.
- [31] M. Astorino, G. Compère, R. Oliveri, N. Vandevorode, Mass of Kerr-Newman black holes in an external magnetic field, *Phys. Rev. D* **94**, 024019 (2016), 11 pages, arXiv:1602.08110 [gr-qc].
- [32] A. R. King, J. P. Lasota and W. Kundt, Black holes and magnetic fields, *Phys. Rev. D* **12**, 3037–3042 (1975).
- [33] J. Bičák, V. Janiš, Magnetic fluxes across black holes, *Mon. Not. R. Astron. Soc.* **212**, 899-915 (1985).
- [34] J. Bičák and L. Dvořák, Stationary electromagnetic fields around black holes. III. General solutions and the fields of current loops near the Reissner-Nordström black hole, *Phys. Rev. D* **22**, 2933–2940 (1980).
- [35] R. F. Penna, Black hole Meissner effect and Blandford-Znajek jets, *Phys. Rev. D* **89**, 104057 (2014), 10 pages, arXiv:1403.0938 [astro-ph.HE].
- [36] R. F. Penna, Black hole Meissner effect and entanglement, *Phys. Rev. D* **90**, 043003 (2014), 6 pages, arXiv:1406.2976 [hep-th].

- [37] N. Gürlebeck, M. Scholtz, Meissner effect for weakly isolated horizons, *Phys. Rev. D* **95**, 064010 (2017), 7 pages, arXiv:1702.06155 [gr-qc].
- [38] N. Gürlebeck, M. Scholtz, Meissner effect for axially symmetric charged black holes, *Phys. Rev. D* **97**, 084042 (2018), 12 pages, arXiv:1802.05423 [gr-qc].
- [39] B. Zhang, Mergers of charged black holes: Gravitational-wave events, short gamma-ray bursts, and fast radio bursts, *Astrophys. J. Lett.* **827**, L31 (2016), 5 pages, arXiv:1602.04542 [astro-ph.HE].
- [40] B. Punsly, D. Bini, General relativistic considerations of the field shedding model of fast radio bursts, *Mon. Not. R. Astron. Soc.* **459**, L41–L45 (2016), arXiv:1603.05509 [astro-ph.HE].
- [41] A. Nathanail, E. R. Most, L. Rezzolla, Gravitational collapse to a Kerr–Newman black hole, *Mon. Not. R. Astron. Soc.* **469**, L31–L35 (2017), arXiv:1703.03223 [astro-ph.HE].
- [42] M. Zajaček, A. Tursunov, A. Eckart, S. Britzen, On the charge of the Galactic centre black hole, *Mon. Not. R. Astron. Soc.* **480**, 4408–4423 (2018), arXiv:1808.07327 [astro-ph.GA].
- [43] R. Penrose, Gravitational Collapse: the Role of General Relativity, *Gen. Relat. Gravit.* **34**, 1141–1165 (2002). Original edition: *Riv. Nuovo Cimento, Numero Speciale* **1**, 252–276 (1969).
- [44] D. Christodoulou, Reversible and Irreversible Transformations in Black-Hole Physics, *Phys. Rev. Lett.* **25**, 1596–1597 (1970).
- [45] J. M. Bardeen, W. H. Press, S. A. Teukolsky, Rotating black holes: Locally nonrotating frames, energy extraction, and scalar synchrotron radiation, *Astrophys. J.* **178**, 347–370 (1972).
- [46] R. M. Wald, Energy Limits on the Penrose Process, *Astrophys. J.* **191**, 231–233 (1974).
- [47] D. Christodoulou, R. Ruffini, Reversible Transformations of a Charged Black Hole, *Phys. Rev. D* **4**, 3552–3555 (1971).

- [48] G. Denardo, R. Ruffini, On the energetics of Reissner Nordstrøm geometries, *Phys. Lett. B* **45**, 259-262 (1973).
- [49] S. M. Wagh, S. V. Dhurandhar, N. Dadhich, Revival of the Penrose Process for Astrophysical Applications, *Astrophys. J.* **290**, 12-14 (1985).
- [50] S. M. Wagh, N. Dadhich, The energetics of black holes in electromagnetic fields by the Penrose process, *Physics Reports* **183**, 137-192 (1989).
- [51] T. Piran, J. Shaham, J. Katz, High efficiency of the Penrose mechanism for particle collisions, *Astrophys. J. Lett.* **196**, L107-L108 (1975).
- [52] T. Piran, J. Shaham, Upper bounds on collisional Penrose processes near rotating black-hole horizons, *Phys. Rev. D* **16**, 1615–1635 (1977).
- [53] M. Bañados, J. Silk, S. M. West, Kerr Black Holes as Particle Accelerators to Arbitrarily High Energy, *Phys. Rev. Lett.* **103**, 111102 (2009), 4 pages, arXiv:0909.0169 [hep-ph].
- [54] K. S. Thorne, Disk accretion on to a black hole. II. Evolution of the hole, *Astrophys. J.* **191**, 507-519 (1974).
- [55] E. Berti, V. Cardoso, L. Gualtieri, F. Pretorius, U. Sperhake, Comment on “Kerr Black Holes as Particle Accelerators to Arbitrarily High Energy”, *Phys. Rev. Lett.* **103**, 239001 (2009), 1 page, arXiv:0911.2243 [gr-qc].
- [56] T. Jacobson, T. P. Sotiriou, Spinning Black Holes as Particle Accelerators, *Phys. Rev. Lett.* **104**, 021101 (2010), 3 pages, arXiv:0911.3363 [gr-qc].
- [57] A. A. Grib, Yu. V. Pavlov, On particle collisions near rotating black holes, *Gravitation and Cosmology* **17**, 42–46 (2011), arXiv:1010.2052 [gr-qc].
- [58] T. Harada, M. Kimura, Black holes as particle accelerators: a brief review, *Classical and Quantum Gravity* **31**, 243001 (2014), 17 pages, arXiv:1409.7502 [gr-qc].
- [59] M. Bañados, B. Hassanain, J. Silk, S. M. West, Emergent flux from particle collisions near a Kerr black hole, *Phys. Rev. D* **83**, 023004 (2011), 10 pages, arXiv:1010.2724 [astro-ph.CO].

- [60] S. T. McWilliams, Black Holes are Neither Particle Accelerators Nor Dark Matter Probes, *Phys. Rev. Lett.* **110**, 011102 (2013), 5 pages, arXiv:1212.1235 [gr-qc].
- [61] J. D. Schnittman, The Distribution and Annihilation of Dark Matter Around Black Holes, *Astrophys. J.* **806**, 264 (2015), 18 pages, arXiv:1506.06728 [astro-ph.HE].
- [62] A. A. Grib, Yu. V. Pavlov, On the collisions between particles in the vicinity of rotating black holes, *JETP Letters* **92**, 125-129 (2010), arXiv:1004.0913 [gr-qc].
- [63] O. B. Zaslavskii, Acceleration of particles as a universal property of rotating black holes, *Phys. Rev. D* **82**, 083004 (2010), 5 pages, arXiv:1007.3678 [gr-qc].
- [64] S.-W. Wei, Y.-X. Liu, H. Guo, C.-E. Fu, Charged spinning black holes as particle accelerators, *Phys. Rev. D* **82**, 103005 (2010), 6 pages, arXiv:1006.1056 [hep-th].
- [65] Ch.-Q. Liu, Collision of Two General Geodesic Particles around a Kerr—Newman Black Hole, *Chinese Physics Letters* **30**, 100401 (2013), 5 pages.
- [66] O. B. Zaslavskii, Acceleration of particles by nonrotating charged black holes? *JETP Letters* **92**, 571-574 (2010).
- [67] O. B. Zaslavskii, Acceleration of particles by black holes—a general explanation. *Classical Quant. Grav.* **28**, 105010 (2011), 7 pages, arXiv:1011.0167 [gr-qc].
- [68] O. B. Zaslavskii, Acceleration of particles by black holes: Kinematic explanation. *Phys. Rev. D* **84**, 024007 (2011), 6 pages, arXiv:1104.4802 [gr-qc].
- [69] T. Harada, M. Kimura, Collision of two general geodesic particles around a Kerr black hole, *Phys. Rev. D* **83** 084041 (2011), 9 pages, arXiv:1102.3316 [gr-qc].
- [70] O. B. Zaslavskii, Ultra-high energy collisions of nonequatorial geodesic particles near dirty black holes, *Journal of High Energy Physics* 12 (2012) 32, 9 pages, arXiv:1209.4987 [gr-qc].
- [71] M. Bejger, T. Piran, M. Abramowicz, F. Håkanson, Collisional Penrose Process near the Horizon of Extreme Kerr Black Holes, *Phys. Rev. Lett.* **109**, 121101 (2012), 5 pages, arXiv:1205.4350 [astro-ph.HE].

- [72] T. Harada, H. Nemoto, U. Miyamoto, Upper limits of particle emission from high-energy collision and reaction near a maximally rotating Kerr black hole, *Phys. Rev. D* **86**, 024027 (2012), 10 pages, arXiv:1205.7088 [gr-qc].
- [73] O. B. Zaslavskii, Energetics of particle collisions near dirty rotating extremal black holes: Banados-Silk-West effect versus Penrose process, *Phys. Rev. D* **86**, 084030 (2012), 14 pages, arXiv:1205.4410 [gr-qc].
- [74] J. D. Schnittman, Revised Upper Limit to Energy Extraction from a Kerr Black Hole, *Phys. Rev. Lett.* **113**, 261102 (2014), 5 pages, arXiv:1410.6446 [astro-ph.HE].
- [75] K. Ogasawara, T. Harada, U. Miyamoto, High efficiency of collisional Penrose process requires heavy particle production, *Phys. Rev. D* **93**, 044054 (2016), 9 pages, arXiv:1511.00110 [gr-qc].
- [76] O. B. Zaslavskii, Maximum efficiency of the collisional Penrose process, *Phys. Rev. D* **94**, 064048 (2016), 9 pages, arXiv:1607.00651 [gr-qc].
- [77] E. Berti, R. Brito, V. Cardoso, Ultrahigh-Energy Debris from the Collisional Penrose Process, *Phys. Rev. Lett.* **114**, 251103 (2015), 5 pages, arXiv:1410.8534 [gr-qc].
- [78] E. Leiderschneider, T. Piran, Maximal efficiency of the collisional Penrose process, *Phys. Rev. D* **93**, 043015 (2016), 13 pages, arXiv:1510.06764 [gr-qc].
- [79] O. B. Zaslavskii, General limitations on trajectories suitable for super-Penrose process, *Europhys. Lett.* **111**, 50004 (2015), 4 pages, arXiv:1506.06527 [gr-qc].
- [80] O. B. Zaslavskii, Energy extraction from extremal charged black holes due to the Banados-Silk-West effect, *Phys. Rev. D* **86**, 124039 (2012), 4 pages, arXiv:1207.5209 [gr-qc].
- [81] H. Nemoto, U. Miyamoto, T. Harada, T. Kokubu, Escape of superheavy and highly energetic particles produced by particle collisions near maximally charged black holes, *Phys. Rev. D* **87**, 127502 (2013), 4 pages, arXiv:1212.6701 [gr-qc].
- [82] M. Kimura, K.-i. Nakao, and H. Tagoshi, Acceleration of colliding shells around a black hole: Validity of the test particle approximation in the Banados-Silk-West process, *Phys. Rev. D* **83**, 044013 (2011), 8 pages, arXiv:1010.5438 [gr-qc].

- [83] K.-i. Nakao, H. Okawa, K.-i. Maeda, Non-linear collisional Penrose process: How much energy can a black hole release? *Prog. Theor. Exp. Phys.*, 013E01 (2018), 21 pages, arXiv:1708.04003 [gr-qc].
- [84] K. Ogasawara, N. Tsukamoto, Effect of the self-gravity of shells on a high energy collision in a rotating Bañados-Teitelboim-Zanelli spacetime, *Phys. Rev. D* **99**, 024016 (2019), 10 pages, arXiv:1810.03294 [gr-qc].
- [85] T. Harada, M. Kimura, Collision of an object in the transition from adiabatic inspiral to plunge around a Kerr black hole, *Phys. Rev. D* **84**, 124032 (2011), 8 pages, arXiv:1109.6722 [gr-qc].
- [86] I. V. Tanatarov, O. B. Zaslavskii, Bañados-Silk-West effect with nongeodesic particles: Extremal horizons, *Phys. Rev. D* **88**, 064036 (2013), 14 pages, arXiv:1307.0034 [gr-qc].
- [87] O. B. Zaslavskii, Geometry of nonextreme black holes near the extreme state, *Phys. Rev. D* **56**, 2188-2191 (1997), arXiv:gr-qc/9707015.
- [88] O. B. Zaslavskii, Horizon/matter systems near the extreme state, *Classical Quant. Grav.* **15**, 3251-3257 (1998), arXiv:gr-qc/9712007.
- [89] O. B. Zaslavskii, Extreme State of a Charged Black Hole in a Grand Canonical Ensemble, *Phys. Rev. Lett.* **76**, 2211-2213 (1996).
- [90] M. Halilsoy, Interpolation of the Schwarzschild and Bertotti-Robinson solutions, *Gen. Relat. Gravit.* **25**, 275-280 (1993).
- [91] J. Maldacena, J. Michelson, A. Strominger, Anti-de Sitter fragmentation, *J. High Energy Phys.* **2**, 011 (1999), 23 pages, arXiv:hep-th/9812073.
- [92] J. Bardeen, G. T. Horowitz, Extreme Kerr throat geometry: A vacuum analog of  $\text{AdS}_2 \times S^2$ , *Phys. Rev. D* **60**, 104030 (1999), 10 pages, arXiv:hep-th/9905099.
- [93] Ó. J. C. Dias, J. P. S. Lemos, Extremal limits of the  $C$  metric: Nariai, Bertotti-Robinson, and anti-Nariai  $C$  metrics, *Phys. Rev. D* **68**, 104010 (2003), 19 pages, arXiv:hep-th/0306194.

- [94] G. Compère, The Kerr/CFT Correspondence and its Extensions, *Living Rev. Relativ.* **15** (2012), 81 pages, arXiv:1203.3561 [hep-th].
- [95] H. K. Kunduri, J. Lucietti, H. S. Reall, Near-horizon symmetries of extremal black holes, *Classical Quant. Grav.* **24**, 4169-4189 (2007), arXiv:0705.4214 [hep-th].
- [96] H. K. Kunduri, J. Lucietti, Classification of near-horizon geometries of extremal black holes, *Living Rev. Relativ.* **16** (2013), 71 pages, arXiv:1306.2517 [hep-th].
- [97] R. Debever, N. Kamran, R. G. McLenaghan, Exhaustive integration and a single expression for the general solution of the type D vacuum and electrovac field equations with cosmological constant for a nonsingular aligned Maxwell field, *J. Math. Phys.* **25**, 1955-1972 (1984).
- [98] B. Carter, Black hole equilibrium states, in *Black holes (Les Houches lectures)*, eds. B. DeWitt and C. DeWitt, (Gordon and Breach, New York, 1972).
- [99] B. Carter, Republication of: Black hole equilibrium states, Part I Analytic and geometric properties of the Kerr solutions, *Gen. Relat. Gravit.* **41**, 2873-2938 (2009).
- [100] N. Kamran, A. Krasinski, Editorial note to: Brandon Carter, Black hole equilibrium states Part I. Analytic and geometric properties of the Kerr solutions, *Gen. Relat. Gravit.* **41**, 2867-2871 (2009).
- [101] N. Bretón Baez, A. García Díaz, Magnetic generalizations of the Reissner-Nordstrøm class of metrics and Bertotti-Robinson solutions, *Nuovo Cimento B*, **91**, 83-99 (1986).
- [102] F. Hejda, *Particles and fields in curved spacetimes (selected problems)*, Master thesis (Institute of Theoretical Physics, Charles University in Prague, 2013).
- [103] J. Lewandowski, T. Pawłowski, Extremal isolated horizons: a local uniqueness theorem, *Classical Quant. Grav.* **20**, 587-606 (2003), arXiv:gr-qc/0208032.
- [104] Z. Stuchlík, S. Hledík, Photon capture cones and embedding diagrams of the Ernst spacetime, *Classical Quant. Grav.* **16**, 1377-1387 (1999), arXiv:0803.2536 [gr-qc].
- [105] V. P. Frolov, I. D. Novikov, *Black hole physics: basic concepts and new developments* (Springer, Dordrecht, 1998).

- [106] J. Bičák, F. Hejda, Near-horizon description of extremal magnetized stationary black holes and Meissner effect, *Phys. Rev. D* **92**, 104006 (2015), 19 pages, arXiv:1510.01911 [gr-qc].
- [107] J. M. Bardeen, Timelike and Null Geodesics in the Kerr Metric, in *Black holes (Les Houches lectures)*, eds. B. DeWitt and C. DeWitt, (Gordon and Breach, New York, 1972).
- [108] N. A. Sharp, Geodesics in black hole space-times, *General Relativity and Gravitation* **10**, 659–670 (1979).
- [109] R. M. Wald, *General Relativity* (Univ. of Chicago Press, Chicago, 1984).
- [110] A. J. M. Medved, D. Martin, M. Visser, Dirty black holes: Symmetries at stationary nonstatic horizons, *Phys. Rev. D* **70**, 024009 (2004), 8 pages, arXiv:gr-qc/0403026.
- [111] O. B. Zaslavskii, Is the super-Penrose process possible near black holes? *Phys. Rev. D* **93**, 024056 (2016), 7 pages, arXiv:1511.07501 [gr-qc].
- [112] T. Jacobson, Where is the extremal Kerr ISCO? *Classical Quant. Grav.* **28**, 187001 (2011), 5 pages, arXiv:1107.5081 [gr-qc].
- [113] F. Hejda, J. Bičák, Kinematic restrictions on particle collisions near extremal black holes: A unified picture, *Phys. Rev. D* **95**, 084055 (2017), 22 pages, arXiv:1612.04959 [gr-qc].
- [114] T. Harada, M. Kimura, Collision of an innermost stable circular orbit particle around a Kerr black hole, *Phys. Rev. D* **83**, 024002 (2011), 11 pages, arXiv:1010.0962 [gr-qc].
- [115] O. B. Zaslavskii, Near-horizon circular orbits and extremal limit for dirty rotating black holes, *Phys. Rev. D* **92**, 044017 (2015), 12 pages, arXiv:1506.00148 [gr-qc].
- [116] J. Bičák, Z. Stuchlík, V. Balek, The motion of charged particles in the field of rotating charged black holes and naked singularities, *Bulletin of the Astronomical Institutes of Czechoslovakia* **40**, 65-92 (1989).
- [117] E. A. Power, J. A. Wheeler, Thermal geons, *Reviews of Modern Physics* **29**, 480-495 (1957).

- [118] F. de Felice, Equatorial Geodesic Motion in the Gravitational Field of a Rotating Source, *Il Nuovo Cimento B* **57**, 351-388 (1968).
- [119] P. V. P. Cunha, J. Grover, C. Herdeiro, E. Radu, H. Rúnarsson, A. Wittig, Chaotic lensing around boson stars and Kerr black holes with scalar hair, *Phys. Rev. D* **94**, 104023 (2016), 28 pages, arXiv:1609.01340 [gr-qc].
- [120] F. Hejda, J. Bičák, O. B. Zaslavskii, Extraction of energy from an extremal rotating electrovacuum black hole: Particle collisions along the axis of symmetry, *Phys. Rev. D* **100**, 064041 (2019), 12 pages, arXiv:1904.02035 [gr-qc].
- [121] E. Poisson, A. Pound, I. Vega, The Motion of Point Particles in Curved Spacetime, *Living Rev. Relativ.* **14**, 7 (2011), 190 pages, arXiv:1102.0529 [gr-qc].
- [122] J. Rasmussen, On hidden symmetries of extremal Kerr–NUT–AdS–dS black holes, *Journal of Geometry and Physics* **61**, 922-926 (2011), arXiv:1009.4388 [gr-qc].
- [123] A. Galajinsky, K. Orekhov,  $N = 2$  superparticle near horizon of extreme Kerr–Newman–AdS–dS black hole, *Nucl. Phys. B* **850**, 339 (2011), arXiv:1103.1047 [hep-th].
- [124] A. M. Al Zahrani, V. P. Frolov, A. A. Shoom, Particle dynamics in weakly charged extreme Kerr throat, *International Journal of Modern Physics D* **20**, 649-660 (2011), arXiv:1010.1570 [gr-qc].